This project has received funding from the European Union's Horizon 2020 research and innovation programme under grant agreement No 101006927.

Verification through Accelerated testing Leading to Improved wave energy Designs

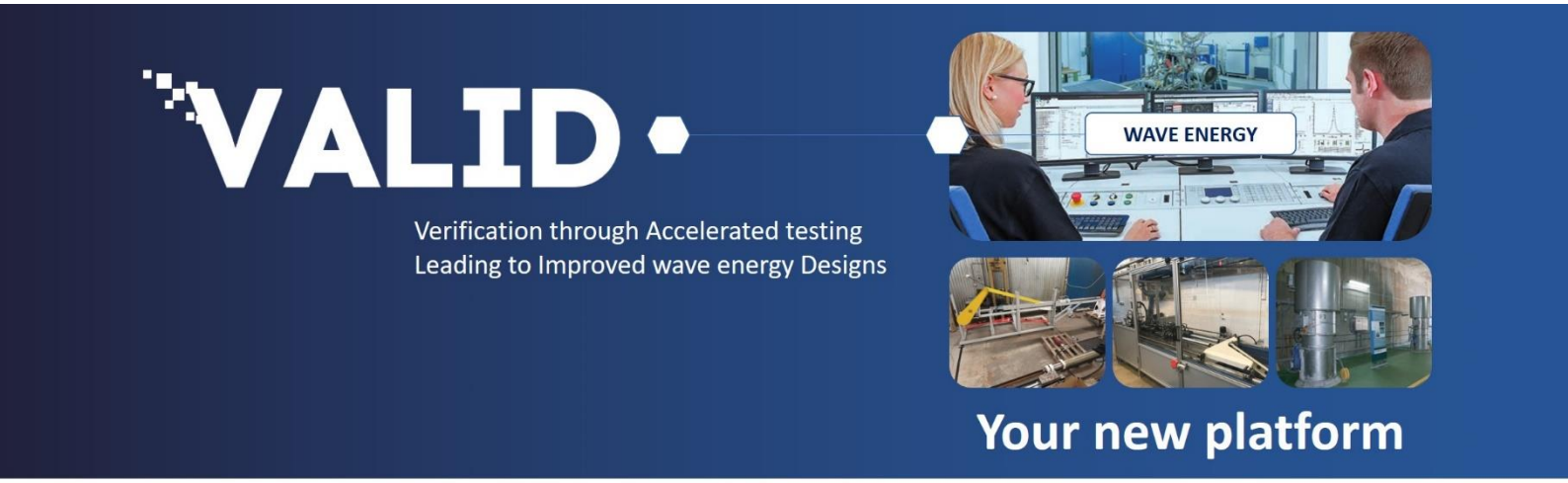

Deliverable D1.2

Critical Components and Modelling Limitations

Version 1.0

2021-12-14

Lead participant: TECNALIA

Dissemination level: Public

This project has received funding from the European Union's Horizon 2020 research and innovation programme under grant agreement No 101006927.

DOCUMENT STATUS

Authors

Name	Organisation
Pablo Ruiz-Minguela	TECNALIA
Eider Robles	TECNALIA
Joseba Lopez-Mendia	TECNALIA
Imanol Touzon	TECNALIA
Joao Cruz	Y4C
Michele Martini	Y4C
José Guadalupe Rangel Ramirez	AAU
Claes Eskilsson	AAU
Johan Sandström	RISE
George Lavidas	TUD
Günter Lang	AVL
Jon Lekube	BIMEP

Approval

Name	Organisation	Date
Julia Fernández Chozas	JFC	2021-11-23

Document History

Version	Description	Reviewer	Date
0.0	Initial ToC for partners review	T1.2 partners	2020-12-21
0.2	Partial draft (up to section 4)	T1.2 partners	2021-06-30
0.5	Analysis of limitations and framework	TECNALIA	2021-10-29
0.9	Full draft for quality review - JFC	Y4C/RISE	2021-11-12
1.0	Final version for the Commision	EC	2021-12-14

Dissemination level

Short	Type	
PU	Public	X
PP	Restricted to other programme participants (including the Commission Services)	
RE	Restricted to a group specified by the consortium (including the Commission Services)	
CO	Confidential, only for members of the consortium (including the Commission Services)	

EU PROJECT NO: 101006927

This project has received funding from the European Union's Horizon 2020 research and innovation programme under grant agreement No 101006927.

Executive Summary

This report reviews and defines the theoretical, numerical and experimental modelling approaches to be considered in the VALID project to address the design and accelerated testing of critical components and subsystems of Wave Energy Converters (WECs). It is part of WP1 activities, which aim to devise a methodology for accelerated hybrid testing that is compatible with the corresponding architecture proposed in WP2.

The report gives a brief review of the key findings about the critical components and sub-systems of WECs identified in the project, before describing and assessing the various modelling approaches that may be relevant in the context of accelerated testing of critical components of WECs. It first classifies and describes the theoretical models, which are simplified and schematic representations of the theory applicable to WECs, focusing the environmental characterisation, wave-structure interaction, affecting effects and deterioration and, reliability and survivability. Then, a review of numerical modelling methods most typically applied in WEC and WEC sub-system design is presented. Basic formulations covering the range of most common approaches used to date (e.g. frequency-domain solvers; time-domain solvers), a brief introduction of the concept of design situations and design load cases and, a qualitative ranking of numerical modelling methods as a function of specific design situations are described. Recent representative examples of WEC numerical models and models for critical sub-systems of WECs are also overviewed. The last modelling approach is the experimental modelling or physical testing. Experimental models for hydrodynamic interaction, energy transformation and, degradation and failure are reviewed in this document. In addition, different kind of testing and additional considerations such as scaling are reviewed.

This initial analysis has led to the classification and description of the models, test rigs and testing platforms that are currently available for its use in the VALID project within the partnership. Although upgrade needs will be analysed within the user cases, this report addresses a preliminary assessment of the value provided by these models and facilities for the hybrid testing methodology. This allows an initial guidance on improvement needs for the future steps of the project.

The report also discusses the limitations, impact and practicalities associated with the implementation of these modelling approaches in the future VALID testing framework.

Finally, the performed review allows for a selection of best candidate methods to be considered, leading to a preliminary selection and an outline of a new framework for accelerated hybrid testing. Such considerations will have a first application in the VALID user cases, assisting in the conceptualisation of a testing methodology. The learnings from such initial application of this framework will inform the re-contextualisation of a final methodology, promoting its wider adoption in the wave energy community.

This project has received funding from the European Union's Horizon 2020 research and innovation programme under grant agreement No 101006927.

Project partner names

RISE	RISE Research Institutes of Sweden AB
TECNALIA	Fundacion Tecnalia Research and Innovation
CORPOWER OCEAN	Corpower Ocean AB
RINA-C	RINA Consulting S.p.A.
BiMEP	Biscay Marine Energy Platform SA
IDOM	IDOM Consulting, Engineering, Architecture, S.A.U.
AAU	Aalborg University
AVL	AVL List GMBH
Wavepiston	Wavepiston AS
TU Delft	Delft University of Technology
Aquatera	Aquatera Sustainability Ireland LTD
JFC	Julia F. Chozas, Consulting Engineer
Y4C	Yavin Four Consultants, Unipessoal LDA

This project has received funding from the European Union's Horizon 2020 research and innovation programme under grant agreement No 101006927.

Table of Contents

This project has received funding from the European Union's Horizon 2020 research and innovation programme under grant agreement No 101006927.

This project has received funding from the European Union's Horizon 2020 research and innovation programme under grant agreement No 101006927.

Tables

This project has received funding from the European Union's Horizon 2020 research and innovation programme under grant agreement No 101006927.

Figures

This project has received funding from the European Union's Horizon 2020 research and innovation programme under grant agreement No 101006927.

1 Introduction

1.1 Project background

A recurrent problem in the wave energy sector is that reliability testing at low TRLs (early development stages) is too costly, and there are many uncertainties and design-decisions that need to be explored; but at high TRLs (late development stages) the design is too rigid to make changes, and associated costs can be prohibitive.

The VALID project aims to develop, implement and enforce a new test procedure based on accelerated hybrid testing techniques. Accelerated hybrid testing allows to integrate knowledge from a real environment (ocean, uncontrolled testing), a simplified lab environment (physical test rigs, controlled testing) and a virtually enhanced environment (numerical models, controlled testing). Once implemented, it will enable the industry to scale-up simulated lab conditions and test a virtual model of the existing structure, and hence reducing uncertainties, increasing confidence in results, empowering informed decision-making, and thus, largely assisting in the design and development process of WECs, especially at low TRLs.

Specifically, WP1 establishes the overall framework for the development of the VALID Hybrid Testing Platform (VHTP) that is at the core of the VALID project. Overall, the activities of WP1 aim to assess and define the range of numerical and physical approaches to be considered under the project, including their interaction, with the ultimate goal of devising a methodology for accelerated hybrid testing that is compatible with the VHTP architecture to be defined in WP2. The specific objectives of WP1 stem beyond the VALID project, i.e. WP 1 aims to provide guidance for the entire ocean energy sector. The identification of critical components / subsystems, the interactions between theoretical, numerical and physical modelling and the uncertainties associated with each approach is considered in detail. Specific attention is given to scaling effects.

1.2 Aim

This deliverable aims to review and define the modelling approaches (theoretical, numerical and experimental / physical) to be considered in the VALID project to address the design and accelerated testing of the critical components / subsystems identified in D1.1 [1]. It is expected that a mix of methods will be considered, leading to a selection of best candidates.

D1.2 informs the overall architecture of the VHTP to be developed in WP2, by identifying the critical modules that shall be addressed theoretically, numerically or physically. To ensure that physical inputs are considered and the benefits of hybrid testing maximised, key information regarding the test rigs available to the VALID project are compiled and reviewed, to ascertain (where applicable) the updates required to address critical components / subsystems.

Additionally, and where applicable, scale considerations are also considered when aligning and prioritising case studies applicable to the VALID project. In addition to the ability to replicate the dominant loads related to the dominant metocean conditions (at a range of suitable scales) in a VHTP, D1.2 also focuses on other potentially dominant environmental effects that affect the long-term reliability of critical components / subsystems, such as e.g. potential ageing effects for components in direct contact with sea water (e.g. biofouling, corrosion, etc.).

1.3 Structure of the report

The report is structured in 7 main sections:

- **Section 1: Introduction**. It presents the scope, aim and structure of the report.
- **Section 2: Critical components / sub-system identification**. It reviews the key findings regarding the critical components / sub-systems of WECs identified in D1.1.
- **Section 3: Review of modelling approaches**. It assesses the theoretical, numerical and experimental methods that may be relevant in the context of accelerated testing of critical WEC sub-systems and / or components.
- **Section 4: Current models, test rigs and testing platforms**. This section reviews the numerical models, test rigs and platforms currently available for use in the VALID project.
- **Section 5: Analysis of limitations**. This section discusses the limitations, impact and practicalities associated with the implementation of modelling approaches in the future VALID testing framework.
- **Section 6: Moving forward: hybrid testing platform**. It presents initial considerations related to a new framework for accelerated hybrid testing.
- **Section 7: Concluding remarks**. This section summarises key findings and next steps.

2 Critical components / sub-systems identification

Within WP1 of the VALID project, Task 1.1 aimed to identify critical components / sub-systems for WECs, while also overviewing the associated key design requirements and the fundamental principles of accelerated testing. At the conclusion of Task 1.1, D1.1 *"Accelerated Testing Requirements"* was compiled [1]. To facilitate the reading of D1.2, this section provides a brief summary of D1.1, focusing on the key findings related to critical component / sub-system identification. The interested reader is directed to [1] for a more completed overview.

2.1 Definition of critical

Following the definitions provided in best practices such as *Offshore Safety Directive 2013/30/EU*, a critical component / sub-system can be defined as an element (or elements) that, if failing, may contribute significantly to a major accident. In this regard, *major accident* can be defined as an event that has severe consequences, either in a context of loss of human life and / or damage to the environment, or in terms of lack of functionality that leads to the inoperability of the system and consequently, economic loss. An immediate connection between reliability and criticality can be made, noting that in [2] a component is defined as reliable if it is able to "*perform the function for which it was designed under certain conditions and for a specified period of time"*. Further detailed commentary regarding the concept of reliability and survivability is issued in Section 3.

2.2 Identification of critical components / sub-systems in VALID

As detailed in [1], the methodology followed to identify critical components / sub-systems of WECs followed a three-stage approach. The approach is illustrated in Figure 1, where the literature review, industry engagement survey and user-case FMEA assessment stages are outlined. Some of the key steps and features associated with each stage include:

- The literature review provided an initial basis to frame the envelope of sub-system that may affect a WEC. In particular, guidance from the Structural Design of Wave Energy Devices (SDWED) project [3] was followed, leading to the definition of five main WEC sub-systems – see Figure 2.
- The PTO sub-system was identified as being of particular importance to both the sector and to the VALID project', as the three proposed user cases – to be 'explored in WP3, WP4 and WP5 – are dedicated to this specific sub-system.
- A review of deterministic-based risk analysis methodologies was compiled in [1]. Particular emphasis was given to FMECA / FMEA based approaches, noting their wide adoption in industry, as evidenced in the survey results (see Figure 3), and their use as a framework in all VALID user-cases. Further insight into both deterministic and probabilistic methodologies for risk analysis is provided in Section 3.

The combined assessment of the three stages followed to identify critical components / sub-systems of WECs led to a VALID ranking – which is summarised in Section 2.3.

This project has received funding from the European Union's Horizon 2020 research and innovation programme under grant agreement No 101006927.

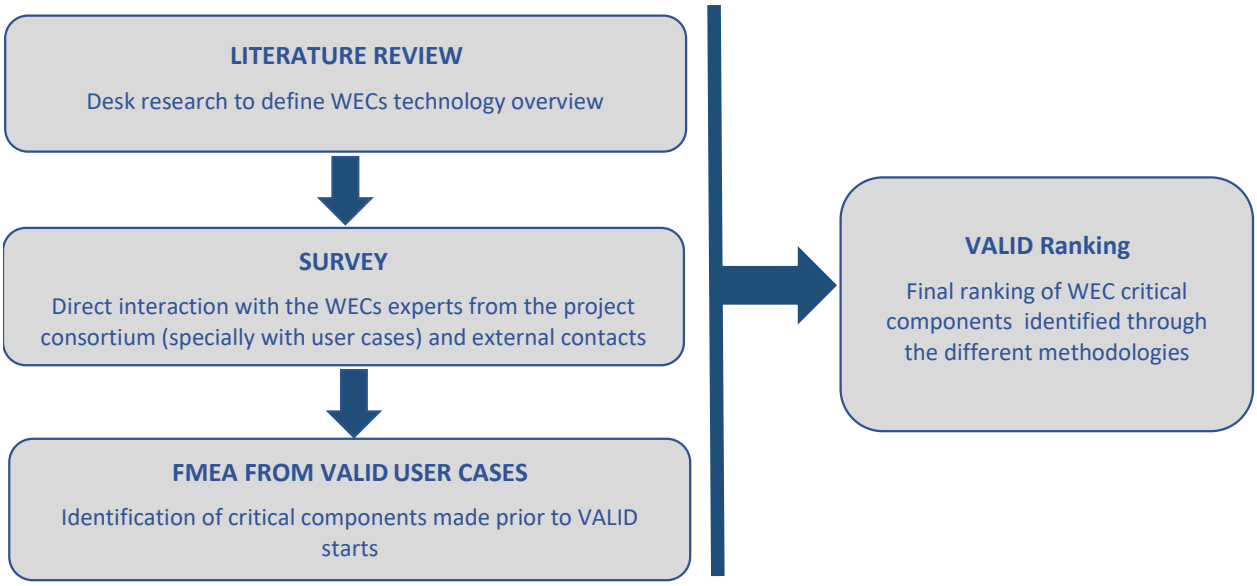

Figure 1: Schematic of the methodology behind VALID's Deliverable 1.1 [1]

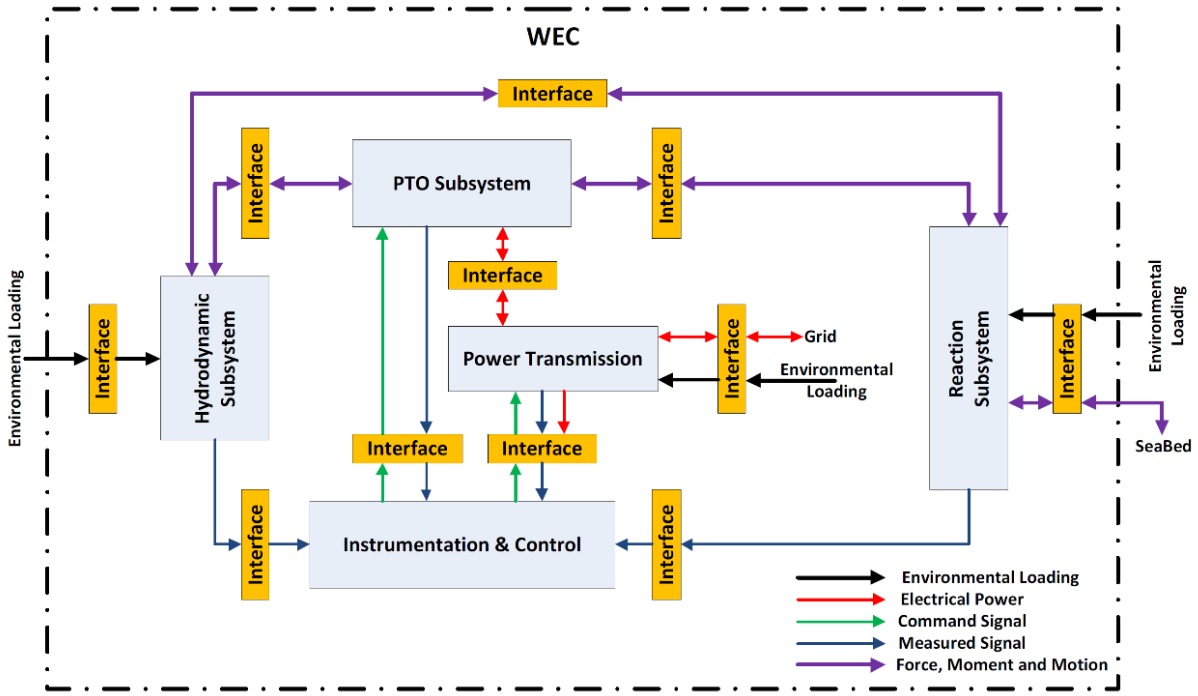

Figure 2: Typical WEC sub-system breakdown [3]

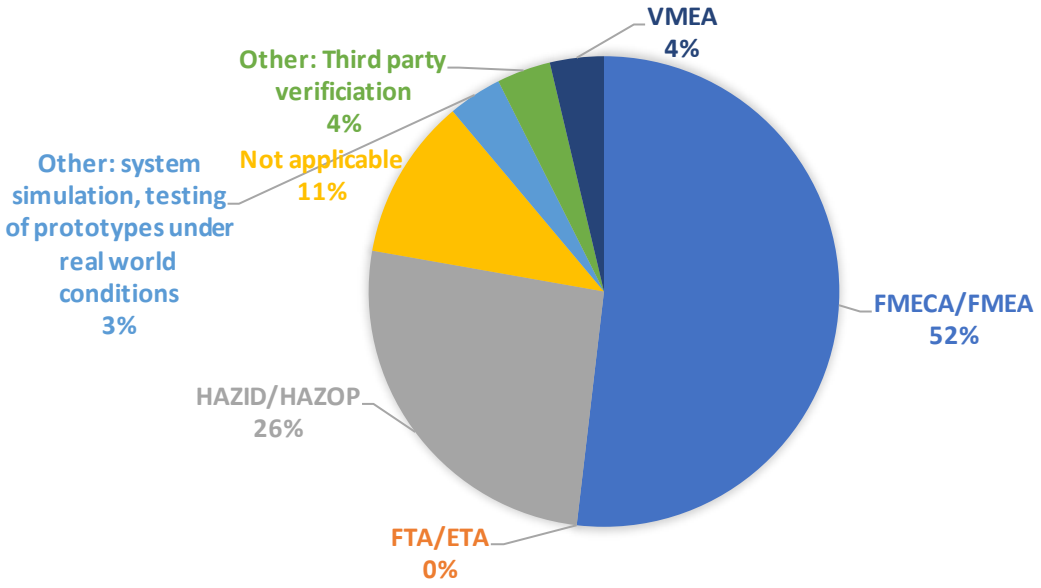

Figure 3: Methodologies used to identify and prioritize the critical sub-systems and components – survey results [1]

2.3 Summary of the Key Findings

Following the methodology outlined in Section 2.2, a VALID ranking of critical components and sub-systems was compiled in D1.1. This is summarised in Table 1, where it is clear that only the PTO sub-system was identified as critical in all the consultations conducted (i.e. literature review; industry survey; FMECA analysis conducted by the user-case lead partners).

Such a finding makes the PTO sub-system of particular interest to the VALID project, although other components should still be considered of interest, in particular in the context of the wider wave energy sector. It is expectable that as the VALID activities progress, a deeper understanding of the influence(s) of critical components will be gathered at sub-system level, which will in turn inform the wider VALID methodology (see also Section 6).

Table 1 VALID D1.1- Ranking of critical sub-systems and components [1]

Critical Component / sub-system	Criticality identified from the literature review	Criticality identified from the survey	Criticality identified from the User Case FMECA analysis
Energy Conversion			
PTO	X	X	X
Electric generator	X		X
Rotor	X		X
Power electronic equipment	X		
Marine Interface			
Mooring	X	X	
Hydrodynamic		X	
Auxiliary Components			
Rod (actuators)	X		X

Critical Component / sub-system	Criticality identified from the literature review	Criticality identified from the survey	Criticality identified from the User Case FMECA analysis
Bearings	X		
Valves	X		X
Seals			X

3 Review of modelling approaches

In this section the modelling approaches that are considered in the VALID project are reviewed. Theoretical, numerical and experimental methods are assessed in Sections 3.1, 3.2 and 3.3 respectively. The main objective of Section 3 is to present formulations that may be relevant in the context of WEC design, in particular in the context of accelerated testing of critical WEC sub-systems and / or components. Where applicable, illustrative examples of previous work in the field are provided, from both research and commercial environments.

It is however worthwhile mentioning that inherent to the VALID concept is hybrid modelling, an innovative approach combining the conventional methods to overcome the limitations of pure modelling. The review allows a selection of best candidate methods to be considered, leading to a preliminary selection and an outline of a testing framework (see Sections 6).

3.1 Theoretical models

In [4] theoretical models are defined as "simplified and schematic representations of a theory's essence/skeleton, linked to the disciplinary approach within which the theory is embedded". Another definition is given in [5], which describes a theoretical model as a "synthesis of a phenomenon, described from a series of accepted and reliable theoretical and observational statements (equations), and whose usefulness lies in the prediction (using a deductive calculation) of new formulas and measurements of reality".

In the context of the VALID project, theoretical models can be associated with the following three engineering domains:

1. Environmental characterisation.
2. Hybrid testing, both at pre- and post-processing level.
3. Reliability and survivability (R&S).

Each of the above-defined types of theoretical models is detailed in the following sub-sections. Although for simple cases (e.g. limited degrees-of-freedom, simple geometries, etc.) theoretical WEC models could be conceived, it is noted that in the current state-of-the-art WEC models, including models of the key sub-systems, are likely to be numerical or physical, underpinned by a range of theoretical principles – see also Sections 3.2 and 3.3.

3.1.1 Environmental characterisation

Theoretical models related to environmental characterisation aim to inform on the representative metocean conditions at the intended deployment site. The theoretical models can be based on linear or nonlinear wave theories (deterministic approach), or spectral methods (probabilistic approach) – see e.g. [6], [7].

The characterisation of the environmental conditions is vital for offshore activities, leading to a better understanding of reliability, survivability, and system design. Their estimation also created a range of realistic environmental inputs to be used in either numerical or experimental models when attempting to characterise WEC response – see e.g. [8] and [9].

The most direct impacts of environmental conditions on WEC design are related to wave conditions. However, and depending on device and materials used, other ocean parameters and mechanisms can be important. For example, ocean temperature, salinity and scour are also elements that can affect the reliability and survivability of a WEC. Such conditions can be diverse from region to region, and they may have significant effects. Environmental parameters such as salinity and temperature are most relevant in specific areas: for example, higher ocean temperatures are encountered in equatorial regions, while Europe is amongst the most saline waters [10], [11]. On the other hand, wave conditions have larger variation in magnitude and distribution, tending to differ from region to region [12], [13]. Knowledge of local environmental

and wave conditions can therefore reduce uncertainties, enhance design decisions, and improve survivability in extreme conditions.

3.1.1.1 ***Metocean data acquisition***

3.1.1.1.1 In-situ instruments

Buoys, wave gauges, and Acoustic Doppler Current Profilers (ADCPs) are some of the instrumentations used for localised measurements of wave and environmental parameters. In situ observations are scarce in locations retained for wave energy exploitation, these data that correspond to the real environmental conditions. Buoys are most used for in-situ measurements and can provide a wide array of parameters such as surface elevation, lateral motion, significant wave height (H_{m0}), wave direction (P_{kDir}, Dir), and spectral information. Buoys have relatively good temporal resolution with sampling intervals in the range of 10–30 min and can be deployed over a long-period of time. Two types of datasets are traditionally available: standard integrated wave parameters (H_{m0}, T_p, T_{m-10}, etc.) and spectral wave data. These are typically the wave energy density over frequencies, and/or over frequencies and directions depending on the directional/omnidirectional capabilities of wave measuring buoys [14].

In situ observations have been exploited in resource assessments to (i) refine the quantification of available wave power (based on real sea conditions), (ii) exhibit waves temporal variability (trends in wave heights, periods, power, etc.), and (iii) evaluate the reliability of simplified wave power formulations based on integrated parameters (such as peak or mean wave periods). The exploitation of in situ observations was also particularly useful to assess uncertainties associated with simplified formulations of the available wave power density based on significant wave height and default statistical periods (such as T_p, mean period T_{m01} or the zero-crossing mean period T_{m02}). Guillou showed that a formulation based on H_{m0} and T_p (with a default calibration coefficient $\alpha = 0.9$ matching JONSWAP spectrum) overestimated the yearly averaged available wave energy flux with differences exceedingly locally 8% [15].

However, they do not come without limitations: firstly, measurements are influenced by deployment depth. Waves transform as they propagate from deeper to nearshore water due to various physical processes such as depth-induced breaking. This means that their measurements are applicable only at that location and cannot be arbitrary extended over several other "nearby" locations, which may be characterised by different depths and nearby coastal masses. Buoys are also limited by the length of their moorings, affecting their maxima of vertical displacements (in case of extreme events), often slipping around incoming crests, and giving erroneous measurements.

Finally, their recordings are often not "full", i.e. hours, days, weeks, months are absent, and their deployments are not continuous but subject to recurring maintenance and re-calibration [16].

3.1.1.1.2 Satellites

Satellites represent another potential long-term and extensive monitoring mean of sea states and other environmental parameters. The exploitation of these large-scale observations, most of the time integrated in publicly available databases, can be used to produce spatial maps of wave energy density at any location in the world.

These maps may derive from a combination of multi-satellite altimeters to produce a large-scale synoptic representation of the mean power density and/or associated energy metrics.

Satellite observations represent therefore an interesting alternative to local in situ measurements or time-consuming numerical simulations. Two types of space-born radars may be considered for resource characterization: (i) altimeter which measures the time taken by a

radar pulse to travel from the satellite to the sea surface and return, and (ii) Synthetic Aperture Radar (SAR) which exploits a large bandwidth of the electromagnetic spectrum [17], [18].

SARs increase the spatial resolution of observations and give access to the wave energy spectrum. The great number of wave energy assessments based on satellite observations relies on altimetry [19]. Exploitation of satellite altimeters provides (i) an evaluation of the significant wave height and associated wave power in coastal locations considered for WEC setup (where wave-buoy measurements are not always available), and (ii) preliminary assessments of the temporal variability of the wave climate.

Satellite altimeter data acquisition started in the mid-eighties (with the launch of Geostat) giving, today, access to decades of measurements. The exploitation of satellite data from several past and present altimeter missions (e.g. ENVISAT, TOPEX/Poseidon, Jason-1, Jason-32, etc.) provided thus first large-scale assessments of the annual and seasonal variabilities of the wave energy resource based on observations.

Satellite measurements depend on orbital trajectories, i.e. the time-interval they pass over the same location, with orbital periods of around 10–35 days, widely spared ground tracks (over hundreds of kilometres) and uncertainties particularly pronounced in the vicinity of the coastline. Satellite observations show important spatial and temporal limitations for assessing the available wave energy resource.

Lately, satellites measurements have improved and can offer information at higher resolution (i.e. every 12h). This does not mean that they are available immediately, as in the case of buoys. In fact, most satellite altimeter data must be corrected and filtered, before any meaningful data are retrieved; this can take up to several months. There is the possibility of shorter releases, so-called real-time products, that are from ongoing missions and are made available within a few hours, but only for specific processes, such as short-term wave forecasting.

Another limitation is the fact that the data have "blind" spots for nearshore locations. When trying to measure waves close to the coastlines (≈20km), satellites cannot properly distinguish land from water masses [20].This creates some issues with regards to their performance. Cavaleri et al compared data from four different altimeter missions, and came to the interesting conclusion that in nearshore areas, though measurements were obtained, they did not match H_{m0} in magnitude, and depending on data frequency resolution, displayed "noise" measurements at ≤20 km from the coast. Smaller differences were given by surface wind recordings, but the complexity of waves increased the differences in H_{m0} by almost 12% [21].

3.1.1.2 *Metocean data accuracy*

The conceptualisation of a robust design, covering key reliability and survivability aspects, requires access of data that characterises the long-term environmental conditions. However, to date most countries/regions do not have data with the necessary spatiotemporal resolution requirements.

To optimise design loads, structure size and power production, a minimum of 10 years of hourly spectral conditions are needed – see e.g. [22], [14]. Furthermore, to have a good understanding of climate conditions and their persistence, additional considerations on Climatological Standard Normals (CSN) are required.

CSN suggest a minimum period that allows long-term extrapolation and proper estimation of averages for climatological parameters, computed for consecutive periods of ≥30 years [23]. Failure to consider long term wave condition into estimates or use very limited information as a source, may lead to under and/or overdesign of components. Figure 4 and Figure 5 showcase the large variations the mean and maxima values of wave conditions that occur, which can affect considerations on survivability and reliability.

This project has received funding from the European Union's Horizon 2020 research and innovation programme under grant agreement No 101006927.

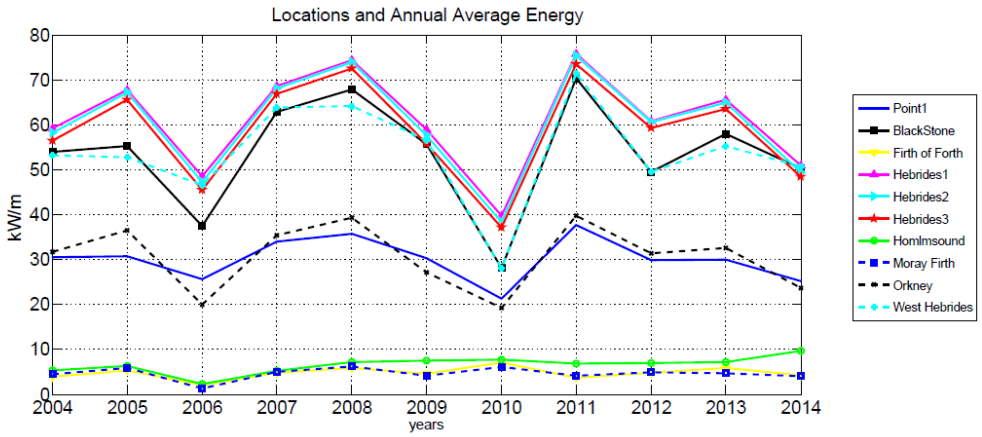

Figure 4: Variations of annual mean wave energy flux at sample North Atlantic sites [24]

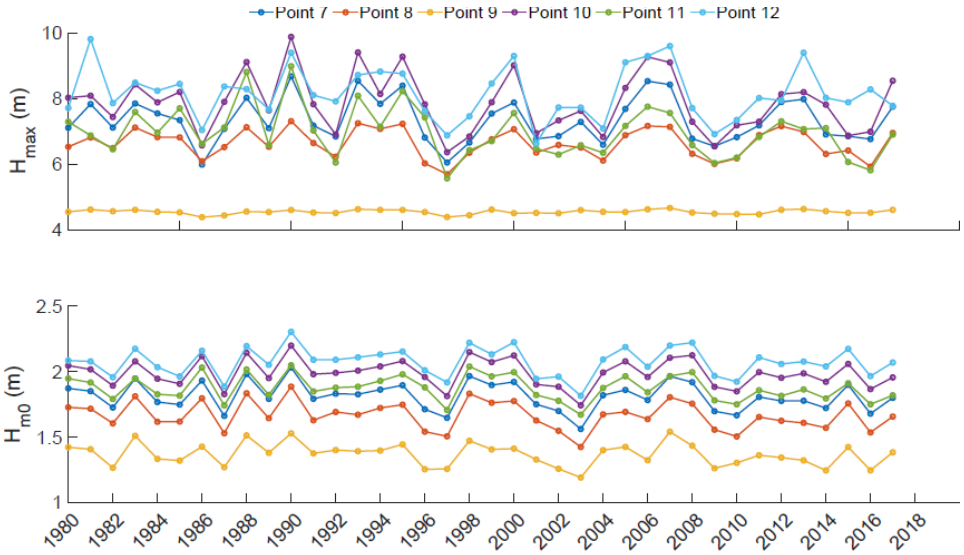

Figure 5: Long term variation of H_{max} and mean H_{m0} at sample North Sea sites [25]. On the top panel the H_{max} shows the highest H_{m0} value for that year, the bottom panel is the mean H_{m0} value

To capture climate variations the minimum 30-years duration allows to also estimate extreme value (return wave) values for 100-years without using probabilistic modelling that depend on very general assumptions that are often not realistic [22]**.** Using long-term spectral conditions, power analysis can be better represented and adhere to best scientific practices as in [26], [27] and suggested standards [28].

To date, majority of information originates from oceanic models, which are not able to provide realistic spectral data at shallow water sites with depths below 100 m, with their spatial resolution affecting spectral estimates and non-linear terms in the energy density function [21], [29]. This means that ocean model results often over-estimate low waves providing unrealistic spectral components and leading to over-ambitious estimates [21]**.** Wind inputs highly affect the wave hindcast results, with most products leading to different wave estimates often with differences over 1 m [30], [31]**.** Figure 6 shows some of the impacts of wave model results in comparison to buoy data, and how they can affect the estimates that are used.

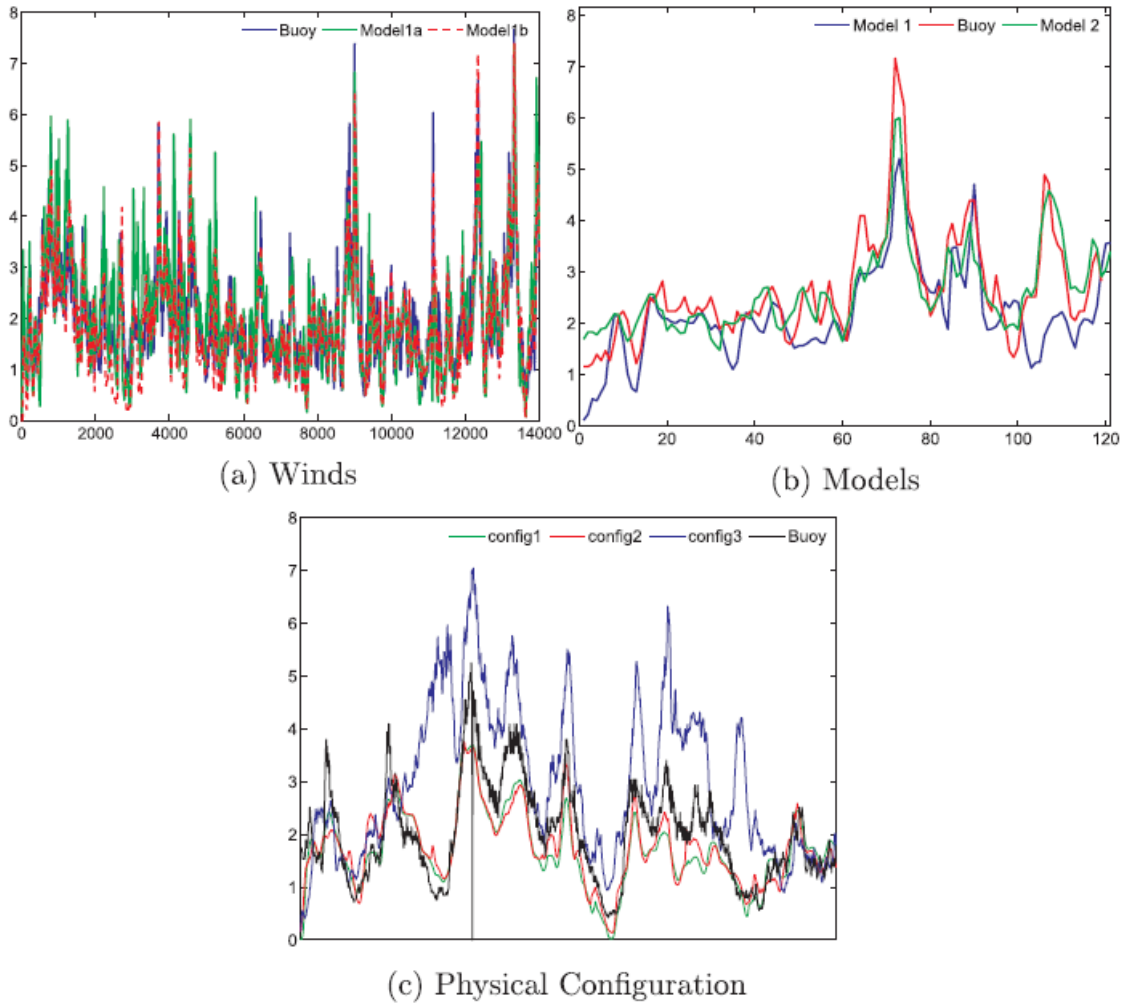

Figure 6: H_{m0} (m) results with inter/cross model and physical tuning. Top left panel shows the differences of the same model driven by different winds, top right panel indicates the difference between an oceanic (Model 2) and nearshore model (Model 1), and the lower panel shows the differences physical tuning can have on the same model

3.1.1.3 ***Extreme value analysis: estimating long-term return period environmental conditions***

Several engineering applications require the knowledge of statistically derived events, since the forecasting ability of numerical models is limited to a short-term timeframe The investigation of expected extreme events improves our understanding of the offshore environment, the construction, survivability of WECs and offshore structures by reducing the uncertainty [32], and avoiding increases in capital expenses.

The investigation of metocean events, helps to characterises the maxima values that may occur for in the future, given a reference year. Extreme Value Analysis (EVA) is an important process which is being used throughout the marine field for the estimation and determination of probabilities of exceedance of parameters such as Hm0. Awareness of extreme events and expected return values is vital to the design in offshore industries.

In order to estimate extreme events of 20, 50, 100 or more years, sufficient data are necessary at least 20% in length of the desired return value [22], [33], [34], for example if a 50 year period is investigated at least 10 years of data should be available. Many studies have stressed the necessity of long time-series of wave parameters [22], [35]–[38]. This poses a problem since

most operational buoys usually do not extend so far back. The existence of such datasets is often quite limited and their reliability at high storm events may be questionable [39].

These limitations lead to higher uncertainty levels, poor estimations in statistical parameters and reduce the validity of the produced results. Moreover, spatial properties of the available datasets pose an additional major issue, since the quantities differ from deep to shallow and are not the same at every location, while potential effects of climate parameters pose another obstacle for limited recordings [29], [40]. Use of satellite data or numerical models, both with having inherit limitations, but can be more useful for EVA analysis. Studies have examined both options, and used the data for further seasonal and extreme value analysis [41], [42].

The inputs for the EVA analysis shall rely on suitable long-term measurements in order to minimize uncertainty. For nearshore location a suitable model should be developed (in absence of ≥10 years), as indicated by previous research which outlined the limitations and the potential differentiation of EVA for shallow locales [43]–[46].

Estimating return wave values (extreme) needs attention and can utilise a variety of models; in the seminal work of Coles, the variants and detailed differences are presented [47]. When working with metocean long-term data, two are the main methods suggested [36], [37], the Generalised Extreme Value (GEV) and the Generalised Pareto Distribution (GPD).

A consideration which must be taken while preparing the data for EVA, is that the values used in the analysis have to be identically independent distributed (iid). This entails "filtering" of the primary input to ensure non-interference to the final extreme value, this can be achieved by several methods of threshold modelling [47], with examples being the Peak-Over-Threshold (POT) or Annual Maxima Method (AMM).

3.1.1.3.1 Generalised Extreme Value (GEV)

These families of distributions (GEV, GPD) though used widely in EVA, are significantly different to each other. This can be attributed to the way and the number of parameters calculated for the distributions and selection of best fit. A summation of the wave environment can be characterized by the fitting of a Rayleigh distribution, though several other attempts have used Weibull or Rayleigh as fit functions.

The existence of the Central Limit Theorem suggests the mean of a large number of random variables has a Gaussian distribution, regardless of the distributions of each variable. This leads to treat the potential distribution of a large sample as an "unknown" component, which have a sequence of random iid variables, which can be expressed by a common distribution (F). This constitutes the recorded events (X_n) (independent random variables) over a period or observations (n) will comprise the maximum of the distribution (M_n) over the investigated period having a common distribution F:

$$P_r\{M_n\} = P_r\{X_1 \leq z, X_2 \leq z, \dots., X_n \leq z\}$$

$$\mathrm{P_r\{M_n\} = P_r\{\{X_1 \leq z\} \cdot \{X_2 \leq z\} \cdot \dots \cdot \{X_n \leq z\}\}} \qquad (1)$$

$$P_r\{M_n\} = \{F(z)\}^n$$

The problem is that by having a large sample, even the smallest deviation leads to the disruption of a proper fit, with the upper points (z) being easily affected. Overcoming this issue means that the distribution F is considered as unknown while at the same time the variables are normalized with a linear approach, see Equation 2.

$$\mathrm{M_n^* = \frac{M_n - b_n}{a_n}} \qquad (2)$$

This means that by applying an EVA, our aim is to reduce the de-generation of a distribution over a point (z), stabilizing it with appropriate selection of parameters. The distributions belong to one of three potential families, Gumbel (Type I), Frechet (Type II), Weibull (Type III), as determined by the value of the location parameter. to examine the behaviour of the data, the GEV includes all these families of distribution while treating the initial guess as unknown, allowing to fit the data and determine the distribution which best describes our data. Thus, G{z} can be described by the application of the data to a GEV as follows in Equation 3.

$$G\{z\} = \begin{cases} \exp\left\{-\left[1+\xi\left(\frac{z-\mu}{\sigma}\right)\right]^{\frac{1}{\xi}}\right. & \xi \neq 0 \\ \exp\left\{-\exp\left[-\left(\frac{z-\mu}{\sigma}\right)\right]\right. & \xi = 0 \end{cases} \quad (3)$$

Where ξ is thy shape parameter, μ the location parameter and σ the scale parameter, with the appropriate distribution based on the derived shape parameter of the block data investigated and the following conditions satisfied.

The unification of the families within the GEV, allows for the examination of various datasets with unknown retrieval statistics and the determination the most appropriate behaviour of the tail (i.e. Type I ($\xi = 0$), Type II ($\xi > 0$), or Type III ($\xi < 0$),). The determination of ξ is dependent on the set and length of data used, as mentioned annual of monthly maxima lead to a smaller array of values examined leading to bias, while very large datasets increase the variance.

Establishing a GEV distribution which describes the data, the estimation of specific quantiles assists in calculating the return levels (return periods). By estimating return values, information gained on the annual maximum value that is exceed once a year in every years of investigation (N) and the probability of exceedance at least once during time span of N years. The return period expressed by the GEV selection can be estimated as the interpretation of the selected family describing the data and the log of the probability (p). Where z_p is the return level (see Equation 4) associated with the (1/p) and the probability of exceedance (see Equation 5) at least one time during the time of investigation (see Equation 6).

$$z_p = \begin{cases} \mu - \frac{\sigma}{\xi}\left[1 - \{-\log(p)\}^{-\xi}\right] & \xi \neq 0 \\ \mu - \sigma \cdot \log\{-\log(p)\} & \xi = 0 \end{cases} \quad (4)$$

$$p = 1 - \frac{1}{N} \quad (5)$$

$$(1 - z_p)^N = 1 - 1/e \quad (6)$$

3.1.1.3.2 Generalized Pareto Distribution (GPD)

The GPD was developed to alleviate the issues of using large amounts of data to provide better extreme value estimates. One of the advantages of the GPD is that it can handle larger datasets and associate them with a threshold value, to refine the estimated distribution for the location. As in the case of GEV the tails are associated with the location parameter and correspond to Type I, II, III, although depending on the different distribution are fitted to the data. The GPD is characterized and fitted to the threshold providing with the estimated distributions F{z} as in:

$$F\{z\} = \begin{cases} 1 - \left(1 + \xi\frac{z}{\breve{\sigma}}\right)^{-\frac{1}{\xi}} & \xi \neq 0 \\ 1 - \exp\left(-\frac{z}{\breve{\sigma}}\right) & \xi = 0 \end{cases} \quad (7)$$

With ξ describing the shape parameter and $\breve{\sigma}$ expressing the scale parameter. The GPD has less parameters involved in the calculation. While the following criteria must be valid in order to estimate the tail Type and appropriate distribution. In the GPD depending on shape parameter, the data are fitted on a generalized Pareto, a special case of Beta, or an exponential.

As in the case of the GEV, having established which distribution describes the sample, an estimation on the return values can be considered. Although, prior to estimation of the actual value one has not only to set the years (N) of investigation but also the threshold (λ_u) (see Equation 8), according to the notion that a Poisson process is considered. The final reduced dataset expresses the samples filtered by the POT method of peaks (k), with the (n_{years}) represent the years of the sample duration. This reveals the cyclic nature of repetition within the dataset, see Equation 9. The threshold is imposed over the available long-term data to ensure that the data are iid and true severe conditions are represented; such can be a high percentile value of conditions that analyse or the duration of severity [48].

$$\lambda_u = \frac{k}{n_{years}} \quad (8)$$

$$z_p = u + \frac{\breve{\sigma}}{\xi}[(N \cdot \lambda_u)^{\xi} - 1] \quad (9)$$

3.1.1.3.3 Practical steps for implementation

The pillars of EVA are GEV and GPD from that point onwards, however, different distribution methods can be used, though using the same filtering processes that is either AMM, POT, etc. Michelen underlined that while application of different EVA methods can be used, it is important to consider the underlying limitations and error in the different methods [49]. Such alternatives can be the All-Peaks Weibull, Weibull Tail-Fit.

Therefore, when using long-term datasets, several steps are required:

1. Filter timeseries, ensuring iid behaviour.
2. Set threshold value.
3. Filter iid sample with threshold values.
4. EVA of new timeseries (GEV, GPD, Weibull, etc).
5. Evaluation of goodness of fit for EVA.
6. Evaluation of return period, based on most appropriate fit, by quantile-quantile plots, probability plots and goodness of fit.

3.1.1.4 ***Environmental contours***

Environmental contours represent a method that can be useful to identify extreme environmental conditions. For the marine environment [50], [51] suggested use of joint distribution of H_{m0} and wave period to assist in the estimation of offshore structure design criteria with application at the Norway seas. Environmental contours allow us to jointly represent the complex wave environment and are constructed based on wave parameters that describe specific locations [52]. These are often used to derive the response of a structure for return wave conditions of N years. Environmental contours is an approximate reliability method that can be fast, but also requires attention.

Its application in metocean conditions is dependent on three (3) main steps (see Figure 7): step (1) obtain long-term reliable metocean data, step (2) estimate the joint distributions of variables and step (3) construct the environmental contour based on the joint distribution data [53].

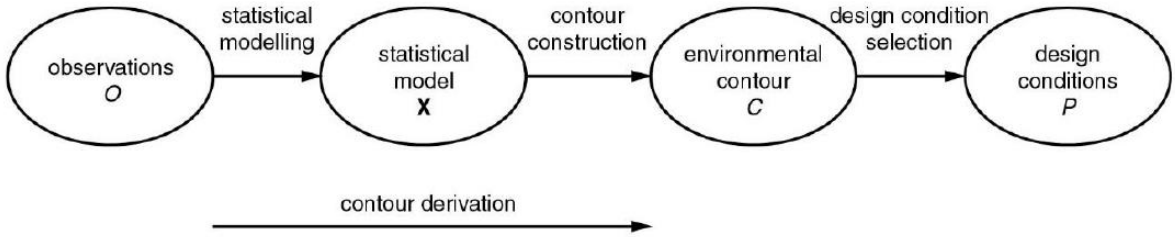

Figure 7: Steps suggested to obtain environmental contours and design criteria based [53]

It is important to note that deriving environmental contours can be done with a variety of ways, hence the fitted distribution will influence the reliability of the data. The range of uncertainty of the environmental contours method is not only based on the fit method, but also on the duration, length and quality of the dataset i.e. a larger sample of variables increases the "accuracy" of the method, see Figure 8.

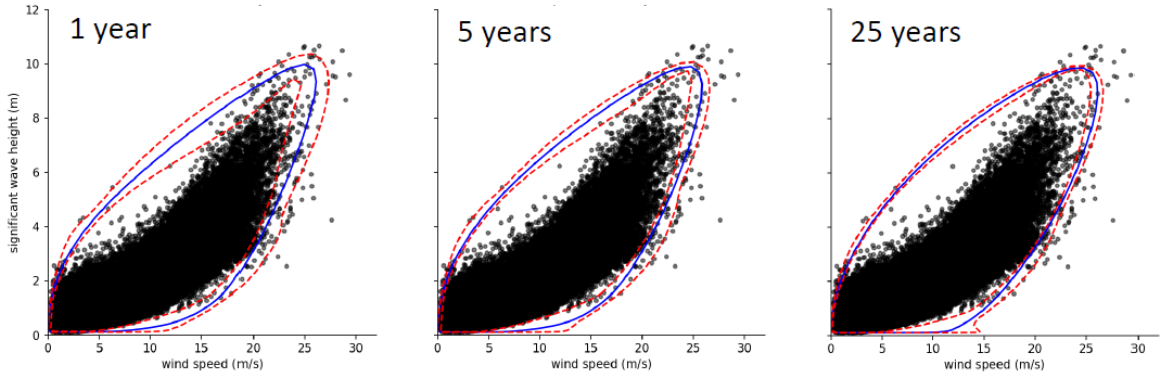

Figure 8: Uncertainty associated with the sample usage in the construction of environmental contours. The larger the size the higher the confidence [53]

3.1.1.5 ***Principal Component Analysis (PCA)***

Principal Component Analysis (PCA) was first mentioned by [54], and usually consists of a linear transformation technique to reduce the multi-dimensionality of dataset, by transforming large datasets into smaller ones, whilst maintaining most of the information, though sometimes at expense of accuracy.

An advantage of PCA is that it is a descriptive tool, that is not bound by 'a-priori' assumptions on distribution characteristics datasets, and different variables. PCA is beneficial to multi-layered datasets for different variables (p), their temporal duration, and with different units e.g. meters for H_{m0} and seconds for T_p [55]. This means that variables in the PCA will have to be standardised (see Equation 10) and to avoid biases when multi-variate analysis is concerned.

$$z_{ij} = \frac{x_{ij} - \bar{x_j}}{s_j} \qquad (10)$$

Each data value xij is both centred and divided by the standard deviation sj of the n observations of variable j. The next step is to estimate the covariance matrix of the input

dataset i.e. their variation around the mean. Subsequently, from the covariance matrix the principal components of the data can be estimated, by computing eigenvectors and eigenvalues. Principal components are new variables that are constructed as linear combinations or mixtures of the initial variables. These combinations are done in such a way that the principal components are uncorrelated and most of the information within the initial variables is squeezed or compressed into the first components [55]. PCA can be also combined with environmental contours to accelerate potential harsh condition estimations.

3.1.1.6 ***Long-term data acquisition***

Without long-term data, any estimation of environmental parameters for coastal infrastructure / ocean energy devices design, will make any reliability estimation flawed, since it will not account for resource changes and variability. Hence, it is important to consider the high value of resource assessments in any offshore activity.

3.1.1.6.1 Numerical modelling

In a spectral numerical model, the wave spectrum is described in time (t) by the action density equation (E), dependent upon direction (θ), frequency (f), latitude (φ) and longitude (λ). Sink source terms are used to estimate the wave parameters (see Equation 11), given a specific set of inputs and physical coefficients, with wind input (S_{in}), triads (S_{nl3}), quadruplet interactions (S_{nl4}), whitecapping ($S_{ds,w}$), bottom friction ($S_{ds,b}$) and depth breaking ($S_{ds,br}$).

$$S_{tot} = S_{in} + S_{nl3} + S_{nl4} + S_{ds,w} + S_{ds,b} + S_{ds,br} \quad (11)$$

This allows to estimate the available wave energy flux (wave energy potential per unit crest, in Wm^{-1}) and wave characteristics, for any site at any depth, without limitations with high accuracy; it is defined as the integral of the wave energy spectrum:

$$P = \rho g \int_0^{2\pi} \int_0^{\infty} c_g(\sigma) E(f,\theta) df d\theta \quad (12)$$

where ρ is the density of seawater, g is the acceleration due to gravity, E is the wave energy density distributed over intrinsic frequencies and propagation directions, and c_g is the group velocity. With use of a properly developed, calibrated, validated wave model important wave conditions like the significant wave height (see Equation 13) and the spectral peak period (see Equation 14) can be acquired.

$$H_{m0} = 4\sqrt{m_0} \quad (13)$$

$$T_{m-10} = \frac{m_{-1}}{m_0} \quad (14)$$

with m_0 the variance and m_{-1} the minus one n^{th} order spectral moment. These represent the conditions over the wave spectrum, and from them a matrix of wave probabilities of occurrences with all sea states (over e.g. H_{m0} and T_{m-10}) can be constructed.

3.1.1.6.2 Calibrating and validating a wave model

Calibration of a wave model involves "random errors", such as deviations from the site measurements due to the dependency of components (i.e. wave heights, wave period) on

wave spectrum and solutions applied [56]–[58]. While alterations are usually not major, they are affected depending on the model [59], [60], set-up [61], [62], coefficients and solvers for physical process, spatio-temporal quality of inputs and boundaries [63], [64].

One major disadvantage of numerical wave models is the missing of the "peaks" phenomenon. Most models tend to under-estimate wave heights at low frequencies and over-estimate at higher ones.

Replacing a low temporal wind component with higher resolution may alleviate some of the under-estimations, but physical tuning is required to ensure that an optimal performance of a wave model with regards to the wind input, bathymetry, location, physics and solving approaches. Several physical problems are resolved within the wave models by "suggested" coefficient, which the user must bear in mind that they may not have universal applications for optimal results [65], [66]. Several of the models presented in Section 3.2.1, offer significant parametrisation options which can improve the results after calibration.

In the calibration phase it can be decided whether to assess spectral derived variables such as H_{m0}, T_p and/or to also compare the one- and two-dimensional variance (or energy) spectrum. The focus of the calibration will be on wind drag precomputations that have limitations especially for higher wind speeds, where they are known to under-estimate and even limit wave growth, therefore, for every different configuration, the CD should be adjusted. This will result in smaller maxima biases, that will allow us to capture extreme conditions better, allowing the reliability and survivability analysis to be based on optimally realistic conditions. Performance and uncertainty of the results will be conducted according to proposed metrics in [67].

After an optimal model is determined the defined 30-year dataset will be produced to use in reliability and survivability methodologies. The validation of this dataset will include multi-year comparisons with in-situ and satellite data. Validation phase will allow us to underline the regions for which uncertainty is higher or lower, taking also into account intra-annual changes.

3.1.2 Wave-structure interaction formulations for WECs

Numerical modelling methods have the potential of greatly accelerating the development process of any system. Such acceleration can be related to the ability of rapidly and relatively inexpensively assessing a wide range of design iterations, addressing key design drivers and multiple input variables (e.g. multiple environmental conditions). Although this is particularly clear at the conceptual design stage, the same potential and opportunity applies throughout all the stages of the design process, including the detailed design stage.

In the context of WEC design, the above-mentioned potential is alluded to in e.g. [68] and [69], where the most commonly applied basic formulations for WEC models are introduced and described. Essentially, these can be broadly divided in:

- Frequency-domain models.
- Time-domain models.

Both formulations build on the theoretical principles developed in the 1970s by e.g. [70], [71] and [72]. Such principles stem from a hydrodynamic modelling approach, aiming to solve the wave-structure interaction problem, and in their simplest / linear forms both types of models share the same fundamental assumptions. These are primarily related to the underlying principles of linear wave theory, which include:

- The free-surface and the body boundary conditions are linearised.
- The fluid is incompressible and the flow is irrotational (potential flow).
- Viscous effects like shear stresses and flow separation are neglected.
- The bottom is assumed to be flat (and uniform).

Under such simplifying assumptions, the superposition principle applies, i.e. an incident wave field can be derived via the superposition of individual harmonic waves. Furthermore, and where applicable, body motions are assumed to be small when compared to the dominant wavelength(s).

From the perspective of frequency-domain models, the outline principles are used to solve two fundamental problems: the *diffraction* problem, when a body is held fixed while under the action of an incident wave field; and the *radiation* problem, when a body is excited to move in an otherwise undisturbed wave field. Analytical solutions can be found for simple geometric shapes. For other cases, these two fundamental problems are typically solved via a numerical model based on the Boundary Element Method (BEM)[1], where the body geometry is discretised and the velocity potential estimated using different formulations (e.g. source formulation, which uses exclusively source terms to solve the dominant equations). A review of each formulation is beyond the scope of this report; the interested reader is directed to [73], where the principles behind the application of BEM to marine hydrodynamics are detailed.

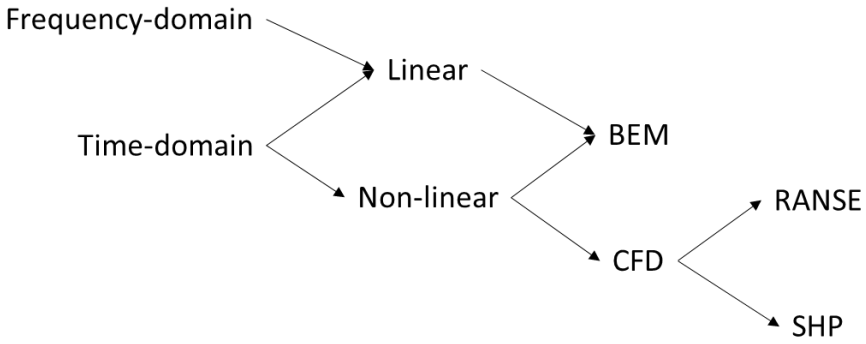

Figure 9: Overview of hydrodynamic modelling approaches

Linear and nonlinear BEM formulations can be followed. In the linear version, the geometry discretisation applied is based on a mean, undisturbed wetted profile. If nonlinear BEM approaches are followed, an expansion of potential flow theory typically uses the instantaneous wetted profile at each time-step to add additional terms to the solution of the wave-structure interaction problem. Therefore, and at the expense of computational effort, nonlinear BEM methods carry the potential to address more aggressive wave-structure interaction problems with increased accuracy. However, other assumptions of potential flow remain applicable (e.g. inviscid fluid). When compared to its linear equivalent, limited applications of nonlinear BEM codes have been made to date in the context of WEC design. An example of an application to wave energy, including comparisons with experimental results, is presented in e.g. [74].

Although both frequency and time-domain models may share the same principles when addressing a WEC's hydrodynamic response, a fundamental difference can be associated with the treatment of the overall WEC dynamics, namely the possibility to include nonlinear applied forces and constraints. Such capacity is only present in time-domain models, conferring a potential increase in the accuracy and fidelity of time-domain numerical model. This is particularly critical when key sub-systems such as the power take-off (PTO), moorings and / or control system have highly nonlinear characteristics, which would be addressed in a linear (or linearised) way in a pure frequency-domain model.

Finally, and when considering more complex wave-structure interaction formulations where e.g. viscous effects are implicitly included, more advanced time-domain models are usually

[1] Also referred to as 'panel method'.

proposed. These are often described under a Computational Fluid Dynamics (CFD) umbrella, which offers the potential to address highly nonlinear problems such as slap and slam loading on ocean-based structures. As described in e.g. [75], CFD models aim to solve the Navier-Stokes equations, a system of partial differential equations (PDEs) that describe the fundamental laws of fluid flow (e.g. conversation of mass and momentum), under a set of boundary conditions that define the fluid domain and, in the case of wave energy, the WEC geometry. As analytical solutions of the PDEs cannot be obtained in a general sense, approximate solutions are derived via numerical models (solvers) based on a range of formulations.

At a high-level, the formulation of CFD models can assume one of two forms: Eulerian, where the domain is discretised in a finite set of points (forming a mesh) and an approximate solution is estimated at such points; or Lagrangian, where the domain is discretised in a set of particles which respect the local flow velocity and approximate solutions are estimated at the position of each particle at each discrete time. Common options of numerical methods to solve the underlying equations following the Eulerian and Lagrangian formulations are Reynolds-Averaged Navier-Stokes Equations (RANSE) and Smooth Particle Hydrodynamics (SPH) solvers, respectively. The application of the latter (SPH) to WEC research is relatively recent, thus there are more examples of RANSE models being developed for specific WEC design problems. However, and as described in [76], due to its inherent characteristics SPH may be "particularly suitable for extreme wave events with wave breaking", thus active developments are ongoing.

A comparison of the dominant characteristics of the basic formulations introduced in this sub-section is presented in Table 2. A qualitative ranking is illustrated in Table 2, with the green tick marks indicating the capability to delivered certain features, or where applicable, a low effort and high availability, the red crossed indicated the opposite, i.e. inability to implement certain features, high effort and low availability, and the yellow question marks indicated potential add-ons to certain features, medium effort and potential solver stability issues.

Table 2: Dominant characteristics of the basic numerical model formulations

		Frequency-Domain	*Linear BEM time-domain*	*Nonlinear BEM time-domain*	*CFD*
Key Features	*Hydrodynamic formulation*	✓	✓	✓	✓
	Nonlinear hydrodynamics	✗	?	✓	✓
	Nonlinear dynamics	✗	✓	✓	✓
	Viscous losses	✗	?	?	✓
	Load coupling	?	✓	?	?
IT Requirements	*Computational effort*	✓	?	✗	✗
	Solver stability	✓	?	✓	?

		Frequency-Domain	*Linear BEM time-domain*	*Nonlinear BEM time-domain*	*CFD*
Usability	*User skills*	✓	?	✗	✗
	Software availability	✓	✓	✗	✓

The following key remarks can be made from the analysis of Table 2:

- With regard to key features, and while noting that CFD formulation discretise the fluid domain while all others discretise the body geometry, it is immediately clear only CFD approaches allow an inherent definition of all listed key features. However, all other time-domain formulations offer potential corrections to specific issues (e.g. weakly nonlinear hydrodynamic solutions and empirical corrections for the inclusion of viscous forces may be considered in linear BEM time-domain solvers).
- Linear BEM time-domain solvers allow, in a more direct and practical way, all load sources to be accounted for, and thus the creation of fully coupled models where all key sub-systems are defined (in different degrees of complexity). Frequency-domain solvers require linearisation of all load sources, and thus a limited coupling potential. Additionally, and at a high-level, it is somewhat unclear if the ability to model mechanical / electrical systems is readily available, or even numerically feasible when consider detailed sub-system descriptions, in nonlinear BEM time-domain and CFD solvers. The use of e.g. CFD solvers to inform partial inputs to other less onerous time-domain solvers may therefore offer merits if computational effort and the coupling of load sources is judged critical.
- The computational effort is particularly high for nonlinear BEM time-domain and CFD solvers, requiring the use of cloud-based and / or supercomputer solutions. Furthermore, it may prove impractical to use such approaches for design situations that demand long simulation output lengths. Additionally, solver stability may present particular challenges to linear BEM time-domain and CFD solvers.
- Frequency and linear BEM time-domain solvers offer less challenges from a user perspective, and can thus be used by a wider community. This is particularly applicable to frequency-domain models, owing to their simplicity.
- All time-domain solvers are widely available in either commercial or open-source formats, with the exception of nonlinear BEM, which are mostly kept to a research background.

As alluded to above, the ability to create fully coupled models can be of particular importance in WEC design. In such models, all relevant load sources, and therefore all relevant sub-systems, are simultaneously accounted for, ensuring that the dominant loads propagate throughout the WEC device, and that critical load paths can be more immediately and correctly identified. Should uncoupled and / or loosely-coupled models be used, where e.g. a sub-system is neglected and / or greatly simplified to allow advanced methods to solve specific problems such as wave-structure interaction in more detail, the overall model accuracy to represent the dominant physics of wave energy conversion may be compromised. Similar results are reported in related industries, e.g. in [77] up to 25% variation in the estimated amplitudes of forces and moments on an offshore wind jacket foundation were reported when comparing fully-coupled with uncoupled load models, with the latter resulting mostly from a

combination of input data sources (e.g. loads model from turbine developer; foundation model from structural design contractor).

3.1.3 Hybrid testing

In hybrid testing, also referred to as hybrid simulation [78], depends on two sub-domains:

i. Hybrid testing.
ii. Assessment measures.

In the first sub-domain (hybrid testing), the virtual simulation and physical setup interact. In virtual simulation environments, numerical models are used to describe the WEC, backed by theoretical models and/or methods. Numerical models follow different theoretical formulations and combine representation of different WEC sub-system to describe its response in an information systems context, considering different baseline formulations, algorithms, etc.

In the sub-domain of assessment measure for hybrid testing, theoretical and numerical models support the best practices to assure the fidelity of a hybrid test [79]. The fidelity can be understood as the virtual-physical compatibility and degree of exactness, considering information systems and communication systems, numerical and theoretical models, and test rig conditions.

3.1.4 Effects and deterioration

A non-exhaustive list of effects that may be assessed via hybrid testing with support from theoretical methods is provided below. For example, and where applicable, forces, stresses, magnetic fields and thermal effects in a WEC are product of their interaction with environmental loads, causing deterioration or damage that can be assessed depending on:

a. *Type of damage*. Depending on the damage or deterioration mechanism, fatigue theory such as fracture mechanics theory [80], fatigue damage accumulation theory [81]. Other damage phenomena are corrosion, see [82]; fatigue-corrosion [83], friction and wear, see [84].
b. *The scale of damage/deterioration*. The scale of interest for addressing the damage condition is relevantly dictating the theoretical models involved to represent the damage conditions, i.e. micro-scale (µm or mm), medium-scale (cm) or macro-scale (m). For example, with fatigue, these scales can be identified as near crack-tip stress field (µm), notch stress field (mm), near joint-stress field (cm), far cross-section stress field (m) and far frame stress field (m).
c. *Established limit states.* The limit state equation is a mathematical model representing a specific system/sub-system in state conditions regarding the load, deterioration mechanism, sub-system characteristics. The formulation of these limits states depends on the previously mentioned models, i.e. WEC, environmental loads, interaction and deterioration models, see [85]–[87]. Some examples of limit states proposed for WEC are presented in [88], i.e. serviceability (SLS), ultimate (ULS), fatigue (FAT) and accidental limit states (ALS).

3.1.4.1 *Fatigue*

Fatigue is the degradation process when a material is subjected to cyclic loading with magnitudes below the static strength [89]. It manifests as a crack that slowly grows, load cycle by load cycle, until final rapture occurs when the crack is large enough. In engineering applications, a fatigue crack initiates at small defects in the material and/or at a stress concentration. The fatigue strength (the resistance to fatigue failure) is highly dependent on

the crack initiation. Fatigue can be aggravated be several factors. An environmental effect that has the most severe effect is corrosion that is described in section 3.3.3.4.

Fatigue is subjected to large amounts of scatter, far more than for other types of mechanical failure modes such as yielding, fracturing and instability (buckling). It is for example not uncommon, for the same load level, to have the number of cycles to failure vary by a factor of two. Designing against fatigue therefore requires statistical methods to handle the scatter. In the VALID project, uncertainty and reliability is the topic in the upcoming deliverable D1.3.

Fatigue is usually divided in low cycle fatigue (LCF) where the fatigue life is up to about 10,000 cycles and high cycle fatigue (HCF) for longer fatigue life. Both these regimes are relevant for WECs. The relation between fatigue life N (number of cycles to failure) to applied load cycling amplitude S is described with the SN curve. One equation describing the SN curve is Basquin's equation

$$S = aN^{-b} \tag{15}$$

where a and b are material constants. Since always $b < 1$, increased load amplitude causes significant decrease of fatigue life, e.g. doubling the load amplitude reduces the fatigue life by much more than a factor of two. More complicated models than Basquin's equation also exist for plastic straining, multiaxiality and variable amplitude but the same effects apply also for these models. This allows for accelerated testing as described later.

The large fatigue damage caused by large load cycles poses a challenge for wave power since a WEC often operates at the high forces and at the relative low frequency from the incoming waves. This can be compared to hydro, wind and thermal power plants where mechanical energy is transferred via a turbine, that operates at higher frequencies and lower forces [90], [91]. This results in that components subjected to fatigue in a WEC needs a stronger design against fatigue.

3.1.4.2 *Wear of seals*

Wear is when material is worn away from the surfaces where bodies are in contact and slide relative to each other [92]. In engineering scenarios many different materials can be in sliding contact and subjected to wear. In WEC applications and for the VAILD project, wear of seals is of particular interest. In these seals, metal is typically in contact with a polymer where sliding is present while water tightness is required. The softer polymer material in the seal is then abraded away, gradually decreasing the sealing function.

The failure of seals due to wear is caused by loss of material of the seal. Abrasion is the wear mechanism active here and is essentially a hard surface tearing material away from a softer material which in this case is the seal. The amount of wear inflicted on a seal per slid distance and contact pressure is referred to as wear rate. The wear rate has units of mm^3/Nm which is equivalent to mm/MPa/m and can be interpreted as depth of wear per pressure and slid distance. The wear rate for a particular situation depends on several parameters, e.g. contact pressure, sliding velocity, temperature and lubrication. For seals, the fluid pressure that the seal is to contain also comes in as a parameter.

Wear is often described with a so-called wear map where the wear rate is presented on a map with contact pressure and sliding velocity on the axes (see Figure 10). Wear maps are regularly used for wear of metals, but the principles also apply for polymers including PTFE [93]. The foremost information from the wear maps are different regions with considerable different amounts of wear. The region where the wear is moderate, and probably acceptable in an engineering application, is called mild wear. The opposite region is where the wear is severe. This region will be entered for high contact pressures where abrasive wear is shifted to adhesive wear which can cause e.g. delamination of the polymer material (effects like galling and seizure can come into effect for metals). For high sliding velocities, severe wear can also happen due to e.g. high frictional heat or due to effects from formation of an oxidized layer.

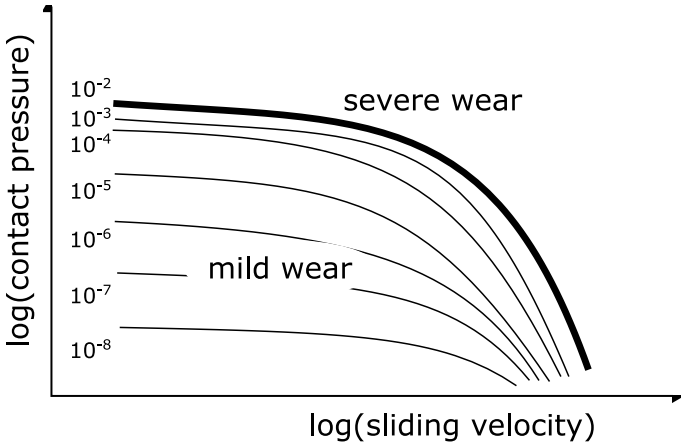

Figure 10 Principal and simplified wear map with wear rates [mm³/Nm]

In the mild wear regime, the wear rate is constant with respect to contact pressure and sliding velocity [94]. This situation is described by Archard's wear equation where the total volume of material worn away is proportional to the contact pressure and total slid distance.

3.1.4.3 ***Corrosion***

Corrosion can be defined as a deterioration of a metal by chemical or electrochemical reactions with its environment [95]. Seawater is one of the harshest electrolytes and the corrosion process is dependent on multiple factors (chemical, biological, mechanical) and parameters (e.g. salinity, temperature, pH, dissolved oxygen, dissolved inorganic nitrogen, and water velocity) [96]. This is very site specific and one further needs to consider which marine-zone is relevant (buried, immersion, tidal, splash, atmospheric zone) [97]. The corrosion rate and character (e.g. uniform, localized) are further dependant of course on the metal/alloy in use and other design features such as welds, sharp edges, and crevices can play an important role in the durability a structure. Furthermore, highly rapid corrosion degradation phenomena such as Accelerated Low Water Corrosion (ALWC) [98] and Microbially Influenced Corrosion (MIC) [99], [100] can cause detrimental effects on marine structures leading to considerable economic impacts.

To design products durable in marine environment it is thus important to take into consideration all the above-mentioned factors throughout the development process and throughout the device lifetime. Protective measures include the use of organic and inorganic coatings, and cathodic protection through sacrificial anodes or impressed current. The protective coatings will degrade over time and leave bare metal vulnerable to the harsh environment. So, it is highly relevant to know as much as possible of the rate of degradation of both the protective coating and the base material. To reduce risks, prolong lifetime and avoid complete failure of WEC devices it is pivotal to adopt a standardised procedure of testing, and design maintenance programs to suit the intended lifetime. The maritime industry has implemented a several maintenance practices such as preventive maintenance (PM), condition based maintenance (CBM), risk-based maintenance (RBM), and structural health monitoring (SHM) [101]. These are implemented to control the degradation rate, increase operational uptime, reduce life-cycle costs, and extend the service lifetime [102].

3.1.4.4 ***Biofouling***

Biofouling is a major problem shared among all maritime sectors employing submerged structures where it leads to substantially increased costs and lowered operational lifespans if poorly addressed. A major economic impact of biofouling to WECs relates to loss of structural integrity and performance caused, for example, by the added weight and thickness/rugosity to

devices and components and obstruction of sensors. Key macrofouling organisms, such as acorn barnacles, mussels, calcareous tubeworms, bryozoans, and kelp, are those most frequently referred in the literature as responsible for those impacts. Other major economic impacts to wave energy relate to corrosion promoted by microfouling and macrofouling organisms. Corrosion may be induced and/or accelerated by anaerobic marine microorganisms via so-called microbiologically influenced corrosion (MIC).

Macrofouling may further facilitate MIC initiated by the microbial communities that grow under the macrofoulers in oxygen-depleted conditions. Furthermore, some macrofoulers may promote localized corrosion as they employ endogenous compounds to adhere to (e.g. acorn barnacles) or perforate (e.g. boring bivalves) substrata. Corrosion may be further accelerated if the coating of fouled devices is physically damaged by the attached organisms, for example when exposed to the pulling forces of waves and currents or upon their removal during maintenance.

The fouling composition and magnitude on any submerged manmade surface depends on both surface specific characteristics and local condition at immersion place.

Of specific concern for wave energy sector is the fact that information on biofouling composition and magnitude across geographies is dispersed throughout published papers and consulting reports. VALID project will test both materials and surface treatments and will include state of the art information on geographical distribution and pressure for marine biofouling [103].

3.1.5 Reliability and survivability (R&S)

The third domain, reliability and survivability (R&S), has two main sub-domains:

i. Identification for reliability, survivability and performance purposes; and
ii. R&S assessment.

The identification for R&S purposes is a stage to couple the hybrid testing domain data, thinking that hybrid testing data has to be pre-processed, to later focus on the risk identification purposes. Such stage may combine hazardous conditions identification and risk management options, i.e. strategies to achieve the establish reliability levels and meet survivability targets. The sub-domain of R&S assessment aims to estimate and evaluate risk, involving e.g. uncertainty characterisation, selection of principles for risk acceptance and tolerance levels, consequence assessment and selection of risk management options (RMO) to achieve the target reliability objectives. In the next section, the reliability and risk theoretical models and related work is commented on in detail.

3.1.5.1 *Methods for assessing reliability in WEC design*

In its fundamental sense, reliability can be understood as the probability of non-failure performance [104], making it necessary to contextualise and define failure and performance. In a relevant context (e.g. mechanical, electrical/electronic subsystems), the failure criterion not only includes the component's physical failure (e.g. fatigue failure), but could also consider metrics related to usability focusing on the failure of performance, i.e. effectiveness, efficiency and satisfaction, following the definitions listed in [105].

From a theoretical perspective, reliability approaches for addressing different problems can be deterministic, pseudo-probabilistic and probabilistic – see Figure 11.

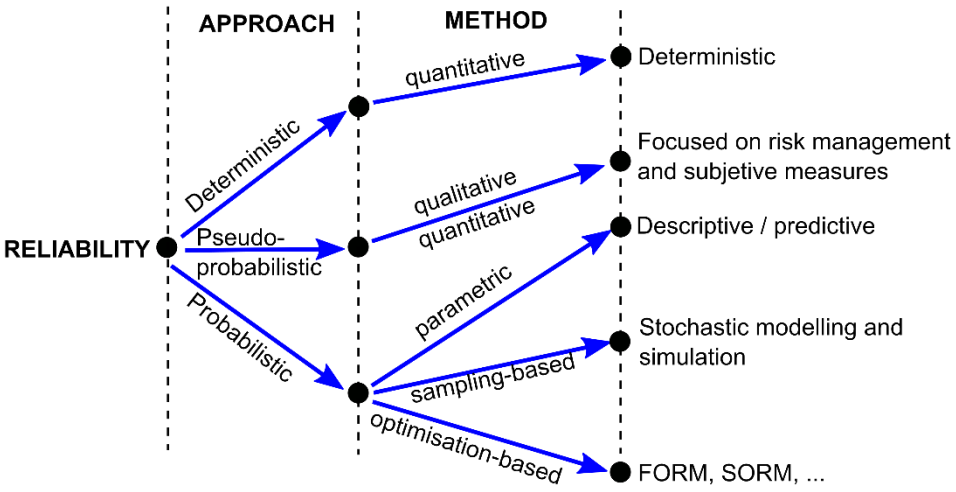

Figure 11: Summary of reliability approaches

An example of a deterministic approach is presented in [106], where the reliability is presented as a methodology for assessing different components in their degree of damage and threshold passing, without further exploring any statistically modelling.

The pseudo-probabilistic approaches are risk assessment tools (used in risk management) with a degree of subjectivity - see [107] and [108]. Relevant examples are summarised in Table 3.

Table 3: Risk assessment tools

Hazard Identification	*Causal-and-frequency analysis*	*Consequence-sequence of scenarios*	*Barrier-Safeguards Analysis*	*Multi-purpose tools*
Hazard log Checklist method PHA, Preliminary Hazard Analysis FMECA: Failure Modes, Effects and Criticality Analysis HAZOP: Hazard and Operability studies SWIFT, Structured What-if technique MLD, master logic diagram	CEA, cause-and-effect diagram analysis FTA, Fault tree analysis	ETA, Event tree analysis ESA, Event Sequence Analysis CCA, Cause consequence Analysis EP, Escalation problems CoM, Consequence Models	BTA, Bowtie Analysis diagram LPA, Layer of protection analysis BORA, Barrier and Operational Risk Analysis EFBA, Energy Flow/Barrier Analysis	Risk matrix Heat Map Risk indexing Delphi technique Expert elicitation

An example of an application of some of the previous models is shown in [109], and in a more general context, are explained in detail in [107]. The probabilistic approach has different branches (see Figure 11): parametric, sampling-based (SB) and optimisation-based (OB) methods. Examples of these methodologies or framework can be found in the following references:

- *Parametric*: [110] addressing different methods and components by using well-known standard distribution described by the different parameters. In [111], the correlation is used for reliability assessment with testing measurements in WECs.
- *Simulation-based*:
  - Monte Carlo Simulation in all its variations, see [112] and [113].
  - Random fields, Stochastic finite element, response surface, see [114].
- *Optimisation-based methods*:
  - FORM stands for first-order reliability methods, see [86].
  - SORM refers to second-order reliability methods, see [115].

In the case of the WECs, the simulation- and optimisation-based methods have been applied in the following references:

- Optimisation-based: [116] and [117].
- Different applications of probabilistic methods in WECs: [118] and [119].

The reliability assessment is related to limit states, at WEC-system or sub-system level, performance and usability metrics. Also, reliability can be extended to cover asset integrity management, combining limit states, performance indicators and efficiency/effectiveness of resource/power delivery, e.g. reliability, availability, maintainability and Survivability/Safety (RAMS); see e.g. [120]. In some cases, e.g. [121], the reliability formulation is used to estimate the extreme response of the WEC system in a probabilistic sense. In [122], [123], the extreme response of WECs is assessed for a given reliability index related to a one-hour extreme response (as a deterministic risk level). The i-FORM (inverse first-order reliability method) method - see [124] – is used to estimate specific stochastic variables or parameters (e.g. significant wave height), which in turn are used as input to derive estimates of forces and displacements related to extreme response – using a range of extreme value distributions.

Reliability assessment/design methods in WECs have been applied to structural, mechanical, electrical and electronic components in WECs. Table 4 shows a summary of the relevant existing literature addressing reliability assessment of all these components. In addition to the type of component, reliability assessment approaches and methods can vary depending on the limit state and damage mechanism. Some of these approaches can better be described as frameworks that propose risk - or reliability - methodologies using different reliability tools; for example, [125] propose one of the first theoretical frameworks for assessing the reliability of WEC components from a systemic perspective, using a probabilistic approach considering failure data of components. Alternatively, methodologies based on failure information (descriptive/predictive reliability) are dependent on testing that may not be economically feasible, or events that could have a low probability, thus limiting their applicability.

A more recent framework is presented in [126], where the probabilistic design and reliability analysis of WECs is considered, based on structural reliability methods from civil-structural engineering; see also [87]. A more pragmatic framework is proposed by [127], which focuses on integrating the information and reliability assessment to develop a WEC concept. The work in [128] presents a framework for fatigue reliability with the calibration of fatigue design factors that is the only current work integrating SN-approach (fatigue capacity using the curve of stress ranges – number of cycles, SN-curve) and FM-approach (damage capacity simulating fracture mechanics process) for considering different strategies for inspection (and perfect reparation) for calibrating fatigue factors for WECs design. The authors consider FORM/SORM (optimisation-based methods) and Monte Carlo simulation (sampling methods). Within the fatigue reliability topic, the work of [129] presents a different methodology using response surface jointly with FORM and comparing with Monte Carlo simulation, providing the accumulated reliability indexes during the fatigue life – see also [115].

Table 4: Comparison of recent literature on reliability in wave energy

	RELIABILITY	*STRUCTURAL*	*MECHANICAL / ELECTRICAL / ELECTRONIC / SYSTEMIC*
EXTREME LOAD	*Deterministic*	-	[86], [92]
	Semi-probabilistic	-	[80], [81], [82], [84], [71]
	Descriptive/Predictive	-	[75], [93], [94], [71]
	Sampling-based	-	[71]
	Optimisation-based	[87], [68]	-
FATIGUE	*Deterministic*	-	[86]
	Semi-probabilistic	-	[80], [81], [82], [84], [71]
	Descriptive/Predictive	-	[75], [93], [94], [71]
	Sampling-based	[78], [79]	[71]
	Optimisation-based	[78],[79], [87]	[67], [91]
Other	*Fatigue Framework***	[76], [77], [78], [83], [73], [41]	-
	*Extreme load Framework***	[76], [83], [72], [73], [8], [20], [41]	-
	Load characterisation	[83], [72], [73], [87], [74]	-
	Performance/Efficiency	[85], [88], [89], [92], [71]	[92], [71]

**The theoretical frameworks consider different methods and aspects of the reliability of the WEC. These frameworks can include probabilistic load characterisation or different methods.

In the context of WECs, few references address mechanical component design from a quantitative perspective. Notable exception includes the work of [116], which focuses on PTO bearings' damage from a wear and fatigue capacity perspective by assessing reliability indexes for the bearings' life cycle using FORM. The work of [130] addresses a hydraulic turbine using the fatigue reliability assessment methodology presented in [128].

Some of the mentioned work in Table 2 addresses WECs from a systemic perspective in the reliability-based design and assessment. Some examples are the work of [125] and [131], where the WECs system's reliability is based on failure information in a descriptive/predictive probability approach. Additionally, [132] focuses on system reliability assessment where parallel and series systems interact differently, using the mean operating time between successive failures. Finally, [133] is a more recent work addressing reliability in terms of the system performance without probabilistic metrics.

When a systemic reliability assessment is considered, some authors e.g. [134], [135] and [136] use reliability assessment tools inside risk assessment, e.g. FMECA (Failure Modes, Effects and Criticality Analysis), risk matrix and heat map. Such tools can be used mainly for hazard identification, which is useful for risk management purposes but not for estimating a reliability metric. A FMECA may deliver two primary outcomes: i) the risk priority number (RPN) as a criterion for assuring the following actions; and ii) responsible for actions. The first is a quantitative representation of the chances (probability) and severity (consequences), using metric related to failure rates and specific severity risk ranking from stakeholders' subjective considerations. The RPN is intended to be a quantity to identify risk-mitigation priority actions and not an index to estimate reliability. As such, a FMECA focuses on identifying risk

management options to pursue the system's risk objective. The assessment of reliability would typically follow once the risk(s) have been identified.

3.1.5.2 *Theoretical formulations for assessing survivability and reliability in WEC design*

The definitions of survivability related to reliability take different connotations in the current literature for different systems. Survivability is related to reliability as a probability or performance metric and as a state- or risk-related framework.

In the context of WEC / WEC sub-system design, eight schemes of interpretation of survivability are potentially applicable:

1. *Indirect survivability,* as metric of the impact of environmental load in WEC, e.g. [137].
2. *Reliability-survivability*, e.g. [132].
3. *Active survivability*, e.g. [138].
4. *Functional survivability*, e.g. [139].
5. *Operational survivability*, e.g. [140].
6. *Survivability post-failure state* [141].
7. *Safety survivability* [139].
8. *Risk-directed survivability*, e.g. [142].

The previous survivability-related definitions can be explained using the following six attributes:

- *Metric*: indirect, deterministic and probabilistic. This metric is textually encountered in the definition that could mention that survivability is a measure or capability referencing a deterministic metric, while others mention survivability explicitly in terms of reliability (probability). There are cases, see e.g. [142], where survivability is presented as a measure (deterministic metric), but there are further implications of probabilistic metrics in the same framework.
- *WEC-Operational condition*. The performance after the event that can be planned or unexpected such as the immediate failure condition, survival state where WEC is staying in the site not strictly in any operational state, standstill operational state due to integrity management, limited efficiency in the presence of damage of any time and operation in an efficient manner.
- *System identification*, i.e. series, parallel or another complex system. While the WEC system identification (could be a task included in risk identification, different survivability definitions do not define the system features or assumed that the damage/deterioration mechanism is an indirect description of the WEC system. While the damage mechanism for failure is a simplistic overall picture of system attributes for failure, the implication of knowing-identification of the WEC system will give a detailed picture of the system's attributes, e.g. failure mechanism, the consequence of component failure, sequence of failure and system robustness, as defined in [143].
- *Damage mechanisms*, such as the sudden occurrence of failure, cumulative damage or another mixed mechanism, e.g. a cumulative mechanism (fatigue, corrosion, fatigue-corrosion), sudden (brittle) failure or another complex mechanism.
- *Risk management*. In a recent conceptual framework, [142] frame survivability with risk analysis traits (risk management and assessment). It is vital to differentiate between risk management, i.e. a management process based on a framework that includes organisational preferences, values and policies, and risk assessment, i.e. science- and evidence-based task(s). The reliability assessment is inside risk estimation, where it is also including uncertainty characterisation, likelihood estimation, risk characterisation, etc.

- *Adaptative system considerations*, e.g. conditional on reparation (tactical adaptation) or active system adapting to planned or unexpected events.

In Figure 12, a visual comparison of the eight definitions of survivability related to WECs is presented. Indirect survivability definitions are presented as the least comprehensive definition, while the risk-directed survivability is the most comprehensive definition, presented as a framework. Additionally, Figure 13 depicts the survivability definitions in a timeline where planed and unexpected events are relevant to define the occurrence of a local or global failure scenario. Detailed commentary regarding each of the defined types of survivability is provided following Figure 13.

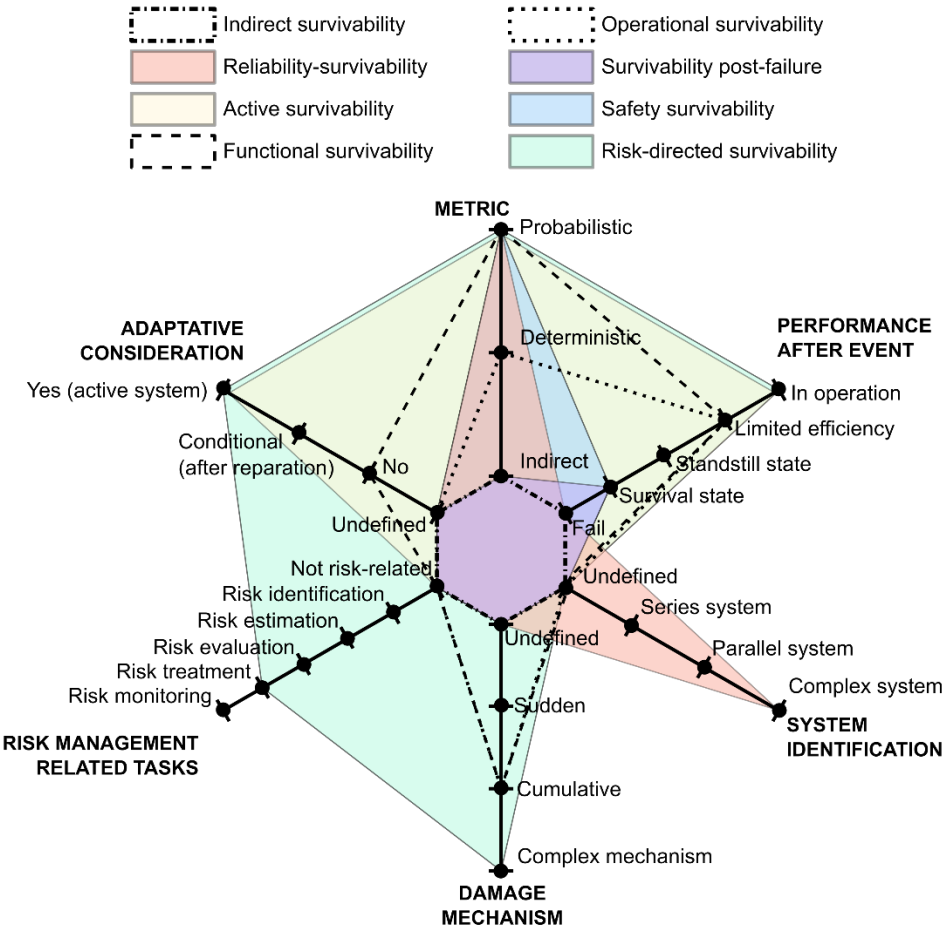

Figure 12: Aspects that shape the definitions of survivability

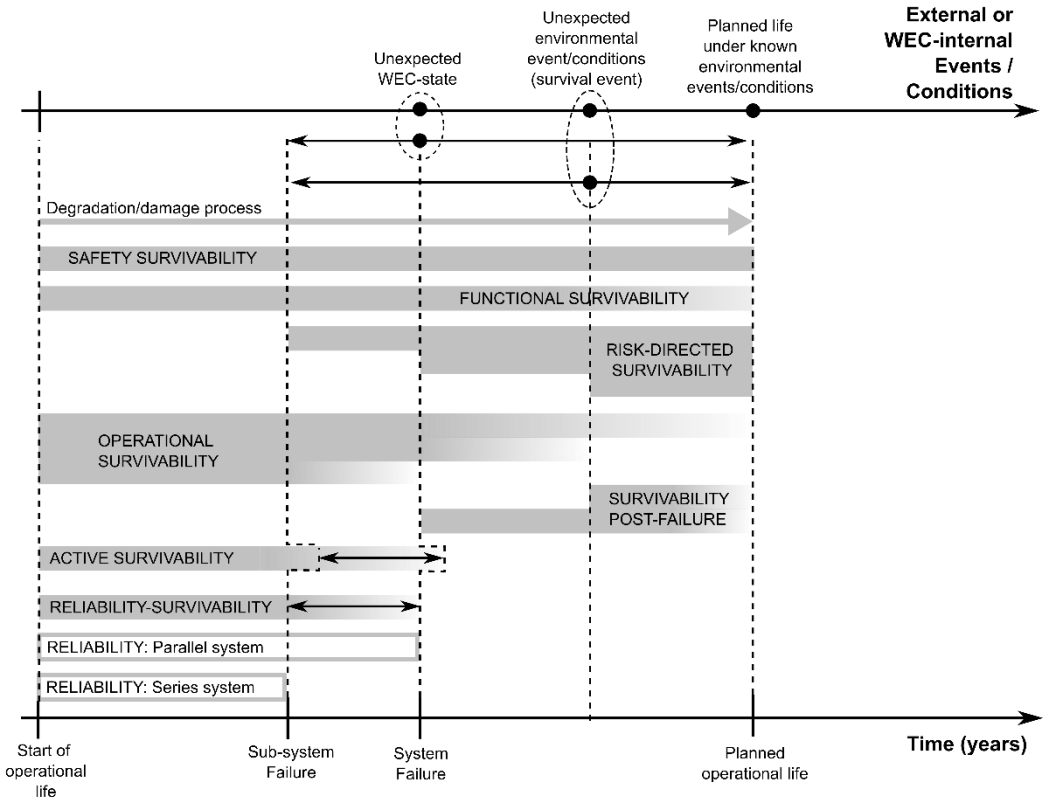

Figure 13: Survivability definitions vs. timeline

Starting with the least comprehensive approach, *indirect survivability* can be defined as an indirect measure concerning the influence of environmental load intensity and effects in the WEC, see [137]. The previous work is not precise in the definition of survivability and is not related to reliability (probability).

Additionally, *reliability-survivability* can be defined the survivability state linked to the system / sub-system probability of non-failure performance. When the failure occurs at the local (sub-system level) or global level, the system operational life ends as the system does not survive and does not reach the planned operational life - see also Figure 13. This survivability definition is centred in reliability as a probability, without any implications concerning the type of system and its attributes, failure/damage mechanism, or sub-system performance metric [132]. In Figure 13, reliability-survivability is depicted with an ending ranging between the series and parallel system failure. The failure can come from unexpected WEC sub-systems conditions (local failure event) or an unexpected event (survival event) triggering the local or global failure.

When the WEC is a series system with n-sub-systems, the failure of any sub-system implies the entire system's failure. These sub-systems' failures are taken as independent random events A_i, denoting the reliability (probability of non-failure performance), of the sub-system E_i by R_i. Then, the reliability of the WEC system is given by:

$$R = P(\bar{A}_1\, \bar{A}_2 \dots \bar{A}_n) = P(\bar{A}_1)\, P(\bar{A}_2) \dots P(\bar{A}_n) = R_1 R_2 \dots R_n = \prod_{k=1}^{n} R_k \qquad (16)$$

Where $P(\bar{A}_n)$ is the complementary probability of the event (failure) of $P(A_n)$, with $P(\bar{A}_n) = 1 - P(A_n)$ and R_k being the reliability of the sub-system k. The reliability does not exceed unity, and the multiplication of the sub-systems' reliability makes for a decrease of the overall system reliability R as the number of sub-systems increases. A fact is that R cannot exceed the reliability of the weakest sub-systems, being $R \leq min(R_1 R_2 \dots R_n)$.

When the WEC system is considered as a parallel system, the system fails when all the components fail, and the probability of failure and reliability of the entire system is given by:

$$P(A_1\, A_2 \dots A_n) = P(A_1)\, P(A_2) \dots P(A_n) = (1 - R_1)(1 - R_2) \dots (1 - R_n) \quad (17)$$

$$R = 1 - (1 - R_1)(1 - R_2) \dots (1 - R_n) = 1 - \prod_{k=1}^{n} (1 - R_k) \quad (18)$$

This system reliability formulation is considered in [132] for WECs.

Active survivability can be defined as dynamic reliability for an active system where the system can define/modify target operational states to avoid dangerous conditions leading to failure. This definition is used in the defence system, see [138]. The WEC's instrumentation and control sub-systems dealing with the response could be thought of as an active system modifying the impact of actions (wave load), and therefore the WEC response and failure conditions. The control system as an active sub-system has limitations, so any adaptative strategy is limited when the WEC system or sub-system fails, and the reliability is conditional on the tactical control strategies as a reserve of the system/sub-system capacity. The word "reserve" means that additional configuration in case of a specific performance level, unextreme event or deteriorating condition; therefore, the conditional reliability can be expressed as follow:

$$R = P(A_1\, A_2 \dots A_n \,|\theta_{ct}) \quad (19)$$

Where θ_{ct} is the set of parameters in the control configuration that provide an active/adaptative response for given hazardous detected conditions, e.g. real-time active control based on forecasted environmental loads. The definition of controllability in [142] established that controllability is the ability for control systems to be implemented to sub-systems or device and incorporate evaluation of the benefits control can deliver and the reliance of a sub-system or device on it. Supporting the definition of active survivability, the "reliance on control" is to what extent the sub-system or device requires the control system to achieve basic/improved/optimal functionality and the impact of control system failure.

Functional survivability is the probability that the system will perform at its expectable rate (or at an allowable degraded rating) without damage that would require the need for significant unplanned removal or repair over the stated operational life [139]. This definition implies that the system is under a degradation process throughout its operational life, and that the degradation influences its power production performance. Such definition is similar to *operational survivability*, used in communication networks and defined as the capability of the system to fulfil its mission [140]. However, functional survivability implies that the damage mechanism can be a gradual process, at local or global level, e.g. fatigue damage, electronic components degradation; however, in the definition of operational survivability, the failure of components could not be necessarily gradual, but sudden and limited to specific sub-system or system level. In other words, function survivability includes probability (reliability), damage mechanism (not implicitly including WEC system attributes) and the performance metric, while in operational survivability is ambiguous about the definition of "presence of failure", maybe implying system attributes such as robustness [143] or different type of system, i.e. parallel system.

Survivability post-failure state is also addressed in the current literature, see e.g. [141]. It implies a survivability state in which the system stays on the installation site and with specific integrity conditions, while not performing effectively with the presence of damage or local/global failure. It can therefore be considered a sub-case of functional survivability, where the WEC maintains physical integrity but not performance integrity.

Additionally, *safety survivability* has also been proposed - see [120] and [139]. It has been defined as the probability that the WEC will stay on station over the stated operational life. This definition only implies that the reliability levels allow accomplishing the entire planned

operational life, excluding considerations concerning the damage/failure mechanism, system characteristics, performance and environmental load.

The last definition of survivability is related to *risk-directed survivability (RDS)*, which is presented in [142] as a measure that could be defined as a risk management related framework for survivability. The framework is not systematically presented as a risk framework, see e.g. [144], [108] or Appendix B of [145]; but it is possible to identify traits of risk analysis (risk management and risk assessment). Risk-directed survivability is defined as a measure (not probability explicitly) of the ability of a sub-system or device to experience an event (survival event) outside the expected design conditions, while not sustaining damage or loss of functionality beyond an acceptable level, allowing a return to an acceptable level of operation after the event has passed. In RDS as presented in [142], survivability is differentiated from reliability, controllability and maintainability aspects, following an external risk management options (ERMO) approach, and as part of a combined risk framework, asset integrity management framework and engineering risk assessment.

Unlike the other definitions of survivability, the RDS definition establishes that survivability is a mixed risk management and assessment-based framework supported by key aspects illustrated in Figure 14.

In conclusion, RDS is at the present the most complete survivability definition to be suggested for WEC design. However, it is accompanied by the following undefined or unprecise characteristics:

1. One of the standard-based principles for establishing the risk levels is ALARP, which is a principle for characterising the acceptable and tolerable level that can be used for design. The definition of survivability does not address what is the risk level domain (acceptable or tolerable risk domain) in ALARP. There are constraints, possible to introduce in the risk evaluation and risk treatment, e.g. best available technology (BAT), CAPEX vs OPEX, etc.; however, if the risk levels are not dictated by a economic policy, the CAPEX vs OPEX is used in risk treatment to assess the chosen strategies to mitigate risk.
2. When the word "reasonably" is used in ALARP, the question is "according to what and to whom?". Is it an engineering decision for BAT? Is this the stakeholders' decision in the design process?
3. The risk evaluation part is not proposing a portfolio of design decisions when risk levels are or not met.

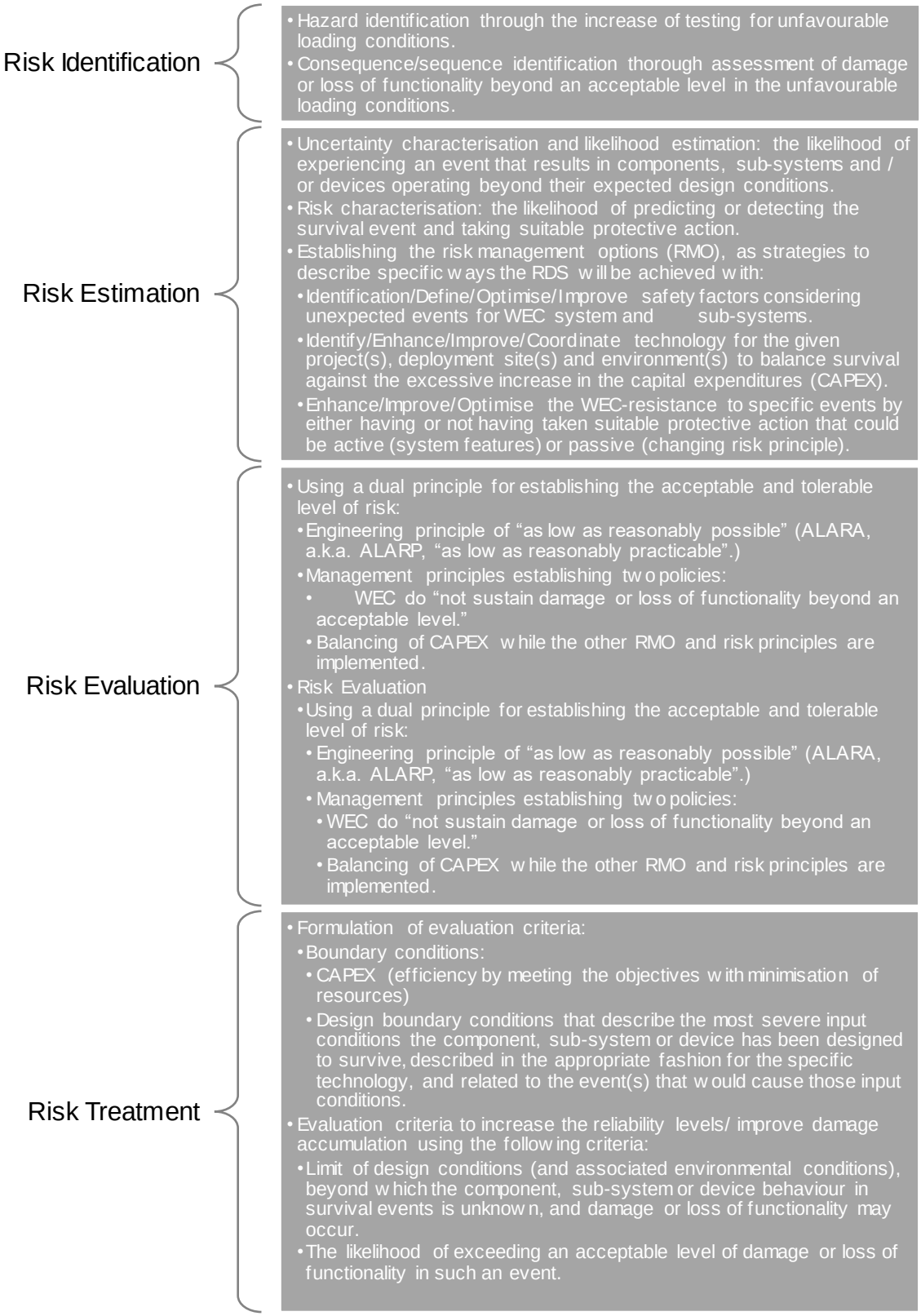

Figure 14: Key aspects related to the risk-directed survivability (RDS) framework [122]

One of the papers dealing with the framing analysis of survivability is [146], concentrating mainly the efforts of the study in the semantics of survivability concerning reliability, without delving into the relationship with failure mechanism and minimising the use of a metric of reliability based on production performance, i.e. the mean time between failures (MTBF) and not in terms of components performance or components damage mechanism, i.e. probability of exceedance of specific state.

In summary, survivability definitions are not unified (not in the WEC context, neither in other engineering areas), which offers the possibility to issue considerations specific to the context of the VALID project.

3.2 Numerical models

In this sub-section, a review of numerical modelling methods most typically applied in WEC and WEC sub-system design is presented. Firstly, basic formulations are overviewed in Section 3.2.1, covering the range of most common approaches used to date (e.g. frequency-domain solvers; time-domain solvers). Following a brief introduction of the concept of design situations and design load cases (DLCs), a qualitative ranking of numerical modelling methods is illustrated in Section 3.2.2 as a function of specific design situations, which in turn may assist future VALID decisions should particular DLCs be targeted in the accelerated testing of specific sub-systems. Recent representative examples of WEC numerical models, include code comparison exercises, are then presented in Section 3.2.3. Models for critical sub-systems of WECs are also overviewed in Section 3.2.5.

3.2.1 Numerical wave models

The exploitation of available hindcast databases and reanalysis archives, derived from large-scale numerical wave simulations, may be of interest in the reconnaissance stage of a wave energy project saving time in the implementation, computation and validation of refined simulations dedicated to resource assessment. Validated and assimilated against a series of in situ and satellite observations, these datasets reach good estimations of the wave conditions in offshore waters.

However, for the development, design and detail characterisation of wave energy projects higher resolution wave hindcasts covering long periods of time, typically ≈30 years should be used, offering a longer temporal coverage than satellite measurements and providing (according to the technical specifications) valuable information to (i) investigate the temporal variability of the wave energy resource at monthly, seasonal and annual time scales, and (ii) exhibit the long-term evolutions by identifying decadal changes in wave power density.

Wave models can be separated into two distinct categories, oceanic and coastal. While, most wave models can be applied to both large and small domains, their computational demands, efficiency, and accuracy determine their preferred use. The popular well known ocean scale models are WAve Model (WAM) and WaveWatch (WWIII), coastal or shelf-sea models are Simulating WAves Nearshore (SWAN), MIKE21-SW1 and TOMAWAC. Except MIKE21, the majority of wave models are open sourced.

Although several limitations exist, developments to alleviate inaccuracies continue. It is important to note that this separation is not deterministic, and in fact all models can be used for ocean and/or smaller domains, however the intricacies behind source terms, numerical solutions schemes, and computational requirements contribute to this classification.

One major difference of the models lay in the way they resolve the action balance density equation, with a range of available source terms. The nature of a model is also a distinguishable part, with varying options whether they are deterministic, probabilistic, using phase resolving or phased averaged approaches. Their ability to reproduce wave conditions

and provide spectral information for shallow or dee- water locations, depends on the physical approaches used in the solvers within a specific wave model. While commonalities exist in some source terms, available options, and parametrisations differ significantly within the models.

Considering the spatial limitations of in-situ, altimeter/satellite datasets (not suitable for resolution <100 Km), numerical wave models are a still high-quality option [147].

3.2.2 Design load cases

Following [148], and at a high-level, the WEC design process involves three main stages: design basis, concept design and detailed design. These are illustrated in Figure 15, where an outline of the key objectives and tasks associated with each stage is also given. The initial stage - design basis – aims to devise a preliminary selection of design load cases (DLCs), which can be defined as sets of input conditions, covering environmental, system and sub-system(s) variables and states, each of which aligned with specific design situations (e.g. power production, power production with faults, etc.). Together, a collection of DLCs aim to represent all loading scenarios to be experienced by a WEC during its lifetime. For sub-systems such as the PTO that may experience multiple input conditions, and / or to which a range of operational states apply for the same design condition, the settings leading to the highest loads should be selected per DLC.

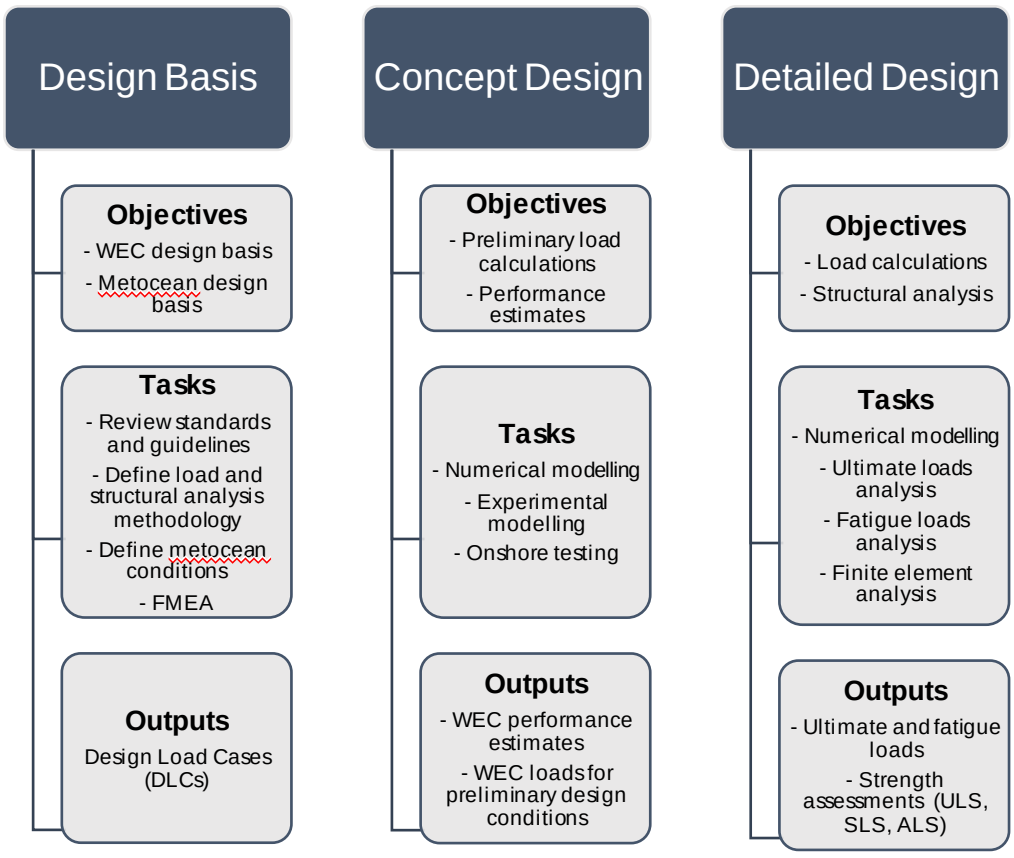

Figure 15: Key objectives and tasks: WEC design process [148]

Some DLCs may be excluded on a WEC or site-specific basis (e.g. if certain environmental conditions do not apply). Furthermore, at the design basis stage a shortlist of DLCs may be obtained following a risk assessment, conducted via e.g. a Failure Mode and Effects Analysis

(FMEA) study targeting all critical sub-systems, which may assist in identifying the DLCs that are most critical to the design stages of interest in order to propose a specific design methodology. The design basis will assist in directing concept and detailed design studies. Typically, load and structural integrity assessments are conducted at these stages, initially for preliminary design conditions and ultimately for a complete set of DLCs, covering fatigue (F) and ultimate strength (U) scenarios. An example DLC table specifically derived for WECs is provided in Appendix B of D1.1 [1], where it is immediately clear that coupled methods offer the greatest potential to simultaneously take into account the cross-influence of all relevant sub-systems.

3.2.3 Coupled numerical models of WECs

With the advent of computational power, numerical modelling of WECs became widespread in the academic, research and industrial communities. Their inherent ability to analyse a wide range of design variables, configurations and iterations of multiple WEC designs make numerical models ideally suited for a range of investigations, from early stage to detailed design, that are critical in a technical development roadmap.

Owing to the history and wide range of solvers outlined above, and while noting the importance of coupled models that account for the influences of all critical sub-systems to estimate the overall WEC response (see also Section 3.1.2), it is somewhat unsurprising that multiple software packages, mostly with a fluid-structure background, have been proposed and / or used in WEC design. A first appraisal of multiple software tools used in wave & tidal energy converter design was presented in McCabe [149], where commercial packages were presented in a standardised way to allow an assessment of their capabilities. More recently, several software / code comparison initiatives have also been conducted, specifically for WEC design tools. For example, in [150] the results of the WEC^3 project (Wave Energy Converter Code Comparison) are presented. WEC^3 focused on mid-fidelity codes that simulate WECs using time-domain multibody dynamics methods to model device motions and hydrodynamic coefficients to model hydrodynamic forces, given the predominance of such formulations in the research community.

Table 5 outlines the characteristics of the software tools tested and compared in WEC^3. The preliminary results showed overall good agreement between all codes for the tested scenarios, with the largest differences being attributed to the different approaches to empirically introduce the influence of viscous effects. Importantly, the WEC^3 project was dedicated solely to code comparisons, thus limited conclusions could be extracted. A similar study, presented in [151], compared a shortlist of numerical modelling tools. In addition to code comparisons, initial comparisons with experimental results from a single degree-of-freedom scale model were presented. The study concluded that for small to moderate incident seas all models tested, linear, weakly nonlinear and fully nonlinear, yielded similar results under the test conditions – which may prove useful to specific design situations that warrant a large number of simulations.

Table 5: WEC[3] code features comparisons ('' denotes a feature under development at the time of writing; [150])*

Code Name	InWave	WaveDyn	ProteusDS	WEC-Sim v1.0
Code Developer	INNOSEA/ECN	DNV GL	DSA	NREL/SNL
Multibody Mechanics	Relative coordinate algorithm	Proprietary multibody method	Articulated Body Algorithm	SimMechanics
Hydrodynamics	Linear potential, Nonlinear Froude-Krylov	Linear potential, Nonlinear Froude-Krylov*	Linear potential, Nonlinear Froude-Krylov	Linear potential, Nonlinear Froude-Krylov*
BEM Solver	Integrated (NEMOH)	Multiple options (inc. WAMIT and AQWA)	Multiple options (inc. WAMIT and SHIPMO3D)	Multiple options (inc. WAMIT, AQWA, and NEMOH)
Hydro-Mechanics Coupling	Relative coordinates	Generalized coordinates	Generalized coordinates	Generalized coordinates
Hydrostatics	Linear*, Nonlinear	Linear, Nonlinear	Linear, Nonlinear	Linear, Nonlinear*
Body-to-Body Hydrodynamic Interactions	Yes	Yes	Yes*	Yes*
Viscous Drag Formulation	Morison elements with relative velocity	Morison elements with relative velocity	Morison elements with relative velocity	Quadratic damping using body velocity, Morison elements with relative velocity*
Mooring (Linear Stiffness/Quasi-Static/Dynamic)	Yes/Yes/No	Yes/Yes/No	Yes/No/Yes	Yes/No/No
PTO and Control	Linear, Look-up table, and API	Linear and API	Linear, PID control, and API	User-defined in MATLAB/Simulink
License	Commercial	Commercial	Commercial	Apache 2.0
External Software	None	None	None	MATLAB, Simulink, SimMechanics

In the context of developing numerical models, code comparisons and further comparisons with experimental results are particularly relevant, especially for novel applications such as WEC design. The definitions introduced by Roache [152] can be followed to introduce the concepts of verification and validation. By verification, it is assumed that comparisons between numerical estimates are made (attempting to answer the question '*are we solving the dominant equations in the right way?*'); whereas in validation, comparisons between numerical estimates and experimental results are made, in attempt to assess if the fundamental physics are well capture numerically (answering the question '*are we solving the right equations?*').

In addition to the novelty and infancy of the wave energy sector, the specificities of WEC design make verification and validation activities particularly relevant, as it is not guaranteed that any software, even commercial software validated for a similar yet different application, is directly applicable to WEC design activities. Such principles were stressed in e.g. the PerAWaT project (Performance Assessment of Wave and Tidal Array Systems), which aimed to develop, verify and validate a range of software tools for wave & tidal energy systems, including a first commercial design tool for WEC design (see e.g. [153]). Results from the PerAWaT project are available in e.g. [154] and [155], where applications to different WECs and comparisons with physical model results at a range of scales is presented. Stressing the importance of

coupled numerical models, and in addition to the fluid-structure interaction problem, particular attention was given to the description of the key sub-systems, most notoriously the PTO.

As an example, results comparing numerical model (WaveDyn) estimates with those from a 1:19 scale model of the WaveBob WEC, tested at the Seakeeping and Manoeuvring Basin at MARIN (The Netherlands), are illustrated in Figure 16 to Figure 19. Firstly, the scale model is shown in Figure 16, where the two main hydrodynamic bodies that constitute the WaveBob WEC are clear: the torus and a central spar, referred to as the float-neck-tank (FNT). At full-scale, the torus has a diameter of 17.6m, a draft of 4.86m and a freeboard of 3.0m, whereas the FNT has a draft of 57m. The model PTO was connected to a six degree-of-freedom force frame to measure the forces and moments between the torus and FNT (see Figure 17). Such measurements allow a feedback loop in the control algorithm to be created, to compensate for losses (friction and stiction), allowing linear and nonlinear PTO profiles to be accurately implemented experimentally. Examples of the measured and modelled PTO force profiles are given in Figure 18. The level of detail given in PerAWaT to minimise discrepancies between numerical and experimental models (and experimental error) led to excellent comparisons between the data sets, as Figure 19 illustrates. It is noted that moderate wave conditions were the focus of the PerAWaT project – thus additional work would be required to assess the degree of numerical to experimental estimates correlation in more aggressive / steep input seas – and the eventual need for additional numerical formulations to be considered.

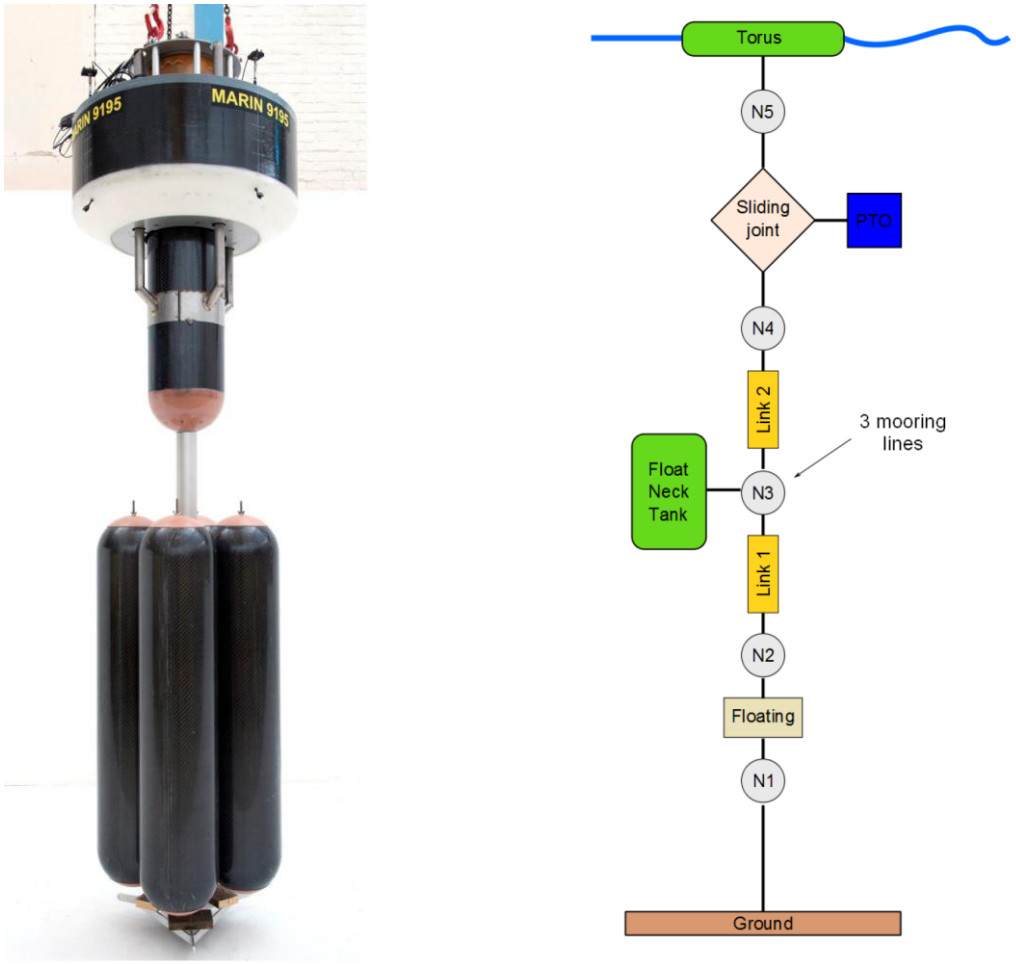

Figure 16: Left - WaveBob WEC 1:19 scale model; Right – schematic of the WaveDyn numerical model of the WaveBob WEC [155]

This project has received funding from the European Union's Horizon 2020 research and innovation programme under grant agreement No 101006927.

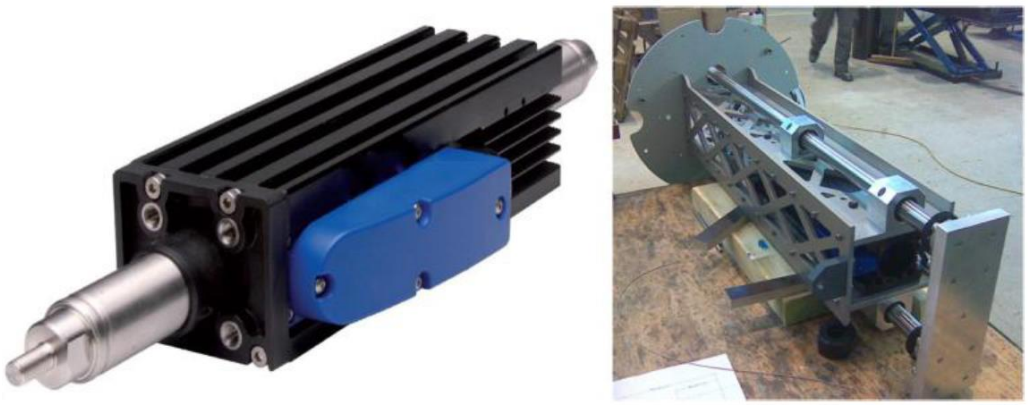

Figure 17: Left - Linear motor used in the WaveBob model PTO. Right: PTO joint frame. Lattice structure is connected to torus. Rectangular section in bottom right of picture is connected to 6 DOF force frame on FNT [155]

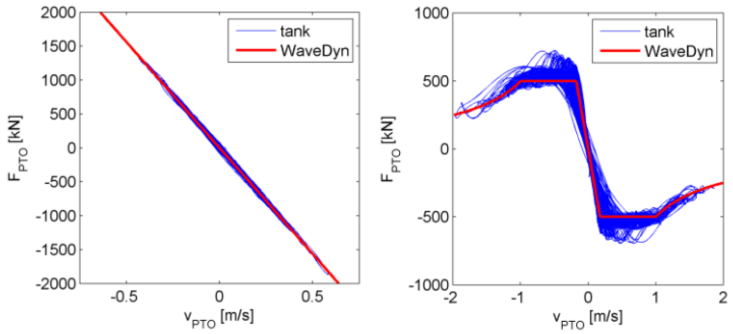

Figure 18: Examples of measured and numerically implemented PTO force vs. velocity profiles for linear and nonlinear scenarios [155]

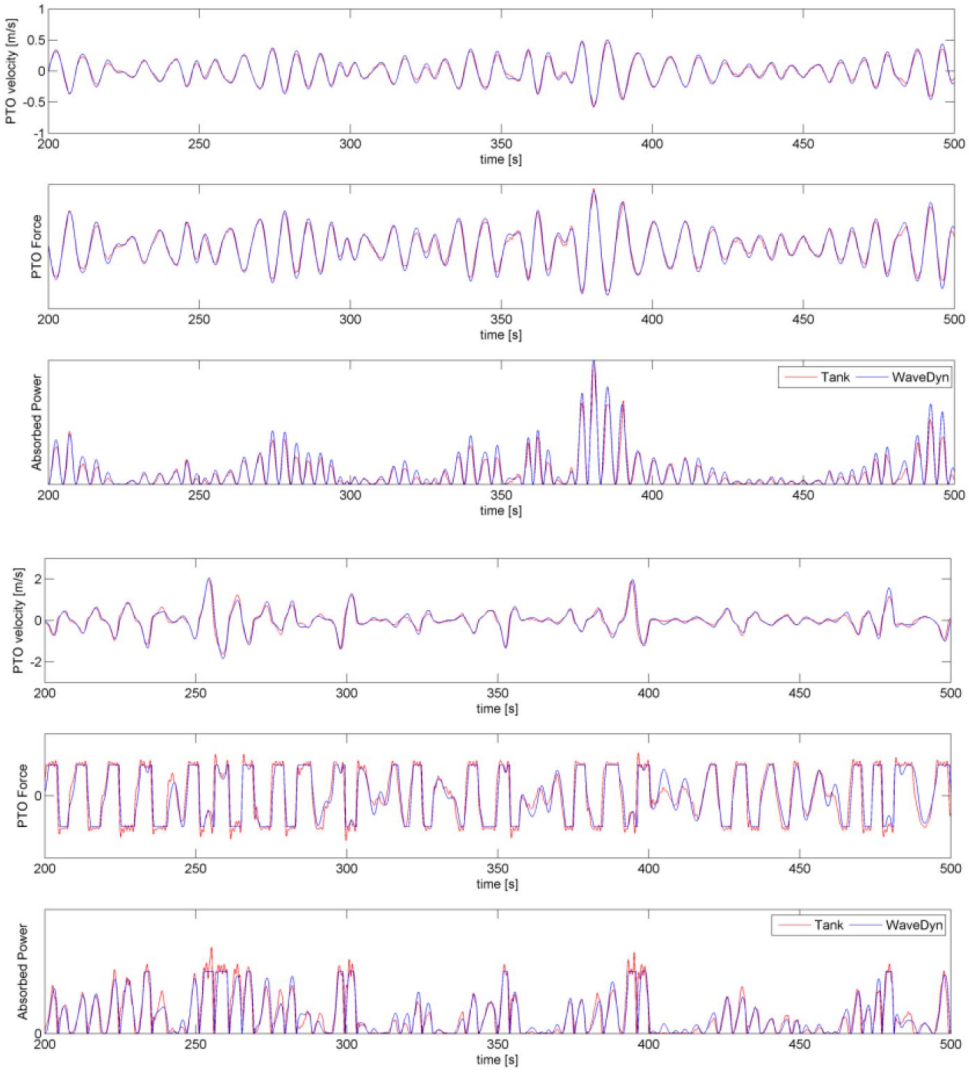

Figure 19: Comparisons of Wavebob PTO time-series from experimental (tank) and numerical (WaveDyn) for an input sea state with H_s=1.8m and T_e=11.3s. *Top: linear controls, unidirectional irregular waves. Bottom: nonlinear controls, directional spread waves with SDIR = 40° [155]*

Further comparisons, including with full-scale data from open ocean, grid connected trials, were also made in PerAWaT in connection with the Pelamis P2 WEC full-scale prototype testing programme. The Pelamis WEC design process remains to date as a valid example of one of the most comprehensive development programmes in the wave energy sector. The Pelamis development programme was hinged on the PEL software, developed by Pelamis Wave Power Ltd and detailed in [156]. In alignment with the formulations introduced in Section 3.1.2 and the remit of applicability discussed in Section 3.2.2, three main software tools are described (see also Table 6):

- *Pel_freq*, a frequency-domain based tool for performance related scoping studies with simplified control.
- *Pel_ltime*, a linear time-domain based tool dedicated to power production in small to moderate seas.

- *Pel_nltime*, a nonlinear time-domain based tool aimed at assessment the WEC response in large seas (survivability focus).

Verification of the PEL suite was made via comparisons with commercial software (e.g. AQWA and Orcaflex). A validation programme was also followed, allowing comparisons of numerical estimates with physical results gathered in experimental tests at multiple scales (from 1:80 to 1:1).

Table 6: PEL software tools [156]

Program	*Body Dynamics*	*Hydrodynamics*	*Control*	*Applications*
Pel_freq linear frequency domain	linear	3D freq. dep. coef. 2D freq. dep. coef.	linear	large parametric studies with simplified control
Pel_ltime linear time domain	linear	3D impulse response 3D freq. dep. coef. 2D freq. dep. coef.	Arbitrary non-linear	power absorption in small and moderate seas
Pel_nltime non-linear time domain	non-linear	2D freq. dep coef.	Arbitrary non-linear	survivability in large seas

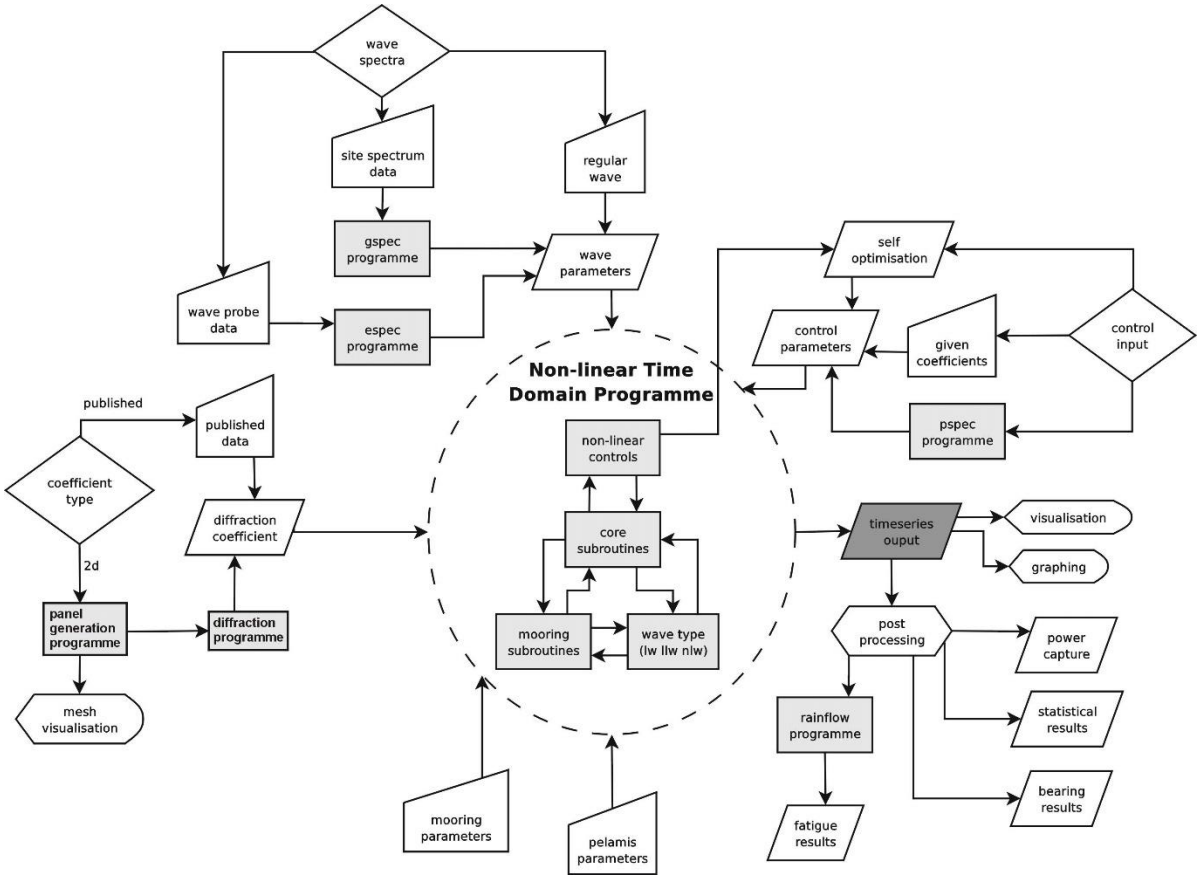

Figure 20: Schematic of the PEL nonlinear time-domain software tool [156]

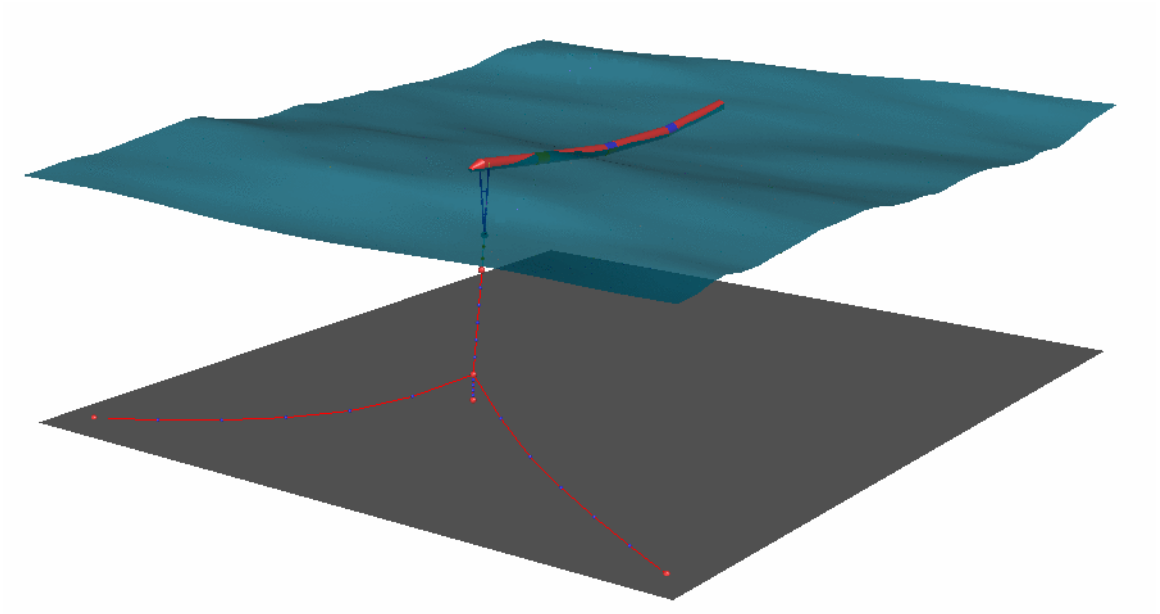

Figure 21: Screenshot of the visualisation interface of the PEL software tools [156]

The time-domain PEL models included dedicated modules of critical sub-system, such as the PTO and control system. For the PTO, the effects of a hydraulic system were included, to a component level, in order to emulate the physical system; whereas for the control system, estimated joint angles were used as inputs, to mimic the data flow that transducers would

create in the physical system. The numerical implementation of the PTO and control modules was ultimately validated via comparisons with experimental tests conducted on a full-scale PTO test rig, where a 1:1 replica of a Pelamis PTO physical module was created, with all its components, and actuated via an external set of hydraulic cylinders that replicated representative load scenarios (see Section 4.3.3 for further details).

Recently, the most advanced numerical formulations based on CFD principles have become increasingly popular. Although conceptually capable of addressing WEC design with a fully coupled approach, owing to practical limitations and / or implementation difficulties, sub-system simplification is still observed in a dominant number of examples. However, and as highlighted in Table 7, the potential of CFD-based formulation(s) to address a range of complex wave-structure interaction problems is evident.

The most prevalent applications of CFD formulations to WEC design to date have focused on extreme wave interaction with the prime mover, in an attempt to capture nonlinear phenomena such as wave breaking and wave overtopping. Examples include [157], where wave slamming loads on oscillating wave surge converters (OWSCs) was characterised experimentally (1:25 scale) and numerically, using both RANSE and SPH based formulations. The tests were undertaken with the flap undamped, i.e. simulating a condition in which the PTO is not operating. Overall, excellent agreement between the experimental results and numerical estimates was reported, as Figure 22 illustrates. The results are encouraging, in particular for design situations that warrant more advanced formulations (see also Table 7). However, the approach carries substantial computational effort challenges, as reported in [157] – e.g. for the SPH simulations, 13 seconds of simulations were completed in approximately 70 hours, using 72 processors of the ICHEC's (Irish Centre for High-End Computing) Stokes supercomputer.

Schmitt and Elsaesser [158] also addressed the modelling of OWSCs using an open-source RANSE solver – see Figure 23. Numerical estimates of the WEC's pitch motion are compared with small scale experimental data, showing overall good agreement. The results illustrate the capacity of a RANSE based formulation to capture nonlinearities in the wave-structure interaction problem, in particular those associated with viscous effects. However, it should be noted that small scale experimental modelling carries inherent limitations, which may include e.g. an exacerbated influence of viscous forces with regard to the inertial forces, when compared with their full-scale equivalent – see e.g. [159]. Additionally, no mechanical torque was applied, and thus no power absorbed by the WEC, in [158]. Both these assumptions were addressed in [160], where a PTO optimisation exercise was performed for a full-scale OWSC using the same solver (OpenFOAM) and a range of monochromatic waves as inputs. The findings demonstrated that RANSE simulations may identify nonlinearities even in moderate environmental conditions related to power production.

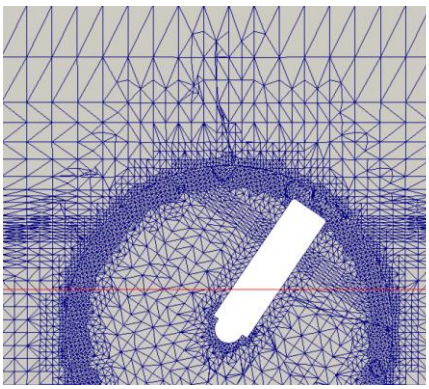

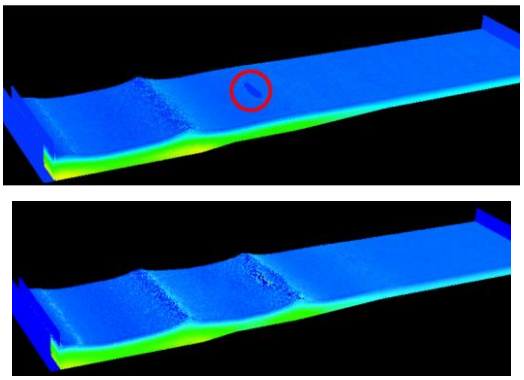

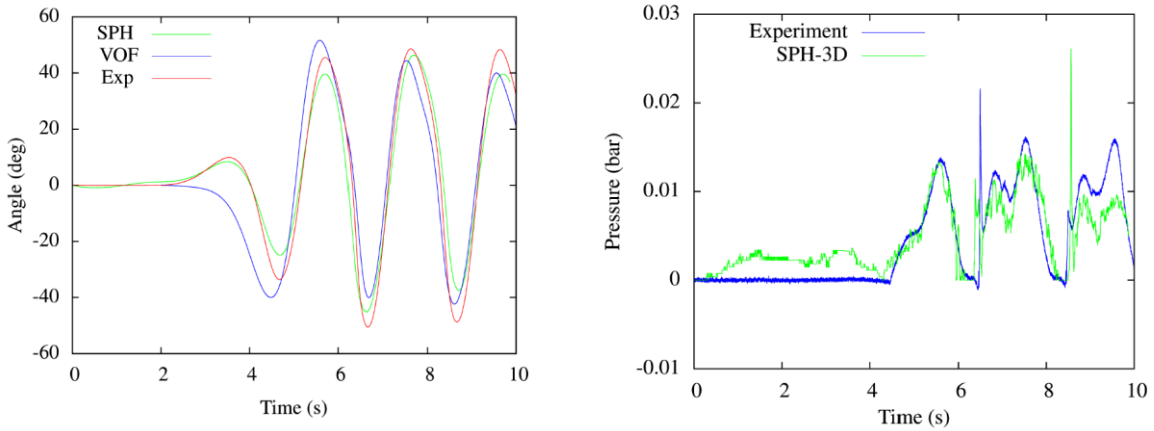

Figure 22: Example of the computational domain (top left: RANSE; top right: SPH) and selected results (bottom left: flap pitch; bottom right: flap pressure) reported in[157].

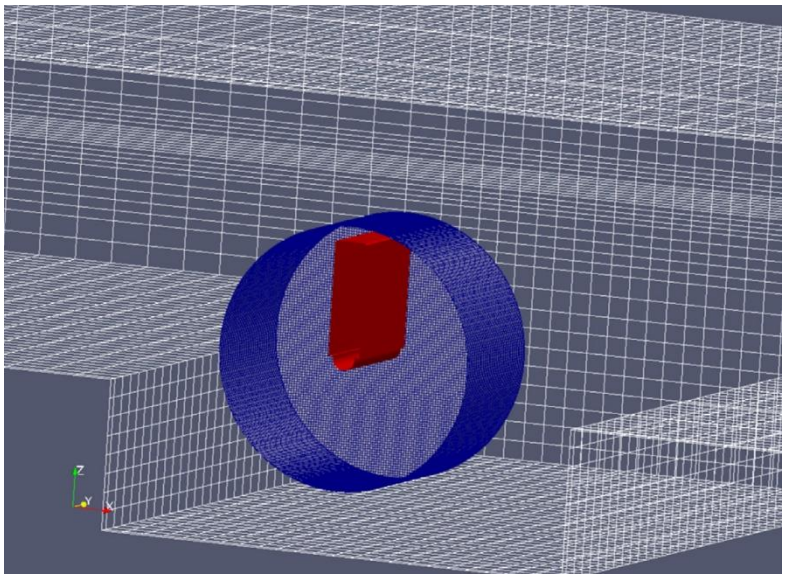

Figure 23: Example of the computational domain in [158]. The rotating mesh is represented in blue, with the flap in read and the fixed outer mesh in white.

For floating WECs, mesh and meshless (SPH) formulations were used in [161] to assess a point absorber's prime mover response under nonlinear wave action. A highly nonlinear single wave (NewWave), a concept first introduced to offshore engineering by Tromans et al. [162] as a means of deriving a design wave, was used as input, and the displacement of the floating prime mover was assessed. Overall good agreement was observed between numerical estimates at the 70th scale experimental test. However, the authors note that '*During all tests no power was taken off the system and the friction in the pulley support is negligible*', thus the conclusions are somewhat limited from a WEC design perspective. Furthermore, and as noted by the authors, the use of a NewWave may provide insight into extreme loading on the floating structure, but "*In reality, irregular waves excite the body continuously and these long-term irregular waves are needed to model the final device with mooring and PTO*".

Further examples of point absorber modelling in CFD numerical models include [163], where numerical and experimental estimates of the CETO 5 WEC response are compared. In particular, linear time-domain and RANSE estimates were compared with 1:20 scale experimental results. A simplified PTO was assumed in both numerical models, and the linear

time-domain model included an empirical viscous drag correction, whereby drag coefficients were estimated in OpenFOAM via forced oscillation tests. As illustrated in Figure 24, a constant drag coefficient was extracted in the surge, heave and pitch degrees-of-freedom. Overall, the results showed good agreement between the RANSE simulations and the experimental results, with the linear time-domain model showing a more pronounced overestimation tendency (see e.g. Figure 25).

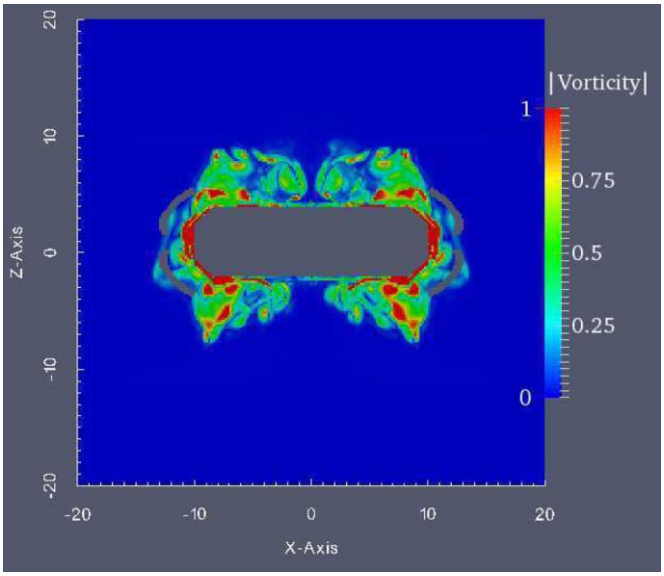

Figure 24: OpenFOAM vorticity field in forced heave oscillation – drag coefficient estimation [163]

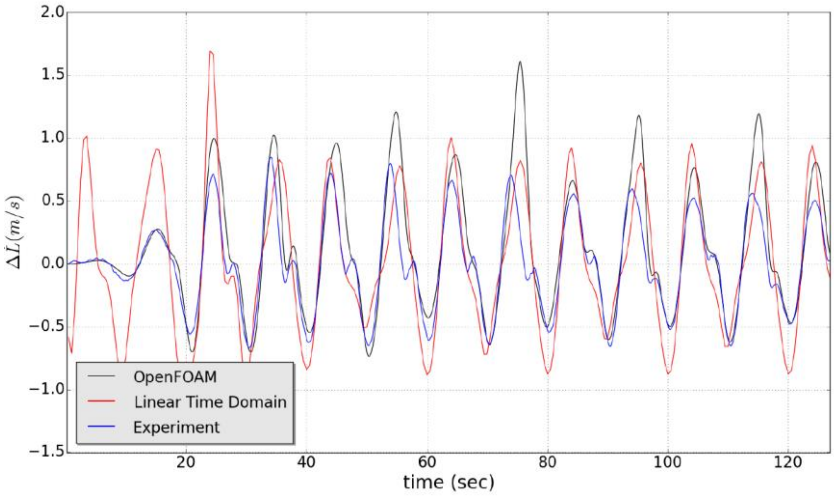

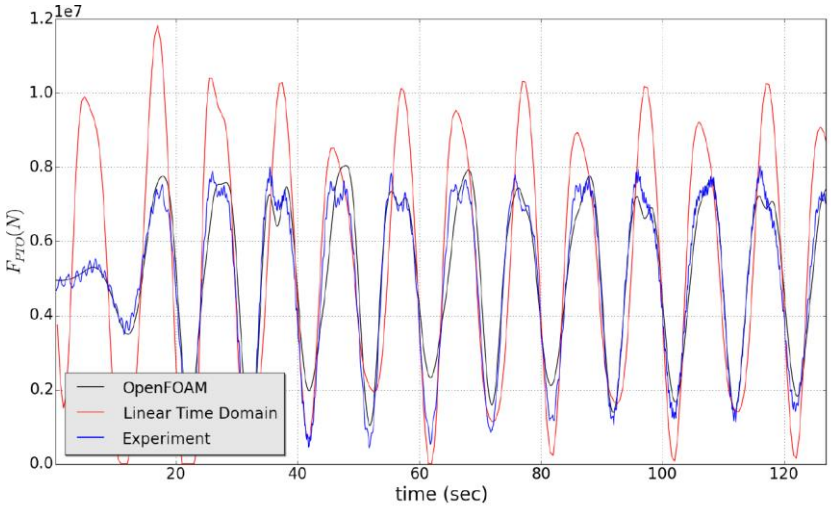

Figure 25: PTO velocity (top) and PTO force (bottom) comparisons under regular waves [163]

However, and although the authors note that the contribution of the Morison correction to the linear time-domain approach is small, the potential disproportionate contribution of viscous effects in small scale testing is not discussed in [163]– and may warrant further work. Such phenomena could mean that RANSE results computed at scale may yield similar estimates to their experimental equivalent, yet both may differ from the full-scale equivalent.

Extreme loads were also estimated in the RANSE solver and compared to their experimental equivalent. Rather than a direct comparison, the RANSE simulation uses a NewWave profile to compare directly with the largest single experimental waves. The authors concluded that the numerical method underestimates the experimental result; however, and noting that the input conditions vary between numerical and experimental setups, the initial work would benefit from additional comparisons to ascertain if e.g. an experimental NewWave input would yield similar results. The proposed used of a focused wave group such as the NewWave profile has the merit of greatly reducing computational time when estimating the WEC response in highly energetic sea states, at the expense of the estimation of memory/dynamic state effects which can dominate the overall system dynamic response. A review of this and other methods, such as the most-likely-extreme-response (MLER) method, is provided in [123]. An application of the MLER method, along with comparisons between modified linear time-domain and CFD approaches, are detailed in [164], yielding good comparisons and demonstrating the potential for using modified lower fidelity models up to highly nonlinear wave-structure interaction events.

In addition to the definition of suitable metrics, and as the final rows of Table 7 suggest, survivability assessment remains an active topic of research in WEC design, owing to e.g. the complexity of modelling a WEC as a coupled system. The conflicting requirements of simultaneously accounting for all relevant load sources, accurate modelling the wave-structure problem for steep input seas, and covering a wide range of design situations within reasonable computational power limits represent a challenge, even if considered in isolation. The use of multiple tools / formulations for different design situations may address some of these requirements, while introducing the need for additional expertise of the software developer(s) and / or user(s). An alternative is to consider a domain decomposition approach, where lower-fidelity models are used for the majority of the simulations and are loosely coupled to higher-fidelity models for a discrete part of the simulations. This approach was followed in e.g. [165], which describe a WaveDyn-OpenFOAM loose link to address extreme loading events on a point absorber WEC. The authors compared the loosely coupled approach to experimental results related to the WEC's response under extreme deterministic events (NewWave). As

Figure 26 illustrates, the approach shows promise when investigating means of adapting a single software tool to cover a wider range of design load cases, with the modified WaveDyn estimates being closely aligned with the estimated motion in all degrees-of-freedom except surge.

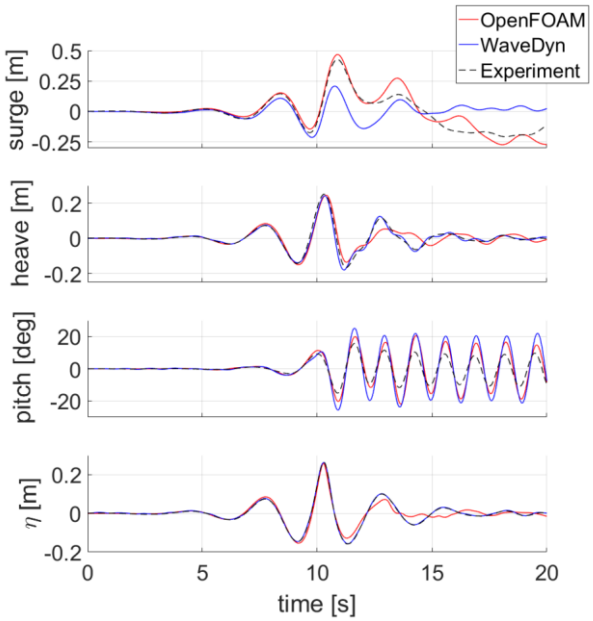

Figure 26: Comparisons of WEC response from different formulations under a NewWave [165]

Overall, the acknowledgement that the best type of numerical formulation will, among other variables, depend on the design situation being analysed, appears to offer a promising avenue for coupled WEC modelling. This opportunity is stressed in e.g. [148] and [166]. In addition to domain decomposition, the use of surrogate models such as polynomial chaos expansion (PCE) may offer the possibility to estimate long-term return period load estimates at a vastly reduced computational effort (see e.g. [167]). Alternatively, the development of open-source WEC simulation software may offer further advantages by stimulating the use of a combination of tools that is best suited for the design challenges, while avoiding the requirement(s) of acquiring and obtaining training in a range of commercial packages.

3.2.4 Suitability of numerical model formulations

Having introduced both the basic numerical formulations (see Section 3.1.2) and the concept of a DLC (see Section 3.2.3), the problem of relating a specific numerical modelling formulation with a specific DLC remains unaddressed. From a WEC design perspective, it is of paramount importance that each DLC is modelled with a suitable formulation, to mitigate the risk of inaccurately estimating dominant load effects. From a numerical perspective, a similar assessment was made in [148], where similar formulations to those introduced in Section 3.1.2 were qualitatively ranked with regard to their applicability to the design situations defined in Appendix A.

Using [148] as a starting point, a revised assessment of the suitability of basic formulations for each design situations is illustrated in Table 7. It is clear from Table 7 that only a frequency-domain formulation presents fundamental limitations that can be associated with the formulation itself – and can thus be considered mostly for early-stage, performance related assessments. All other surveyed options offer the potential to address the range of design

situations proposed in Appendix A, with different degrees of development effort, which in turn can be associated with e.g. model availability (in commercial and / or open-source format), ease of development (from a programmer and user perspective), suitability to assess highly transient phenomena, etc. As an example, and while all time-domain based options are fundamentally suited to the *Power Production plus Faults* design situation, linear time-domain based solutions are more readily available – warranting the classification presented in Table 7.

Time-domain based methods offer the opportunity to address performance, reliability and survivability related aspects. From those proposed in Section 3.1.2, the least advanced time-domain formulation provides sufficient detail to cover a wide range of performance and reliability related aspects, which if allied to its usability profile – see Table 2 – makes it a usual first option from a WEC and sub-system design perspective. The more advanced formulations, especially those related to CFD, theoretically offer the greatest potential to address survivability related aspects – in particular if e.g. specific modes of operation in such state dictate that critical sub-systems are in an idle mode, which may in turn facilitate the overall system modelling task.

While a single formulation may be unsuitable to address all key design situations detailed in Appendix A, it remains unclear if hybrid formulations, using outputs from advanced methods to enhance physical descriptions of specific inputs in other formulations, may be conceptualised in this regard. It is also noted that no distinction is made in Table 7 with regard to the specificities of each model in further design related aspects. For example, it is assumed that point loads models are considered; however, distributed loads models may offer advantages when e.g. transitioning the assessment from a load to a strength assessment perspective. To demonstrate the current state-of-the-art, examples of flagship and recent work involving numerical models of WECs are presented in Section 3.2.3, to ascertain potential avenues for development.

Table 7: Suitable of numerical modelling formulations to specific design situations (adapted from [148])

Design Situation	*Frequency-domain*	*Linear BEM time-domain*	*Nonlinear BEM time-domain*	*CFD*
1. Power production				
2. Power production plus faults				
3. Start-up				
4. Normal shut-down				
5. Emergency shutdown				
6. Parked (standstill or idling)				
7. Parked plus fault conditions				
8. Transport, installation, maintenance and repair				
9. Accidental / abnormal events				
10. Damaged stability				

Rating System Key

Formulation fundamentally suitable	Formulation suitable with minor development efforts	Formulation suitable with significant development efforts	Formulation suitable with major development efforts	Formulation fundamentally unsuitable

3.2.5 Critical sub-system models for WEC design

The creation of a fully coupled WEC model implies that all relevant sub-systems will be described numerically. Using the definitions introduced in VALID's D1.1 [1], this notion requires that, where applicable and depending on the development stage, the hydrodynamic, PTO, reaction, power transmission and instrumentation & control sub-systems need to be explicitly considered when creating a WEC numerical model.

If in-house codes are not used, the creation of a fully coupled WEC model therefore relies on a numerical simulation platform. These often use object-oriented, high-level programming languages to model a range of e.g. mechanical and electrical sub-systems, intrinsically facilitating their coupling, and exist in both open-source and commercial formats. Examples of numerical platforms of this type and that can be used in WEC modelling include MATLAB / Simulink, Modelica and Simcenter Amesim. Once applied, the creation of a coupled WEC model can be considered a first step towards hybrid testing, by enabling a virtual platform where all relevant sub-systems are considered.

Due to the number of publications and its open-source status, a noteworthy example for WEC design is WEC-Sim (Wave Energy Converter SIMulator), an open-source WEC simulation tool developed in MATLAB / Simulink using the multi-body dynamics (MBD) solver Simscape Multibody. The WEC-Sim project is an ongoing effort funded by the U.S. Department of Energy's Wind and Water Power Technologies Office, with the code development effort being a collaboration between the National Renewable Energy Laboratory (NREL) and Sandia National Laboratories (SNL). Due to its open-source nature, in the research community multiple developments are active, all of which gradually contribute to the extension of WEC-Sim's application remit. Further details regarding WEC-Sim can be found in http://wec-sim.github.io/WEC-Sim/.

WEC-Sim was originally conceived to model devices that involve rigid bodies, PTO sub-systems and moorings. Simulations are performed in the time-domain by solving the governing WEC equations of motion in all relevant degrees-of-freedom, in a fully coupled format. Given the importance of the PTO sub-system in the VALID project, an example of how WEC-Sim allows PTO modelling is detailed in this sub-section.

WEC-Sim allows PTO properties to be applied to any joint in the system, where energy converted from the relative motion between adjacent bodies may be used to drive the WEC powertrain. In addition to allowing simplistic representations of a PTO subsystem via e.g. mass-spring-damper representations, a specific module, PTO-Sim, has been developed to allow a first decomposition of individual features and components that are presented in specific types of PTOs. The approach is detailed in [168], where the ambition of eventually modelling all of the main Power Conversion Chain (PCC) options applicable to WEC designs is presented – see also Figure 27. Due to their popularity in WEC developments, hydraulic PTOs were first targeted in PTO-Sim, emulating the critical components in a hydraulic circuit. An example of a single degree-of-freedom hydraulic PTO implemented in PTO-Sim is illustrated in Figure 28, where the potential to add more detailed representations of each critical component is also clear, noting that each individual block is fully editable.

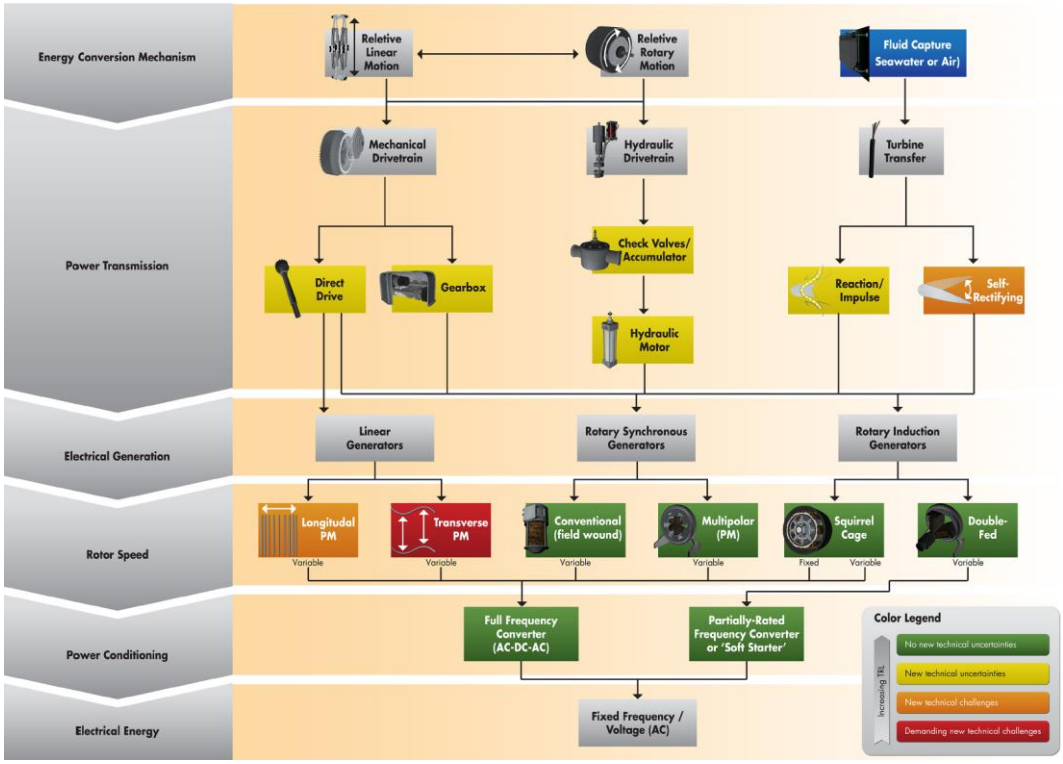

Figure 27: Typical Power Conversion Chain (PCC) options in WEC design [168]

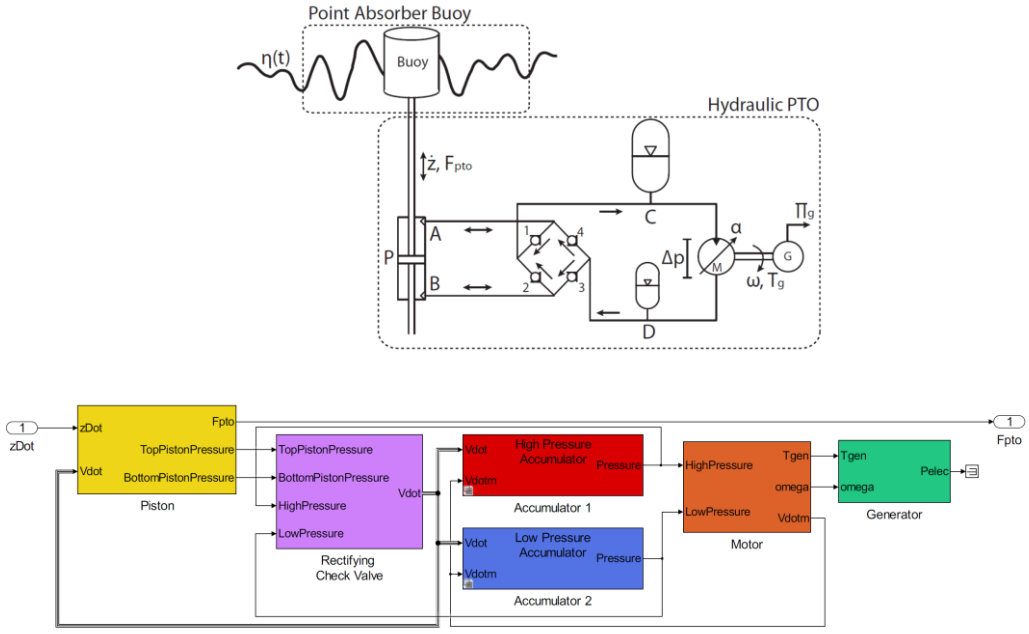

Figure 28: Schematic of a generic hydraulic PTO (top) and of its PTO-Sim representation (bottom) [168]

The challenges of PTO modelling, especially when considering reliability and survivability aspects, are well described in [169], where it is made clear that the "(…) *modelling of PTO systems both physically and numerically is challenging due to the difficulty in accounting for*

coupling between PTO systems and loads, the influence of scaling effects, and the generation of realistic and repeatable model conditions". Ultimately, the capacity to numerically model a PTO down to component level (or to a level where key component effects are captured) should be seen as an ambition of a WEC development programme, given its ability to test and iterate key design options in a controlled environment. A hybrid testing platform may provide a means to more rapidly develop and validate a numerical model of a critical sub-system, which may in turn allow component-level modelling to be included in a global, fully coupled WEC model. This potential is particularly clear if e.g. a full-scale critical system is tested in the hybrid platform, leading to a sub-system digital twin (see also Sections 3.2.3 and 3.2.5 for example of previous programmes and some recommendations for next steps, respectively).

To conclude, and recognising that alternative sub-systems may be critical in other WEC designs, additional developments to WEC-Sim that may affect different sub-systems are reported in [170]. These include:

- For floating WEC configurations, the potential effects of the Reaction sub-system in the overall dynamic response of the WEC can be of particular importance. Recognising such importance, a specific module – MoorDyn – has been created in the form of a lump-mass based mooring line model. MoorDyn is loosely coupled to WEC-sim, which in practice requires a small-time step in WEC-Sim to reach a stable solution. A verification and validation effort involving MoorDyn + WEC-Sim is reported in [171], where comparisons with OrcaFlex and 1:25 scale experimental results are presented for a three-legged catenary system connected to a single floating body. Overall, good agreement is found between the MoorDyn + WEC-Sim and OrcaFlex, as illustrated in Figure 29. Both numerical line tension estimates show similar discrepancies to the experimental results, with the authors attributing both numerical and experimental setup parameters (e.g. scale) to the root-cause of such discrepancies.
- Historically, load analysis in WEC design has been based on point load models, which inherently assume that rigid bodies are connected via series of constraints. Such approach may somewhat condition the transition from loads to stresses, by assuming that the hydro-elastic coupling is negligible. The introduction of flexible bodies in WEC-Sim via its coupling with a Finite Element Analysis (FEA) software tool was presented in [172], where a load analysis exercise was conducted for an OWSC WEC in the context of the MegaRoller project. The results showed that for specific DLCs the hydro-elastic coupling may lead to variations in the estimated peak PTO loads, which may in turn affect the design of (multiple) critical sub-systems – see Figure 30.
- The application of WEC-Sim to derive PTO load metrics over a wide range of design situations, leading to a design envelope for a novel PTO, was also reported in [173], where it was clear that the consideration of multiple DLCs is required from a critical sub-system design perspective at an early design stage (see also Section 3.2.2). Additionally, [174] analysed multiple methods to derive WEC design loads, with load estimates from WEC-Sim being compared to both experimental results and estimates from alternative formulations. The impact of post-processing methods when deriving design loads was also quantified in [175], where the VMEA methodology was applied to assess the uncertainty related to load estimates derived in WEC-Sim. Further consideration regarding uncertainty quantification will be explored in VALID's D1.3.

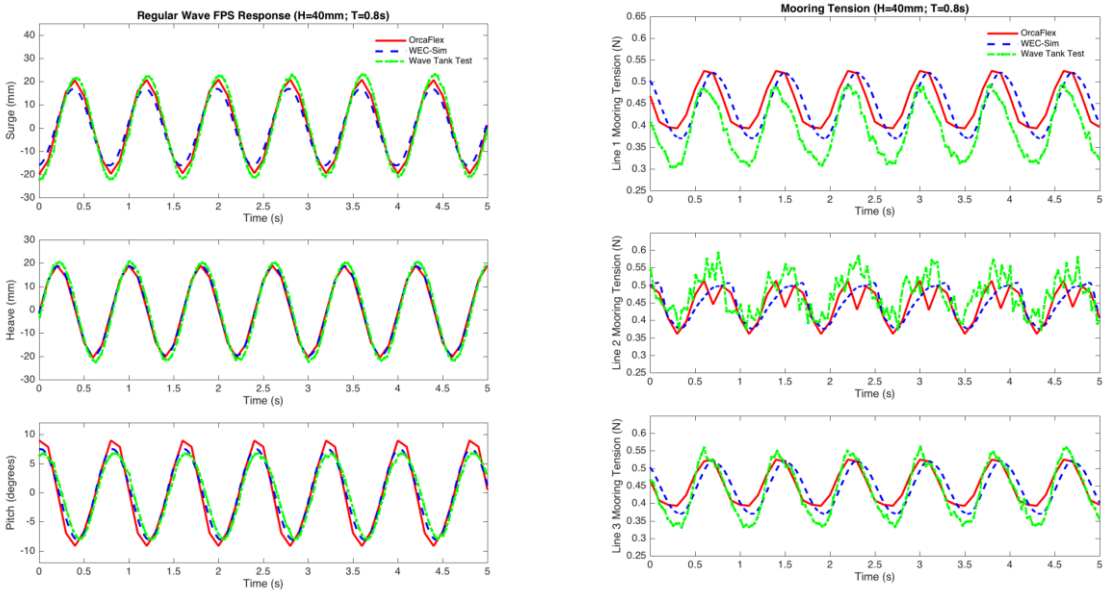

Figure 29: Comparisons between numerical and 1:25 experimental model floating body response (left) and line tension (right) – single body, three-legged moored WEC system [171]

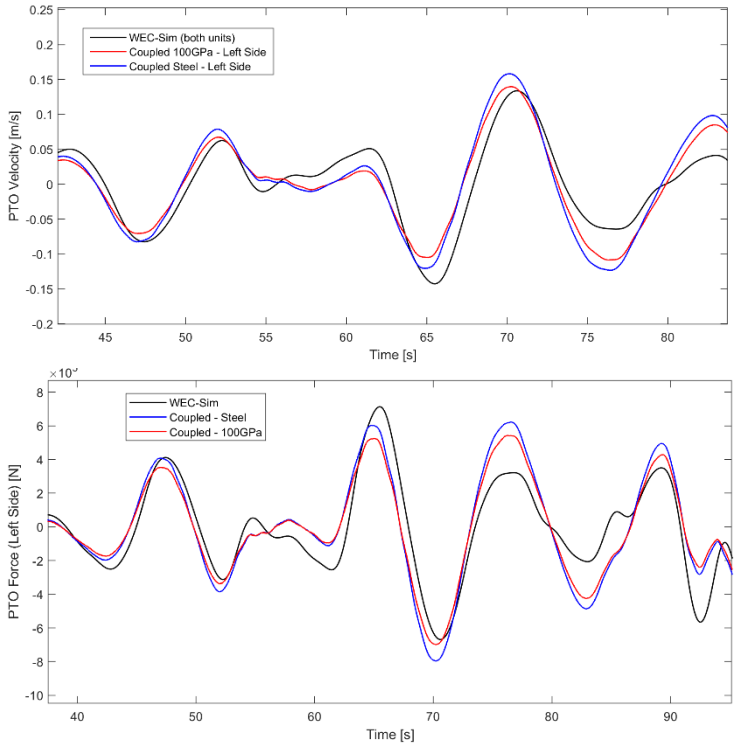

Figure 30: Comparisons between estimates of PTO velocity (top) and PTO force (bottom) on a 1MW OWSC WEC design using a rigid-body formulation (original WEC-Sim) and a hydro-elastic modification of the code [172]

The modelling developments described in this sub-section are examples of advancements that contribute to the increase in the fidelity of a time-domain linear BEM model as an emulator of a given WEC design, by allowing additional detail to be consider in each critical sub-system while considering their overall interaction (in a fully-coupled format) with all relevant sub-system that constitute the WEC. The role of fully coupled numerical models, either as creators

of input (actuation) load time-series to critical sub-system test rigs and / or as the core engine of real-time, hybrid testing platforms, is briefly discussed in this section and later detailed in Section 6.

3.2.6 Uncertainty quantification

A comparatively little effort is often devoted to the analysis and quantification of uncertainty that inevitably characterize computational models. Uncertainty in input parameters, model structure, loads, and boundary conditions originate from the inherent variability of physical quantities as well as from incompleteness of information about the object or system being modelled.

Uncertainty quantification (UQ) associated to computational models is part of the Verification and Validation (V&V) process, which systematically addresses the comparison between model predictions and experimental data. V&V and UQ are necessary activities for the credibility assessment of the results of numerical simulations, particularly in the case of novel engineering fields where standardized requirements for design and testing are not available or in safety-critical applications where underestimation of risk and variability may lead to hazardous consequences and financial loss.

The majority of UQ methods found in industrial applications rely on probabilistic frameworks, wherein uncertain variables are modelled as continuous probability distributions derived from experimental data and expert elicitation. Pseudo-random number generators and sampling algorithms such as Monte Carlo and Latin Hypercube can be used to evaluate the probability distributions and explore the design space where the input variables and parameters are defined.

Simulation based methods like Monte Carlo quickly becomes computationally expensive especially for non-linear model. Thus, surrogate models that are computationally cheap to evaluate can be useful. There exist many choices for surrogate modelling, e.g. Kriging [176], artificial neural networks (ANN) [177], and generalized Polynomial Chaos (gPC) [178], [179].

Analytical methods for UQ can use sensitivity analysis and investigate how the uncertainties propagate through the system to the output variable. One such approach is the Variation Mode and Effect Analysis (VMEA), [180]–[184]. VMEA is a probabilistic method that studies the variation and uncertainty around a nominal design. The VMEA approach represents a first-order, second-moment method. "First-order" is due to the fact that the influence of each term is approximated by one single linear term. "Second-moment" is that the probabilistic influence is approximated by second-moment statistics, i.e. variances and covariances.

The literature on V&V and UQ is formidably vast and diversified, spanning areas of fundamental math and statistics, numerical methods, and applications in virtually any field of engineering. For a concise and pragmatic introduction to UQ for computational models, the guide authored by the Stochastics Working Group at NAFEMS is a reasonable starting point [185]. A comprehensive guide to the expression of uncertainty for computational models is the "Handbook of Uncertainty Quantification" [186]. For an overview of existing standards for V&V and UQ in modelling and simulation, it is referred to this recent review by Freitas [187]. Uncertainty Quantification in Numerical Modelling and Simulation will be extensively covered in the upcoming VALID deliverable D1.3.

3.3 Experimental / physical models

Experimental modelling is the technique of investigating the behaviour of a system with an experimental model in the real world. Other naming of this technique that can be seen is physical modelling, simulation, testing. In the VALID project the term experimental modelling and sometimes testing will be used for this technique. Experimental modelling is different and

in some sense the opposite to the virtual, mathematical or numerical model where the system is described and simulated with computations. Numerical modelling is assessed in Section 3.2.

Experimental modelling has two potential main advantages over numerical modelling. The first one is that systems and fundamental phenomena that are not fully understood can be investigated, if the testing scale is appropriate. The other is that results from experiments may inspire more confidence in the estimates, by offering a source of validation [188]. The main disadvantages are that experiments most often are more expensive and time consuming. Often only a quite limited number of experiments can be conducted.

Experiments are in the VALID project categorized into three levels:

- The first level is small scale testing on materials and smaller specimens. The purpose of this testing is usually to determine or validate/certify certain properties such as material behaviour. It can also be used to investigate fundamental behaviour. This type of experiments is generally not replaced by numerical modelling. Instead, they lay grounds for numerical modelling by supplying properties such as material data and validated numerical methods. The first level of experiments is therefore not the in scope of VALID apart from suppling in-data.
- The second level is testing on components and systems. This is the testing that is the focus of the VALID project and will be extensively described and developed through the course of the project.
- The third level is complete product testing. It can be scaled or full-scale versions of the product. Examples are demonstration and prototype testing. From the VALID project perspective, this testing is at the other end as compared to the first level of testing. This is the most expensive and time-consuming type of testing. It is also the least flexible in the sense that it is difficult to include design modifications, improvements, change of requirements or inclusion of new information. In the VALID project, it is a direct objective to reduce the need of this type of testing. Ocean testing is primarily performed for full system testing of the WEC, either in full-scale or reduced scale. There is a potential for applying hybrid testing also to ocean testing. For example, sub-systems that have not been fully implemented in the experimental model, can be modelled by a virtual representation that can be simulated and connected to the experimental ocean testing.

The categories for experimental modelling for WECs that are addressed in the following subsection are:

- Experimental models for hydrodynamic interaction.
- Experimental models for energy transformation.
- Experimental models for degradation and failure.

3.3.1 Hydrodynamic models

Experimental testing of scale models is a vital component of a standard WEC development programme. Its complementarity regarding numerical modelling estimates is also critical (see also Section 3.2). By definition, numerical models simplify the physical representation of a system, and experimental tests can be used to assess if such simplifications do not affect the realism of its estimates, i.e. if the numerical representation is valid. However, it is important to note that experimental models are themselves limited by a range of variables, and therefore their response should not be automatically assumed to be an exact replica of the behaviour of a full-scale WEC. An overview of existing tank testing guidelines is presented in Section 3.3.1.1.

Items that condition the realism of experimental models include environmental variables (e.g. wave conditions) and WEC variables (e.g. sub-system model characteristics). For example, and despite the controlled nature of wave conditions in a tank environment, the generated

waves are not a perfect representation of the conditions in an open ocean environment, due to e.g. reflections from the tank's side walls. Additionally, specific hydrodynamic effects may be ill-represented in scale model tests, in particularly in small scale tests. For example, the ratio between inertial and gravitational forces scales at a different rate when compared to the ratio of inertial and viscous forces. As gravitational and inertial forces tend to dominate the response of a WEC, typically the scale is chosen so that these are dynamically similar to the full-scale design, at the expense of other forces acting on the hydrodynamic bodies (e.g. viscous forces). Section 3.3.1.2 presents an overview of the scaling laws to be considered for experimental tests.

A further complication of modelling WECs at small scale is the representation key sub-systems such as power take-off (PTO) sub-system. The standard approach is to use simplified models that replicable the effects of their full-scale equivalent, but that are not necessarily replicas down to component level. The construction of experimental WEC models is discussed in Section 3.3.1.3, with examples of previous wave tank testing campaigns presented in Section 3.3.1.4.

Within these limitations, if experiments are carefully set-up results from experimental tests can provide valuable data to estimate full-scale WEC response and validate numerical models. There are considerable synergies with the offshore engineering industry and a strong legacy regarding the importance of tank testing that can also be used to acquire relevant know-how.

3.3.1.1 *Overview of wave tank testing guidelines*

Guidelines and protocols for the development of offshore structures have long been established and subsequent standards have been issued by certification bodies such as the American Bureau of Shipping (ABS) and Det Norske Veritas (DNV), among others.

A number of specific guidelines for the tank testing of WECs have been published, including:

- Sarmento A. and Thomas G. *Laboratory Testing of Wave Energy Devices. Wave Energy Converters Generic Technical Evaluation Summary*, Annex Report B1, Device Fundamentals / Hydrodynamics. CEC, Brussels. 1993. Also summarised in Cruz (Ed.) Ocean Wave Energy, Springer [189].
- Hydraulic & Marine Research Centre (HMRC). *Ocean Energy: Development and Evaluation Protocol, Part 1: Wave Power* [190].
- Supergen Marine – *Guidance for the Experimental Tank Testing of Wave Energy Converters*. University of Edinburgh [191].
- EMEC Marine Renewable Energy Guide – *Tank Testing of Wave Energy Conversion Systems* [192].
- EquiMar Deliverable *D3.3 – Assessment of Current Practices for Tank Testing of Small Marine Energy Devices*. Universities of Strathclyde, Cork, Southampton and Aalborg, and DNV [193].
- EquiMar *Deliverable D3.4 – Best Practice Testing of Small Marine Energy Devices*. Universities of Strathclyde, Cork, Southampton and Aalborg, and DNV [194].
- International Energy Agency (IEA) Ocean Energy Systems (OES) Annex II Report. Task 2.1 *Guidelines for the Development and Testing of Wave Energy Systems* [195].
- International Towing Tank Conference (ITTC) *Recommended Guidelines. Wave Energy Converter Model Test Experiments* (7.5-02-07-03.7) [196].
- IEC TS 62600-103:2018 Marine Energy – Wave, Tidal, and Other Water Current Converters – Part 103: *Guidelines for the Early Stage Development of Wave Energy Converters – Best Practices and Recommended Procedures for the Testing of Pre-Prototype Devices* [197].

Most recently, the IEC have issued a technical specification (TS), IEC TS 62600-103, for the development of wave, tidal and other water current converters, including best practices and recommended procedures for the testing of pre-prototype devices. The TS covers guidance on wave tank test programmes and the first large-scale sea trials.

Key stages involved in planning and executing a testing campaign can be summarised as follows:

1. Planning an experimental programme

- Presenting a clear statement of testing objectives, e.g. proof of concept, optimisation of design, validation of numerical model(s), testing of specific components.
- Consideration of model scaling, including geometric similitude, structural similitude, hydrodynamic similitude and power conversion chain similitude.
- Define the experimental device, including technical drawings and description of experimental subsystems and their functionalities.

2. Choice of test facility and outline test plan

- Identify required test facility specifications, e.g. dimensions, wave making capabilities, tank instrumentation and data acquisition, logistics and technical support.
- Determine tests to be conducted and identify variables to be monitored.

3. Model design, construction and calibration

- Determine the appropriate testing scale for the test objectives, considering appropriate scaling laws.
- Consider: material selection, model construction methods, mass distribution, simulation of representative device subsystems.
- In-situ checking and calibration of models and sensors

4. Testing and reporting

- Determine layout of models and sensors in the tank
- Calibration of waves in absence of models
- Test runs
- Analysis and documentation

3.3.1.2 *Scaling*

Scaling laws / similitude

In order to estimate the behaviour of a full-scale WEC from scale model tests, geometric, kinematic and dynamic similarity with the full-scale device must be ensured. These respectively imply the following requirements:

- Geometric similarity requires that there is a fixed ratio of dimensions between the model and the full-scale device.
- Kinematic similarity requires that there is a fixed ratio of velocities between the model and the full-scale device.
- Dynamic similarity requires that there is a fixed ratio of forces between the model and the full-scale device.

Due to the wide range of load sources that affects a WEC, it is not possible to scale all of these load sources at the same ratio. The standard approach taken in tank testing is to use a scaling criterion that keeps the dominant load sources on the WEC in a fixed ratio.

Typically, in the majority of concepts proposed to date the response of a WEC is governed by gravitational and inertial forces. The ratio between inertial and gravitational forces is represented by the Froude number, F_n, given by $F_n = \frac{U}{\sqrt{gL}}$, where U and L are velocity and length scales, respectively, and g is the modulus of the acceleration due to gravity. Froude scaling can be therefore be described as a set of scaling laws that maintain the same F_n between model scale and full-scale.

Under Froude scaling all lengths are scaled by the same factor k (e.g. WEC dimensions, water depth, wave height, wavelength, etc.). Typically, this means that the chosen model scale will be limited by practical limits associated with e.g. the size of the wave tank and the size of the waves which can be generated. For example, to model a WEC operating in 50m water depth in a tank of 2m depth the maximum scale possible is limited to 1:25. Additionally, wave tanks typically contain freshwater rather than sea water. The ratio between the density of sea water and fresh water, r, is usually taken as 1.025, and should be considered.

Scaling factors for a range of relevant physical properties are listed in Table 8.

Table 8: Froude scaling factors

Quantity	*Scale factor*
Length	k
Angle	1
Time	$k^{0.5}$
Linear velocity	$k^{0.5}$
Angular velocity	$k^{-0.5}$
Linear acceleration	1
Angular acceleration	k^{-1}
Volume	k^3
Density	r
Mass	rk^3
Force	rk^3
Moment	rk^4
Power	$rk^{3.5}$
Linear stiffness	k^2
Angular stiffness	k^4
Linear damping	$k^{2.5}$
Angular damping	$k^{4.5}$

Froude scaling applies when gravitational and inertial forces, therefore disregarding viscous forces as the correct ratio between inertial and viscous forces is not maintained. To keep the latter ratio at model scale, the Reynolds number, R_e, where $R_e = \frac{UL}{\nu}$ and ν is the kinematic viscosity of the fluid, would need be maintained (between model and full-scale). As the kinematic viscosity is a property of the fluid and the ratio between U and L is determined by the Froude number, it is not possible to simultaneously maintain the same Froude and Reynolds numbers at model scale.

The practical effect of this inconsistency is that viscous effects, such as vortex shedding and drag, may not be correctly scaled. Additionally, such effects may be more significant at small scale, e.g. viscous damping on the hydrodynamic bodies and mooring lines will be greater at model scale than at full-scale. Other viscous properties include surface tension effects, should also be considered when planning tank tests to ensure that their effects are noted and where applicable, mitigated.

Scale selection

The model scale used for a particular set of experimental tests is dependent, amongst other variables, on the objective of the tests. The IEC TS 62600-103 emphasises the need to test at a range of scales as part of a staged development program leading to a full-scale WEC.

An overview of the staged development approach outlined in the IEC TS 62600-103, and the requirements for each stage and including the scale guidance for physical tests, is provided in *Table 9*.

Table 9: the typical stages of a WEC development programme (experimental testing)

Stage 1: Concept Model (TRL 1 - 3)
• Aims to validate the initial design concept through small scale tests in regular waves with a basic PTO. Obtain a first indication of power performance. • Extends to device optimisation trials in irregular waves, where initial design parameters should be explored e.g. changes in geometry. • Scale guide: 1:100 – 1:25.
Stage 2: Design Model (TRL 4)
• Aims to produce a more realistic model with more accurate PTO and mooring system such that Stage 1 results can be validated. Survivability check to observe device response in survival conditions. • Monitoring of component, power-take-off and control systems. • Scale guide: 1:25 – 1:10.
Stage 3: Sub-System Model (TRL 5 - 6)
• Aims to prove components in realistic conditions and determine their effects upon the device performance. • Sheltered site to allow the testing of device at larger scale, e.g. deployment check, operational check, survivability check, galvanic corrosion check and fatigue stress evaluation. • Scale guide: 1:5 – 1:2.
Stage 4: Solo Device Proving (TRL 7 - 8)
• Aims to prove the device with full-scale components. • Scale guide: 1:2 – 1:1.
Stage 5: Multi-Device Demonstration (TRL 9)
• Recommendations of final commercial unit, i.e. fully optimised device with grid connection and electricity sale. • Possible deployment of small array trials (3 – 5 devices). • Scale guide: 1:1.

3.3.1.3 *Model construction*

The construction of a WEC model should include the manufacture and successive integration of its main subsystems, which can generally be identified as:

- Hydrodynamic sub-system
- Power Take-Off (PTO) sub-system

- Reaction sub-system
- Power conversion & control sub-system

It is understood that, depending on the scale selected for the experiments, creating a representative model of the system may not be possible, i.e. it may not be feasible to construct a model where the effects of the dominant load sources are scaled consistently. This is especially true for Stage 1 and Stage 2 models, i.e. up to 1:10 scale (see Section 3.3.1.2), on which this sub-section will focus [196].

Practical scaled models can be constructed with the purpose of fulfilling the test objectives, which may allow making specific assumptions with regard to the scaling of the different sub-systems without invalidating the testing process, depending on e.g. operational modes and environmental conditions [192].

Construction of a scaled hydrodynamic sub-system

The main goal in constructing a scaled version of the hydrodynamic sub-system is to replicate, in a controlled environment, the behaviour of its full-scale equivalent. This requires scaling geometry and mass-based properties for all the bodies involved. Mass distributions can be replicated by designing the model with movable and weight-adjustable lumped-masses.

From a geometric and inertial perspective, model accuracy may be checked by different methods for the centre of gravity position, including the suspension method, and by the bifilar suspension method for inertias [192].

Multiple types of structural materials may be used in scaled models, with light materials allowing additional flexibility to accommodate movable lumped masses, which may be beneficial to e.g. fine tune the distribution of inertial properties. Additionally, if the full-scale hydrodynamic sub-system is made of flexible materials, additional measures may need to be taken to ensure these dynamic effects are modelled at scale.

Finally, and in particular at small scales, sharp edges should be avoided when considering model construction, as these may introduce viscous effects that are not representative of their full-scale equivalent due to the scaling law followed.

Construction of a scaled PTO sub-system

The main objective of a scaled version of the PTO sub-system is to correctly scale the forces that are exchanged between the PTO and the other sub-systems, for specific design situations (which in turn combine operational mode and environmental conditions). The interaction between the hydrodynamic response of the WEC and PTO force affects the overall WEC dynamics and, as such, the overall system response and power absorption.

Practically, it is typically not possible to build exact replicas of the full-scale PTO due to e.g. unavailability of components at small scale. Therefore, the construction of a PTO model may require simplifications. This typically does not represent any shortcoming as, for the purposes of scaled testing, it is the PTO effects on the critical sub-system(s) and on the WEC response that shall be scaled, rather than the PTO itself.

Overall, a simple yet representative mechanism able to provide a scaled reaction force to the hydrodynamic sub-system is sufficient to mimic the dominant effects of the PTO – as illustrated in the examples of Section 3.3.1.4. If the scaled reaction force consists in a constant damping coefficient, this can be achieved using variable-aperture orifice systems, mechanical dampers or brushless DC motors coupled with simple mechanical levers.

The fidelity of such model(s) can be checked by e.g. imposing constant speed profiles at PTO and measuring the reaction force through a load cell. The average force to speed ratio shall be equal to the scaled (linear) damping coefficient.

Within this modelling process, it is important to note that dynamic and static friction forces may represent a large portion of the total (scaled) PTO force, which in turn may not be representative of the full-scale system. As such, friction forces in the PTO model should be minimised.

Construction of a scaled reaction sub-system

The main objective of a scaled version of the reaction sub-system is to station-keep the WEC, and correctly scale the forces that are exchanged with the sub-system that it is attached to, most often the hydrodynamic sub-system.

Typically, for WECs that involve a fixed connection to the seabed, the creation of a scaled reaction sub-system can be relatively straightforward, although careful planning should involve e.g. an instrumentation layout that allows the connection of excitation forces at the attachment point(s).

Scale modelling of mooring-based reaction systems may offer additional challenges. In catenary arrangements the model should consider a target scaled mass per unit length [192]. The fidelity of the model may be checked by e.g. hanging weights on the mooring and record the displacement of the line. For taut systems, on the other hand, the line tension should be the key measurement. For the target scales under consideration, the station-keeping features of anchors can be typically replicated by appropriate clump weights.

Construction of a scaled power conversion & control sub-system

At reduced scale, the modelling of the power conversion module of a WEC is usually not required, as the power levels involved are often very low – thus power absorption is limited to mechanical absorption. More typically, the control sub-system may have a role in scaled experiments.

However, and in particular for small scale tests, experiments may not require any active control mechanism. In such cases, constant PTO settings are applied throughout the experiments. If specific tests require the variation of PTO settings, coefficients and / or the implementation of a control logic during the tests, this may be achieved with the support of programmable digital controllers [198].

3.3.1.4 *Examples of previous wave tank testing campaigns*

To conclude Section 3.3.1, a non-exhaustive overview of examples of scale testing campaigns is provided. In particular, scale tests related to two of the WECs considered in the VALID user cases are initially overviewed.

Examples from VALID Participants

In 2010, WavePiston performed 1:30 scaled tests at Aalborg University's deep-water basin [199], [200]. The WEC consists in a number of collectors which can oscillate back and forth in surge. Each collector is a thin plate, and their relative motion contributes to pressurize sea-water which is then transported to an onshore collector to either power a turbine or be used for desalination purposes (see *Figure 31*).

The testing campaign involved developing a different model to facilitate PTO force measurement and reduce as much as possible viscous effects which may not be representative of a full-scale effect (see also Section 3.3.1.2). The floating collectors were mounted on vertical aluminium tubes, which were allowed to rotate around a pivot point far above the still water level. This allowed the collectors to move in an almost perfect horizontal fashion, reproducing the motion they would have at full-scale. Furthermore, the PTO model consisted in friction wagons placed outside the water and connected to the pivoting aluminium tubes; the friction force could be adjusted by means of increasing or decreasing the mass of the wagons. This represents a clear example of building scaled models of different WEC sub-systems, focusing on the effects they have on each other rather than building their scaled representations (see Section 3.3.1.2).

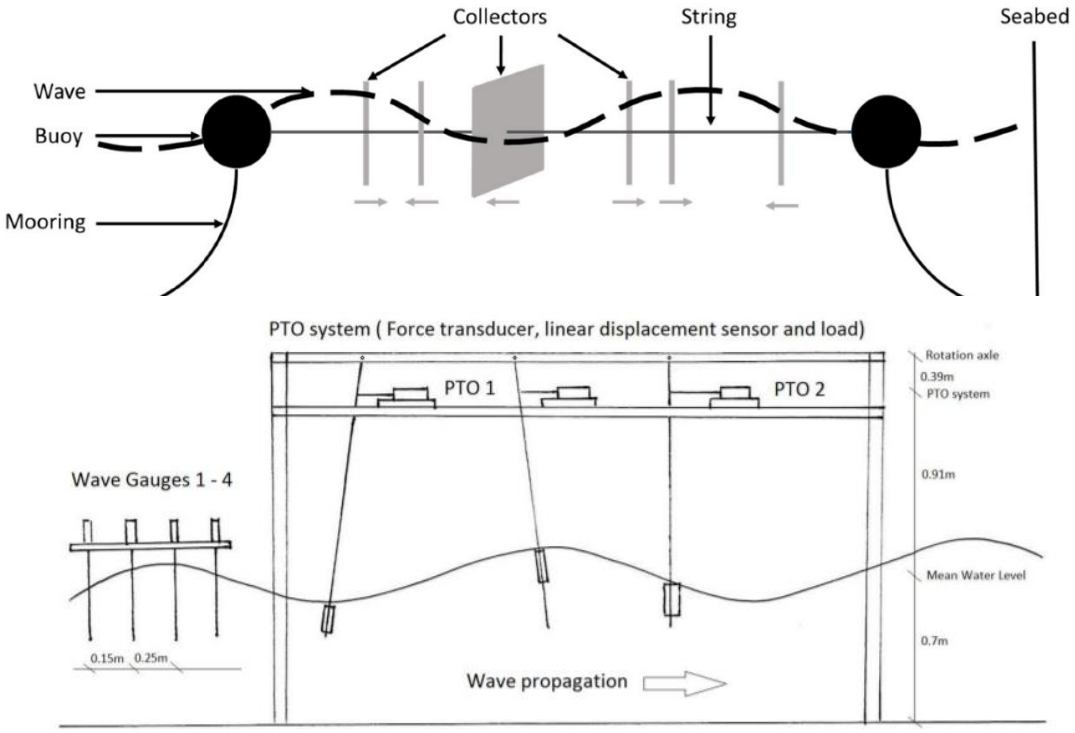

Figure 31: Wavepiston full-scale architecture (top) [201] and experimental setup for tank tests (bottom) [200]

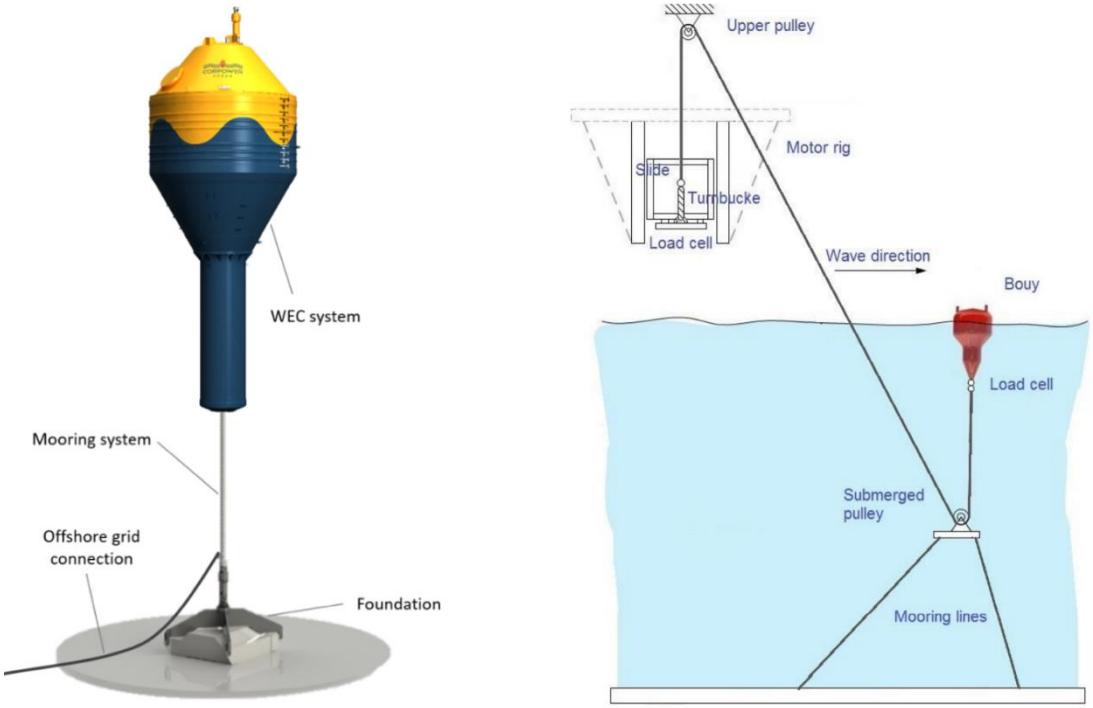

Figure 32: CorPower Ocean full-scale device rendering (left) and experimental setup for tank tests (right) [202]

In 2015, CorPower Ocean conducted, within the Marinet project, 1:16 scaled tests in the ECN Hydrodynamic and Ocean Engineering Tank in Nantes, France [202]. The device under study consists of a floater moored to the sea bottom by means of a pre-tensioned mooring system. The PTO, including the pre-tensioning and power conversion system, is located inside the buoy (see *Figure 32*). To facilitate and speed-up the testing campaign, a hybrid setup was used, where all the machinery were simulated by means of a motor rig located outside the water connected to the buoy by means of a rope and pulley system (see *Figure 32*). This is another example of constructing PTO model so that its effects on the scaled hydrodynamic sub-system are reproduced, rather than the PTO itself.

3.3.2 Energy transformation

3.3.2.1 *Overview*

Energy transformation comprises all the subsystems and components necessary to transform the captured hydrodynamic energy into the electrical device output. It often requires several transformation stages. These critical subsystems are commonly referred as Power Take-Off or PTO for short.

Many different typologies of PTO systems exist and often the PTO type are dependent on the WEC type. The main PTO typologies were introduced in deliverable D1.1 [1]. Figure *33* presents an overview of the different energy conversion paths of a WEC's main transformation stages.

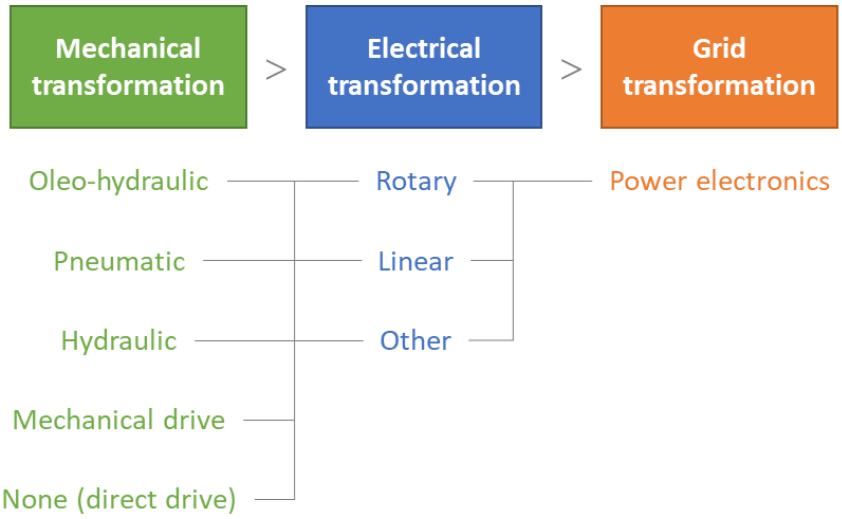

Figure 33: Schematic of PTO types

The main components per transformation stage and alternative path are as follows:

- Mechanical transformation:
  - Oleo-hydraulic system: Piston, Accumulator, Hydraulic motor
  - Pneumatic system: Air chamber, Air turbine
  - Hydro system: Reservoir, Hydro turbine
  - Mechanical drive system; Pulley, Rack-and-pinion, Gearbox, Flywheel
  - None (for direct drive PTOs)
- Electrical transformation:
  - Rotary electrical generator
  - Linear generator
  - Others: Dielectric elastomer generator, etc.
- Grid conditioning: Power electronics

Note that the greatest diversity of alternatives for energy conversion belongs to the mechanical transformation stage. The rotary electrical generators are mainstream, except for direct drive PTOs that often use linear generators or other unconventional methods such as the dielectric elastomeric generators.

Since the test rigs and experimental models required for component testing need to be tailored to each energy transformation path and PTO component, this review does not aim to cover all the potential combinations, but to provide key information about the experimental modelling approaches used in wave energy.

In this regard, the most common experimental modelling approach for PTO components is **Hardware-in-the-Loop (HIL) testing**. HIL testing is a technique where real signals from a test rig controller are connected to an emulated system that simulates reality, tricking the controller into thinking it is in the complete product. Test and design iteration take place as though the real-world system is being used. The advantage of HIL testing is that some subsystems can be real, while others are mathematical models. Figure 34 shows a generic HIL architecture used for testing energy transformation subsystems and components.

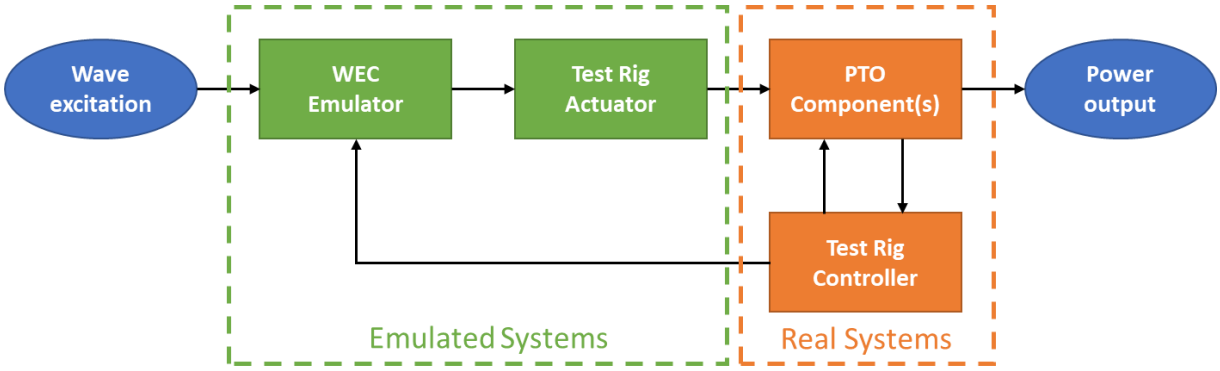

Figure 34: Generic HIL architecture

The WEC emulator software implements a numerical model of the device hydrodynamic interaction with the wave excitation forces to generate the primary power. The computed input parameters are then emulated through the test rig actuator. Several actuators can be used. However, based on the type of the primary actuation that the PTO component gets as an input, the experimental models can be broadly classified in two main groups:

- Linear actuation based on force and linear velocity commands
- Rotary actuation based on torque and angular velocity commands

The test rig controller sends command signals to and receives sensing signals from the real PTO component under testing in the bench. A signal data acquisition system is often used to compile the data during the tests together with various sensors, transducers, controllers and data loggers. These parameters are then fed back to the WEC emulator to adjust the primary actuation for the next cycle.

The power output transformed in the PTO together with other key parameters can be stored in a database for later analysis of performance and reliability results from the experiments.

One particularity of WECs is the wide variety of concepts under research that may require testing at some point of their development. Especially when describing mechanical transformation rigs, it is notable that many of the existing ones are related to a project and have been developed ad-hoc for testing a particular concept. This fact makes it complex to describe these rigs from a generic perspective. As they are specific and adapted to the concept for which they have being designed.

This is not the case of the electrical transformation test rigs, particularly with rotating generators. As the design of these subsystems is more established, there are different test rigs that have similar characteristics and can be used for most of the WECs under research.

The following sections present illustrative examples of PTO component testing according to the target transformation stage and type of actuation. Finally, the limitations to current experimental modelling approaches are briefly highlighted.

3.3.2.2 *Mechanical transformation rigs*

Oleo-hydraulic system

The Pelamis WEC is an example of a hydraulic PTO system comprising of pistons, accumulators, hydraulic motors and rotary electrical generators.

Experimental tests were conducted on a full-scale PTO test rig, where a 1:1 replica of a Pelamis PTO physical module was created, with all its components, and actuated via an

external set of hydraulic cylinders that replicated representative load scenarios (see Figure 35: The Pelamis PTO module full-scale test rig [203]).

Figure 35: The Pelamis PTO module full-scale test rig [203]

This test rig was developed mainly for validating the functional numerical models of the PTO and control modules, but not for testing reliability and durability of the oleo-hydraulic cylinders or other hydraulic components.

Other wave energy developers have designed and realised similar in-house experimental models. For instance, the WaveStar full scale test-bench also used a hydraulic cylinder as a linear actuator for testing the oleo-hydraulic PTO components. A schematic of the WaveStar test rig is presented in Figure 36.

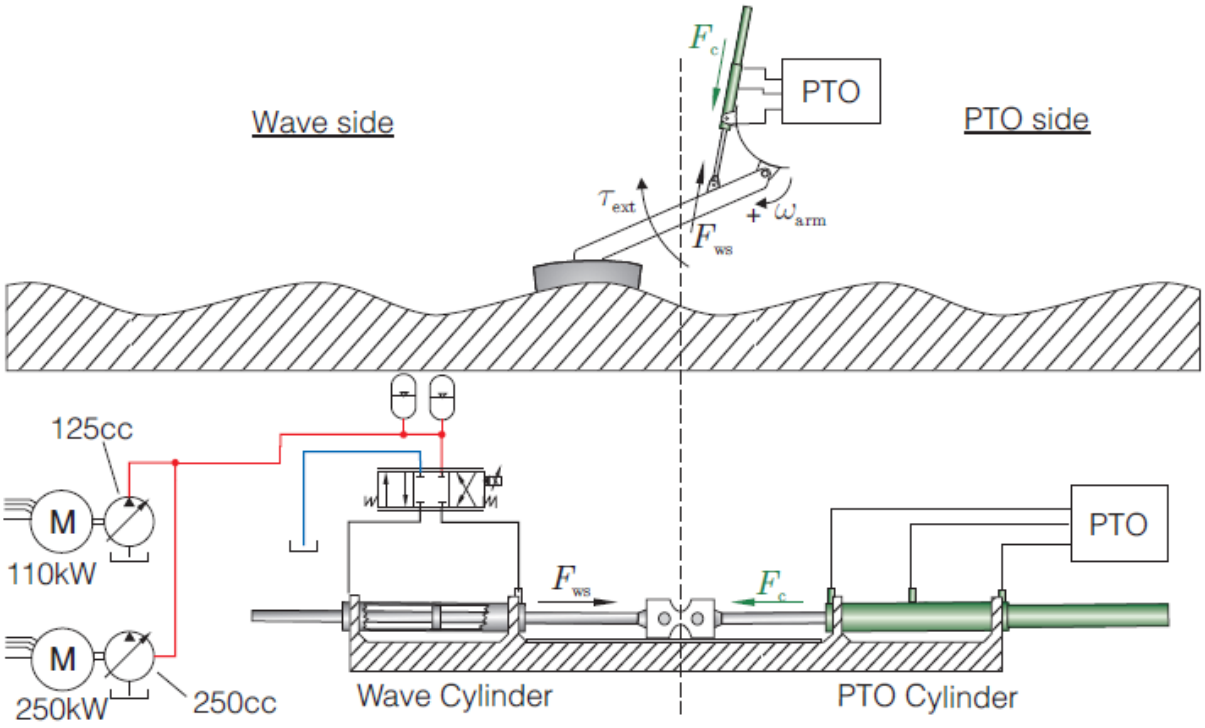

Figure 36: WaveStar PTO module full-scale test rig [204]

Note that both examples use full-scale experimental models since they were built at an advanced development stage of the technology.

Pneumatic system

The oscillating water column (OWC) concept is probably one of the first commercial application of wave energy, namely in navigation buoys. The PTO comprises an air turbine, normally of a self-rectifying form, so that whether the collector is exhaling or inhaling, the turbine is driven in the same direction.

IST developed a 55 kW V-Flow Turbine Lab to experimentally test air turbines and generator sets under unidirectional variable flows within the H2020 OPERA project, see Figure 37 [205]. The variable flows are accurately reproduced with a calibrated air flow valve connected to the radial fan which is forcing the air through the turbine.

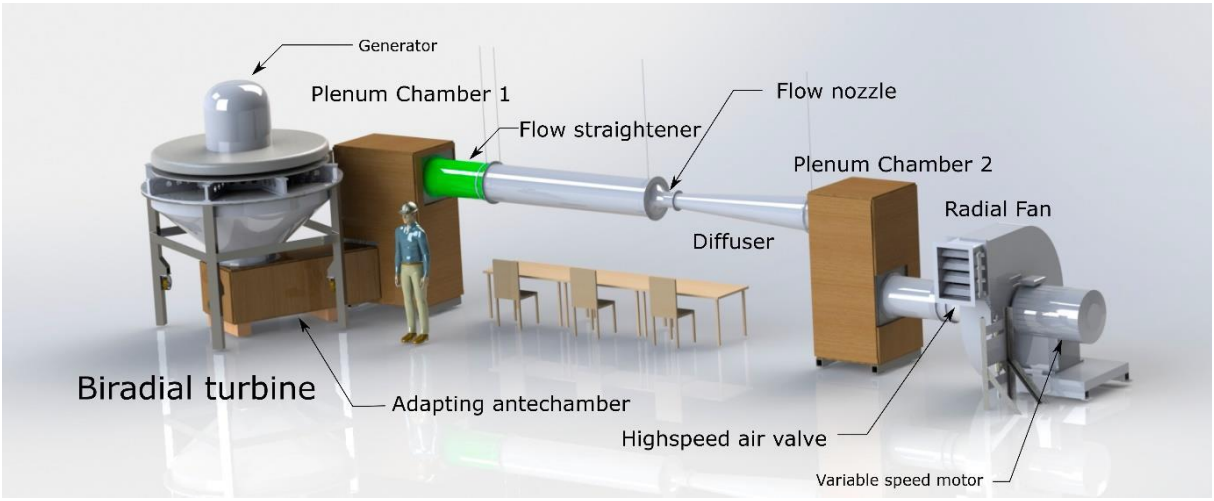

Figure 37: IST 55 kW V-flow turbine test rig representation [205]

The test rig comprises eight major components:

1. Horizontal adapting antechamber. It guides the air flow from the air turbine to the first plenum chamber at low speeds.
2. First plenum chamber. It is designed to significantly reduce the air speed and swirl motions which impairs the correct pressure measurement.
3. Honeycomb flow-straightener. It is required to further minimize the air swirl.
4. Calibrated flow nozzle. It measures the air flow rate through the differential pressure principle.
5. Diffuser, designed to recover kinetic energy.
6. Second plenum chamber. It was devised not only to work as an elbow and connect to a duct at the ground level but also to the smooth out any pressure wave that might be produced by the rapid closure of the high-speed valve.
7. Radial fan. The air flow rate and pressure gradient are imposed by a 55-kW radial fan that is connected to the plenum and controlled by a frequency converter.
8. Automated air valve. It can reproduce the pressure signals imposed by a computer before discharging air onto the atmosphere.

The experimental model can monitor several parameters. The differential pressure at the nozzle together with the air atmospheric pressure and temperature are acquired to calculate the instantaneous air flow rate. A variable frequency drive controls the radial fan rotation speed. A control algorithm imposes the fan's pressure head and air flow rate together with the position control of the air valve attached to the discharge. The static pressure can be measured on six different locations of the air turbine. On each stator (entry and exit), the pressure was measured firstly near to the stator external diameter and secondly close to the turbine rotor. At the conical adapter, two static pressure plugs measure the turbine pressure drop. The turbine-generator is then controlled either in rotation speed or torque through an analogic signal, which subsequently allows advanced control strategies for average power output maximization. For turbine vibration monitoring, two accelerometers are coupled to the turbine structure and the data signal is acquired.

This test rig was developed for dry testing of a biradial air turbine and fine-tuning of its control before installing it at the Mutriku wave power plant for further testing and later on a floating OWC prototype for the final demonstration. The test rig monitored vibration levels that might lead to a mechanical failure if exceeded a certain threshold during the short test programme.

Mechanical drive

EMEC's HIL PTO testing rig provides a sequence of speeds and loads to a power take off by an actuation device, simulating waves on dry land for the purpose of accelerated testing of mechanical PTO systems for WECs [155].

The test rig can also be used to adjust the PTO and the controller parameters to validate assumptions for performance optimisation and survivability modes. Furthermore, it can be used for fatigue, loads or efficiency testing of a specific sub-system of the WEC. The rig has a stroke length of 3.5m, a rated velocity of 2.7m/s and a maximum rack force of 207kN.

Figure 38: Layout of EMEC test rig [155]

Another example of a mechanical drive model is the HIL test rig for the ISWEC PTO consisting of a gyroscope, see Figure 39 [207]. This test rig replicates the motion induced by the waves on the hull. The pitch motion activates the gyroscopic system and it is the main responsible for power absorption. The mechanical structure of the test rig is composed of a fixed base carrying a rocking platform which supports the gyroscope and rotates about a horizontal axis giving rise to the pitching motion and therefore simulating the action of waves. The system is acted by a brushless motor coupled to two sequential gearboxes that provide a total gear ratio of 629:1. The motor can work with either a time history of pitch motions (open loop) or regular waves (closed loop). A PID controller minimises the error within the pitch command to the rocking platform and measured signal. A synchronous machine controls the resisting torque in the output axis of the gyroscope. Finally, the flywheel speed can also be adjusted by the test rig controller.

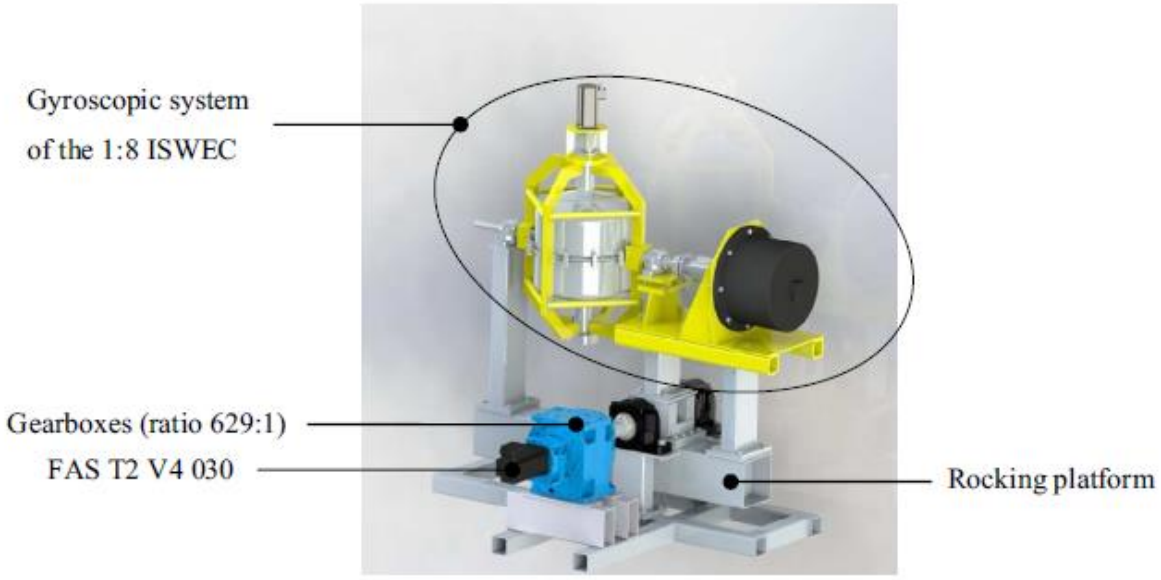

Figure 39: Layout of the ISWEC test rig [207]

The test rig was designed to reproduce the rated conditions of the 1:8 ISWEC prototype. Its main purpose was to research PTO control strategies to enhance power output on different sea conditions. No durability tests were foreseen.

Two partners from the VALID project have built test benches for laboratory testing of specific PTO components. The HIL test benches can simulate the reciprocating motion of a shaft and are used for the reliability of seals. More details are provided in section 4 which describes the modelling approaches of the user cases.

3.3.2.3 *Electrical and grid conditioning rigs*

Direct drive generator

Two H2020 projects have developed laboratory rigs for testing their innovative direct drive PTOs.

On the one hand, the IMAGINE project [208] which aims at developing the Electro-Mechanical Generator (EMG), a PTO concept for wave energy applications able to convert slow speed, reciprocating linear motion into electricity. The EMG is based on the integration of a recirculating ballscrew and a permanent magnet generator. The ballscrew is a mechanical device in which the balls, acting as low friction load-carriers, efficiently convert the low-speed linear motion of the screw into a high-speed rotary motion of the nut. Permanent magnets are integrated in the nut, which acts thus as rotor of the electrical generator.

This PTO test rig is an evolution of the one used in the EMERGE project [209] but at a larger scale (from 100 kW to 265 kW) and with advanced capabilities. It allows both dry and flooded tests to be carried out. The main objective of the testing is to evaluate the PTO performance at a wide range of operating conditions (in terms of axial velocity and electrical damping factor). Besides, durability and reliability are also tested by mean of high load accelerated endurance tests. Figure 40 shows an overview of the test area and test bench.

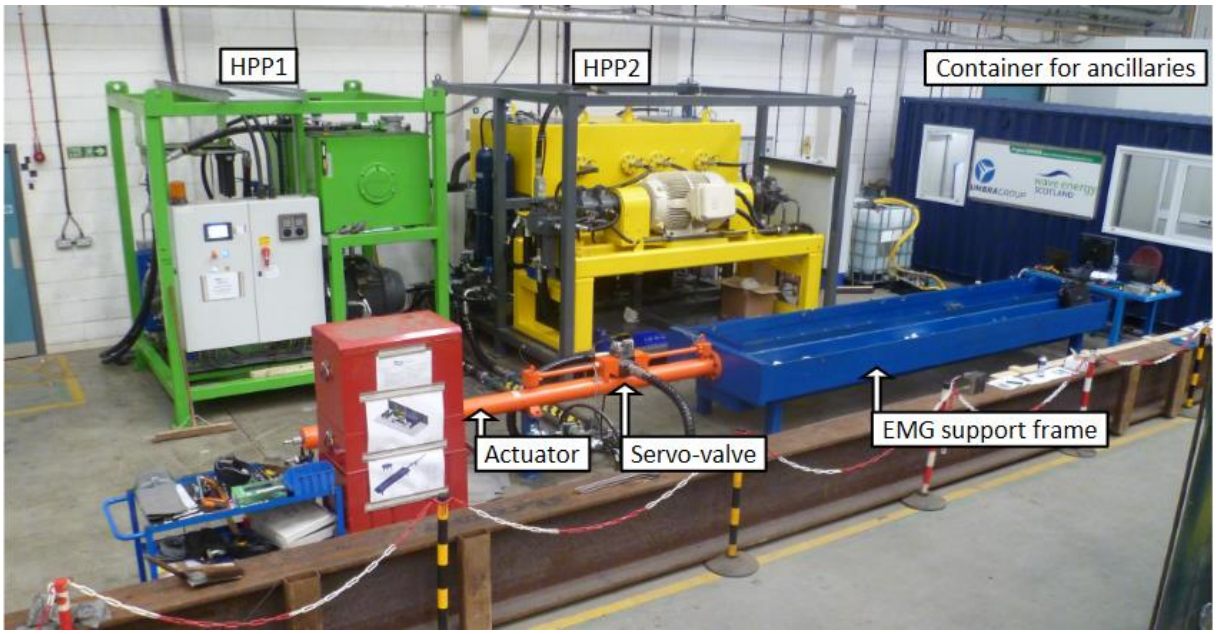

Figure 40: Overview of Test Area and Test Bench [209]

On the other hand, the SEA-TITAN project, which aims at developing an innovative Direct Drive Linear Electric Generator. The three-phase linear generator is based on azimuthal switched reluctance technology. The 50 kW test rig developed in this project comprises three main systems [210]:

- An actuator, in order to mechanically move the linear generator according to the conditions determined by the wave energy converter (WEC) to be emulated, as well as the sea location to be reproduced in the lab;
- The power electronic converters and cabinets that control and feed both the generator and the actuator; and
- The hardware-in-the-loop (HIL) scheme, a control set in order to reproduce different wave scenarios in order to validate the PTO as well as the control platforms developed by the different WEC technology developers.

The WEC emulator provides the force command, based on the generator velocity and control strategies selected. This force reference is used by the linear generator control to ensure that the generator force command is equal to the mechanical force developed by the linear PTO. In order to guarantee the usefulness of the HIL scheme, the generator control must be calibrated properly. The force command is translated into currents when passed through a look-up table, and the gate signals of the IGBTs are generated via a hysteresis band control. The grid connection allows for injecting the generated energy to the network, as well as supplying power to feed the phases of the linear generator. Figure 41 shows the design of the laboratory test rig and facility. Power converters and cabinets are positioned so they can be opened for revision and operation issues without interfering with other equipment. The control platform (HIL) is in a separate room within sight of the test rig.

This project has received funding from the European Union's Horizon 2020 research and innovation programme under grant agreement No 101006927.

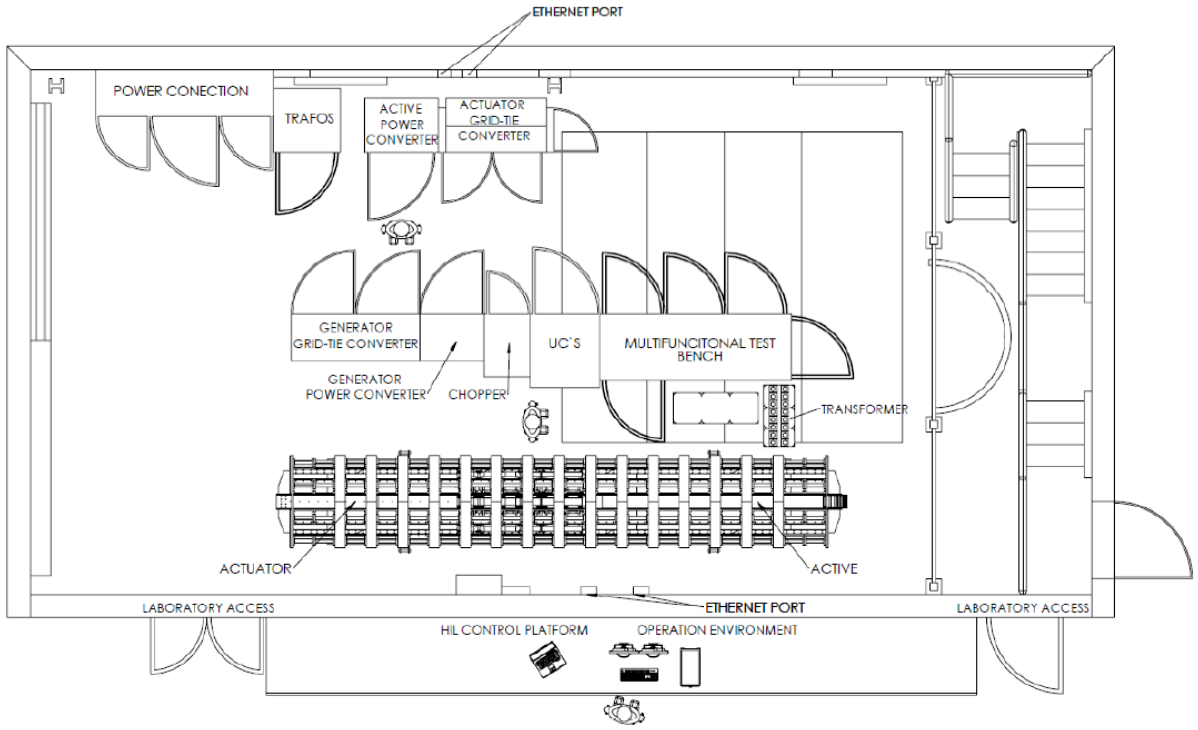

Figure 41: Laboratory test rig equipment and facility [210]

Experimental model testing is mainly aimed at validating the efficiency of the innovative PTO solution under operational conditions. However, other testing procedures may be carried out such as thermal performance (e.g. power electronics, generator coils and bearings), endurance tests and grid compliance.

Conventional rotary generator

The Electrical PTO-Lab is a turbine emulator to reproduce the mechanical output of an ocean energy device/wind turbine. It consists of a HIL test bench for grid connection of wind turbines and ocean energy converters, focused on testing electrical components (i.e. electrical generators and/or power converters and associated control). This test bench simulates the power production of a device with a rotary movement and it can be divided into two key parts [211] [212]:

Emulated part: Devices that capture ocean energy and transform it into rotating motion can be emulated by these facilities. An electrical motor, configured as the ocean energy prime mover, is used to re-create the dynamic response exhibited by an ocean energy device given a specific set of input conditions. The prime mover motion is emulated by drive-controlled electrical motor which is usually coupled to a flywheel via a gearbox.

Real part: This is the physical equipment on the electrical Power Take-Off side. This equipment is an exact scaled replica of the equipment that would exist on the full-scale ocean energy device. The connection between the emulated part and the physical part of the Rotary PTO is the mechanical shaft between the motor and the generator. A full-scale ocean energy device with rotary power take off will include:

- Electrical generator
- Power electronics
- Sensors

- Control
- Cables to connect to the utility grid

The scaled facility includes each of these elements.

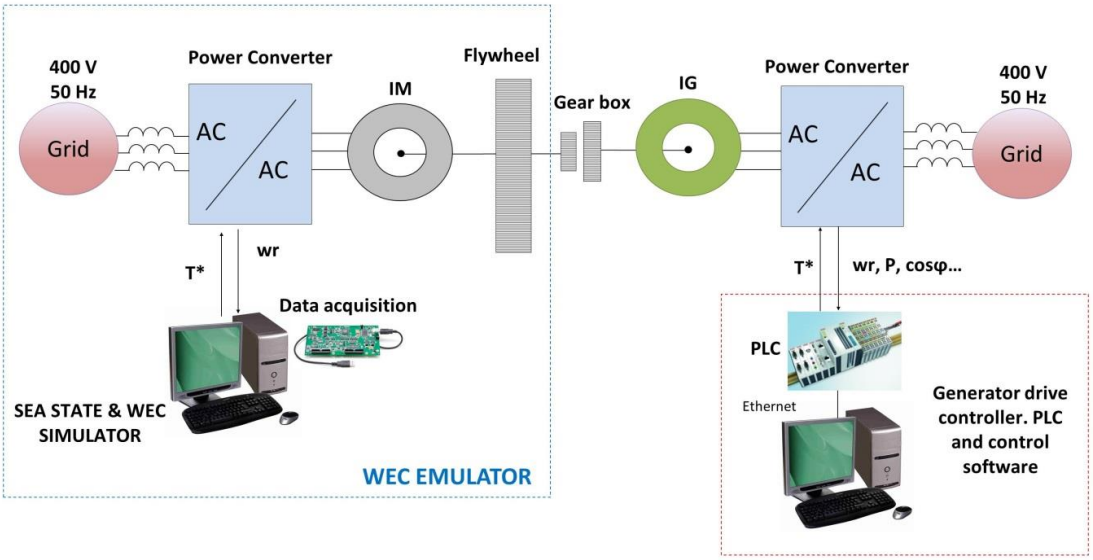

Figure 42: Typical configuration of a testing infrastructure [212]

Figure 42 shows the typical configuration that a generic testing facility could have. The first part surrounded by a blue dotted square represents the emulated part described above. It would have the same behaviour of the real ocean device, where the shaft between the flywheel and the gearbox would behave as the shaft of the real device. The second part of Figure 42 is the real part.

These kind of electrical test rigs with rotary generators such as the HMRC Rotary Rig, SINTEF's SMARTGRID LAB and TECNALIA's Electrical PTO were part of MaRINET and MaRINET2 projects. Round Robin tests were carried out in several facilities in order to tests the accuracy and suitability of HIL testing of WECs [213].

Figure 43: Electrical Rotary Rig HMRC-MaREI [214]

More details are presented in Section 4 describing the experimental models of the three user cases.

Dielectric elastomer generator

Dielectric elastomer generators (DEGs) are soft electrostatic generators based on low-cost electroactive polymer materials. These devices have attracted the attention of the marine energy community as a promising solution to implement economically viable WECs.

Scuola Superiore Sant'Anna has developed a small scale HIL test rig (approx. 1:30 and 1:10) that replicates in a laboratory environment the realistic operating conditions of CD-DEGs (Circular Diaphragm DEG) integrated in OWC devices, while drastically reducing the experimental burden compared to wave tank or sea tests [215].

The HIL simulator is driven by a closed-loop real-time hydrodynamic model. The HIL system combines a hardware scaled implementation of the OWC air chamber, the DEG and its power electronics. A mechanical hardware emulates the action of the water column on the chamber and a software environment simulates the OWC hydrodynamic behaviour and executes the DEG's electrical control logics. The mechanical actuator is based on a vertically mounted pneumatic cylinder that has been purposely designed and built. The linear motion of the piston is driven by a ball-screw stage with maximum force of 4500 N, that is actuated by a brushless motor that features rated continuous power of 2.4 kW, continuous torque (at stall) of 8.67 Nm, and maximum speed of 4590 rpm. This test rig was calibrated with data of a U-OWC plant with CD-DEGs, tested at the NOEL in Reggio Calabria.

Figure 44 shows a schematic of the experimental set-up for the HIL testing of DEGs.

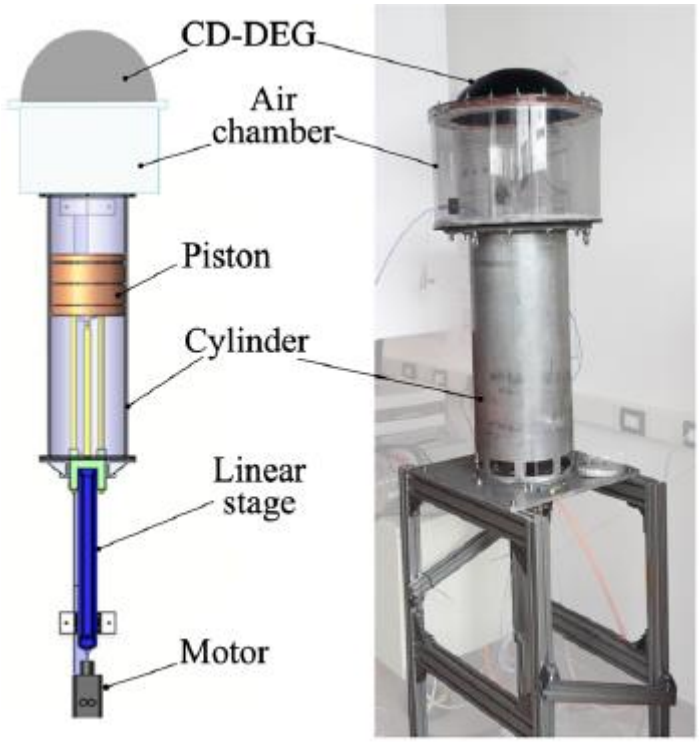

Figure 44: Schematic drawing and picture of the experimental set-up for HIL testing [215]

This test rig provides a powerful tool to test the PTO efficiency of different CD-DEGs configurations and control strategies subject to realistic operating conditions at an early development stage of the technology before sea testing and technology upscaling.

3.3.2.4 *Special test rigs*

SWEPT lab

It is a mobile test lab for WEC PTOs developed by Sandia National Laboratories (Figure 45). This test rig can be used for both linear and rotational PTOs, multiple degrees-of-freedom and independent control. The laboratory can simulate the dynamics (i.e. inertia, damping, stiffness, multi-body links) of full scale WECs, as well as take input from waves and wave-body interactions. The actuator power ranges 5 to 500 kW and up to 2 Hz.

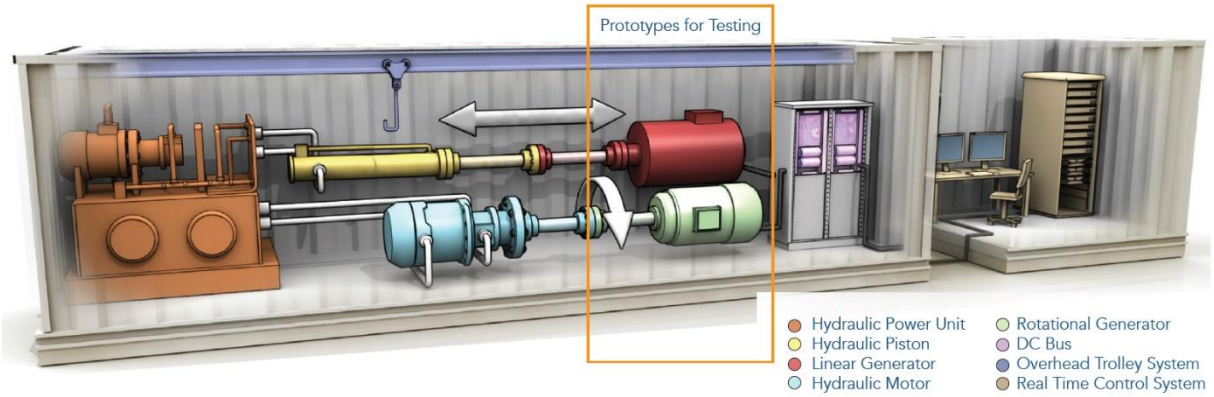

Figure 45: 3D representation of Sandia's mobile test lab [216]

This system allows for PTO studies including system identification, real-time control, reliability analysis and grid interface simulations.

Dual HIL

Funded under the same H2020 call as the VALID project and started at approximately the same time, the H2020 IMPACT project is developing a Dual Hardware-in-the-Loop (DHIL) test rig [217].

The DHIL platform will combine one rig for testing the entire WEC drivetrain either linear or rotary, from the mechanical input to grid compliant power, and another rig for testing structural components and mooring lines, either in dry or wet environment.

State-of-the-art PTOs are often inefficient when working outside design conditions and prone to failure. Other subsystems such as the control system, power management and moorings are deemed to be critical in terms of reliability, that is their failure may cause damages and serious consequences on the overall device operation. The current development approach for WEC technologies usually sees all these subsystems tested in isolation at different scales and various levels of technology maturity due to testing restrictions, economic and time constraints. Techno-economical aspects, optimization and control functions are often considered as consecutive independent phases while they are interlinked.

The novel methodologies proposed by the IMPACT project will reduce the test duration with respect to a typical endurance tests and focus on key aspects such as reliability, performance and survivability.

3.3.2.5 *Additional considerations*

Scaling issues

Laboratory scaled testing may bring many advantages in terms of investment costs in particular for early stages of wave energy technology development. However, the method of scaling must be carefully selected to correctly represent the dominant forces of the device under test because it is not always possible to achieve perfect similitude (i.e. geometric, kinematic and dynamic). Several force ratios have been proven of interest in engineering problems. Since surface waves in the ocean are gravity driven, Froude is used as the typical scaling rule.

The power range of the full-scale device and that of test rig will largely determine the test rig scale [212]. The peak mechanical power at the test rig must be within the power range of test equipment. This is usually the first step in determining a suitable scale for the experiment. Once a first guess at a suitable scale has been determined, other parameters need to be checked to ensure they are within the physical limits of the test rig.

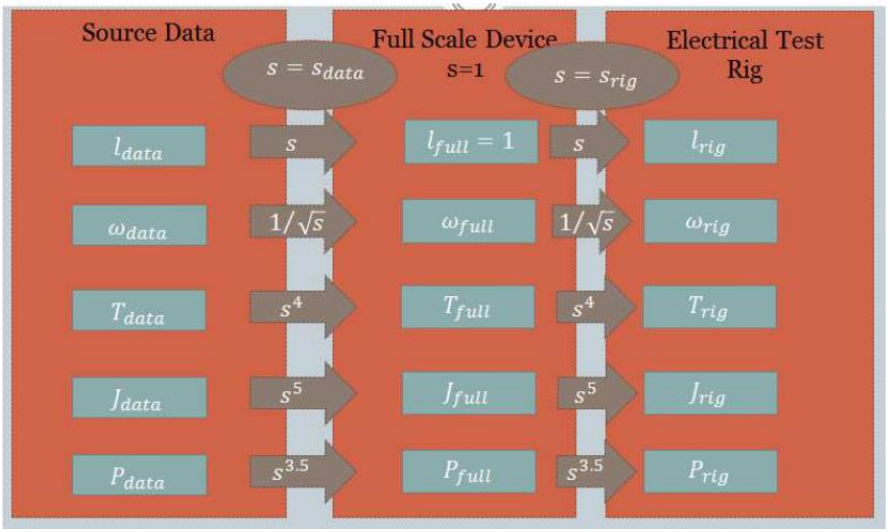

Figure 46: Important parameters to consider for electrical testing [212]

Given these physical limitations, certain devices may not fit every laboratory test rig. For instance, if the speed and torque parameters do not fit in an electrical experimental model, then a virtual gearbox can be added. The scaled model running on the system controller e.g. Programmable Logic Controller (PLC) can operate at a different speed and torque to that of the electrical test rig. Another strategy could be to add inertia to the virtual device model that is controlling the motor.

Simulation of mechanical loads

PTOs can be placed either in a horizontal or vertical position. For instance, heaving buoys are commonly coupled to linear PTOs that move up and down. However, testing components this way and reproducing the same mechanical conditions in terms of transversal loads, leads to a very expensive testing infrastructure and sometimes even limitations due to the height requirement. Therefore, it is common to design the PTO test rigs in a horizontal position. On the other hand, PTOs mounted on floating WECs are exposed to accelerations that cannot be easily reproduced in horizontal laboratory tests rigs.

We must be aware that the mechanical conditions during these tests are not equivalent to those during the real operation and test cases should be selected to ensure the components will never behave in harder situations.

Multiple failure mechanisms

The experimental model set-up might limit the failure mechanisms that can be tested at laboratory. Some test rigs are designed for a dry environmental whereas other can also operate in a flooded situation which can be closer to the real open sea conditions.

Moreover, the environmental effects such as humidity, salinity, temperature, biofouling might play an important role in the reduction of useful life of PTO components. It is therefore needed to carefully assess whether these phenomena should be combined, or it is sufficient to be tested separately.

Degradation and failure models are discussed in Section 3.3.3.

Testing procedures

Laboratory testing of PTOs can be useful for various purposes such as proof of concept testing, numerical model validation, performance optimization, power quality, reliability, endurance, climate and/or accelerated testing.

Nevertheless, the results are highly dependent on the system identification tests aimed at calibrating the dynamics of the test rig actuator and PTO system.

As recommended in the CEN-CENELEC Workshop Agreement draft document [218], testing procedures should include the test rig set-up and calibration of the actuators. Furthermore, actuator performance should be assessed by means of their frequency response functions, understanding how well the measured signals (e.g. force or torque) from the actuator respond to their respective desired commands. This strategy should also be applied to the characterization of PTO system dynamics, for instance to identify resonant behaviour. Uncertainty ranges should be considered in cases where only limited amounts of data are used to characterize the PTO over a broad range of operational conditions. Figure 47 shows an example of this characterization for a linear actuator.

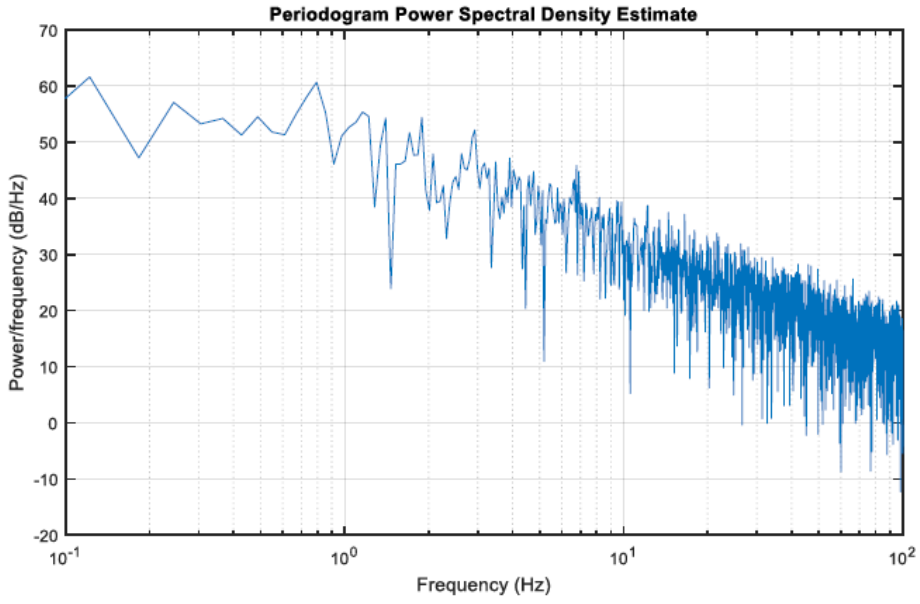

Figure 47: Input signal for system identification of actuator test system [219]

3.3.3 Degradation and Failure

Degradation is the gradual lowering state of the material and/or product performance. Failure is when something breaks or stops working. Failure can be the result of degradation or the result of a sudden event such as overloads or pre-existing defects.

This section focusses on the material and mechanical aspects of degradation and failure. This also includes the growth of marine organisms on WECs as it has a direct and detrimental effect on material and mechanical performance.

Experiments on the gradual deterioration are the most challenging. One reason for this is the large uncertainties related to gradual degradation process in it-self [183]. The others are the practical difficulties of performing experiments in degrading environments for long periods of time. It is the purpose of the VALID project to develop methods that combine numerical simulation to make such experiments faster and less costly.

3.3.3.1 *Critical subsystems*

The WEC subsystems that are critical and subject to mechanical degradation are categorized in this section. The distinguishment into these categories are general and made to serve the different mechanical degradation mechanisms. In D1.1 [1], the critical systems and components are listed in more detailed for the VALID user cases. A comprehensive report on reliability relating to different subsystems is also available from the RiaSor projects [183].

Structural

The structural parts of a WEC are the features that bear the loading on the product or the device. Loading can be self-weight, inertia forces, external forces and internal forces. Failure of structural parts can cause major malfunction or total loss of the WEC. The load bearing parts are typically beams, trusses and shells. Also joints, e.g. bolted joints, welds, adhesively joined surfaces belong to the structural parts.

Failure modes of the structural parts are mechanical failure in the form of instability, yielding and fatigue. Structural parts can also be subjected to corrosion if exposed to the ocean environment.

Hull, casing and panels

These parts typically have the purpose of shielding the product from the environment, prevent access or provide a visual appearance. These parts can also, in the case of WECs, have the function of properly transferring forces from the incoming waves to the structure for energy conversion. Malfunction of these features will require repair and possibly cause further damage to other subsystems. In some cases, hulls are not load bearing, so forces are instead supported by other structural parts. In other cases, hulls are designed to bear the main loading on the product. In this case, the hull becomes part of the structure, necessitating the aspects of the structural parts described above to be applicable.

Since these are outer parts, constantly affected by the harsh ocean environment, corrosion and biofouling are major causes of deterioration as described in sections 3.1.4.3 and 3.1.4.4. Biofouling also has the adverse effect of increased load levels on the exterior parts due to extra weight and drag in the water.

Machinery

The machinery in a WEC is all the moving components that take part in the energy conversion, from the collection of the energy in the waves, to the powertrain that transmits the mechanical energy to an energy converter such as a generator. Degradation and experimental modelling of generators is described in Section 3.3.2. A WEC can also have supplementary machinery for functions such as pre-tensioning and force actuation to sync movement of the buoy to the incoming waves, e.g. CorPower's Wavespring [220]. For WEC developers, the machinery is usually the most important part. Furthermore, the working principle is often unique and the core innovation of the developing WEC company. This results in a lack of knowledge and experience which makes development and designing slower and more difficult since design guidelines do not exist. The hybrid testing to be developed within the VALID project is foreseen to greatly amend this issue.

Existing design practice for machine parts can be used for WEC machinery. With that said, it needs to be emphasized that considerable uncertainty is added due to the novelty of WEC technology which needs to be addressed with statistical methods [183]. A deterioration mechanism of large impact in WEC machinery, is wear of seals since components of the moving machinery (e.g. pistons, shafts) is partly in contact with the sea water, e.g. the CorPower and WavePiston WEC designs [200], [221]. These components are also then subjected to corrosion and biofouling.

Cabling

Cables are integral components of a WEC farm [222]. They are necessary to transfer the energy collected from a WEC to the grid. Since most WECs are moving with the motion of the waves, the cabling will be constantly moving. This is referred to as dynamic cables. The resulting cyclic straining of the cable material causes degradation of the cable that can decrease the electrical conductance causing lower power output. Further degradation can cause failure of the cable resulting in costly downtime and repairments.

Biofouling is major concern to the cables as large amounts of marine growth is added to the cable making it heavier and subjected to extra drag which in turn increases mechanical loads on the cable.

Mooring

The mooring secures the WEC device to the seabed. WECs that work with energy conversion that relies on external force transfer to the seabed have moorings that are subjected to very large securing forces in the seabed. These forces are also cyclic causing fatigue deterioration [91]. Exposure to the sea water makes moorings also subjected to corrosion and biofouling. Failure of moorings cause downtime and urgent repair or even risk of total loss of the WEC.

3.3.3.2 *Fatigue testing*

Experimental modelling of fatigue is conducted by applying cyclic loading that represents a loading that one wants to investigate or design against. Fatigue testing can be categorized in two different types. The most common type is to apply a varying load on a specimen until it breaks. The other and more advanced type is to monitor a crack as it grows during cyclic loading. This type is called fracture mechanical testing [223]. The first type is a more common approach in engineering, although some uses of the fracture mechanics approach exist for WEC applications [224].

Fatigue testing can be performed on smaller material specimens for which it exists a multitude of standards. This testing on small specimens is valuable for determination of material

properties and further understanding of the fatigue phenomenon. This level of testing is not the focus of the VALID projects where rapid product development is the topic.

Component and product testing [90] with respect to fatigue is instead what is foreseen to be used in the VALID project. This type is usually needed in mechanical engineering to design durable products. The fact that fatigue cracking is initiated at stress concentrations due to the product geometry, further makes component/product testing necessary. Joints, e.g. welds, rivets and bolts are susceptible to fatigue. Environmental effects on the fatigue should also be realistically investigated in component testing.

Methods to combine numerical modelling of fatigue with testing is commonly employed in the automotive industry [183]. A design practice is to measure loading (e.g. accelerations in the vehicle suspension) when the vehicle is driven on a test track with representative road conditions. Testing is then performed on a vehicle where actuation is made on the suspension to simulate the driving on test track. In this way the durability of a vehicle can be adequately tested and validated. The downside is that this testing procedure is expensive and time consuming. To make the development faster and more efficient, numerical simulations are employed to replace some or all steps in the vehicle durability modelling. MBD and FEA methods, as mentioned in Section 3.2.5, can be used to numerically simulate the vehicle dynamics on a virtual road. FEA can be used to evaluate the stress and strain in the vehicle structure to evaluate durability and fatigue damage [225].

The described numerical simulation method for fatigue design used in the automotive industry is similar to the envisioned virtual hybrid testing to be developed in the VALID project. A major issue to address in fatigue testing of components and products is acceleration of the testing. In real operations, cyclic loading is applied over time scales of several years which is impossible to conduct in experimental modelling. The most common way to accelerate fatigue is to exploit the behaviour that the large load cycles cause the most fatigue damage as described in section 3.1.4.1. Fatigue tests can therefore be accelerated by testing only the load cycles that causes most of the damage. Since the aim is to quantify the fatigue life, this can be referenced to as characterization testing as described in the VALID document D1.1 Accelerated Testing Requirements [1].

The WECHULL project (www.wechull.se) addresses testing of composite materials for WEC applications. The levels of testing to be performed are both on material specimen level and component level. Also, hydrodynamic interaction modelling using fluid structural interaction (FSI), as similarly described in Section 3.2.3, is to be used to get load levels for mechanical deterioration.

Both fatigue testing (see Figure 48) and numerical modelling of dynamic movements of the cables were addressed in the project "R&D of dynamic low voltage cables between the buoy and floating hub in a marine energy system" [222]. A current project following the same topic is the OceanERA-NET project Seasnake (oceanenergy-sweden.se/seasnake/). This project features the cable fatigue test bench facilities of The University Gustave Eiffel. Other test facilities for cable testing are Dynamic Marine Component (DMaC) Test Facility of University of Exeter and the cable test rig available from Offshore Renewable Energy (ORE) Catapult.

Figure 48: Fatigue testing at RISE in the project "R&D of dynamic low voltage cables between the buoy and floating hub in a marine energy system" [222].

3.3.3.3 ***Wear of Seals***

To test the wear behaviour between two materials, various testing procedures are available [226]. One test is the "pin on disc" test. This test is fairly simple where a stationary pin is pressed against a rotating disc. In this test, contact force, sliding speed and environmental conditions can be controlled. Results are wearing rate, coefficient of friction and other material investigations of the worn surfaces. The pin on disc test can be categorized as the material testing level where wear properties of certain material combinations can be investigated. Wear maps are typically made from pin on disc tests.

To test wear of seals and their tightness, component testing is needed where seal geometry and a fluid pressure can be included. These types of tests are closer to the topic of the VALID project where product development is made with combined experimental and numerical modelling. Material testing such as pin on disc are valuable for material selecting and laying a foundation for understanding of the physical mechanisms.

Test rigs for component level testing of seals are candidates to be employed by some user cases in the VALID hybrid testing framework. Within the Waveboost project, CorPower has built test rigs for dynamic seals [221]. The test can simulate the reciprocating motion of a shaft on which a seal is containing a pressure up to 300 bar (see Figure 49). The second test rig for seals is built by WavePiston. It is similar to the CorPower test rig. A special feature of the WavePiston test rig is the ability to model the ocean environment by pumping temperature-controlled pH buffered artificial sea water around the seals (see Figure 50).

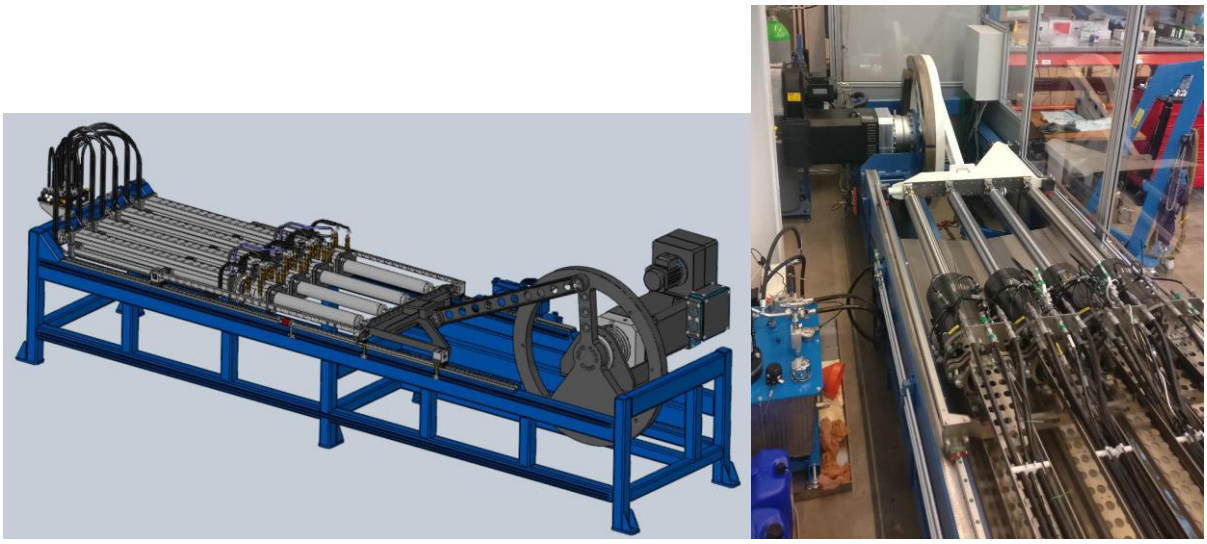

Figure 49: The test rig from the Waveboost project for experimental modelling of wear of dynamic seals [221].

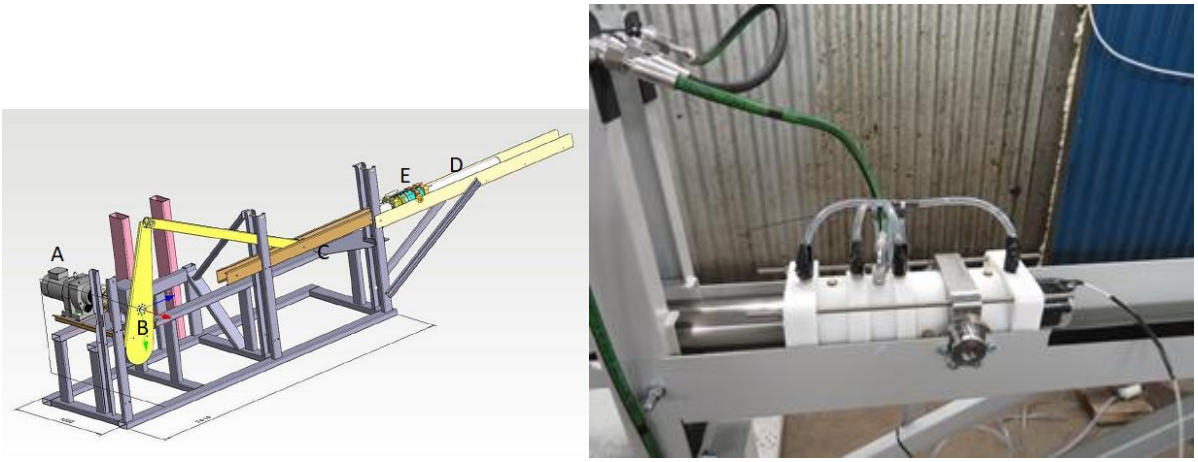

Figure 50: The WavePiston test rig for experimental modelling of wear of dynamic seals.

3.3.3.4 ***Corrosion tests***

Corrosion test methods have been developed over a long time and are now standardised by ASTM and ISO. Many different accelerated tests exist depending on what material you want to study e.g. metals or alloys (ASTM G44, ASTM B117, ISO 9227), inorganic coatings (ISO 10289), organic coatings (ISO 11997-1, ISO 12944-6)[227]–[232]. There are electrochemical tests for detailed studies of corrosion rates and processes (ASTM G 5, 59, 61, 100, 150.) [233]–[237]. Classification societies such as DNV GL have developed standards and recommended practices for corrosion protection in marine environments for offshore wind farms including a variety of tests and design recommendations, based on experiences from the oil and gas industry [238]. The accelerated corrosion tests often recommended, see Table 10, include the standard ISO 12944-9 "Paints and varnishes – Corrosion protection of steel structures by paint systems – Part 9: Protective paint systems and laboratory performance test methods for offshore and related structures"[239]. These tests are designed for painted steel and require tests with a duration of almost half a year of exposure. They mainly make sure that the paint systems are controlled for quality.

Table 10: Recommended qualification tests for painted steel in offshore and related structures adapted from ISO 12944-9 (table 4.)[239].

Test	Scribe line	Environment of corrosivity category CX (offshore)	Environment of combined corrosivity category CX (offshore) and immersion category Im4 (splash and tidal zones)	Environment of immersion category Im4
Cyclic ageing test	Yes	4 200 h	4 200 h	—
Cathodic disbanding (ISO 15711, Method A, unless otherwise agreed)	No (artificial holiday used instead)	—	4 200 h	4 200 h
Sea water* immersion (ISO 2812-2)	Yes	—	4 200 h	4 200 h
* Artificial sea water as defined in ISO 15711:2003, Table 1.				

Salt spray corrosion tests such as ISO 9227 and ASTM B117 are often well designed for rapid analysis of pores, discontinuities, and damage in organic and inorganic coatings [228], [229]. They also work well for quality control purposes where components are coated with the same coating or for comparison of different coating application processes. Comparison between different coatings on the other hand, can only be made if the coatings are adequately similar in nature. Another weakness is the lack of correlation with long-term performance of different coatings due to the corrosion stress in the tests is significantly different from what is encountered in practice. For atmospheric corrosion, the cyclic salt spray tests with intermittent spraying and controlled climate (wet and dry atmosphere) and is often used to improve the correlation with real climate stresses caused from wet/dry exposure. These tests are frequently used in the automotive industry where OEM's quality control and prove the corrosion protection performance for their products (components) meet the requirements. Here, the components are typically exposed to an accelerated exposure test with cyclic salt spray for a duration of six weeks and a visual examination rank the corrosion performance based on visual corrosion.

For component and systems testing which is of focus in the VALID project one needs to define clear criteria for evaluation after the finalised corrosion test. It can be defined, for example as in ISO 10289, as a rating of the coating to protect the underlying base metal from corrosion based on area of the substrate that exhibit corrosion. This is important as it rates the degree of protection after a time in a certain corrosion test and can be used for comparison of different coatings and as a general proof of acceptable protection criteria to meet. Other evaluation criteria of importance are that functionality (electrical or mechanical) is maintained after a corrosion stress has been applied and that no water or salt has leaked through protective seals. For electrical products and components IEC 60068-2-11 test Ka and IEC 60068-2-52 are often recommended practices which utilises continuous and cyclic salt spray tests, respectively [240], [241].

For marine environments artificial seawater can be applicable in corrosion tests instead of the more commonly used electrolyte of sodium chloride to simulate the intended environment more properly. One can go even further and utilise natural seawater as an electrolyte to better

capture degradation processes happening in field. However, one needs to realise the site-specific conditions and its limitations to the reproducibility of the tests. In general, as stated in many of the standards, natural-exposure trials/field tests should always be undertaking as it is clearly understood that artificial ageing will not necessarily have the same effect.

Two examples of corrosion testing for wave energy systems are shortly reviewed next.

- Corrosion testing for wave energy devices includes testing of paint systems and other coatings used for the device. These can be accelerated in the lab to serve as quality control. The tests can also be applied to other small parts or small-scale devices to test functionality after exposure to the harsh electrolyte of seawater. Field tests in the natural ocean environment are also very useful to gain knowledge from natural phenomena. The drawbacks from field testing are that there could be site specific features that are not found at other sites and that with the lack of acceleration factor it takes a long time.
- A PTO system with a cylinder immersed in seawater is commonly used for many WEC devices for generating power from wave action. These cylinders require smooth inorganic coatings that can resist wear, fouling and corrosion. In the Waveboost project, Corpower ocean and RISE performed some corrosion tests on laser cladded test pieces of a PTO cylinder. The corrosion tests were partly performed accelerated in the lab using natural seawater in a conventional salt spray test (ISO 9227) for 1,000 hours duration at 28 °C, see Figure 51. The other part was (not accelerated) at the field test site at Kristineberg Marine Research and Innovation Centre on the west coast of Sweden. The samples were immersed in seawater under a jetty for a total duration of 12 months, see Figure 52, protection of different laser cladded coatings served as an initial validation of the corrosion protection performance. However, one needs to bear in mind that the acceleration factor is unknown, the test pieces were not subject to any wear which can affect the corrosion protection. This test method will be further investigated in the De-RISK project Marine Growth | DE-RISK during 2021, where different electrolytes (sodium chloride, artificial sweater, and natural surface seawater) will be employed in an accelerated salt spray test with continuous spraying.

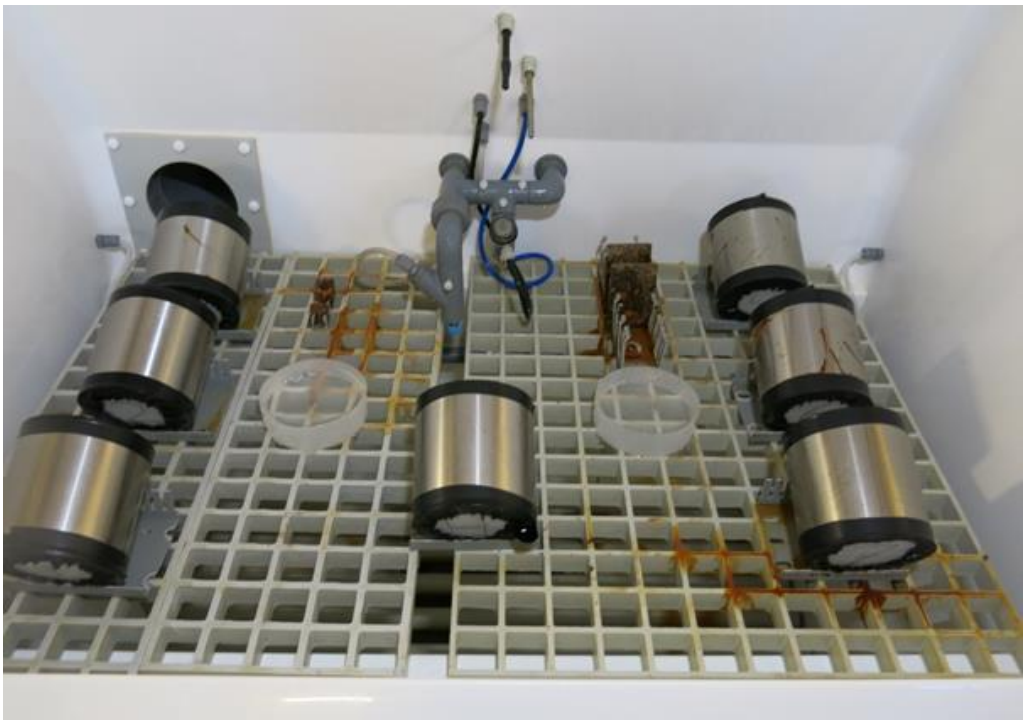

Figure 51: Overview picture of test pieces of laser cladded PTO cylinder in a salt spray test chamber during an accelerated corrosion tests using continuous spraying with natural seawater at a temperature of 28 °C.

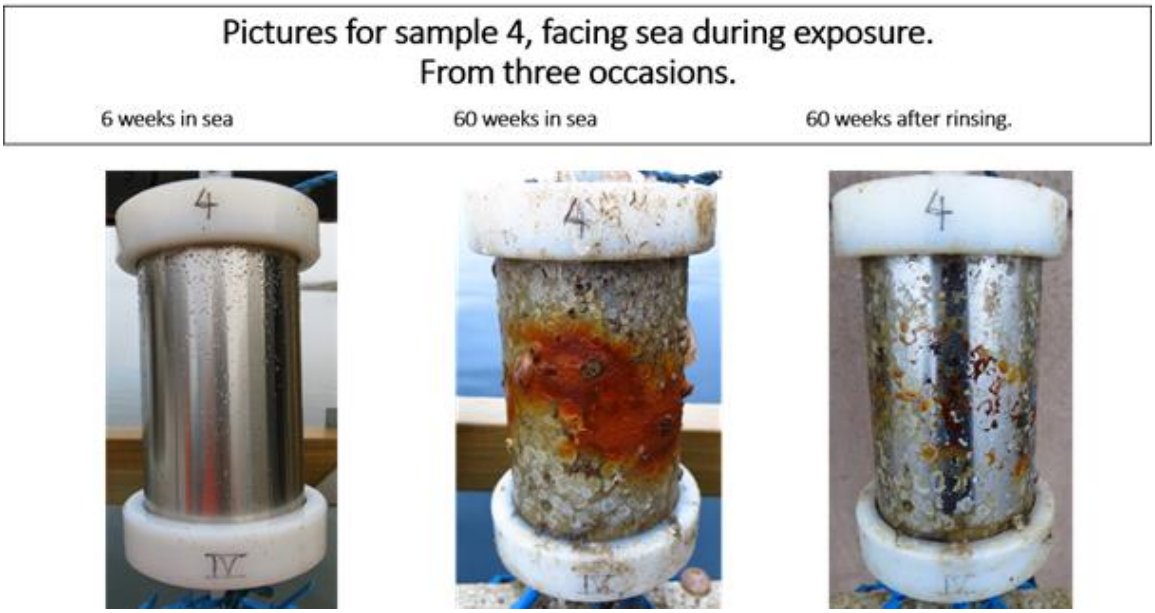

Figure 52: Pictures of a laser cladded test piece of a PTO cylinder submerged in seawater under a jetty at Kristineberg test site in Sweden. The stainless-steel coating revealed severe corrosion pits and were of subject to hard biofouling such as barnacles during field test.

3.3.3.5 ***Marine Biofouling***

Antifouling systems are as old as the human navigation of the seas. In trying to combat the natural phenomenon of marine biofouling on immersed surfaces such as boat hulls humans have treated surfaces with different compounds mixed in paints. Nowadays the antifouling paints can be divided into biocide or biocide free systems. There are also other antifouling systems not based on paint such as mechanical based strategy (in situ cleaning; grooming; washing etc.) and other physical methods. Taking into consideration that the most used countermeasures in the marine sectors (included MRE) are the antifouling paints, the major methods used for evaluating the efficacy of antifouling paints both for biocide paints and biocide free will be reviewed [242], [243].

Figure 53: Efficacy evaluation of antifouling products Conduct and reporting of static raft tests for antifouling efficacy (CEPE 2012) @RISE

Figure 54: Testing the adhesion strength of barnacles, tube worms and bryozoans on fouling release paints according to the standard method ASTM D5618-20.

The VALID consortium includes several marine test sites, where know how and test methods are used to further understand anti-fouling material developments. This information aims to provide guidance on how to lower maintenance costs and contribute to technical standards/technical working groups, ultimately contributing to improving standards and contributing towards the progression of the commercial deployment of wave technologies.

Figure 55: Harslab @TECNALIA. Testing coatings and materials at both immersion zone, splash zone and atmospheric zone.

With the increase in deployments for test and validation of wave energy devices, both at full or smaller scale, the marine biofouling problem has received increasing focus as one key aspect to ensure reliability and functionality in real conditions. During the last years, many different materials, components, subcomponent of marine energy devices have been studied regarding marine biofouling accumulation and impact.

A brief overview of recent projects on biofouling testing related wave energy devices is provided below.

SEASNAKE Project

In the OCEAN-ERANET project "Seasnake" the impact of marine biofouling on dynamic cables is being evaluated and countermeasure evaluated in field test.

Two different paint formulations (made by MWA coating AB, Sweden, partner of the SEASNAKE project) has been tested in immersion test at two locations. In Sweden, at RISE facilities in Kristineberg Center for Marine Research and Innovation, and in Portugal at WavEC facilities (WavEC Offshore Renewables, Portugal, partner of the SEASNAKE project). The two paints have been tested as applied on triplicate samples made of the same polymeric material as the outer jacket of the planned SEASNAKE cable. Each sample is 3 cm in breadth and 5 meter long. At each site, two sets of triplicates painted with the two experimental paint were deployed, as well as a third set of control samples, i.e. non-painted same material.

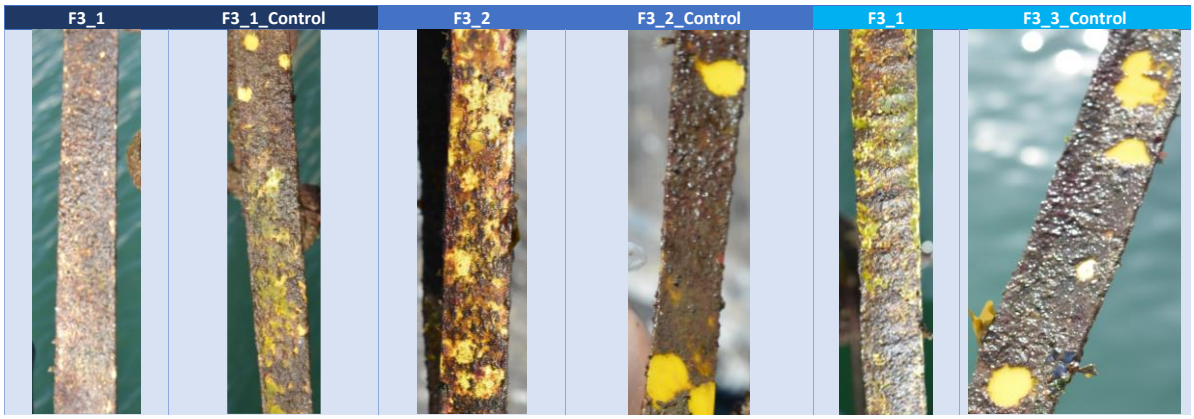

Figure 56: An example of results in Portugal, F3 is one of the two formulation, while control is the non-painted side of samples.

As can be noted in Figure 56, the main difference between the control sides and the painted side (formulation "F3") (similar results were obtained for the formulation called "F6") are the spots left by barnacles once removed by mechanical forces after ca.80 days of immersion. The hypothesis was to achieve a barnacle protection to minimize the possibility for barnacle penetration and disruption of the cable and to remove the microfouling by later mechanical grooming on the cable, using the low surface energy of the paint.

More result needs to be evaluated on the real cable sample during the summer of 2021 and using the ASTM D5618-20 method for measuring the adhesion strength of barnacles and other macro fouling organisms.

WEChull Project

In general, biocide paint is the first choice for reliable efficacy. Some developers are considering the fouling release antifouling systems (i.e. silicone paints) but the WEC movement in the water does not generate enough flow on the surface as the fast-going vessel these systems are designed for. In order to try to find a compromise and have something reliable and functional but still containing less biocide and no metal biocide at all, some initiatives are combining easy cleaning paint with anti-barnacle biotech technologies. This will give the possibility to eliminate the most aggressive and difficult to remove organisms and leave the rest with the fouling release properties of the coating and easy clean aspects, to be used in future planned mechanical grooming/cleaning.

This is the case of the WEChull project, where RISE AB and Corpower Ocean AB will use the mentioned evaluation methods (i.e. CEPE, ASTM) during field testing of the coatings for antifouling properties for specific material selections, based on a mix of easy clean coating, anti-barnacle active substances and mechanical cleaning of the hull. The selection campaign will be run in a nearshore environment with static conditions on panels in order to select the better suited formulations and cleaning intervals on both composite and concrete substrata. Once the formulation with better efficacy/environmental impact/costs will be selected, a demonstration campaign will be run in more exposed areas such as the real deployment site for the project developers participating in the project or in specific testbed offshore.

OCEANIC Project

Beside the polymeric and composite surfaces, there are also metallic parts to be protected both from corrosion but also from marine biofouling. In particular, on these metallic surfaces the marine biofouling can cause the so called biocorrosion. Solutions based on coatings are

often designed for ships and the in-between dry dock intervals for cargo ships are 3-5 years. In the MRE sector, the request is for a longer lifetime. The solution is not easy. In the OCEAN-ERANET project OCEANIC Oceanic Project | European Project (oceanic-project.eu), the idea has been to dope the Thermally Sprayed Aluminium (TSA), a system used for long lasting corrosion protection, with biotech anti-barnacle agent. Based on the project findings, this worked as it is possible to see in Figure 57. In A) and B) there are shown the results of the exposition of the panels under salt spray test according to ASTM B117-11 (1000 h). In C) and D) I can be observed the same thermally sprayed alloy on same substratum panels immersed at EMEC test site in Orkney island for a period of 6 months, attached at 30m depth on the Corpower Ocean AB foundation during the ocean testing. More research is need in order to achieve smooth and long-lasting antifouling and anticorrosion protection systems for metallic parts as one cannot rely on paint systems.

Figure 57: Thermally sprayed aluminium doped with anti-barnacle carrier and sprayed simultaneously on stainless steel panels.

DE-RISK Project

Many WEC devices have a PTO cylinder immersed in water. This part is subject to wear and also needs to go through sealing systems that prevent water from leaking into the hull compartment. For these reasons, paint is not so suited for these parts and thermally sprayed aluminium is not hard enough to resist wear of the high cycles during the lifetime of the WEC. In this case, the solution could be included in the design of the system itself. One way to manage fouling on surfaces is to groome surfaces a little every day (grooming approach). In the De-RISK project Marine Growth | DE-RISK the partners are looking at different alloys to be employed and to change full stroke intervals to keep the piston clean from fouling. The test will be run during the summer of 2021.

3.3.4 Uncertainty quantification

Experimental modelling and the measurements involved are subjected to uncertainty. To make use of the results from the experimental modelling, the uncertainty needs to be understood and quantified.

The type of uncertainty coming from limitations in measurements (e.g. measurements errors) can be handled in standardized ways such as in the GUM framework [244]. Other types of uncertainty come from limitations of the experimental model in representing the reality and operational conditions. Examples of this, as discussed in this deliverable, can be in loads due to e.g. scale effects, ageing effects, unknowns in usage and geographical differences between experiments and real deployment. These latter types of uncertainty are a major topic in the VALID project and are to be extensively covered in the upcoming VALID deliverable D1.3.

4 Current models, test rigs and testing platforms

This section reviews the numerical models, test rigs and platforms currently available for its use in the VALID project. The objective of Section 4 is to find the starting point of the three user cases of the project by a specific review focusing on reliability testing of the critical components in the user cases.

Each section looks at the available numerical models and experimental models for each of the user cases presented in VALID. Each model capabilities, interfaces, software, hardware and communication requirements are analysed, providing an initial assessment of their value for the hybrid testing. This will help to detect the upgrading needs of the facilities that will take part in each user case testing.

4.1 User Case #1: Dynamic seals

4.1.1 Overview of WEC technology

CorPower Ocean (CPO) wave energy converter (WEC) is of the point absorber type, with a heaving buoy on the surface absorbing energy from ocean waves and which is connected to the seabed using a tensioned mooring line. Novel "phase control" technology makes the compact device oscillate in resonance with the incoming waves, strongly amplifying the motion and power capture. This offers five times more energy per ton of device compared to previously proposed technologies. The high structural efficiency allows for a large amount of energy to be harvested using a relatively small and low-cost device, providing competitive cost-of-energy. The system has improved survivability in storms, thanks to its inherent transparency to incoming wave energy, when detuned. Generators and power electronics are standard components known from the wind industry, enabling well known grid connection architecture. The buoys operate autonomously by a programmable logic controller located inside the device, with an interface for remote control and data acquisition to shore over radio-link. These step-change innovations provide a path for wave energy to overtake wind turbines in structural efficiency and competitiveness.

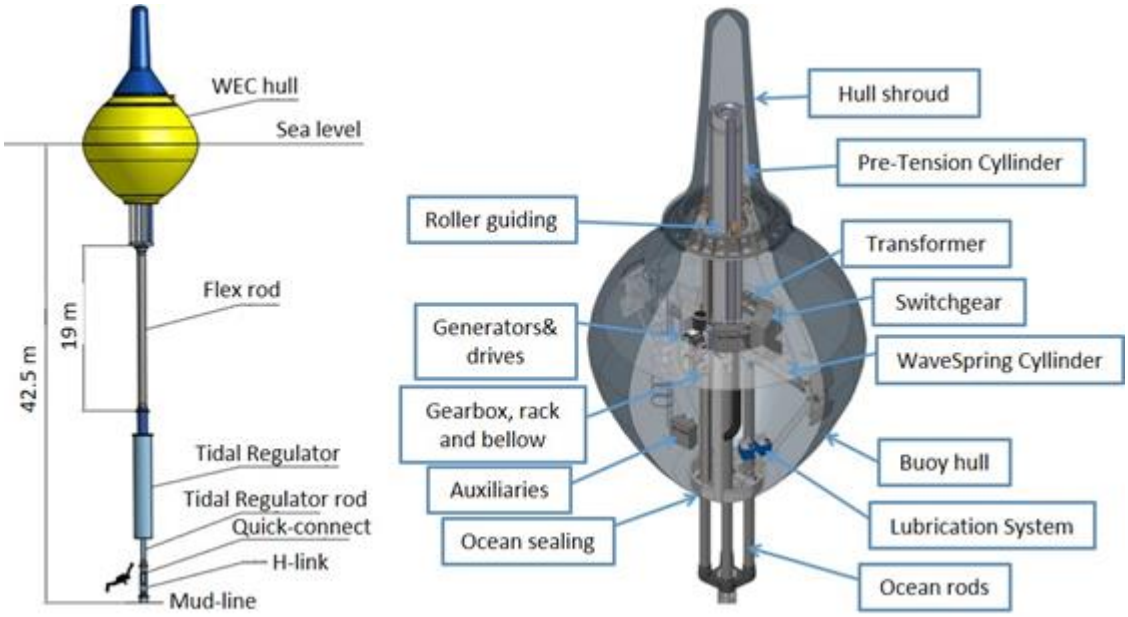

Figure 58: The CPO WEC and subsystem overview.

The CPO WEC addresses the key challenges of efficient wave energy harvesting in a unique way**.** They offer tuning and detuning of the device to the sea conditions, by such introducing a function to wave energy similar to wind turbines pitching the blades to control the driving force of the device.

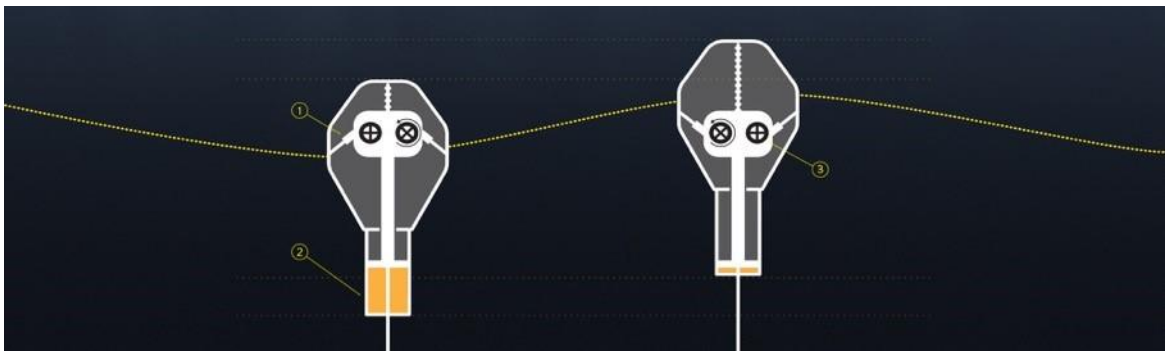

Figure 59: The COP WEC working principle.

Inspired by the pumping principle of the human heart, CorPower uses stored pressure to generate energy from waves in two directions. The human heart uses stored hydraulic pressure in the vascular system to provide force for the return stroke, thereby only requiring the muscles of the heart to pump in one direction. In a similar way, CorPower's WEC uses pneumatic pressure to pull the buoy downwards. It mimics the energy storage aspect of the human heart whereby the upward force of a wave swell pushes the buoy upwards while the stored pneumatic pressure provides the restoring force driving the buoy downwards. This results in an equal energy production in both directions and allows for a lightweight design with high natural frequency.

The CorPower WEC converts renewable energy from waves into electricity through the rise and fall as well as the back and forth motion of waves. A composite buoy, interacting with this wave motion, drives a Power Take Off ("PTO", power train located inside the buoy) that converts the mechanical energy into electricity. The WEC consists of a light buoy connected to the seabed through a power conversion module and a tension leg mooring system. By means of novel and patented technologies the CPO WEC moves in resonance with incoming waves, making it move in and out of the water surface.

In a conventional point absorber, the buoy follows the motion of the waves. The CPO WEC on the other hand uses a combination of pretension and the WaveSpring technology to better leverage the motion of the waves by pushing the buoy into perfect timing with each wave. Consequently, the buoy motion increases due to resonance, along with the power output.

4.1.2 Existing numerical models

4.1.2.1 *Modellable components of the CorPower device*

Modelling of various components is essential to de-risk and validate designs during the WEC development process. Models are used for a variety of purposes such as predicting structural loads on the system, calculating the power output of the WEC in different sea states, and verifying the control system software.

Figure 60 shows a top-level overview of the modelling and testing processes during the WEC development process and how that leads to the WEC deployment. The process is iterative with each stage feeding back into the previous stage, as well as forward into the next stage. The initial machine design is supported by mechanical modelling using ANSYS and Solidworks and hydrodynamic modelling using Orcaflex, as well as the Wave2Wire model.

Once the machine design meets the concept specification the various subsystems can be fully incorporated into the Wave2Wire model. Parameters from subsystem testing (e.g. from the seal rig), as well as previous testing are used as inputs to the Wave2Wire model. Once the proper functioning of the system has been established in the Wave2Wire model and it has been validated against tank testing/ocean test data, all major subcomponents of the WEC prototype can be assembled and tested in the Hardware-in-Loop (HIL) rig. The same wave model as used in the Wave2Wire model is used as an input to the HIL rig, and all hardware and software can be validated and fault-checked. Real sensor outputs can then be fed back into the Wave2Wire model to improve its accuracy. The final stage is WEC ocean deployment. Data from this stage is collected and used to improve the HIL rig design and testing, as well as the Wave2Wire model.

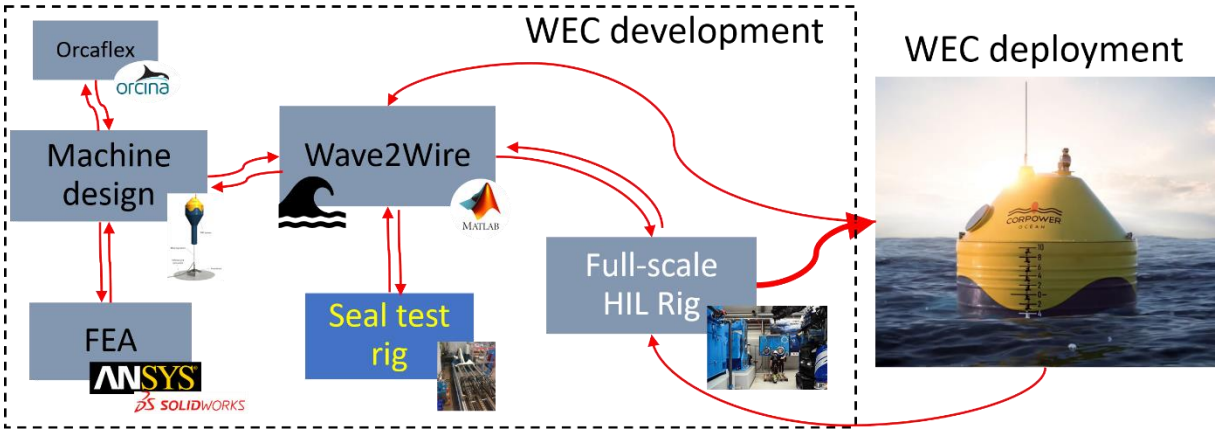

Figure 60: Overview of modelling in the WEC development process.

During the above processes all the major subsystems in the CPO device are modelled at some level. A summary of these as well as the modelled parameters are given in Table 11.

The rest of this section gives a more in detail description of the models used at CPO.

4.2.1.1.1. Models for design validation

There are a number of models that are used for design validation that are summarised in Table 23. The design process typically involves the system architecture design, followed by the concept design, and finally the detailed design. The concept design stage is the first stage that is supported by modelling, typically based on analytical calculations and basic Finite Element Analysis (FEA) according to standards, as well as the basic Wave2Wire model to assess initial system performance. The detailed design process involves more in-depth FEA and validation in the refined Wave2Wire model.

4.2.1.1.2. Models for HIL testing

For the HIL PTO testing the same Wave2Wire model as used for the validation testing is used. Specifically, the hydrodynamics block is used to simulate the wave conditions for particular load cases. The wave amplitudes and frequencies are output from the Wave2Wire model, converted to linear motions by the HIL rig, which are then input into the attached PTO.

The seal rig has its own basic Simulink model, which has been used to validate the rig design.

Table 11: Summary of modelled subsystems and parameters.

Modelled Subsystem		Loads	Reaction forces	Position	Friction forces	Hydrodynamic forces	Mechanical stresses	Mechanical strains	Conversion efficiency	Output power	Sensor inputs	Sensor outputs	Control outputs
Stru-cture	Buoy hull	x	x	x		x	x	x				x	
PTO	Pre-tension cylinder	x	x	x	x		x	x				x	
	Power conversion system (generators, drives)		x		x				x	x		x	
	Control system										x		x
	WaveSpring	x	x	x	x		x	x				x	
	Gearbox	x	x	x	x		x	x				x	
External	Supervisory Control And Data Acquisition										x		x
	Moorings	x	x	x			x	x				x	
	Anchors	x	x	x			x	x					
	Tidal regulation	x	x	x		x	x	x				x	
	Umbilical	x	x	x		x	x	x					

4.1.2.2 *Available numerical models*

The numerical models available for the CPO user case are listed in Table 23.

Table 12: Overview of numerical models for User Case #1.

Num.	Model Type	Software	Comments
1	Hydrodynamic model/Wave2Wire	MATLAB/Simulink	Developed by CPO.
2	Hydrodynamic model	Orcaflex	Developed by Orcina.
3	Hydrodynamic model/Slam loading	Orcaflex, MATLAB/Simulink	Developed by CPO.
4	FEA	SolidWorks	Developed by Dassault Systemes.
5	FEA	ANSYS	Developed by Ansys Inc.
6	Seal rig model	MATLAB/Simulink	Developed by CPO.

4.1.2.2.1. Hydrodynamic modelling

CorPower Ocean is using mainly three different models to generate design load cases:

- A Simulink-based model
- An Orcaflex model
- A stand-alone model for slamming loads calculations

4.1.2.2.1.1. Simulink-based model

The mathematical model developed at CPO to represent dynamics of the buoy, mooring and machinery is based on rigid-body motions and lumped representation of fluid forces. The representation of hydro-pressure forces on the hull are split in hydrostatic forces (buoyancy) and hydrodynamic forces (wave excitation and wave radiation, including added mass effects), and is based on linear hydrodynamic theory with non-linear corrections for drag losses and instantaneous submergence.

This so-called wave-to-wire (W2W) model is validated against tank test data [245] and against a half-scale ocean testing campaign [246] and may be used to investigate system dynamics through time-domain simulations. The model includes functionality for the simulation of faults in for instance grid connection, control or tidal regulation as required to run simulations to derive certain load cases. Quantities like motion signals and machinery forces are output as direct results of the simulation, whereas external pressure distribution on the hull and point loads at hull attachments needs to be derived by post-processing models.

As this model is based on linear wave theory, the uncertainty level associated to simulations increases with wave height. This model is well suited for:

- Deriving fatigue load cases in normal operation
- Estimating the annual electrical production at different sites
- Qualitatively comparing configurations in most sea states
- Producing rough estimates of load cases in extreme sea states

This model is split into four main blocks, each representing a specific part of the system, as illustrated in Figure 61 below. They are presented in more detail in the following sections.

Hydrodynamics Block

Main functions

- Calculate the hydrodynamics forces that apply on the oscillating and stationary parts of the system
- Integrate equations of motion of oscillating and stationary parts of the system
- Input:
    - PTO force calculated by the PTO block
    - Mooring force calculated by the mooring block
- Output
    - Position and velocity of oscillating and stationary parts of the system
    - Hydrodynamic forces

Different variants:

There are two different variants of this block: with two and six degrees of freedom. The two-degree of freedom version can also be used as a one-degree of freedom version.

- The two-degree of freedom version is primarily used to compare different configurations or to eliminate effects that make understanding the system's behaviour more complicated.

- The six-degree of freedom version is the main version of this block and is used to produce load cases or performance estimates.

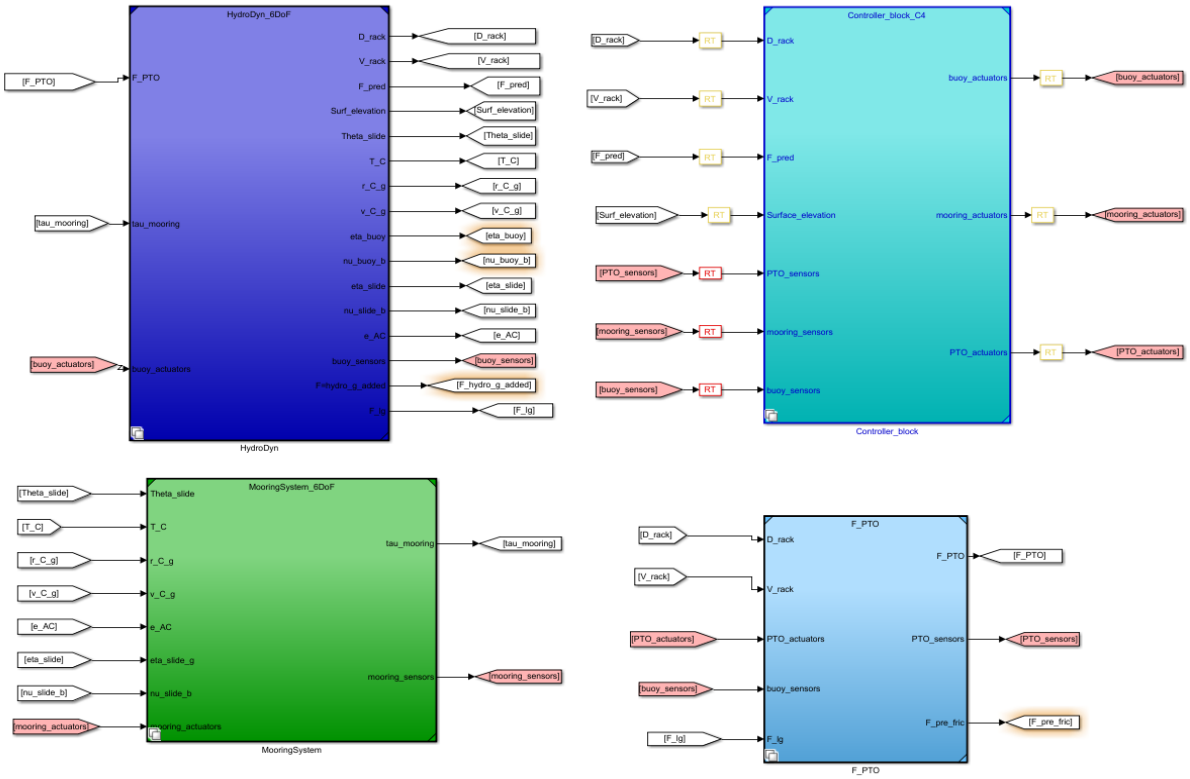

Figure 61: Top-level diagram of Simulink Wave2Wire Model

PTO Block

Main functions:

- Calculate the force applied by the PTO on the oscillating part of the system, taking into account non-linearities such as end-of-stroke braking, the thermo-fluid behaviour of the high-pressure system, or the damping strategy which is used.
- Provide the controller block with sensor values for the relevant properties
- Input:
  - Relative position and velocity of the oscillating and stationary bodies
  - Commands from the control system
- Output:
  - Force applied by the PTO on the oscillating body
  - Sensor values of relevant properties (e.g. pressures, forces, velocities, valve status…)

Different variants:

Different capabilities of this block have been developed to represent the different designs considered throughout the design phase. However, all of these are performed by the same Simulink block.

Control Block

Main functions:

- Represent the control system

- Provide commands to the PTO and the mooring block
- Input:
  - Sensor measurements from all other blocks
- Output
  - Commands to actuators in PTO block and in mooring block

Mooring Block

Main functions

- Calculate the mooring force
- Provide controller block with sensor measurements of the relevant properties in the mooring system
- Input:
  - Position and velocity of the stationary part of the system
  - Position of the connection point of the stationary part of the system to the mooring system
  - Commands from the controller block
- Output
  - Mooring force
  - Sensor measurements of the relevant properties

Different variants:

There are two different variants of this block: with two and six degrees of freedom. The two-degree of freedom version can also be used as a one-degree of freedom version.

- The two-degree of freedom version is primarily used to compare different configurations or to eliminate effects that make understanding the system's behaviour more complicated.
- The six-degree of freedom version is the main version of this block and is used to produce load cases or performance estimates.

Orcaflex model

Orcaflex [247] is an offshore industry standard tool for the simulation of buoys and other structures and in particular mooring systems. During normal operation of the WEC the influence of the PTO on the response are greatest and this is best captured by the Simulink model, but in much larger sea states where the WEC is in a survival model and with small PTO oscillations Orcaflex is a more accurate tool to predict the WEC and mooring loads and motions.

Slam loading model

The slam loading model has been constructed by CPO and uses outputs from Orcaflex, Simulink and Matlab to analyse the maximum slam loads.

Estimation of worst-case water and body kinematics are used to establish a characteristic value for the maximum relative velocity between body and water. This is used to estimate sequences of slamming pressure acting on the hull, which are finally fed to a structural dynamics solver to compute the hull response.

Structural analysis

The structural analysis of the WEC is performed using a combination of classical calculations from standards and finite element analysis (FEA). Loads and constraints are derived from the WEC hydrodynamic model for the system or module under consideration.

At module level structural design is undertaken for all components by either analytical methods following basic calculation or more advanced calculations according to standards where required – such as EN13445 for pressure vessels. Where analytical methods are not sufficient finite element analysis (FEA) is undertaken using tow tools. Solidworks simulation of simpler parts and assemblies and Ansys Mechanical is used for more complex parts and assemblies where great detail can be included as well as utilising combined global analysis with local sub-models [248] to capture as much detail as possible.

Seal rig model

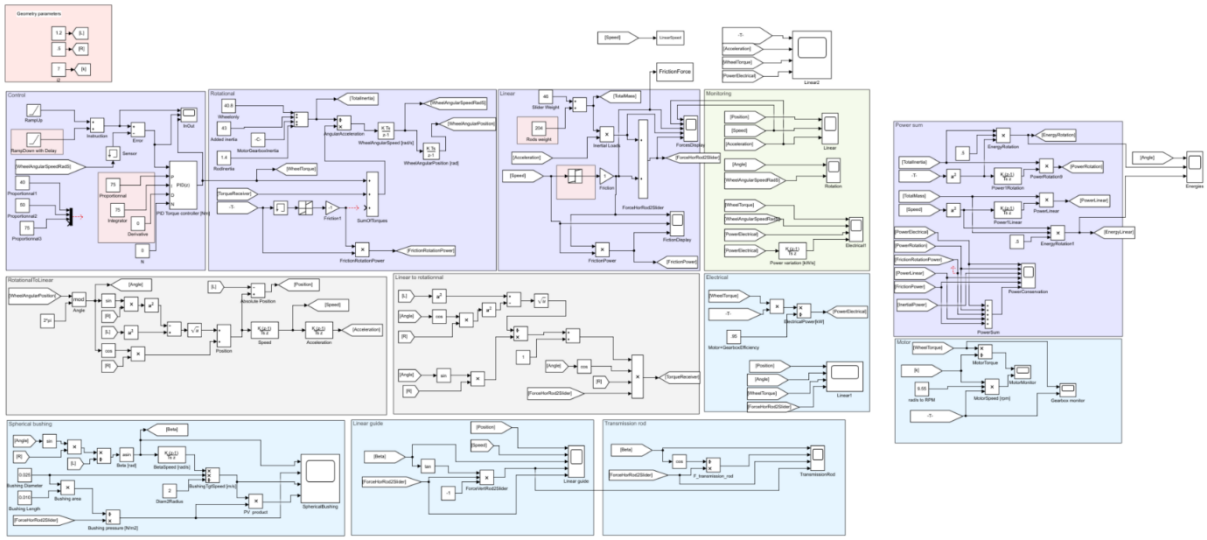

Figure 62: Overview of Simulink seal rig model.

The model of the seal test rig was originally used as a method to validate the concept design of the seal rig prior to construction. The model consists of a number of blocks that convert the control input and motor rotational speed into simulated linear motion of the test rods. Estimations of the friction forces from the seals can also be input. The model was used to validate the forces generated by design cases, as well as the input power required. This helped with dimensioning of components such as the rig frame and motor.

4.1.3 Existing test rigs

This section provides a description of the existing test rigs and capabilities to perform reliability testing of seals for User Case #1. Two test rigs are described: firstly the seal test rig described and developed in the Waveboost project [221]; and secondly the hardware in loop rig that has been developed as part of the HiWave-5 project to test the power take-off system in dry testing before ocean deployment.

4.1.3.1 *Seal test rig*

High-pressure and standard-pressure sealing solutions are used in the Pre-Tension Cylinder, the WaveSprings, and on the ocean rods - all of these being the central modules of the Power Take-Off system. These sealing solutions are reciprocating rod sealing systems that have been identified as critical components and need to be tested and optimized to ensure the performance and reliability targets of future WECs.

4.1.3.1.1. Overall description and capabilities

The test-rig for critical sealing systems is used to assess reliability of seals. The main deterioration mechanism is the wear of the seal polymer material as described in section 3.1.4.2.

The seal test rig is used to assess the wear on the various seals in the CorPower system. It mimics the translation in one degree of freedom of the primary PTO, relative to the mooring to the seabed which in turn is driven by the wave motion.

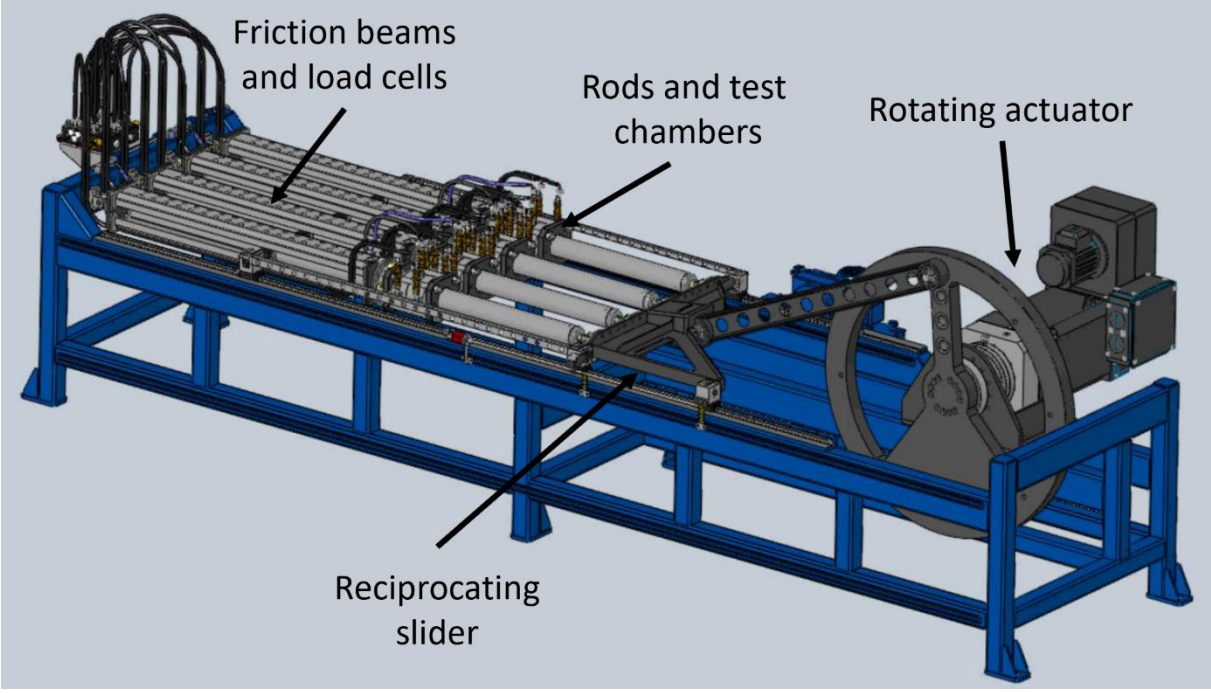

Figure 63: annotated schematic of the seal test rig.

An annotated schematic of the seal test rig is shown in Figure 63. The rig is composed of a crank-slider mechanism that provides a linear reciprocating motion through a motor rotating with a constant speed instruction. This mechanism is particularly suited to test very long travelled distances. The wheel has a high inertia that can store and release energy from and to the reciprocating slider. Thus, the variations of linear speed are not directly seen by the motor, and the electrical power supply is smoothened.

The sealing systems are mounted in test chambers, and the rig can accommodate up to four quarter-scale 80 mm diameter test rods. It is also capable of accommodating one full size ocean rod with a diameter of 360 mm. The test chambers are pressurized cylinders with mounts for seals and guide rings, and which the rods can travel through. The rods are connected to the reciprocating slider. The chambers are held in place by articulated "friction beams" that transfer the friction forces to the structure. Loadcells are inserted in series between the friction beams and the structure. This configuration enables the loadcells to read friction forces only, and not to be affected by inertial loads. This also allows the rig to measure friction accurately even during highly dynamic cycles (up to 7 m/s of linear peak speed).

The articulation of the friction beams is provided by a spherical joint on the loadcell side, and by a "hollow yoke" assembly on the chamber. This makes the system statically determined and prevents the apparition of unwished side loads in the sealing solution due to misalignments. It also allows the simulation of controlled side loads with weights hung under the chambers.

Lubricating oil and pressurized air are supplied to the chambers, and both circuits have pressure, temperature and flow sensors. These signals are monitored, stored and post-processed by a central PLC (programmable logic controller).

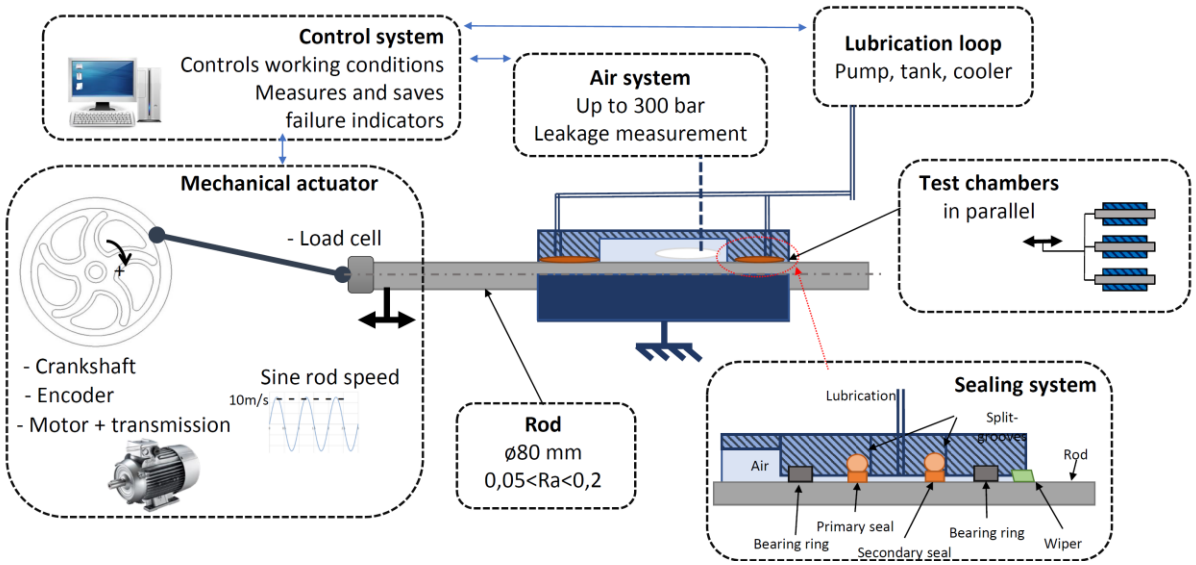

Figure 64 Schematic overview of the CorPower lab for seal testing.

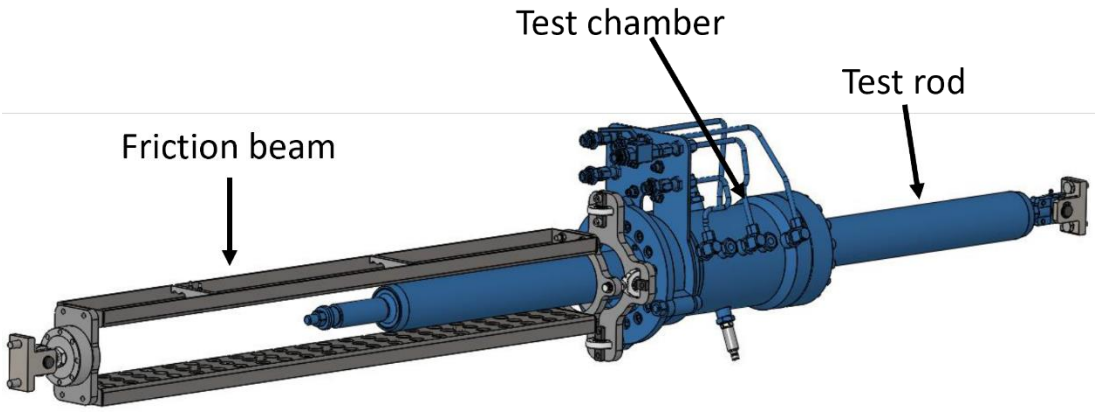

Figure 65 Drawing of a single line of the seal test rig. The friction beams, test chamber, and rod are all shown.

Figure 64 shows a breakdown of the components comprised in the test rig, while Figure 65 shows drawing of a single line within the seal test rig. There are several main parts (as indicated in Figure 64):

- **Test chamber:** cylinder in which the sealing components are mounted, and get the relevant working conditions (pressure, rod speed, lubrication, temperature).
- **Mechanical actuator:** external system that provides the back-and-forth relative motion to the test chamber.
- **Air system:** external system that provides compressed air to the test chamber to simulate the working media of the cylinder.

- **Lubrication:** external system that provides lubricating oil and cooling to the sealing components.
- **Controls & data acquisition:** automation, electronics, and sensors that control the working conditions, measure, and save the investigated metrics for post-treatment.

The crankshaft can be attached at different radii on the crank wheel to achieve different linear velocities. The velocities are given in Table 13.

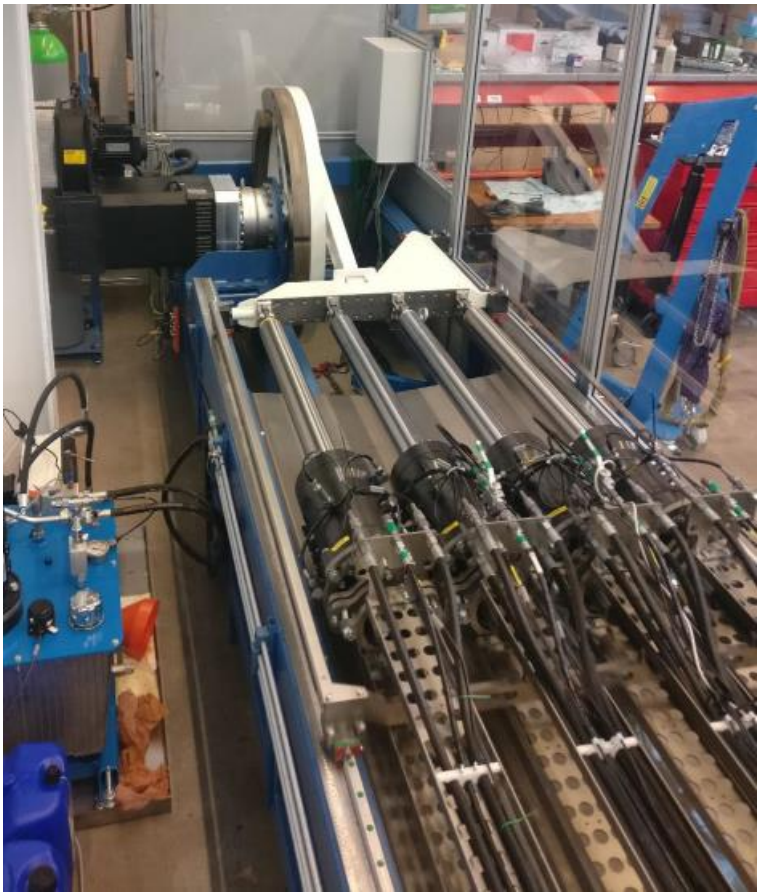

Figure 66: Image of the seal rig.

Table 13: Velocities for different connection rod attachments to crank wheel.

Crank wheel radius [mm]	Crank rpm	Max linear velocity [m/s]
150	260	5
250	200	6
350	170	7
450	150	8

A principal part of the test rig is the test chamber with seals containing an internal pressure Figure 67. The test chambers are composed of a cylinder body and several groove rings. These rings allow easy mounting of the seals thanks to split-grooves. The primary and secondary seal are mounted on a ring that also receives lubrication. The pressurized chamber

serves the purpose of simulating the air pressure in the WEC. This pressure, up to 300 bar, can theoretically also be used to accelerate the wear of the seals.

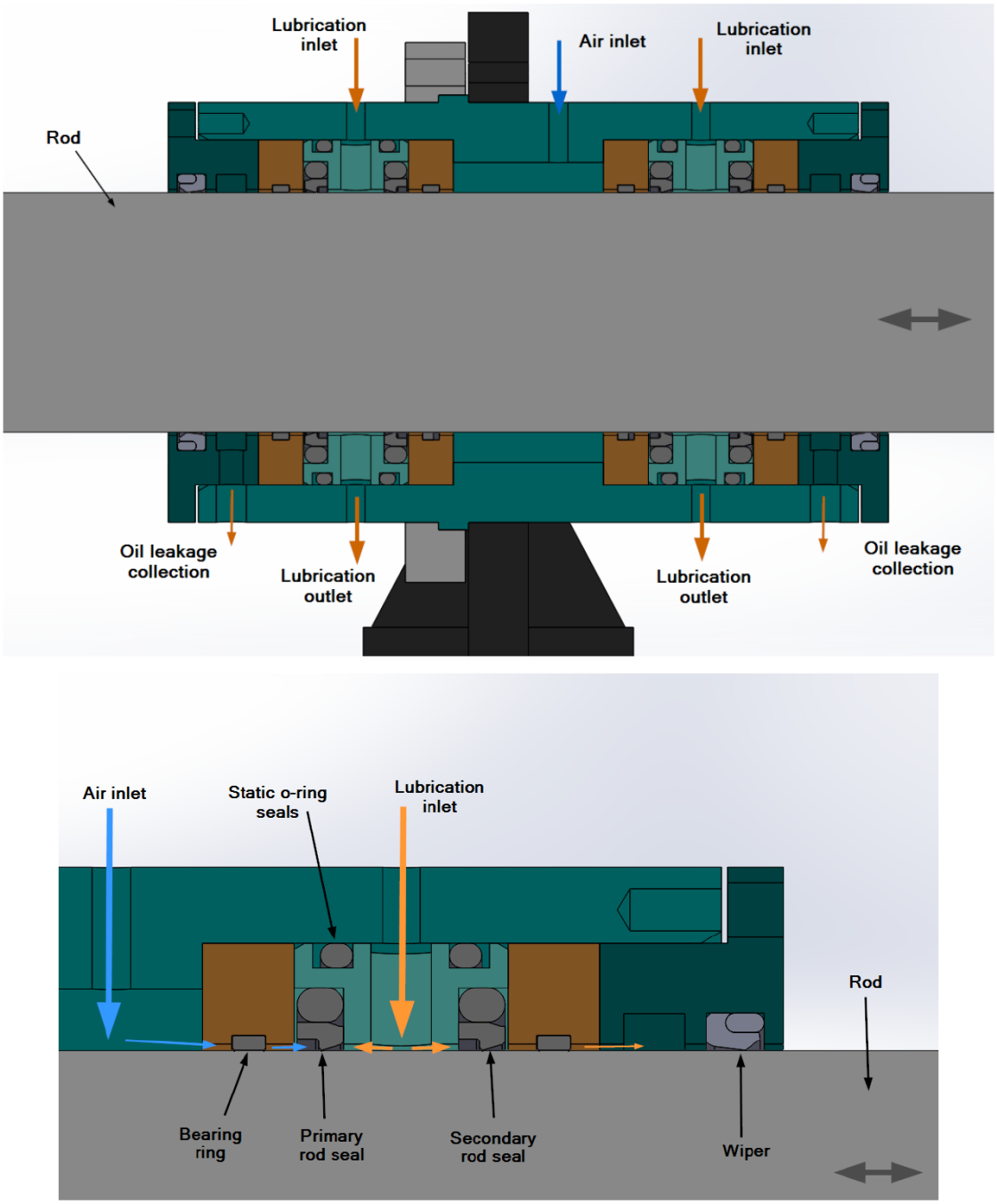

Figure 67: cross-section of test chamber.

The test rig has the following components:

- **Motor:** 92 kW AC induction motor is used. The reference is HDP IP23 H160 from ABB
- **Planetary gearbox:** The reference is PH932 F0120 MELC from Stober.
- **Data acquisition and control system.**

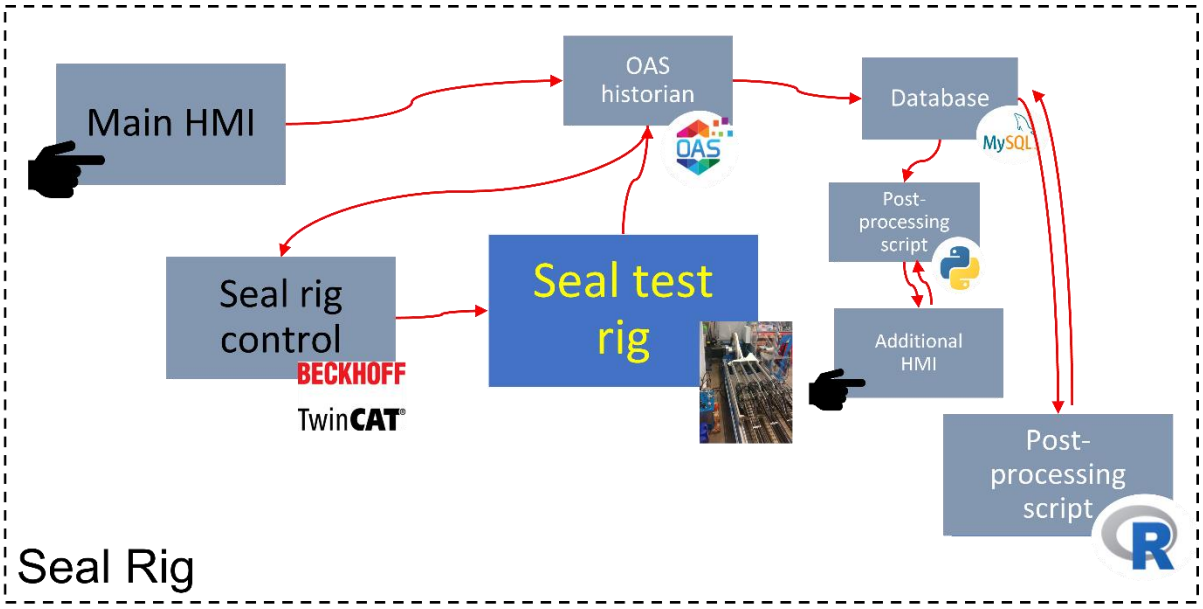

Figure 68: Schematic of seal rig control system.

An overview of the seal rig control system is shown in Figure 68. The seal rig is controlled using *Beckhoff TwinCAT 3 software*. This takes inputs from the main human-machine interface (HMI) via *OAS Historian* software, and outputs control signals to the motor of the seal rig. Sensor information is fed back from the seal rig via *OAS historian*, and back to the *TwinCAT* software. Sensor data is also output from *OAS historian* to *MySQL* databasing software where it is stored. The main post-processing of the data is carried out using algorithms in the *R* programme, while an additional post-processing algorithm can be controlled using another HMI via *Python*.

4.1.3.1.2. Additional communication, software and hardware requirements

In the current setup a lot of data is recorded for every stroke of the seal test rig. This generates a large amount of data, and so it is vital to have algorithms that can process and store this information in a suitable way.

The software that was developed for the control and data acquisition of the reliability test rig is also used to ensure its safe operation. For this, limits or logics have been implemented on each signal that is being recorded. These are called Continuous Buit-In Tests or CBITS.

In most cases, a first level alarm sends a warning to the user, and a second level alarm triggers an emergency stop of the machine.

These limits have been implemented and individually tested. In some cases, the levels have been temporarily changed to make the testing possible without reaching the actual extreme values. Some levels have been refined after the commissioning tests, such as the maximum dynamics.

An enclosure has also been designed and installed around the seal test rig in order to prevent dangerous interactions between the rig and people while the rig is in operation.

4.1.3.1.3 Initial assessment of applicability to the hybrid testing methodology

This rig could most certainly be used as part of a hybrid model, whereby the seal friction and rod speeds are measured physically in the rig, and fed back to a virtual model of the rest of the

WEC as part of the Wave2Wire model. This could potentially allow the effect of seal wear to be included in the Wave2Wire model.

Preliminary identification of needs for upgrading are the following:

- A way to accelerate initiation of seal failure
- Connecting of the Wave2Wire model directly to the seal rig software
- A conversion block to convert inputs/outputs from/to Wave2Wire model to account for scaling effects of using quarter-scale ocean rods
- Accommodation for full scale ocean rod testing (360mm diameter rod)
- Inclusion of corrosion effects (e.g. application of salt water)

4.1.3.2 ***Hardware in the Loop (HIL) Rig***

4.1.3.2.1. Overall description and capabilities

System-level dry testing has been found to be an effective method for characterizing and stabilizing a Wave Energy Converter prior to ocean deployment. During our half-scale prototype testing a dry test campaign was conducted to verify and debug all functions and operational modes of the drive train and control for the C3 WEC.

CPO's full-scale demonstration is now focussed on ocean deployment of the C4 WEC. The redesigned HIL rig is intended to run the WEC machinery in a controllable environment before operation in the ocean. During the dry test campaign, the HIL rig is used to test the machinery in all sea states, from normal operation sea conditions through to storms.

As opposed to the half-scale test rig, the full-scale rig is designed to move the parts of the C4 PTO system that will be moving in the real ocean environment, representing a significant test rig upgrade over the previous HIL rig. The main components of the test rig are described below.

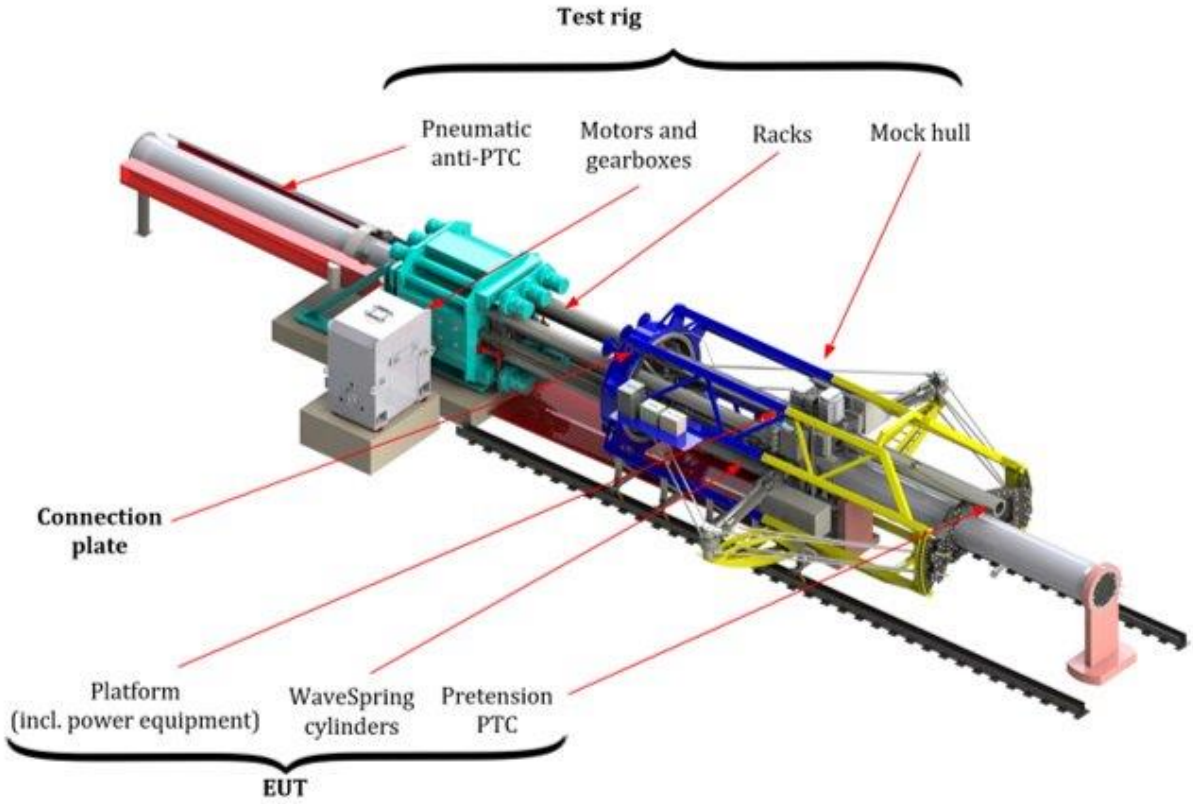

Figure 69: Overview of CPO's full scale HIL rig.

Mock hull - A secondary moving frame (mock hull) replaces the buoy hull which will not be part of the dry testing. The main function of this frame is to hold the extremities of the wave-spring cylinders that are normally attached to the buoy in full WEC configuration.

Anti-PTC - The force that is applied by the test rig on the moving part of the PTO replicates essentially the buoyancy force and other hydrodynamic forces, which exist when the buoy is submerged in the ocean. The buoyancy being dominating, the test rig force is exclusively oriented in one direction. Adding an anti-pretension cylinder subsystem produces the base part of this force (approximatively half of the total maximum force), to reduce the motor max load.

Motor & Energy storage - The motor has been specially designed for the application and has a peak power output of 7 MW. A flywheel-based solution is used to absorb energy during power peaks, so that power consumption from the grid is approximately constant in time.

Gearbox - A cascading gearbox converts rotation to linear motion by sharing the load between several pinions, allowing smaller pinions. Since the goal is to convert the motor speed to a rack velocity, a smaller pinion means that a smaller gear ratio can be used to reach the same generator speed. The gearbox is therefore more compact, lighter, having smaller rotational inertia and cheaper.

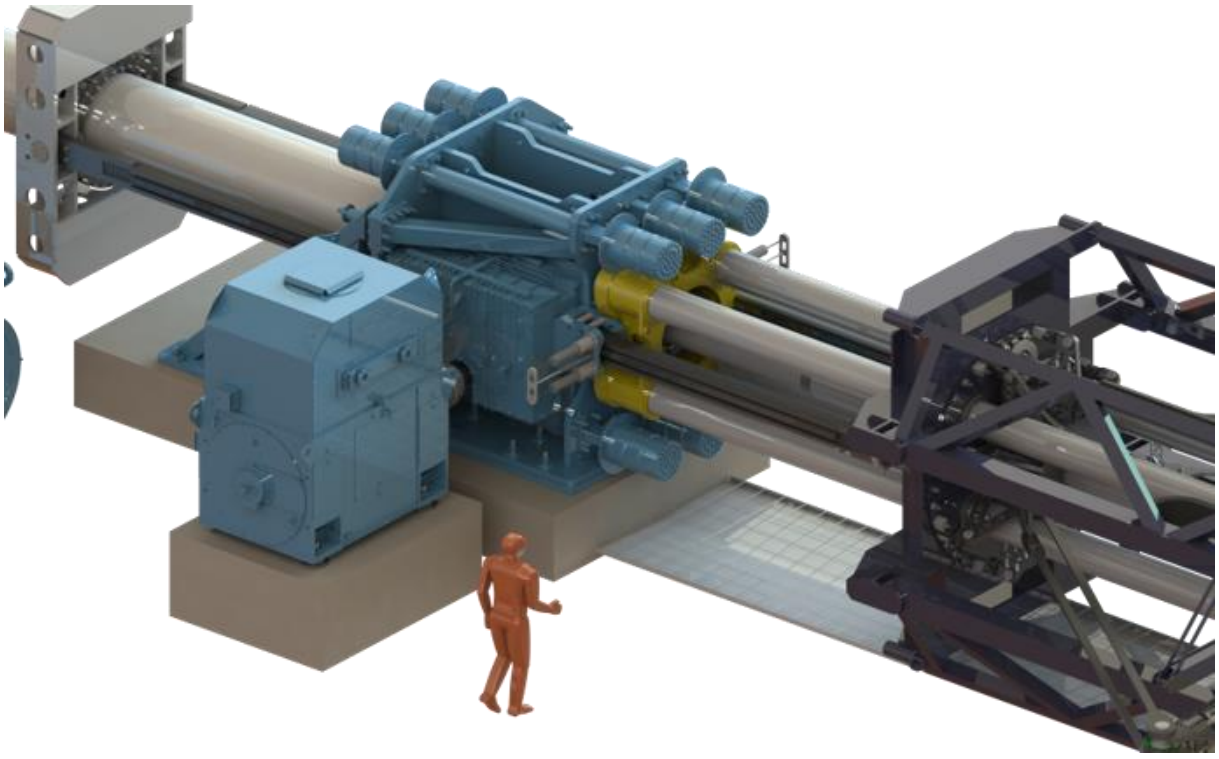

Figure 70: Representation of CPO's HIL rig.

Figure 71: Images of CPO's HIL rig.

Figure 72: Image of CPO's HIL rig.

The controlling of the HIL testing is done in conjunction with the numerical simulation model Wave2Wire. It is a complex numerical model that implements all parts of the power conversion, from wave models, primary converter (WEC hull), through mechanical PTO (linear to rotary), electrical generation conversion, and power export. The numerical model is constantly calibrated by testing the performance of components, sub-systems (modules) and full WEC systems. In this way the HIL test operates close to real conditions which is the topic of the VALID project.

4.1.3.2.2. Additional communication, software and hardware requirements

The test rig is extensively connected to the Wave2Wire numerical model. During dry testing the WEC PTO controller uses several input signals from the simulation model that are measured signals in the ocean, such as surface elevation and excitation force. It is therefore necessary that the control system is capable of taking inputs from the existing Wave2Wire model. The high-performance Power Electronics Controller is used to control the drive motor with the reference signal calculated from CPO's Wave2Wire model. Sensor values from the

PTO are fed back into the model of the WEC at sea to close the loop and reduce the effect of modelling discrepancies. The most important sensors used for control purposes of the HIL rig are:

- Force and torque sensors,
- Encoders for velocity, position and acceleration.

For diagnostics and model validation, the following is also monitored:

- Force (in addition to the sensors mentioned above)
- Acceleration
- Pressure, in pressure tanks and cylinders
- Structural loads, e.g. load on moving secondary rig frame due to the WaveSpring,
- Temperatures,
- Voltage, e.g. bus voltage for rig motors
- Current, e.g. active current from grid.

The control system also handles all required safety aspects e.g. to detect when the behaviour of the PTO is starting to exceed safe operating limits and then stop in a controlled manner. This approach avoids letting the emergency system trigger a hard, and potentially dangerous, stop. There is a separate safety control system that initiates emergency stop in case of faults.

4.1.3.2.3. Initial assessment of applicability to the hybrid testing methodology

The PTO HIL rig that CPO uses is a typical example of hybrid testing. Actual wave data is input to the controller, which converts it into theoretical hydrodynamic loading and then applies corresponding physical loads to the PTO.

This rig will not be upgraded as part of the VALID project and the main focus will be on the seal rig.

4.2 User Case #2: Generator failure

4.2.1 Overview

User case #2 aims to produce a first-of-a-kind practical implementation of the novel testing methodology and hybrid platform on a critical subsystem common to ocean energy devices, namely the electric generator.

The numerical models are set to simulate the electro-mechanical behaviour of the Power Take-Off system of resonant Wave Energy Converters. Particular attention is given to the applicability in the IDOM's [249] OWC device (MARMOK).

The electrical generator is a critical component within the PTO, and it is also in the critical path of the energy conversion steps. It is the core of the WEC where mechanical energy is transformed into electrical power. A failure in this component will directly reduce the Annual Energy Production (AEP) which creates incomes for the wave energy plant. Wave energy devices are not usually easy to be maintained on site due to the constrained working conditions on board (i.e. weather windows, movements and accelerations, reduced working space, ...). If towed onshore for maintenance, the downtime and the maintenance cost increase significantly.

The PTO of the MARMOK WEC device (Figure 73) has been extensively demonstrated at the Mutriku shoreline OWC plant (12 months) and at the BiMEP [250] open-sea testing site (2.5 years) within the H2020 OPERA project [251].

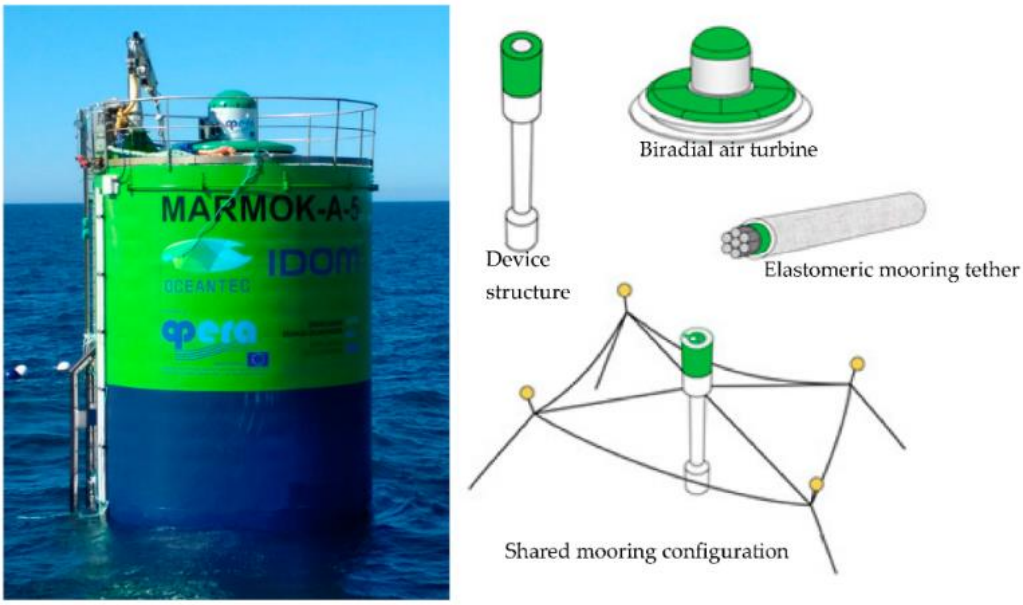

Figure 73: Marmok wave energy converter [251]

To be accurate, Mutriku power plant has been operating for almost 10 years already (Figure 74), wherein significant input data on real conditions has been collected and it can be used to feed into the user case specification.

Figure 74: Mutriku Wave Plant

Although the two WEC configurations presented above differ on the location respect to the shoreline (Mutriku is located nearshore and Marmok offshore), the operational principles of both are the same. Indeed, the operational principle of an Oscillating Water Column or OWC consists of extracting the energy from a bidirectional airflow generated by the oscillating of the sea level in one or more chambers. The chambers are filled with air and seawater. Through an underwater opening to the sea, the incoming waves change the water level inside the chambers. This causes a change of the pneumatic pressure for the air volume inside the chamber. The compressed air leaves through an aperture above the water column, making an air turbine running. The air flow drives a turbine which rotates always in the same direction even though the air flow is bidirectional. When the seawater leaves the WEC, this cycle repeats itself in a different direction, generating a bidirectional airflow in one cycle. The rotation of the turbine is transmitted to an electrical generator to produce electrical power. Hence, the Power Take-Off consists of an Air turbine, Electrical generator and Power electronics. Hence, the

difference between the two concepts is the heave degree of freedom of the floating buoy compared to the fixed chambers attached to the breakwater.

The insulation failure is a significant root cause for the breakdown of high voltage rotating machines. The ageing mechanism is dominated by thermal degradation of the binder resin, mechanical stress caused by vibration and switching pulses and stress caused by the different thermal expansion coefficients of the materials involved. This failure was experienced during the testing of the new turbine-generator set in the OPERA project. Tightly coupled with the electrical generator, the power electronics suffer similar issues. Moreover, the power peaks and the environmental conditions impose very severe conditions on the mechanical design of the generator: bearings, balancing, alignment, etc.

4.2.2 Existing numerical models

4.2.2.1 *Modellable components of an OWC device*

Depending on the final objective pursued, several relevant modelling approaches can be used to simulate a WEC. Objectives may range from the evaluation of energy or structural performance, to optimisation of real time operation and the integration in the power system [252]. With regards to the PTO modelling, time-domain models are widely used to simulate the power flow through the various stages of wave energy converters.

Wave-to-Wire (W2W) models are used to evaluate the behaviour of ocean energy devices [253], the forces acting on them, the loading and stresses, and the electrical power output from a given set of input resource conditions. In the field of wave energy, the term wave-to-wire usually refers to numerical tools that can model the entire chain of energy conversion from the hydrodynamic interaction between the ocean waves and the WEC to the electricity feed into the grid.

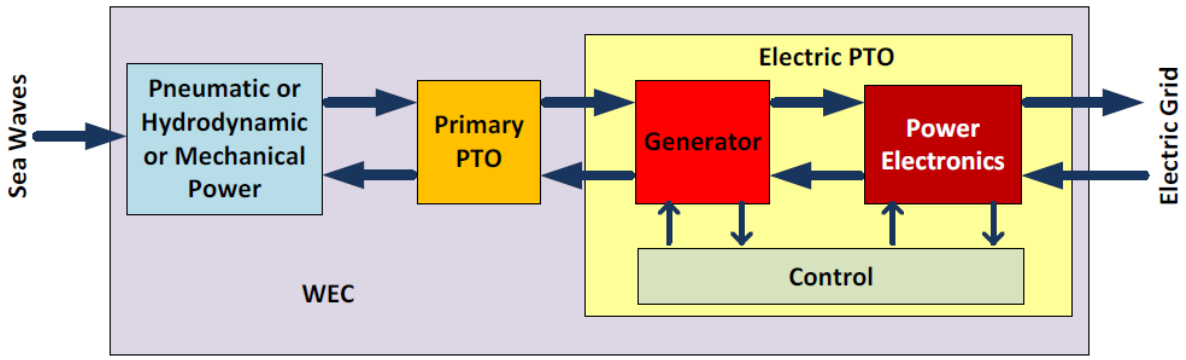

Figure 75: Wave to wire model of a generic wave energy converter [254]

W2W models gather various conversion stages, where each one could be an individual numerical model. Specifically, for OWC operation principle, the W2W model is composed of the following stages:

1. Absorption stage model: from hydrodynamics to pressure conditions in the chamber.

2. Primary PTO: Mechanical stage model: from airflow to rotation of the turbine. Air turbine model.

3. Generator: Mechanical energy to electrical energy transformation.

4. Power Electronics: electrical energy adaptation for grid connection.

5. Control: refers to generator torque/speed control.

4.2.2.1.1 Models for design validation

The best way of validating a particular wave energy technology is throughout experiments and performing them in a controlled environment like a laboratory. For this, mathematical models are necessary to represent the wave resource (the WEC excitation forces) and the different energy transformation steps which cannot be physically tested at the test bench.

Figure 76 shows a simplification of the different subsystems of an OWC WEC, where the PTO is divided by the turbine, generator and power electronics.

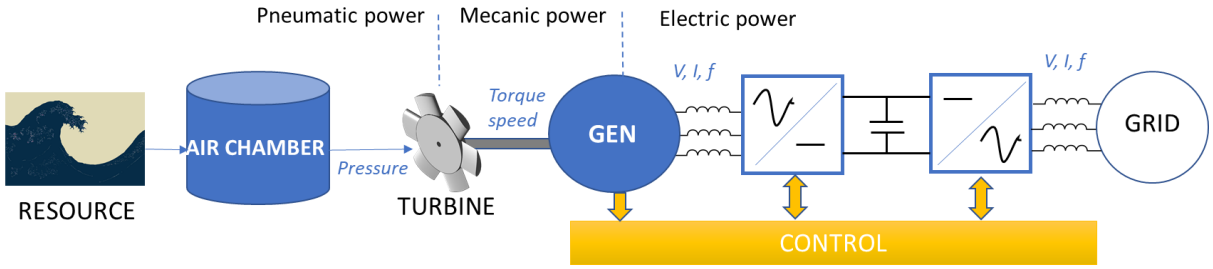

Figure 76: Subsystems of a typical configuration of the different energy transformation steps OWC device

Every single subsystem can be modelled with different level of detail depending on the purpose of the model. It must be noted that a complete model of the device implies modelling subsystems with very different dynamics and couplings.

From the hydrodynamic point of view, the interaction between waves and an OWC can be represented by a boundary-value problem [255] where the only exception is constituted by the boundary condition at the interior free surface which, in case of uniform pressure distribution can be written as

$$-\omega^2\phi + g\frac{\partial\phi}{\partial z} = -\frac{i\omega}{\rho}\hat{p} \quad \text{on } z = 0 \qquad (20)$$

where we clearly assumed the pressure to be oscillating with frequency ω so that it can be described by its complex amplitude. A visual representation of the application of the boundary conditions is given in Figure 77.

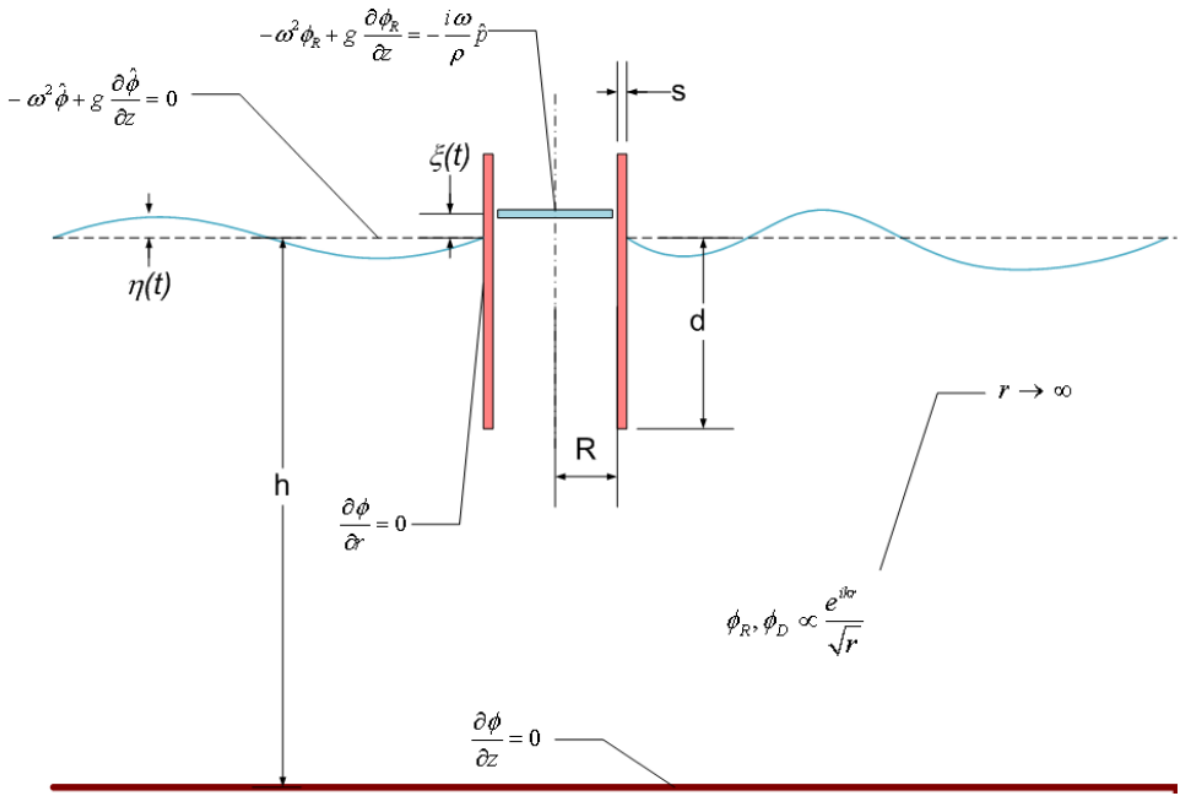

Figure 77: Definition scheme and representation of the boundary-value problem for the solution of the velocity potential due to an oscillating water column [255]

Different commercial BEM codes are available (WAMIT[256], AQWA [257]) to characterise the hydrodynamic response.

4.2.2.1.2 Models for HIL testing

Hardware-In-the-Loop (HIL) means that part of the device to be tested will be emulated in the facility while other part will be a real representation of the device itself. Different facilities will focus on different testing objectives, having different real and emulated parts.

In the case of testing electrical PTO components, the division between hardware and emulated part could be the one shown in Figure 78.

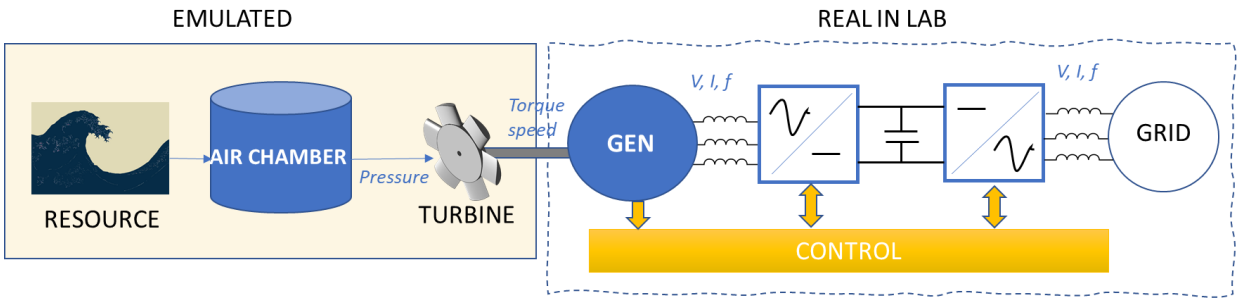

Figure 78: Emulated vs. real subsystems in a HIL electrical facility

HIL testing of electrical PTO components therefore requires a numerical model to emulate the behaviour of the OWC from the resource to the torque and rotational speed in the shaft. Thus, emulated part needed for the hybrid tests could be termed as a **wave to torque model**.

In addition, other software resources are needed in order to operate the facility:

- **Generator control strategy**: a torque or speed control to extract the power from the generator.
- **High level control**: it could be a state-machine to start, operate and stop the device.

These last two controls elements are not strictly models, as they do not represent the mathematical approach of a subsystem. However, they are needed for the facility operation and will be collected and treated as models in this Deliverable.

4.2.2.1.3 Models for full simulation

In the case of a complete simulation, all the subsystems of Figure 76 must be modelled. This will result in a **wave to wire model**. Each subsystem can be modelled with lower or higher detail depending on the objective of the simulation.

The models (or algorithms) necessary for completing the W2W model can be split into:

- **Wave to torque model**: it can be exactly the same model as the one used to emulate this behaviour in the facility. In the case of an OWC device, and depending on the detail level, it will comprise the models of the **resource**, **air chamber** and **air turbine**.
- **Generator model**: it can be represented as a simple electromechanical equation, or it can be more detailed including efficiency and reliability performance.
- **Generator control strategy**: It represents the control algorithm over the generator. The control can be on a torque or speed basis. It will be composed by:
    - Control strategy to obtain the reference speed (or torque)
    - Control loops including the controllers, to extract from the generator the current associated to the reference speed (or torque)
- **Power electronics model**: It represents the behaviour of the power electronics. Depending on the purpose, it can be a simple gain, representing the efficiency (even a unity gain, as the power electronics efficiency is higher than the one of the rest of components), a gain depending on the power load, or a more complex model. If the behaviour of the power converter itself is to be analysed, the switching of the semiconductors can also be modelled. This, however, would have very slow dynamics compared to other subsystems (µs vs. s).
- **Grid model**: this model is not strictly necessary as the outputs of the power electronics can be enough to analyse the performance of the device. The grid model is useful when analysing the behaviour of the device regarding grid connection. A weak or strong grid can be modelled, and perturbations (voltage sags, offset, frequency variations, etc.) can be added.

The inputs and outputs of each of these models are not predefined. They must be adapted in order to fit with the previous and next step.

4.2.2.2 ***Available numerical models***

The numerical models needed for the laboratory testing of the electrical generator encompass the absorption, pneumatic and mechanical energy transformation stages. The principal outputs from this numerical model are the torque and rotational speed. In the context of VALID, we will refer to this part of the W2W models as wave-to-torque models. The rest of the conversion

chain (i.e. electricity generator and grid connection) will be used to control the test rig operation, to model the failure mode and to extrapolate test results.

Table 14: Summary of available models for UC#2.

	Models for HIL testing	**Models for simulation**
Wave to torque	CORES: Input is directly pneumatical power passing through a Wells turbine efficiency curve. Simulink	
	OPERA: hydrodynamic model of Mutriku plant	
	MARMOK model	MARMOK model
Generator		CORES: simple electromechanical equation. Simulink (losses estimation, Matlab-Simulink)
		OPERA: (losses estimation)
		DTOCEAN+: Losses and reliability model. (Python)
Generator Control	CORES: 4 different speed control laws. (Beckhoff-Twincat)	CORES: 4 different speed control laws. (Matlab – Simulink)
	OPERA: 7 different control laws including MPC. (Matlab - Simulink)	OPERA: 7 different control laws including MPC. (Matlab-Simulink)
	MUTRIKU	MUTRIKU (Matlab-Simulink)
Power electronics	Space Vector Modulation and Positive Sequence Detector for a multilevel converter in a DSP	Different switching models of 2 and 3 level power converters.
		DTOCEAN+: Losses and reliability models. (Python)
HIL state machine control *	Tecnalia test rig (Beckhoff-Twincat)	

4.2.2.2.1 Wave-to-torque models

The goal is to translate the environmental loading into relevant inputs to the motor which represents the prime mover mechanical energy obtained from the resource, considering the generator torque

To represent the dynamic of a device, a general approach [258] of the equation of motion for a single body oscillating (f.e. heave) can be represented with de 2nd Newton law:

$$m\ddot{x} = F_e + F_r + F_h + F_{PTO} \qquad (21)$$

Where

m: mass of the device,

$\ddot{x}$: heave acceleration,

F_e: Excitation force,

F_r: Radiation force,

F_h: Hydrostatic force,

F_{PTO} : PTO force.

To take into account nonlinearities, particularly when they can be modelled as time-varying coefficients of a system of Ordinary Differential Equations, it is useful to apply a time-domain model based on the Cummins equation [259], whose use is widespread in seakeeping applications. This is based on a vector integro-differential equation which involves convolution terms responsible for the account of the radiation forces. For a case of a single body floating in heave, the Cummins equation can be expressed in the form:

$$(m + A_\infty)\ddot{x}(t) + \int_{-\infty}^{t} K(t-\tau)\dot{x}(\tau)d\tau + \rho g S x(t) + F_{pto} = F_e(t) \quad (22)$$

Where

A_∞: infinite added mass, the integral term represents the convolution,

ρ: density of the water,

g: gravity,

S: area at the degree of freedom.

The hydrodynamic parameters such as added mass and damping can been obtained using a boundary-element code (ANSYS-AQWA [257]. WAMIT [256]).

4.2.2.2.2 CORES OWC model

Overall description and capabilities

This model was used in CORES project to validate the generator, the power converter and the PLC that were installed in the OE Buoy [260] 4th scale prototype tested in Galway Bay. The model which emulates the buoy and the turbine, gave as output a torque reference to the motor. It directly considered as an input the pneumatic power of the OWC chamber (instead of processing the hydrodynamic iteration of the buoy with the waves). This pneumatic power was empirically obtained on a testing campaign in HMRC [261] wave basin with a floating OWC device at a scale 1:50.

Regarding the definition of the air turbine, the model considers a typical efficiency curve of a Wells turbine as shown in Figure 79. This curve is represented with a look-up table.

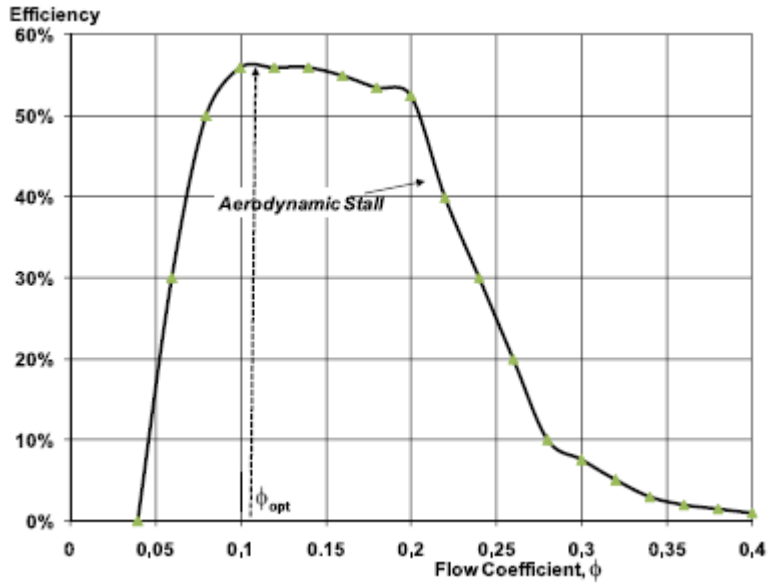

Figure 79: Wells turbine performance characteristic

The nondimensional flow coefficient, φ, input to the look up table, is equivalent to the air velocity to tip velocity ratio and can be expressed as:

$$\phi = \frac{2Q}{(A_{duct} - A_{hub})D\omega} \qquad (23)$$

where Q is the volumetric air flow across the turbine, A_{duct} and A_{hub} are the turbine duct and central hub cross-sectional areas respectively, D is the turbine diameter, and ω is the turbine rotational speed in rad/s.

Mechanical power is considered as $P_{mec} = P_{pneu}\,\eta_{wells}$ and thus, the torque in the shaft can be easily obtained as $T = P_{mec}\,w$.

Communication, software and hardware requirements

Since the test bench was designed for CORES project [262], several users have been working in the lab throughout MARINET1 [263], MARINET2 [206] projects, all of them used Simulink-Matlab [264] to define a time domain model of each device.

In order to guarantee a real time model, a DSpace [265] was used in collaboration with the University of Basque Country. As an output, the model is able to provide the torque reference to the motor taking into account the generator speed.

The generator control laws were developed in the Beckhoff environment (Twincat-Beckhoff [266]) inside the "HIL state machine control". This is an overall control module where a state machine algorithm has been implemented in the PLC. It is divided into 6 states describing the different necessary steps for the correct and safe operation of the system.

At State 1, the system boots up and after a certain time goes directly to State 2, where some verifications are made to be sure that the sensors are operational, and values are inside the requested ranges. For example, it will test the chamber pressure to know if it is within safe operation range [267].

Then State 3 stands for the run up where the brake is released, and the turbine starts rotating and then goes to State 4 where a specific control law can be applied on the generator every sampling period. When an alarm is triggered by sensors or if an error is detected, the machine

system enters in State 5 (low priority) and the turbine slows down until breaking in State 6. If the error is critical, State 6 is directly engaged stopping the operation.

Initial assessment of value provided for the hybrid testing methodology

The model can be used as a fast wave-to-torque model to provide a torque to the generator and analyse the influence of pneumatic power amplitude and variations.

The model takes the pneumatic power as an input. If inputs should be directly correlated with the wave resource, it must be adapted.

4.2.2.2.3 Mutriku OWC model

Overall description and capabilities

This model was initially developed within OPERA H2020 project [251]. Some modifications were developed regarding how to send the speed reference to the motor in real time.

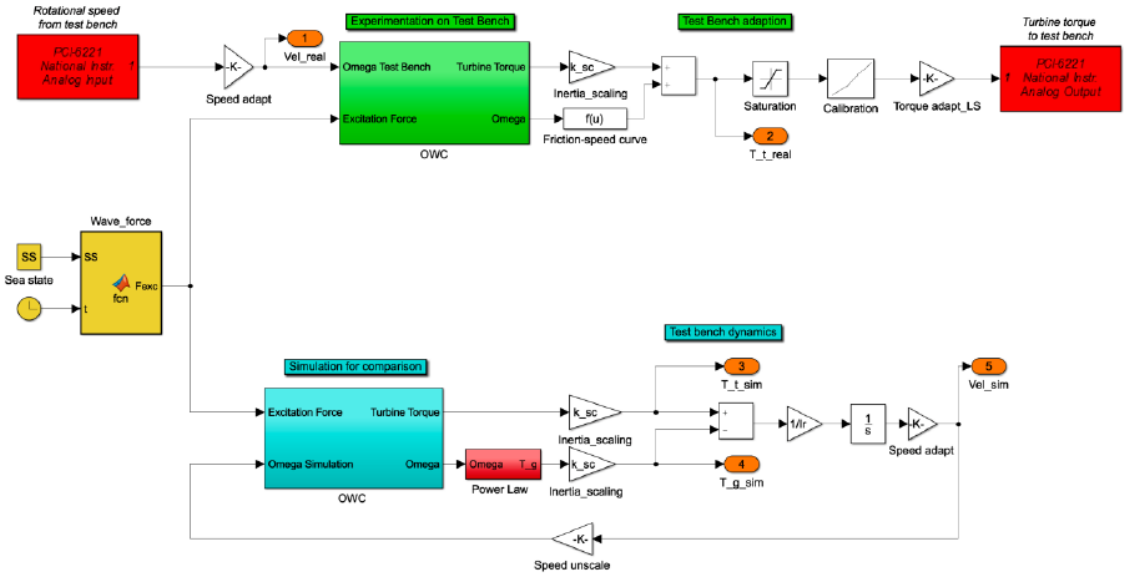

Figure 80: Simulink lay-out for real time experimentation of OWC [267]

Communication, software and hardware requirements

The motor is controlled by a UMV4301 Leroy Somers drive following torque or speed reference provided by the analogue signals coming from the acquisition board **NI PCI 6221** from National Instrument [268].

The simulation is performed by an XPC target configuration which is the real-time architecture from Matlab/Simulink [264]. The generator is an ABB M3BP200MLA 8-pole SCIG of 11 kW rated power for 768 rpm. As the motor, its frequency is 50 Hz and the voltage is 400 V connected in delta. The generator is grid connected via an ABB ACS800 B2B power converter. The PLC controller is a CX1020 [269] from Beckhoff with a series of digital and analogue signal boards.

Initial assessment of value provided for the hybrid testing methodology

The model can be used as a wave-to-torque model that represents the behaviour of the Mutriku plant.

4.2.2.2.4 MARMOK Model

Overall description and capabilities

Marmok model considers the heaving motions of the floating structure and the surface water level as well as the air chamber compressibility and the electric generator. The model can be divided into three parts

- Hydrodynamics: Heave of the floater and Heave of the OWC
- Chamber Pressure and turbine performance
- Generator performance with its internal voltage and current control

The first part represents the energy captured from waves and transformed into WEC motions based on the Cummins Equation (Linear Hydrodynamic coefficients) with state space approximation of the convolution term and two degrees of freedom, heave of the floating structure and heave of the OWC (Figure 81):

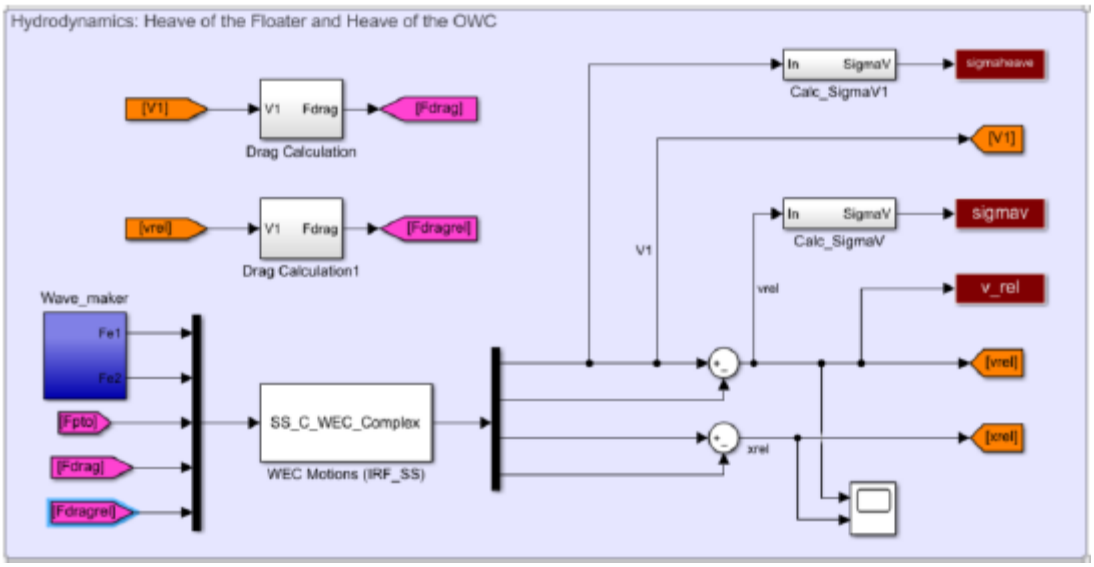

Figure 81: Hydrodynamics: Heave of the floater and Heave of the OWC

The second part represents the energy transformation from WEC motions into a rotating shaft (Figure 82), where the chamber pressure has been added, as well as air turbine non-dimensional curves: airflow / pressure and torque / pressure.

This project has received funding from the European Union's Horizon 2020 research and innovation programme under grant agreement No 101006927.

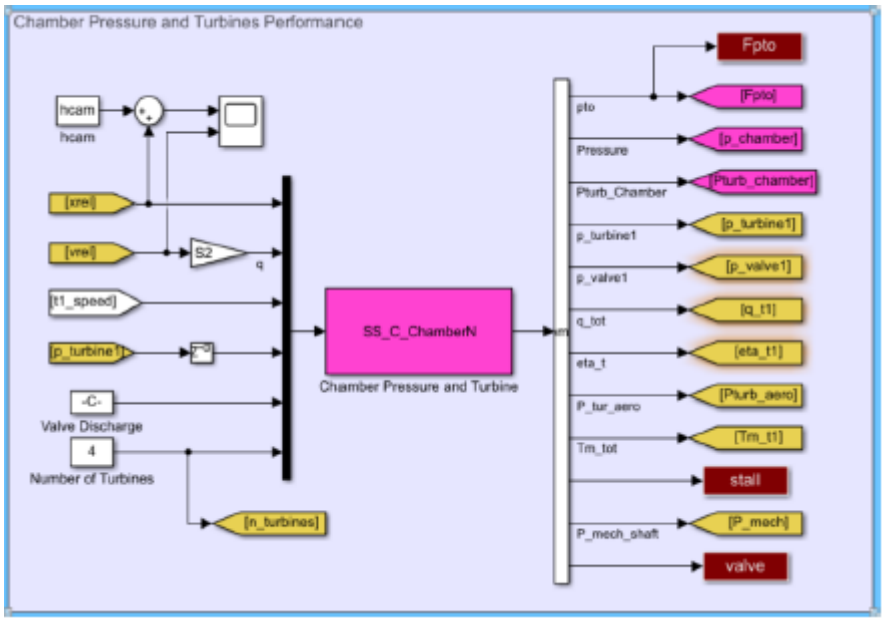

Figure 82 Marmok air chamber pressure and turbines performance

The third part represents the energy transformation from the rotating shaft into electrical current and voltage. There is a stationary model based on energy losses estimation (Figure 83):

- Iron losses
- Winding losses
- Mechanical losses
- Capacity losses

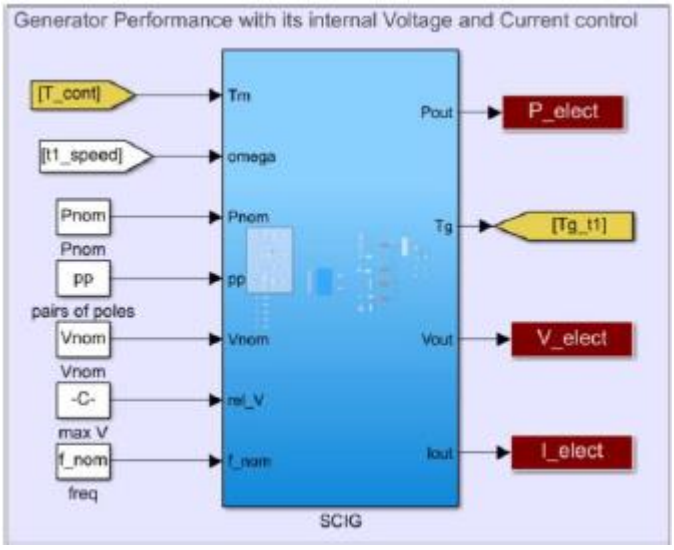

Figure 83: Marmok Generator performance

Initial assessment of value provided for the hybrid testing methodology

The wave to torque model can be used to represent the motion of a floating OWC while the generator model can be used for calculating the losses.

4.2.2.2.5 Electrical generator models - DTOceanPlus model

The ultimate goal is to model the physics of the electrical generator for the critical failure mode, namely thermal fatigue. Most available models have been developed for functional tests (energy yield). However, the usual performance and control models converting input to rque and speed into tension, voltage and thermal losses are not enough to model the generator for the failure mode investigated. Large instantaneous peaks are a feature specific to UC#2.

Overall description and capabilities

The DTOceanPlus project has developed a generator model [270] for reliability analysis. Generator insulation lifetime has been estimated by statistical methods [271]. The machines may withstand temporary, often-repeated high temperatures depending on the duration and amplitude of the temperature peak. A similar shortening of the lifetime applies also to the bearings of the motor, in which heat-resistant grease can be employed.

The generator life is calculated using the mean temperature of the generator given the stator current. Specifically, the total damage on the generator is computed as the sum of the individual damages for each operational sea state.

Electrical insulating materials are thermally rated by test to establish a thermal endurance relationship. This is an expression of aging time to the selected failure criterion as a function of test temperature in an aging test. The former is the number that corresponds to the temperature in °C, derived mathematically or graphically from the thermal endurance relationship at a specified time (often 20,000 hours for utility and industrial machines [272]).

Generator life can be defined from the curves presented in Figure 84, which depend on the class of the generator and winding temperature:

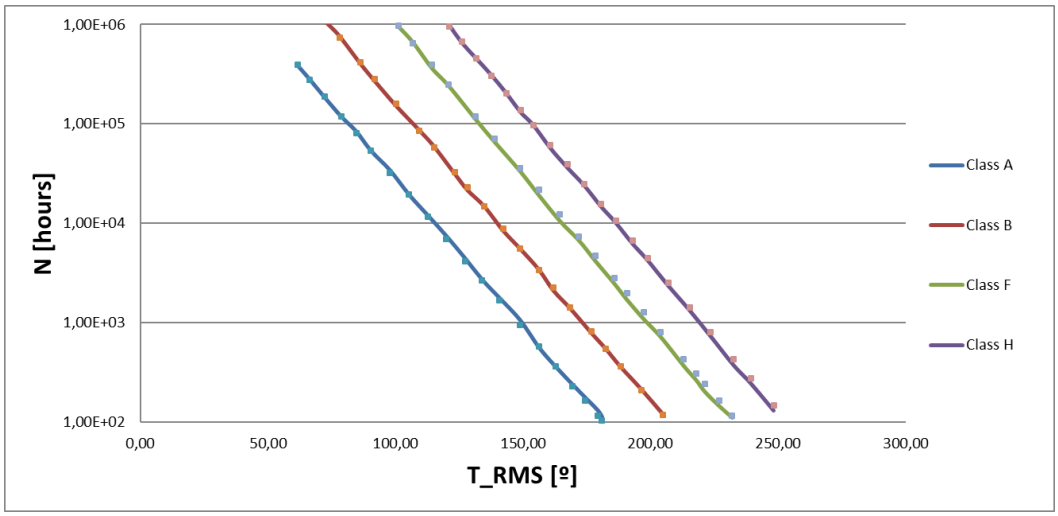

Figure 84: Total winding temperature curves obtained from [273]

Curves of the figure above have been adjusted through logarithmic functions (considering thermal classification of rotating machine insulation materials from IEC 60005 [274]), having obtained the following results: $N = e^{KT+K0}$

Table 15: Life assessment curves adjustment

Life assess adjust	Class A	Class B	Class F	Class H
K	-0.069	-0.069	-0.069	-0.069
K0	17.1288228	18.8974785	20.7619675	22.1243926
T max	105	130	155	180

$T_{RMS}=K*I_{RMS}^2$ (24)

The relation, k, between the RMS current and temperature has been supposed to be the corresponding value to the maximum permissible temperature and the nominal current working point.

Therefore, life damage is computed as the cumulative damage with respect to the predicted life of the generator at every sea state:

$D = \sum_s \frac{n_s}{N_s}$ (25)

This model is integrated in the performance model for two common types of electrical generators: Permanent Magnet Synchronous Generator (PMSG) and Squirrel Cage Induction Generator (SCIG). The performance model computes the mechanical, capacity, winding, iron, rotor and brushes/magnet losses respectively.

Communication, software and hardware requirements

The model has been implemented in Python.

Initial assessment of value provided for the hybrid testing methodology

It can be the starting point for the generator failure assessment model. However, this model only takes into account the impact of the stator current and thus, temperature in the reliability of the generator. Other affecting factors should be included.

4.2.2.2.6 Generator control algorithms

Different control strategies for the optimal performance of the generator and turbine set are available from previous projects. These control strategies were designed for analysing and improving the performance of the device. Even if UC#2 is focused on the reliability of the generator, each control strategy will stress the generator in a different manner. Therefore, the impact of the control law must be taken into account in the tests.

CORES speed control laws (4)

Different control laws were designed within CORES project. Two were focused on low inertia turbines performing a continuous optimum speed control that tried to maintain the turbine working in the maximum efficiency point as much as possible, thus, with the objective of extracting the maximum power [275].

The following expression allows calculation of the optimum speed to maximize the turbine efficiency as a function of air pressure inside the OWC chamber and the actual turbine angular speed, both of which can be measured. This optimum speed reference is commanded to the generator side power converter speed controller:

$$\omega_{opt} = \left(\frac{2P_r}{\left(A_{duct} - A_{hub}\right) K_d D \phi_{opt} \sqrt{\omega}} \right)^{\frac{2}{3}} \quad (26)$$

Usually, the pressure measurement is available. However, if any problem occurs with the pressure sensors it is still possible to control the system, optimizing the turbine efficiency, without the pressure measurement. This can be accomplished by estimating the optimum electrical torque as a function of the rotational speed.

We can easily obtain the maximum mechanical power for a given pneumatic power and $C_{p\_opt}(\phi_{opt})$ being the peak value of the turbine efficiency:

$$P_{mec\_opt} = 0.25 C_{p\_opt}(\phi_{opt}) K_d \phi_{opt}^2 \left(A_{duct} - A_{hub}\right)^2 D^2 \omega_{opt}^3 \quad (27)$$

Due to the pulsating nature of wave energy, the power injected into the grid in these two control laws is highly variable. This fact may seriously affect the grid stability. Additionally, the power electronics of the PTO system must be overrated to withstand high power peaks.

Energy storage systems can be introduced to smooth the electrical power injected into the grid. If the turbine does not have enough inertia, a flywheel can be used to add it. Two new control strategies for a Wells turbine OWC device were designed in CORES [276]. The primary goal of these control strategies was to smooth the profile of the electrical power injected into the grid, so that a high penetration of wave energy does not threaten the grid stability. In both cases, the flywheel also helped to smooth the power through the electric generator. The first high inertia control law tried to extract from the generator the same power that the turbine was receiving in the shaft but filtering it, and thus, avoiding the peaks. This obtained a quasi-constant speed profile, and a smother power output.

The second high-inertia control law designed a sea state basis variable speed control law. It is not possible to follow the speed reference in a wave to wave basis due to the effect of the high inertia. However, it is possible to develop a control law that changes the turbine rotational speed in a sea state by sea state basis. In this case, the rotational speed of the turbine will change until it reaches an optimum value according to the current sea state. It would also be desirable that the speed changes occur automatically without any information or measurement about the sea state. The optimum speed values are obtained through offline simulations. A number of fixed speeds are tested for every sea state and the particular speed that maximizes the efficiency is selected for each.

OPERA speed control laws

One of the objectives of OPERA was the implementation at sea of innovative algorithms for controlling the Power Take Off of wave energy converters that would increase the power production and device reliability

Six (CL1 – CL6) control laws were implemented and tested in the shoreline Mutriku Wave Power Plant during the project and are summarised in the table below. All were previously validated through simulations and dry-lab tests. Unfortunately, the validation of the CL7 was not possible because it required a more accurate estimation of the incoming waves than available.

Table 16: Summary of control laws designed in OPERA

Control Law #	Adaptive/ Predictive	Controls …	Based on …
CL1	Adaptive	Generator torque	Rotational speed
CL2	Adaptive	Generator torque	Chamber pressure
CL3	Adaptive	PTO damping, valve open-close timings	Hourly sea-state data
CL4	Adaptive	Valve open-close timings and position	Rotational speed, chamber pressure and valve position
CL5	Adaptive	Generator torque	Next wave information + output power+ rotational speed
CL6	Predictive	Generator torque	Water column motion in the chamber (position and speed) Pressure in chamber Turbine speed Wave elevation in front of the plant
CL7	Predictive	Valve open-close timings and position	12-24 sec future wave information, rotational speed and chamber pressure and valve position

4.2.2.2.7 Power Electronics models

A complete wave to wire model consists of a variety of systems that integrate different disciplines (e.g. hydrodynamics, aerodynamics, electronics…) and have very different dynamics. Usually, depending on the purpose of the simulation, some subsystems are simplified in order to save computational efforts and focus on the subsystems that have more influence in the objective under study.

Power electronics have very fast dynamics compared to the rest of subsystems in the wave to wire model and present a high efficiency. They are thus, usually not modelled and its performance assumed as ideal. Integrating a complete power converter model, including the switching, would make it really difficult to perform a long simulation if a powerful workstation is not used. In addition, the information it would add is not clear.

However, due to the possibility that the switching of the power converters has some impact in the generator failure mode under study in the UC#2, a compilation of available power converter models has been done.

- Diode rectifier
- Thyristor rectifier
- IGBT 2 level converter with vectorial control
- NPC 3 level converter

4.2.3 Existing test rigs

This section provides a description of the test rigs and capabilities to inform reliability testing of the thermal fatigue in the electrical generator (User Case #2).

The test rigs are set to validate the electro-mechanical behaviour of the Power Take Off system of WECs. Particular attention is given to the applicability in the IDOM's OWC device (MARMOK). However, the capabilities of the rigs can be utilised for other rotating devices such as tidal and wind turbines.

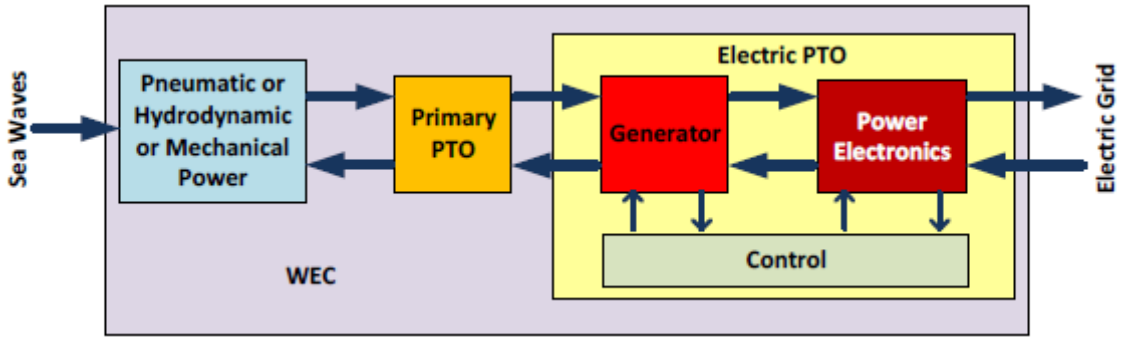

Figure 85: General Test rig schematic

4.2.3.1 ***Electrical PTO test rig (TECNALIA)***

4.2.3.1.1. Overall description and capabilities

The Electrical PTO test rig is a PTO emulator to reproduce the primary mechanical energy captured by ocean energy devices. It provides a controlled lab environment, reducing risks and development time of control laws before the deployment of the system. It facilitates a step-by-step design, fine-tuning and comparison in terms of efficiency, power quality and grid codes. This test rig allows to repeat actual operational conditions (based on field measurements), validate numerical models and identify software errors which may lead to PTO failures.

The following image represents the general scheme of the Electrical PTO Lab.

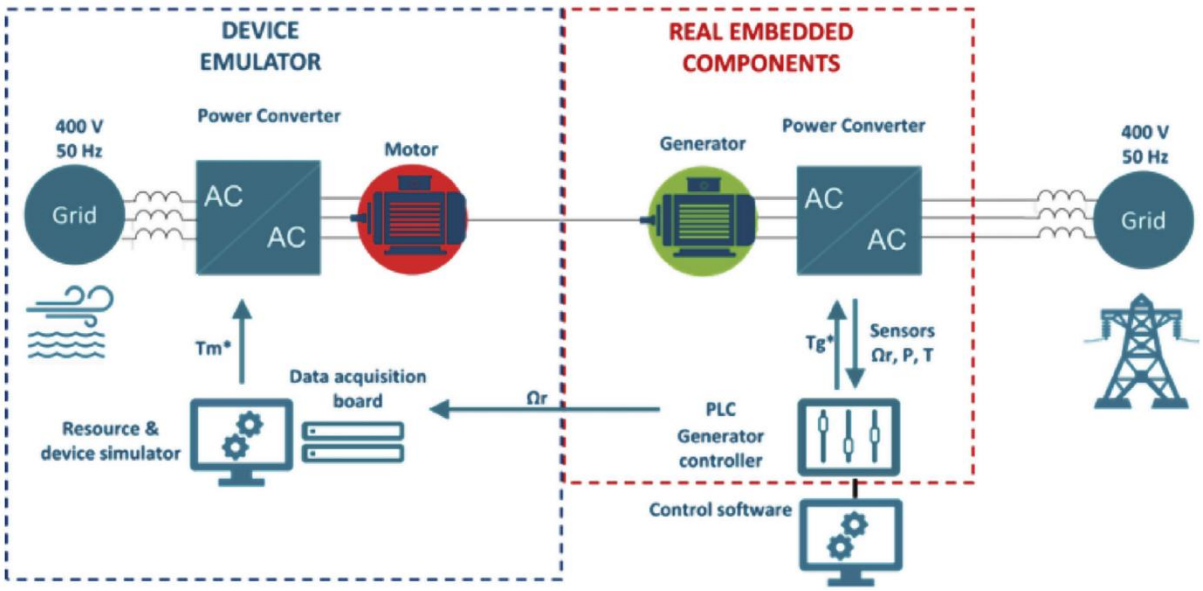

Figure 86: Configuration of the Electrical PTO Lab at Tecnalia.

The test bed can be divided into two key areas, namely the motor and the generator areas. The motor area (device emulator) is composed by the motor, the frequency converter to control

the motor and the motor control software. The aim of these components is to simulate the performance of the WEC and turbine under any sea condition. It is a simulation because the mathematical equations are programmed in the motor control software so that it behaves like the WEC. The generator area (real embedded components) includes the generator, the frequency converter to control the generator and a PLC with the generator control software. This part represents the real equipment that could be connected between the WEC and the grid. The motor and the generator are coupled by means of a gearbox.

The next figure shows the practical setting of the test rig.

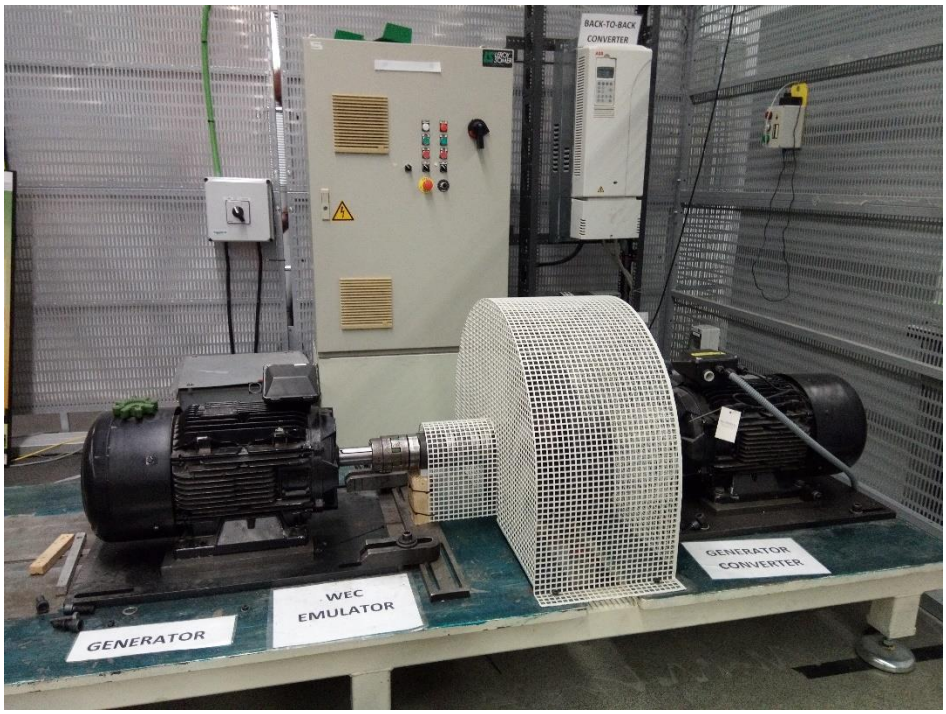

Figure 87: Electrical PTO test rig at Tecnalia.

The test rig has the following components:

Motor and motor frequency converter**:** The motor and motor frequency converter are supplied by Leroy-Somer. They have a rated power of 15 kW and rated speed of 1,460 rpm. The motor is a 2 pole-pairs 15 kW SCIM and allows peaks of power up to 28 kW. The frequency converter is suitable to control motors with a maximum speed up to 3,000 rpm. It can be controlled remotely via external 4/20 mA signals. Motor control is performed via a PC control board. Torque or speed commands updated every 5 ms. Fully controllable in speed or torque control modes. Arbitrary torque or speed waveform references can be followed. Programmable user defined mechanical input characteristics under arbitrary sea states/sea currents/wind conditions can be programmed.

Generator and bidirectional power converter**:** These two components are provided by ABB. The generator is a 4 pole-pairs 11kW SCIG and connected to an isolated grid by the B2B. The converter is rated at 11 kW (heavy-duty use) and permits a flexible remote control of the generator torque or speed via analogical signals. It is possible to adapt the test bed as required by the user to accommodate different generators with different rotational speeds. Currently the test bed is available with:

- 11 kW 768 rpm 400 V squirrel cage induction generator
- 10 kW 1500 rpm 400 V doubly fed induction generator

Generator control is performed by a PLC. Torque or speed commands updated every 10 ms. Fully controllable in speed or torque control modes. Arbitrary torque or speed waveform references. Programmable user defined control software

The motor and generator specifications are listed in the table below:

Table 17: Motor and Generator specifications.

	Motor	Generator	Unit
Model	LSES 160 LUT	M3BP180MLA	-
Rated power	15	11	kW
Rated velocity	1460	768	rpm
Rated torque	97.77	136.77	Nm
Rated current	28.10	27.30	A
cos phi at nom	0.85	0.58	
Nb pairs of pole	2	4	-
Ratio Max/Nom torque	1.86	1.80	-
Nominal voltage	400 Y	400 Delta	V
Nominal frequency	50	50	Hz
Weight	109	239	Kg

Inertia**:** Currently installed with a 1 kgm^2 flywheel. Possibility to increase the inertia up to 8 kgm^2.

Grid connection: Direct grid connection through a full power back-to-back power converter.

Additional communication, software and hardware requirements

The motor is controlled using a real-time simulation based on Matlab/Simulink environment and using an xPC configuration. This type of architecture is composed of a host PC for the development of the numerical model, a target PC operated by the Simulink Real- Time OS and where the model is downloaded and run in real time.

A NI-6221 process board is installed in the target PC. It is the interface to manage the I/O. This setup simulates the performance of the WEC and turbine. The model includes the sea states and the WEC mathematical equations. It receives the turbine speed from the test bench motor encoder and sends the torque that must be applied to the motor using the frequency converter.

The motor frequency converter by Leroy-Somer is rated at 15kW and allows peaks of power up to 28kW. It can be controlled remotely via external 4/20 mA signals. Both speed and torque control modes are available.

The generator is controlled with software programmed in a PLC from Beckhoff. The controller and the generator frequency converter are communicated through several analogical and digital inputs/outputs.

Figure 88: Beckhoff PLC

In this way, the generator rotational speed is fed into the PLC. It is connected to a 400 V grid through a back-to-back bidirectional converter supplied by ABB.

This converter is rated at 11 kW and allows flexible remote control of the generator torque or speed via analogical signals.

In the current application, speed or torque reference are computed by the control law of the generator control software and applied by the back-to-back converter.

The PLC executes a state machine that handles the possible errors and, in case of no error, carries out the speed control algorithms. The output of the speed controller is the electrical torque that needs to be applied to the generator in order to reach the desired turbine speed. This torque reference is sent to the power converter through a 4/20 mA analogue output terminal. The controllers embedded in the commercial frequency converter will follow this torque reference and will control the DC bus voltage and the power injected into the grid. In order to manage the power take-off, the state machine represented in Figure 89 has been implemented in the PLC controller. The state machine is quite simple and just 6 states are used to control the whole system. Transition conditions and actions in each state can be modified to adapt the operation to the desired WEC.

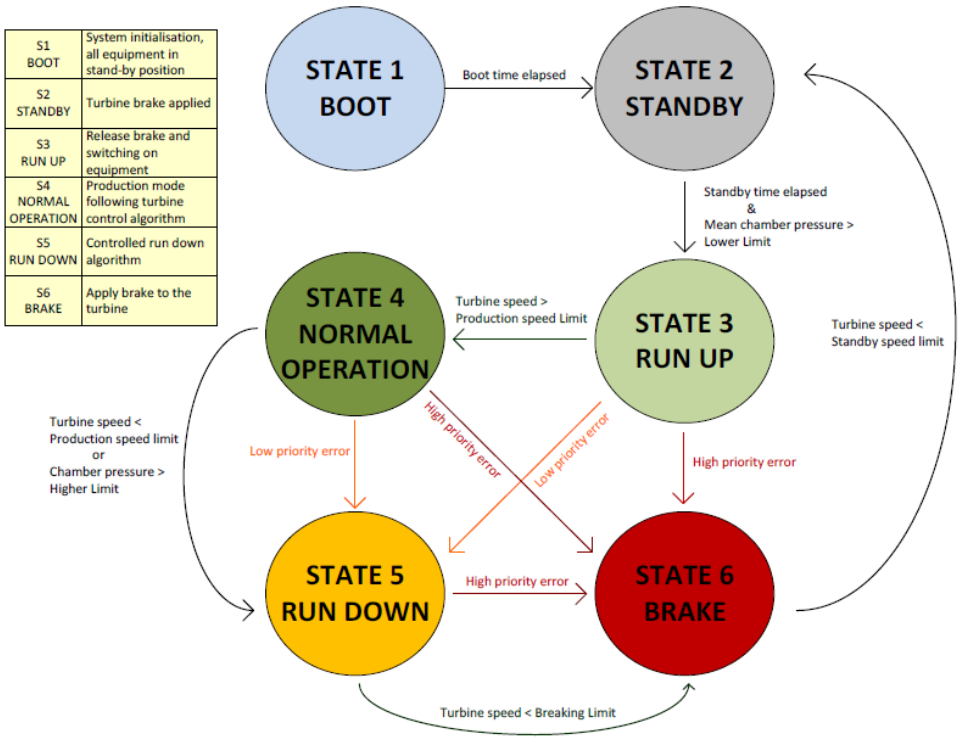

Figure 89: State machine implemented in the PLC controller

4.2.3.1.2. Initial assessment of value provided for the hybrid testing methodology

The Electrical PTO test rig was originally designed for functional tests, namely design and fine-tuning of controllers and comparison of different implementation options in terms of efficiency, power quality and grid codes. The behaviour of the WEC is completely emulated and it is based on the knowledge of the mathematical equations and main parameters of the WEC. The main components that take part on the WEC emulation are the motor, the frequency converter, the programmable inertia and the motor control software. The rest of the WEC components are physical copies of the real ones at small scale. That makes the test bench a *Hardware In the Loop* facility (HIL).

However, the possibility of reproducing actual operational conditions (based on field measurements) opens the way to the investigation of critical failure modes in the electrical generator and corresponding power electronics.

Testing of the generator at full scale is not considered to be a critical requirement, since wave energy devices will have a broad range of nominal powers depending on the deployment site, the specific technology or even the configuration of the PTO (i.e. single or multiple turbines per device). However, some phenomena may not be fully scalable. There is a more fundamental question of how to combine in a controlled laboratory environment the environmental loading which can accelerate the degradation of the insulation under certain conditions.

The analysis of generator performance under specific stress conditions requires the installation of sensors to monitor relevant parameters. Accelerated aging tests will require increasing the stress levels above normal service operation conditions. This could either involve increasing the ambient temperature where testing is performed or undersizing of key components to speed up the failure.

4.2.3.1.3. Preliminary identification of needs for upgrading

The Electrical PTO test rig has suffered some modifications as a result of its use in other research projects. The following picture shows the actual condition of the test rig located in the laboratory of building 700 at Tecnalia. The test rig needs to be put back to work and upgraded with new sensing capabilities. A specific analysis is being done in WP4 leading to the specification of the user case.

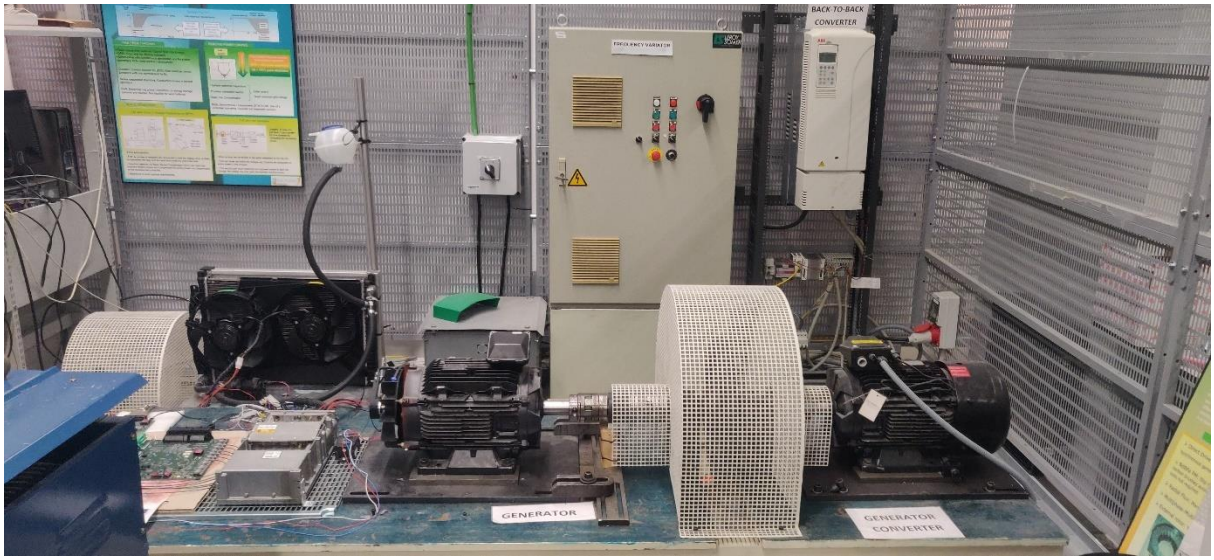

Figure 90: Current status of Electrical PTO test rig at Tecnalia

4.2.3.2 ***Mutriku Wave Power Plant (BiMEP)***

4.2.3.2.1 Overall description and capabilities

The Mutriku Wave Power Plant was commissioned in 2011, the first of its kind being connected to the power grid and currently the only one that has operated for almost ten years. In these ten years of continuous operation the plant has supplied more than 2.000 MWh to the power grid, undoubtedly reaching a significant milestone within the wave energy sector. In addition, the power plant was upgraded with new equipment in order to be used as research and testing infrastructure. Among the equipment, a back-to-back power converter and a control PLC was installed on site, which have already been used during one-year testing of a biradial turbine within the H2020 OPERA project.

However, during this period different components have suffered a significant aging process as the equipment is exposed to a harsh environment with high levels of humidity and salinity, especially in the gallery where turbo-generators are located. Salt accumulation, pitting corrosion and bearing wear are the main causes of component failure. Among the electrical failures stand the generator insulation fault or heatsink overheating due to obstructions produced by salt.

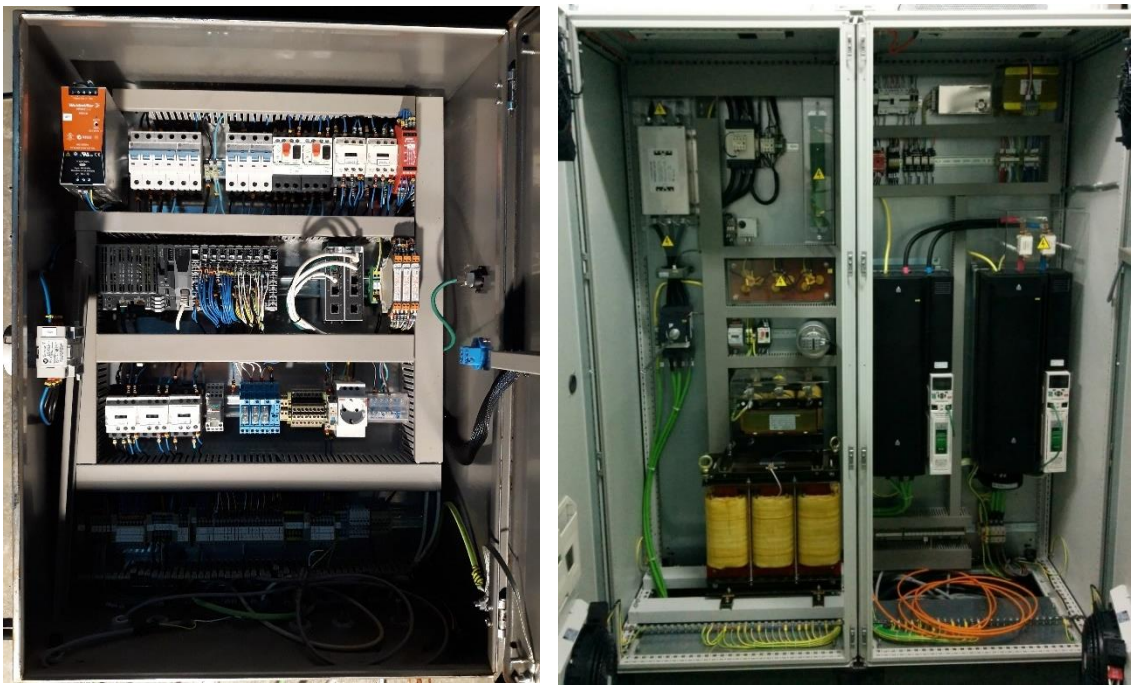

Figure 91: Back-to-back power converter and a control PLC

The following table shows a set of available equipment at Mutriku site.

Table 18: Available equipment at Mutriku.

Equipment ID	Equipment Description	Model
OWC Chamber		
CHB-PS	Chamber Pressure Sensor	Keller-Druck PTX 5072
CHB-LR	Water Column Level Radar	Rosemount 5601
Wells Turbine		
TRB-BV	Motor-operated Butterfly Valve	-
TRB-PS	Damper Position Sensor	Novotechnik RFC 4801
TRB-ACC	Vibration Sensor	IFM VKV021
TRB-DDP	Turbine Duct Differential Pressure	CMR P-Sensor
TRB-TOP	Turbine Outlet Pressure	Druck PTX7533
Induction Generator		
GEN-IM	18.5 kW Induction Generator	VEM
GEN-GWT	Generator Winding Temperature	-
Power Electronics		
PES-B2B	90 kW AC Drive	C. Techniques Unidrive M700
Control Unit		
CTR-PLC	Control & Measurement PLC	B&R X20cCP1584

The Mutriku Wave Power Plant is composed of 16 OWC chambers, from which only 14 are currently equipped by a Wells turbine and an induction generator. The remaining two chambers, located at both ends of the power plant, remain empty as the construction of the breakwater is not fully finished and the side walls are not completely sealed. For this reason,

enough pressure is not obtained in both chambers as the air inside the chamber is lost through small joints and orifices in the side wall.

In addition, one of the 14 chambers in the mid-section of the plant was upgraded with additional instrumentation and is currently used for testing purposes, where new control strategies can be tested as well as novel concepts of turbines and generators. Among the new instrumentation stand the water level radar, control & measurement PLC and the power converter.

Figure below shows the communication topology used in the Mutriku Wave Power Plant.

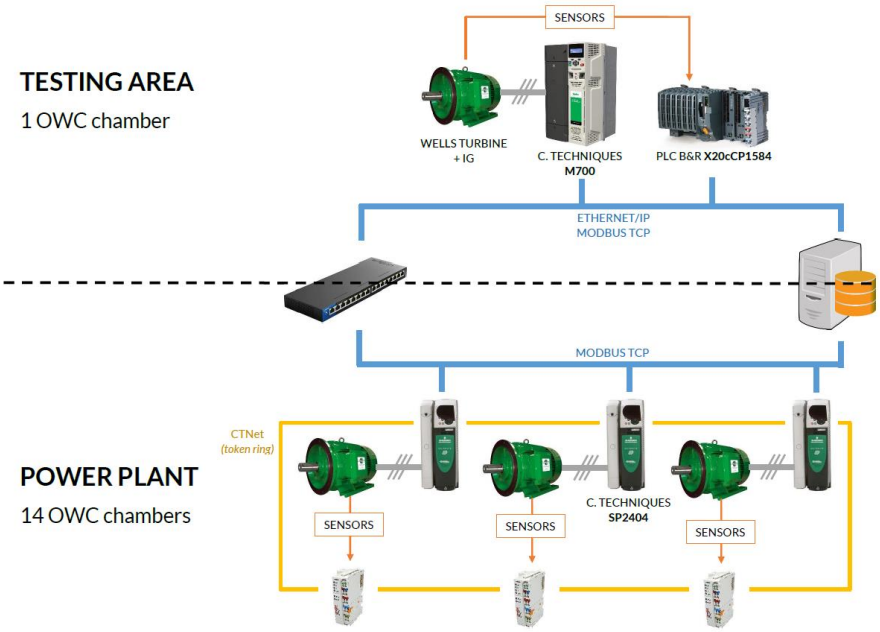

Figure 92: Communication network topology of the Mutriku Wave Power Plant

The original communication system was designed under Control Techniques-brand CTNet topology. CTNet is based on a token ring topology, where the fieldbus headers, control PLCs and servers form a communications ring. The data from the sensors, however, had to be accessed by using specific protocol established by the CTNet system. For this reason, new communication cards were added to access the PLC via Ethernet communication. That means that the PLC itself acts as gateway between Ethernet and CTNet networks. The PLC is attached to the SP2404 power converter, one PLC per power converter and 14 power converters in total.

To improve the communication capabilities, a parallel and separate network was deployed in the testing position where a PLC is responsible for reading from sensors directly and serving the data in an Ethernet network.

4.2.3.2.2 Additional communication, software and hardware requirements

Operation data of each turbine are collected by the plant SCADA and stored in a local database. A sampling period of 100 ms is used to collect data. The list of parameters measured on site is shown below.

Table 19: Measured parameters at Mutriku.

	Pneumatic/mechanical	Electrical
Measured	Pressure (Pa)	Active Current (A)
	Water Column Level (m)	Reactive Current (A)
	Damper Position (º)	Voltage (V)
	Vibration (mmps)	Frequency (Hz)
	Differential Pressure (Pa)	
	Outlet Pressure (Pa)	
	Winding Temperature (ºC)	
Estimated	RMS Pressure (Pa)	Instantaneous Power (kW)
	Rotational Speed (rpm)	Mean Power 1 min (W)
		Mean Power 5 min (W)

4.2.3.2.3 Initial assessment of value provided for the hybrid testing methodology

One of the barriers when analysing the ageing process, material fatigue and their effects, often failure or breakage, is usually a lack of failure events properly recorded and labelled that would allow a post-failure analysis. Fortunately, as mentioned above, overcurrent faults have happened during the operation of the wave power plant. This could have likely been caused by an insulation fault due to thermal stress in the generator windings and it could be worthy of a deeper analysis. Nevertheless, the short number of parameters observed and collected may not provide significant results.

The elevated number of turbo-generator sets placed in Mutriku also makes easier to compare the functioning of different turbines and the stress the machines are subjected to when they are operated under different operating conditions. This may help to analyse those mechanical and electrical parameters able to produce significant alterations on the system which may consequently yield in premature ageing of components.

4.2.3.2.4 Preliminary identification of needs for upgrading

Many sensors show appropriate performances and accuracy class despite the adverse conditions they are subjected to and the fact that they have not been designed for such purposes. Electric meters of the power converter, however, have been designed for the only purpose of protecting electrical equipment, and thus, they do not offer a reliable and accurate measure of many electrical parameters such as voltage, currents and frequency, and other parameters estimated from these measurements such as power and rotor speed. Installation of new and more precise sensors and meters could contribute to improve the accuracy and reliability of the measurements, being it necessary to make some arrangements in the turbo-generator housing for that purpose.

4.2.3.3 ***Available electrical generators for UC#2***

This subsection provides additional information about the technical specification of the electrical generators currently available for testing in UC#2:

- Doubly fed induction generator installed as drive motor in TECNALIA's test rig (15 kW)
- Squirrel cage induction generator (CORES) installed in TECNALIA's test rig (11 kW)
- Induction Generator in TECNALIA, property of IDOM (18.5 kW)
- Squirrel cage induction generator in Mutriku Wave Power Plant (18.5 kW)

The suitability of each generator for thermal fatigue testing will be assessed after the user case is specified in WP4.

Table 20: Doubly fed induction generator installed as drive motor in TECNALIA's test rig

	Motor	Unit
Model	LSES 160 LUT	-
Rated power	15	kW
Rated velocity	1460	rpm
Rated torque	97.77	Nm
Rated current	28.10	A
cos phi at nom	0.85	
Pairs of poles	2	-
Ratio Max/Nom torque	1.86	-
Nominal voltage	400 Y	V
Nominal frequency	50	Hz
Weight	109	Kg

Table 21: Squirrel cage induction generator (CORES) installed in TECNALIA's test rig

	Generator	Unit
Model	M3BP180MLA	-
Rated power	11	kW
Rated velocity	768	rpm
Rated torque	136.77	Nm
Rated current	27.30	A
cos phi at nom	0.58	
Pairs of poles	4	-
Ratio Max/Nom torque	1.80	-
Nominal voltage	400 Delta	V
Nominal frequency	50	Hz
Weight	239	Kg

Figure 93: Induction Generator specifications (property of IDOM)

Table 22: Squirrel cage induction generator in Mutriku Wave Power Plant

	Generator	Unit
Model	GU1V 160L 2	-
Rated power	18.5	kW
Rated velocity	3053	rpm
Rated torque		Nm
Rated current	25	A
cos phi at nom	0.93	
Nb pairs of pole	2	-
Ratio Max/Nom torque	1.80	-
Nominal voltage	460 Delta	V
Nominal frequency	50	Hz
Weight	134	Kg

4.3 User Case #3: Seawater hydraulic pump seals and glider pads

4.3.1 Overview

User Case #3 deals with seawater hydraulic pump seals and glider pads in WECs. The specific case to be demonstrated in the VALID project is based on the Wavepiston WEC. Wavepiston is a multi-body floating oscillating wave surge converter (OWSC) constructed by surging plates connected through beams. The WEC is slacked moored to the bottom (Figure 94, upper panel). Each plate is attached to a wagon, that is connected to two telescopic hydraulic pumps. A unit of plate, wagon, support beam and pumps are called Energy Collectors (Figure 94, lower panel). The hydraulic pump pushes seawater into a transport pipe. The pipe leads the pressurised water to an onshore turbine and/or a reverse osmosis system. Wavepiston has deployed several scaled sea-trials outside Denmark and is presently testing a full-scale system at the PLOCAN test site in the Canary Islands (Figure 95).

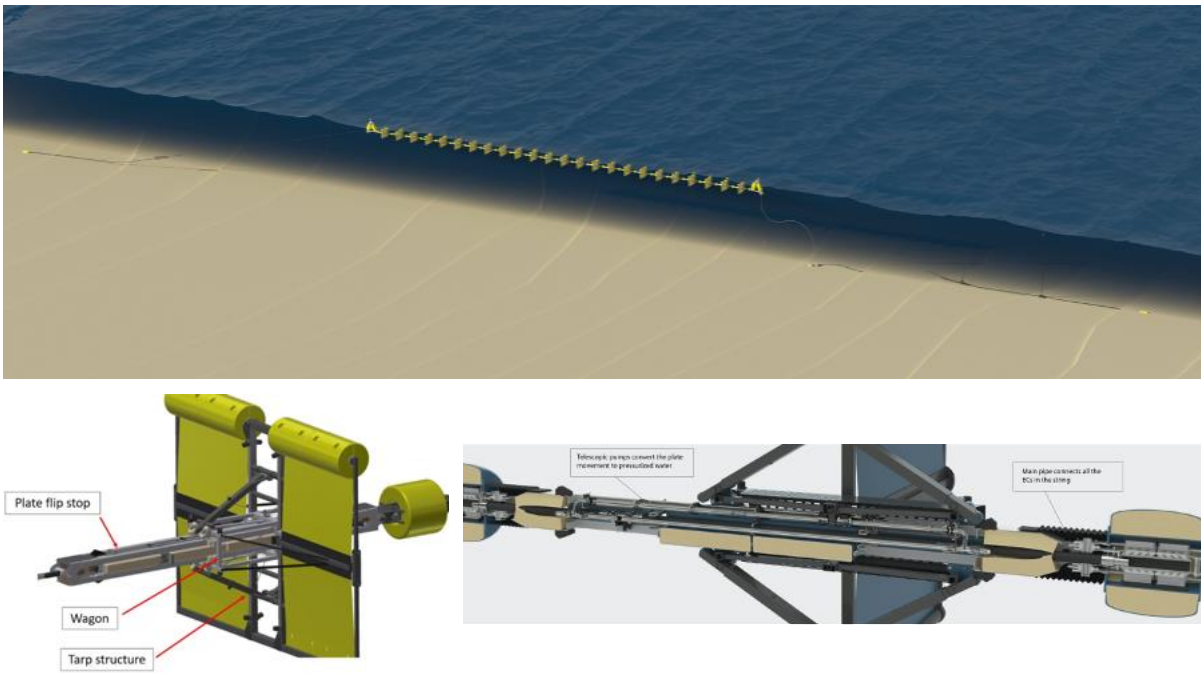

Figure 94: The Wavepiston floating oscillating surge wave energy converter.

Figure 95: Wavepiston with two energy collectors operating at the PLOCAN test site.

The wear of the hydraulic seals has been identified as a critical factor for the Wavepiston device. This is not a unique problem for OWSCs such Wavepiston, but the same problem is present also for all WECs relying on hydraulic pistons in the PTO setting. However, for Wavepiston the hydraulic pumps do not only generate power but also (i) make the energy collectors self-centring, and (ii) are vital for the integrity of the structure by providing damping for the motion of the wagon.

4.3.2 Existing numerical models

4.3.2.1 *Modellable components of an OWSC device*

To fully model a wave energy converter is a multi-disciplinary task. When modelling a WEC the approach is often made up of highly specialised models executed in a sequential manner. These models often represent different sub-systems of a WEC. A general way to breaking it down is presented in Figure 96. Here the different sub-systems are [253]:

1. Hydrodynamic sub-system. This is the system describing the wave energy conversion approach. For the Wavepiston OWSC this is the wave motion causing the surge motion of the plates.
2. PTO sub-system. This system describes the conversion of mechanical power to electricity. This is often a two-stage system. For the Wavepiston OWSC this sub-system consists of a primary PTO in the shape of hydraulic pumps converting the motion of the plates to high-pressure seawater and an electrical generator as secondary PTO that converts the high-pressure seawater into electricity.
3. Power transmission sub-system is the electric system that feeds the converted electricity into the grid.
4. Reaction sub-system. This system provides the reaction point for the PTO. It can be a mooring system or a fixed support structure. For a Wavepiston energy collector this is the support beam that in turn is keep stationary by a slack mooring system.
5. Control sub-system. Consists of sensors and actuators for the electromechanical processes.

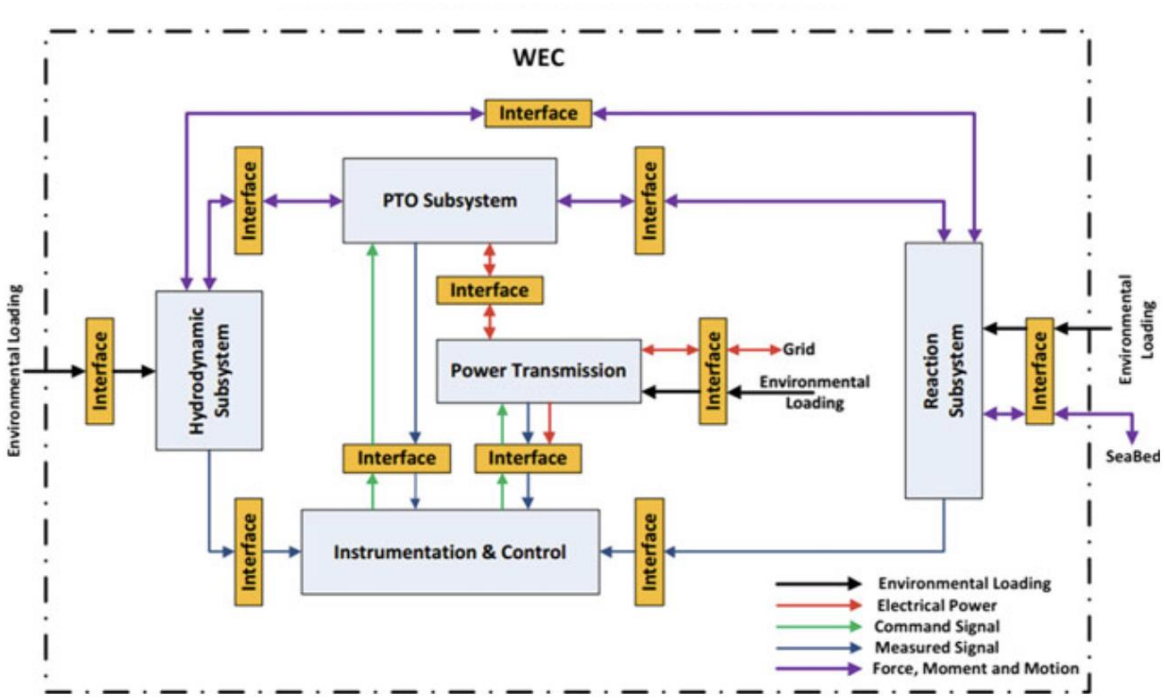

Figure 96: WEC system breakdown. From [253].

4.3.2.1.1 Models for design validation

Due to computational complexity and, mainly, prohibitively large computational times, models used for performing optimization and design of the WEC must often be somewhat simplified. The type of model used for the complete system simulation is referred to as a Wave-to-wire model. A W2W model will typically rely on model equations for all sub-systems listed above, in combination with site specific environmental conditions and grid connection model. For User Case #3 that would count to:

- Environmental model: the operational and survival sea-states are hindcasted from wind-data using a phase averaging wave model such as SWAN.
- Hydrodynamic model: the loads and motions of the WEC are based on linearised hydrodynamic/wave-body interaction and a rigid-body assumption of the WEC.
- Reaction model: Wavepiston is slack moored. The design with many energy collectors per WEC could mean a quasi-static mooring approach to be sufficient. Otherwise, for WECs generally dynamic mooring should be employed.
- Primary PTO model: a dynamic model for the flow and pressure inside the telescopic pump and the transport pipe.
- Secondary PTO model: Generator model
- Grid connection model

Here the specialised numerical models for every sub-system should ideally have been validated against experimental laboratory experiments or against numerical simulations of high-fidelity specialised numerical models.

4.3.2.1.2 *Models for HIL testing*

As mentioned earlier, HIL means that part of the device to be tested will be emulated in the facility while other part will be a real representation of the device itself. The division between hardware and emulated part for User Case #3 is like presented in Figure 97.

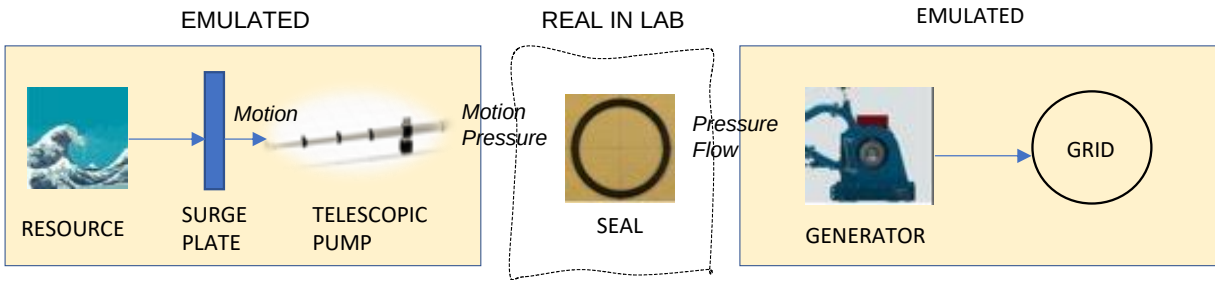

Figure 97: Emulated vs. real subsystems in a HIL seawater hydraulic seal testing facility.

It is assumed that the same sub-system models as used in the W2W model will be used in the emulated parts. However, in the case real-time simulations are required even simpler surrogate models might be necessary for some subsystems.

4.3.2.1.3 *Models for full simulation*

The full simulation model will consist of the W2W model described above but with extra added numerical or heuristic models for estimation of

- Wear, fatigue, and reliability models for the seals
- Wear, fatigue, and reliability models for the glider pads

4.3.2.2 ***Available numerical models***

The numerical models available for the Wavepiston user case are listed in Table 23.

Table 23: Overview of numerical models for User Case #3.

Num.	Model Type	Software	Comments
1	Computation of motion and power production. Frequency domain tool.	WEC-1 [277] [278]: an in-house model developed in MATLAB. Model relies on hydrodynamic coefficients in WAMIT format.	Developed by DTU.
2	Computation of motion and power production. Time domain linear tool.	WEC-2: an in-house model developed in MATLAB. Model relies on hydrodynamic coefficients in WAMIT format.	Developed by DTU. Based on the open-source DTU Motion Simulator [279].
3	Computation of motion and power production. Time domain weakly nonlinear tool.	WEC-SIM [280][281]. The hydrodynamic response uses WEC-SIM standard implementation while there are bespoke implementation of the	Restricted to surge motion only and fixed support structure.

Num.	Model Type	Software	Comments
		PTO and export pipe. Model relies on hydrodynamic coefficients computed by WAMIT and/or NEMOH.	
4	Computation of motion for the macro system including mooring. Time domain weakly linear model.	ORCAFLEX [247]. Orcaflex is able to handle the wave-body motion and restraints from the mooring system. Bespoke external forces can be added using the ORCAFLEX API.	Model setup and execution by external consultants. Model does not include PTO.
5	CFD model (U-RANS) for estimating viscous effects.	STAR-CCM+ [282]. Two-phase simulations using the volume of fluid approach.	Forced surge motion with no waves.
6	Fatigue modelling	Waterfall analysis of WEC-2 results	
7	FEA. Structural mechanics. Nonlinear time dependent.	NASTRAN [283]. Used as an overall structural design tool. Identified "hot spots" are needed for detailed analysis using ABAQUS.	
8	FEA. Structural mechanics. Nonlinear time dependent.	ABAQUS [284]. Used for detailed studies.	Model setup and execution by external consultants: Sigma Energy & Marine

4.3.2.2.1 Models for motion and power estimation

As seen from Table 23, Wavepiston have 3 different numerical models for estimating the power production from the device. They are all based on linear hydrodynamic theory; one solves the motion and the power production in the frequency domain while the other two works in the time domain. The first two are developed by Technical University of Denmark and is based on the open-source linear solver DTU Motion Simulator [279] which is implemented in MATLAB. In this report we will, however, focus on the model based on WEC-SIM [280].

The governing equations to be solved are the Cummings equation for the motion (28), two pressure equations for the pumps (29) and accumulators (30) and, finally, one equation for the continuity of the flow in the pipes (31):

$$(m + A_\infty)\ddot{x} + \int_{-\infty}^{t} K(t-\tau)\dot{x}(\tau)d\tau + \rho g S x + F_{pto} + F_{moor} + F_{drag} = F_{ext}, \quad (28)$$

$$Q_{n-1} - Q_n = |\dot{x_n}|\, S(\dot{x_n}, x_n), \quad (29)$$

$$\dot{p_m} = (Q_{n-1} - Q_n)\frac{p_1}{V_E}\left(\frac{p_m}{p_1}\right)^{1/\gamma+1}, \quad (30)$$

$$\dot{Q_n} = \frac{A_n}{\rho L_n}(p_n - p_{n+1}) - \frac{1}{2D_n A_n} f\left(\frac{Q_n}{A_n}\right) Q_n^2, \quad (31)$$

where *m* is the mass matrix, A_∞ is the added mass matrix at infinity and x is the position vector. Overdots denote differentiation with respect to time. *K* denotes the damping matrix, and the integral is the damping impulse response function. *S* is the water plane area. F_{ext} denotes the wave excitation forces, while F_{pto}, F_{moor} and F_{drag} denotes the possibly nonlinear source functions representing PTO, mooring and viscous drag forces, respectively. Pressure and discharge in the *n*:th pump are denoted p_n and Q_n, while L_n, D_n, A_n describe the length, diameter, and cross-section area of the pipe. p_m is the pressure at the inflow to the accumulator, while p_1 and V_E is the pressure and volume of the bladder containing gas. Finally, γ is the specific heat ratio.

WEC-SIM time domain

WEC-SIM is a multi-body model based on linear hydrodynamics develop in MATLAB/SIMULINK by NREL/Sandia [280][281]. However, as WEC-SIM supports the nonlinear Froude-Krylov approach for the excitation force it can be viewed as a weakly nonlinear model [285]. The external forces can be fully nonlinear. WEC-SIM comes with blocks for PTOs [168] and constraints and supports dynamic mooring [171],[286].

The Wavepiston model in WEC-SIM is for simplicity here shown for the case of two energy collectors only. The approach has been extended to up 24 energy collectors, but the 2 energy collectors case include all modules used. Figure 98 show the main Simulink blocks. The green block is the global frame located at the bottom. The grey blocks are PTO blocks whose main objective is to constrain the motion to surge only. While the grey PTO blocks include classical spring-damper PTO we do not use those but instead couple to a Wavepiston specific PTO block that have been developed to mimic the telescope hydraulic pumps (the red block). The actual plates are the yellow body blocks.

Focusing on the telescopic pump block, the most important parts are show in Figure 99. Here the PTO force is obtained as

$$F_{pto} = \mathrm{p}\, S\, \mathrm{sign}(-u). \quad (32)$$

If we disregard the flow in the export pipe, then the energy collectors basically work independently and there is no coupling between the energy collectors, as seen in Figure 98. If we allow for a time-dependent flow and pressure in the pipes connecting the energy collectors to the on-shore turbine, as well as adding accumulator tanks, the energy collectors become coupled. The corresponding Simulink block become as illustrated in Figure 100. The light-blue blocks solve the continuity equation, including losses, in the pipes. Including these blocks now couples the energy collectors together.

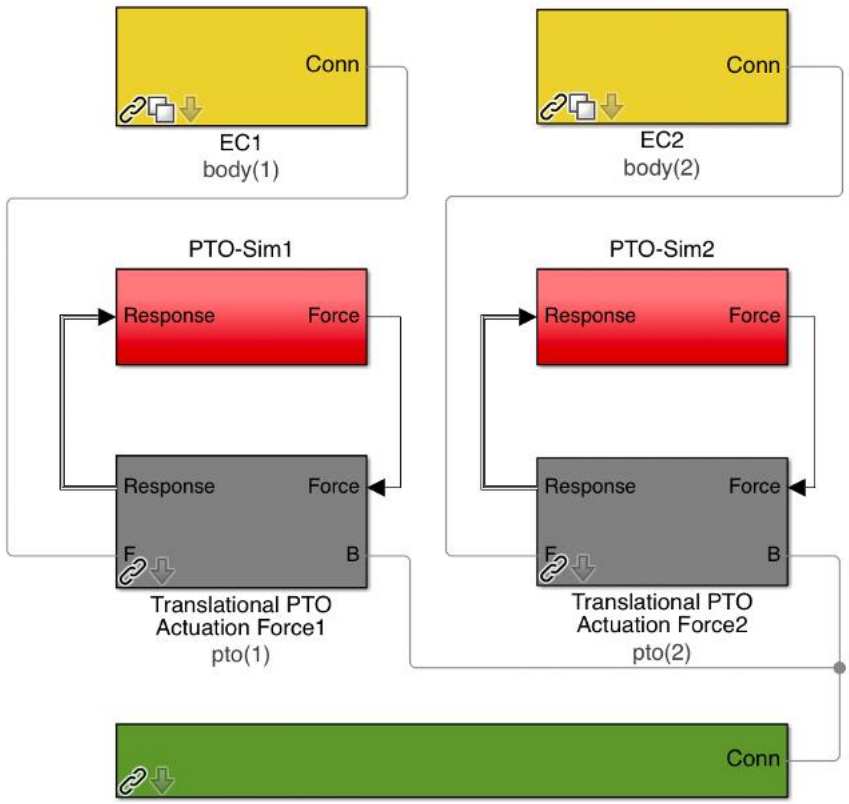

Figure 98: WEC-SIM Simulink representation of the basic Wavepiston WEC (ECx=Energy collector x)

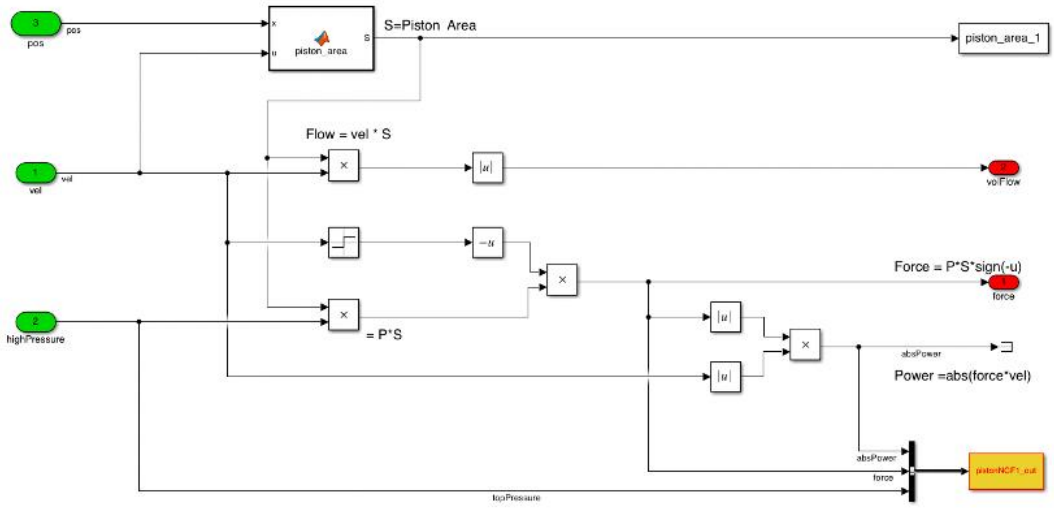

Figure 99: WEC-SIM Simulink representation of the hydraulic pump.

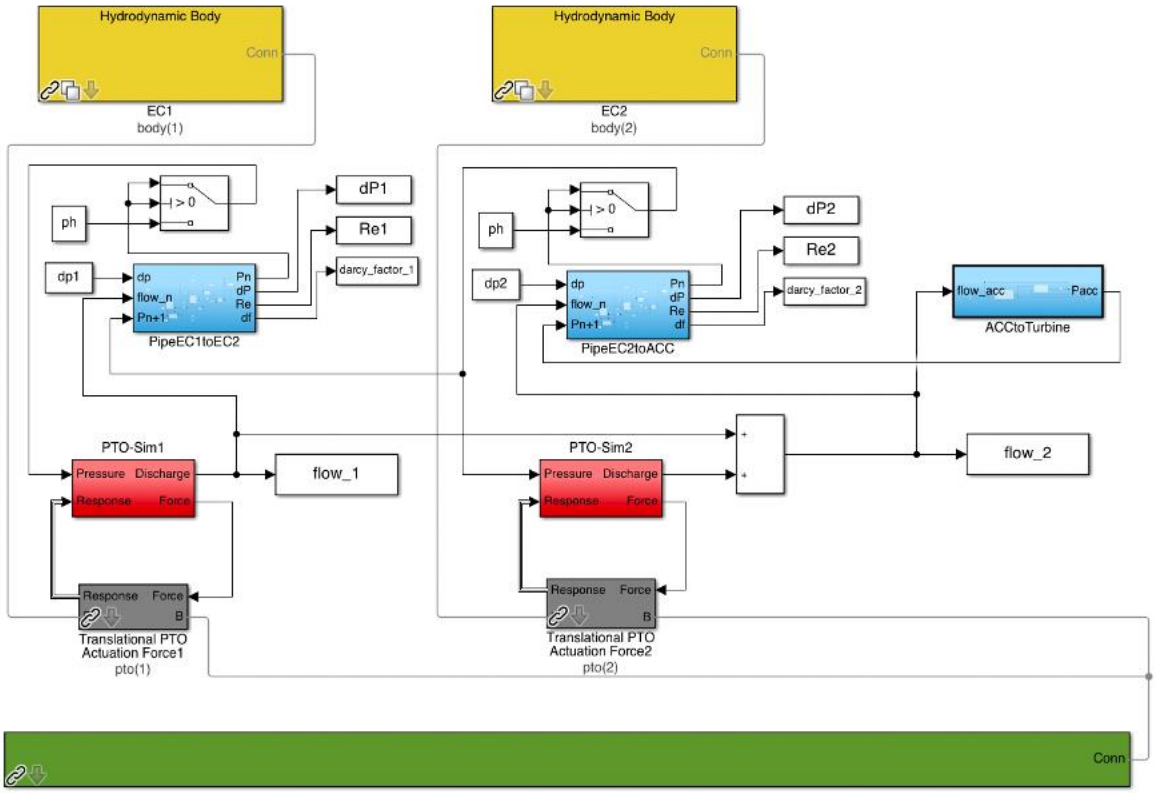

Figure 100: WEC-SIM Simulink representation of the Wavepiston WEC with connecting pipes and accumulator tank.

<u>WEC-SIM time domain compared to WEC-1 and WEC-2.</u>

Generally, the three motion simulation models provide similar results. Figure 101 shows a comparison of the pressure in the pump for a "one pump – one accumulator" tank set-up. In Figure 100 "eps" denotes the steepness of the waves, defined as the ratio of wave height over wavelength. Please note that the reason the WEC-SIM model continues to increase the pressure is that the WEC-SIM model did not have the end-stop forces turned on. End-stop forces are implemented within the PTO block as for WEC-SIM version 4.2. As the WEC-1 model is significantly faster it might be used in an initial part for the hybrid modelling.

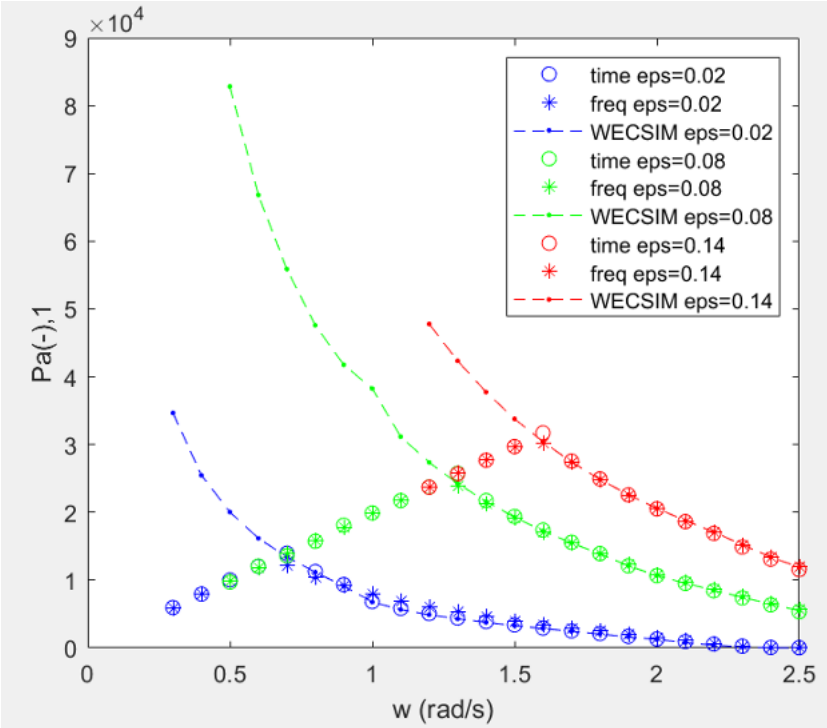

Figure 101: Code-to-code validation of pressure in the hydraulic pump (eps denotes wave steepness, i.e. wave height/wave length).

4.3.2.2.2 Model for survivability cases

While the above models are focused on power production and the motion is presently restricted to surge only, Wavepiston uses yet another model for mooring and export pipe design. This model is set-up in Orcaflex, the commercial industry standard model for mooring and offshore. Orcaflex is like WEC-SIM a weakly nonlinear model (based on linear hydrodynamics with nonlinear Froude-Krylov implementation). However, as this model is mainly focused on survivability, in the Orcaflex Wavepiston model the energy collectors are simplified to be Morison bodies and there is no PTO active (albeit that is presently under implementation). On the other hand, the Orcaflex model supports the "flipping" of the energy collector plates i.e. the plate fold together when the wagon hits the end-stop damper to reduce the load at the extreme position (see the left most energy collectors in Figure 102).

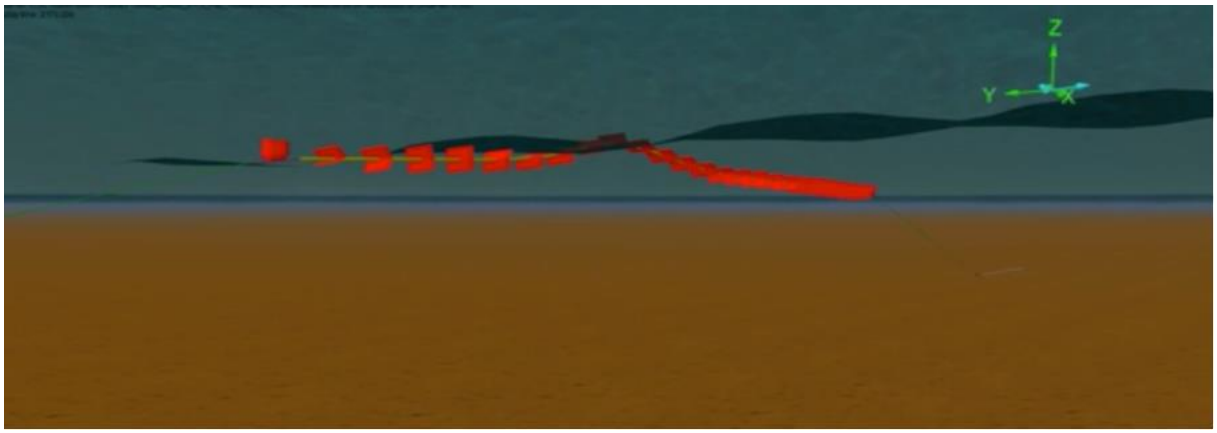

Figure 102: Snapshot of the Wavepiston Orcaflex model [287].

CFD model

The Wavepiston plates clearly cause vortex generation and losses from induced drag (see Figure 103). This is further complicated by several plates in close proximity to both other plates and the free surface. Thus U-RANS simulations has been carried out to get better estimation of drag coefficients. This being an important variable connected with large uncertainty in the weakly nonlinear hydrodynamic models discussed above. The simulations were performed in model-scale and for an earlier design of the plates.

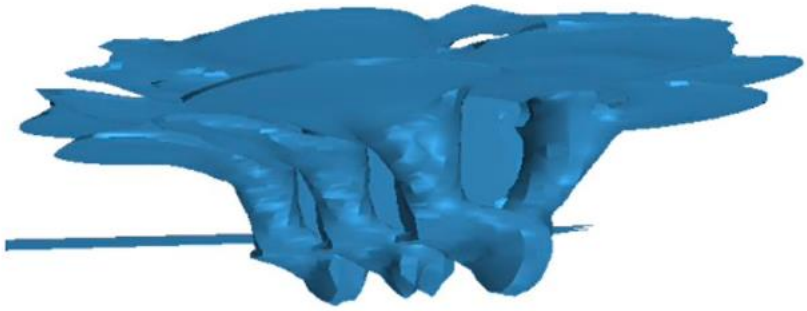

Figure 103: Snaphot of a CFD simulation showing vorticity =2/s iso-contour for three plates in close proximity to each other and to the free surface [288].

Structural dynamic models

The macro Wavepiston system experience significant motion yielding structural loads on the support structure and wagon. The bending and torsion of the beam and wagon is believed to greatly influence the wear and fatigue of the glider pads/wheels. Thus, FEA models have been set-up in NASTRAN and ABAQUS. Figure 104 show the deformation of the wagon due to torsion of the structure. The attachment of the glider pads/wheels are deformed which likely will influence the wear and fatigue.

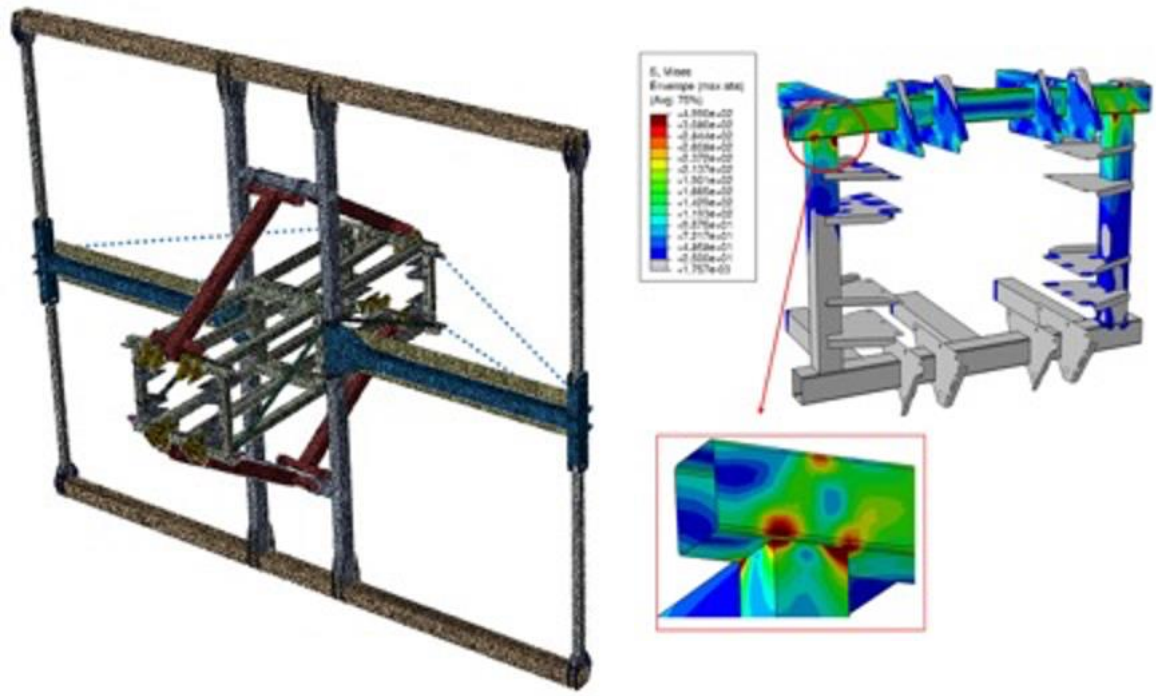

Figure 104: ABAQUS FEA simulation of response to torsion. Left: mesh and Right: Stresses and deformation (exaggerated 5 times) of the wagon/glider pads holder [289].

4.3.2.3 *Communication, software and hardware requirements*

The sub-models are to be coupled by the AVL Model.CONNECT platform. Most of the sub-models are developed in MATLAB/Simulink. The Model.CONNECT already supports the Simulink communication. The sub models and the Model.CONNECT software are to be run on a standard workstation.

4.3.2.4 *Initial assessment of value provided for the hybrid testing methodology*

The numerical models outlined above can provide the fundamental data about the required motion of the wear bar that is needed by the hybrid testing. The models will also be used to get the limits of the unsteady pressure that the seals will be subjected to.

The WEC-SIM model is highly valuable to the project as it forms the basis for the virtual models to be used in the hybrid testing methodology. The WEC-SIM W2W model will provide the motion of the hydraulic pump in the physical test rig and thus form the boundary conditions to the hybrid model. The WEC-SIM model additionally forms the starting point for a more refined hydraulic pump/export pipe model that will be coupled through Model.CONNECT.

The Orcaflex model is valuable as verification/validation of the WEC-SIM model for global motions, but is not foreseen to be coupled to the hybrid test rig.

The CFD model is highly valuable to be used to get a better prediction of the drag the plates are experiencing. To obtain better drag coefficients are vital for the global motions that will drive the physical test rig. This model will thus provide data but not be coupled through the Model.CONNECT.

The NASTRAN/ABAQUS models are valuable to estimate possible bending/torsion of the frame for the glider pads. These models will thus provide data but not be coupled through the Model.CONNECT.

4.3.2.5 *Preliminary identification of needs for upgrading*

- To extend the WEC-SIM model to include the motion of the macro-structure as well as the mooring restoring forces.
- The model is highly sensitive to drag and multi-EC plate simulations for wave-plate interaction should be carried out in CFD to better identify this for the full-scale PLOCAN device.
- There is a critical need to include a higher-fidelity model for the hydraulic pump and to include models for predicting the wear of the seal and glider pads.
- The onshore electrical generator/reverse osmosis system should be included to obtain a more complete W2W model.
- Grid connection should be included to obtain a more complete W2W model.
- Judging from the FEA simulations hydro-elasticity will probably have to be included in a simplified manner in the W2W model if to accurately address the glider pads reliability.

4.3.3 Existing test rigs

This section provides a description of the existing test rigs and capabilities to perform reliability testing of seals and glider rings in seawater hydraulic pumps (User Case #3).

The test rigs are set to validate the behaviour of seawater hydraulic pumps. Particular attention is given to the applicability in the Wavepiston's floating oscillating surge device. Generally, the seawater hydraulic pumps are part of the power take-off (PTO) sub-system acting as the primary PTO. However, the capabilities of the rigs can be utilised for other devices targeting e.g. desalination and pumping storage.

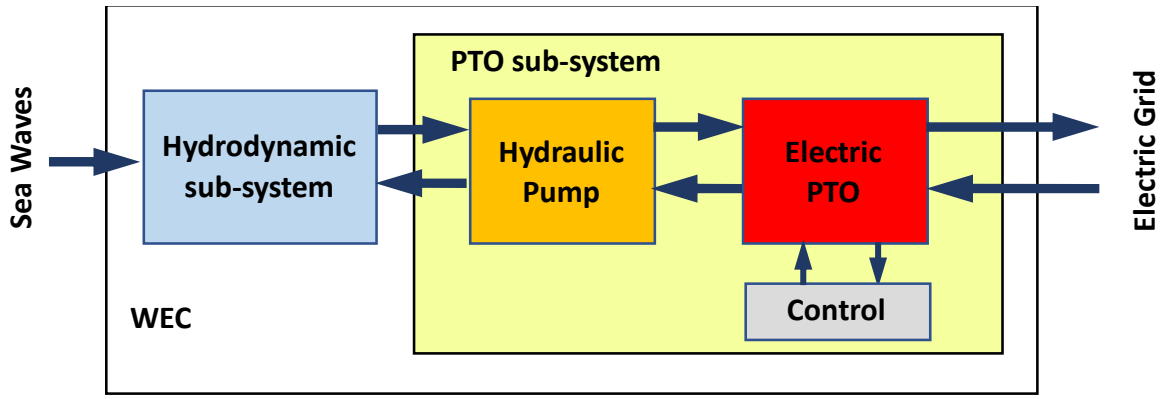

Figure 105: General test rig schematic

4.3.3.1 *Seawater Hydraulic Pump Seal Test Rig (Fiellberg OY)*

Overall description and capabilities

The Seawater hydraulic pump seal test rig is used to assess the wear on the seals and wear on the rods of the hydraulic rams of the Wavepiston system. It mimics the translation in one degree of freedom motion of the primary PTO, which in turn is caused by the wave motion. Looking at the Wavepiston device (Figure 106) the hydro-dynamic sub-system is made up of the energy collectors, i.e. the plate-wagon system. The hydraulic pump is then connected to the wagon which is experiencing a translating single degree of motion.

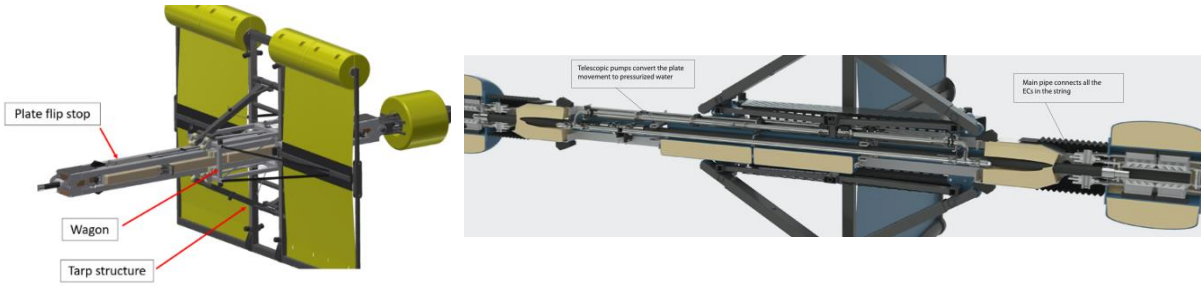

Figure 106: Overview of one Wavepiston energy collector and the seawater hydraulic pump.

Figure 107 presents an overall drawing on the test rig while Figure 108 shows photographs of the test rig. There are several main parts (as indicated in Figure 107):

A. The electrical motor.
B. The arm translating rotation to oscillatory linear motion (prime mover).
C. The support structure holding the wear bar.
D. The wear bar.
E. The seal block package holding up to 4 seals.
F. Pressure tank (not included in Figure 107)

The electrical motor and arm are generating the oscillatory linear motion. The rpm of the motor is controlled by a manually programmed Variable Frequency Drive and sets the frequency of the translating motion of the wear bar. The design of the arm sets the stroke length, which is constant. The wear bar is then pushed back and forth by the arm while the seal block package is locked in place in relation to the support structure. Please note that the resulting motion is close to sinusoidal, but not fully sinusoidal as illustrated in Figure 109. The seal block package consists of up to 4 seals which can be set under pressure. During operation the seals operate fully immersed in water.

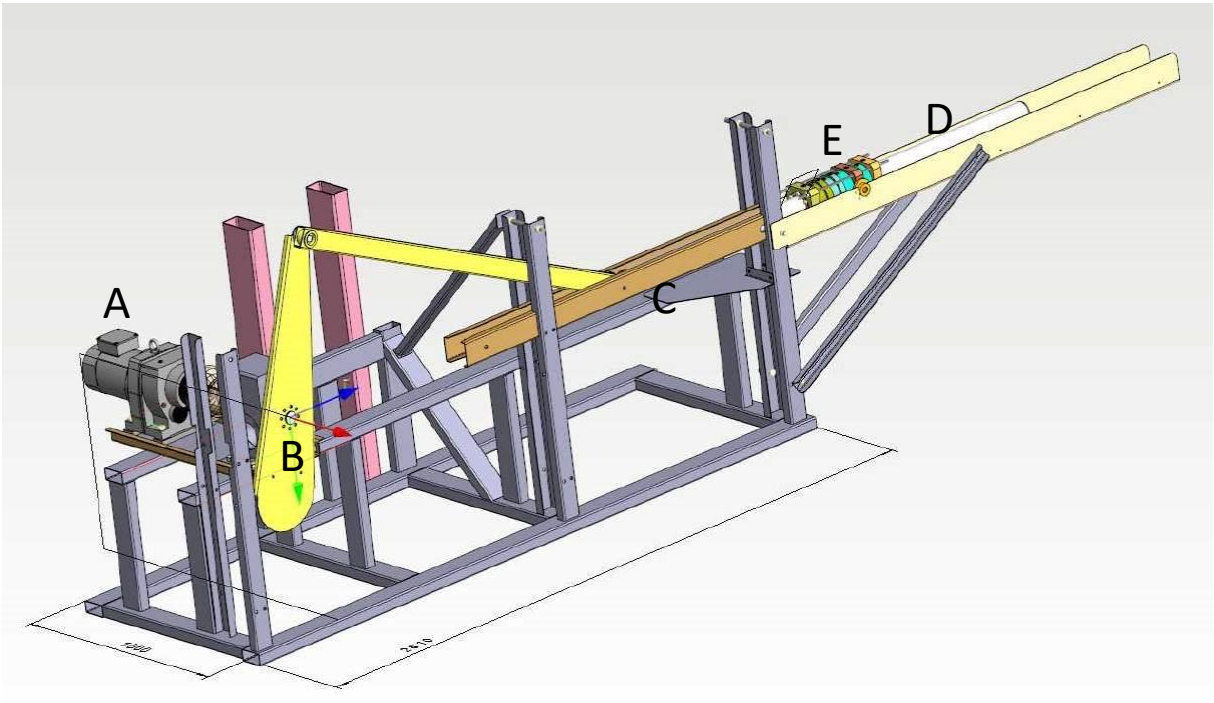

Figure 107: Drawing of the Seawater hydraulic pump seal test rig

Figure 108: Photos of the Seawater hydraulic pump seal test rig. Top: overview. Bottom: Seal block package.

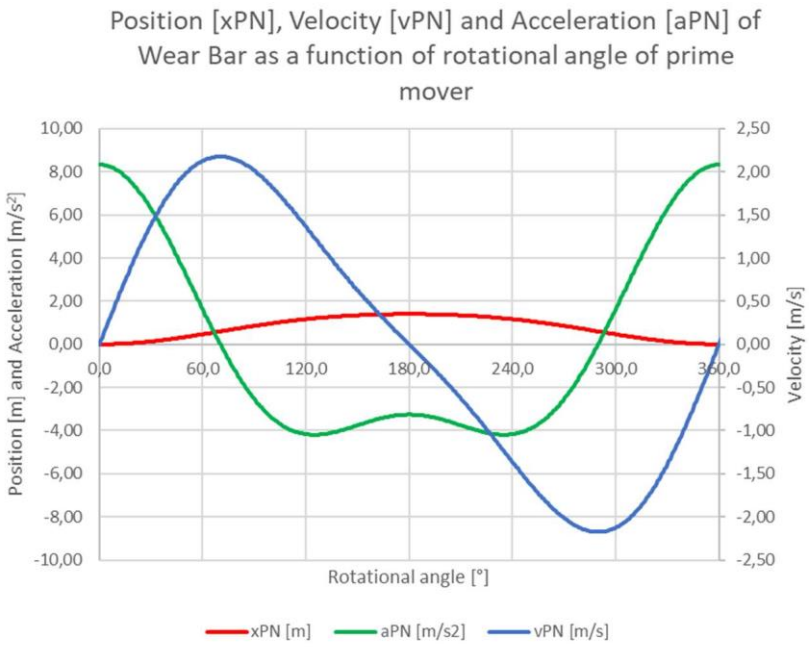

Figure 109: Position, velocity, and acceleration of wear bar as function of the rotational angle of the translating arm.

Table 24 presents the main characteristics of the test rig.

Table 24: Hydraulic Seal Test rig specifications.

	Maximum	Minimum
Motor frequency (rpm)	25 rpm	5 rpm
Stroke length (m)	2 m	(Depending on arm length)
Seal diameter (mm)	60 mm	60 mm
Pressure (Pa)	10 MPa	0 MPa

The test rig has the following components:

- **Motor:** VEM G43A DM100LC4
- **Pressure tank:** Unknown high-pressure pump
- **Data acquisition system:** None, seals and counterpart are inspected manually.

Additional communication, software and hardware requirements

As mentioned above, the test rig is not controlled by any software and there is no automatic collection of data.

Initial assessment of applicability to the hybrid testing methodology

The Seawater hydraulic pump seal test rig has been designed for testing of fatigue and wear of different seals. The behaviour of the WEC is quite simplified as, at present, only regular harmonic motions with a constant stroke length can be emulated.

Another major draw-back of the current setup is that the seals are fully pressurized during the entire test. This is very different from actual operation conditions where the seal is only energized in the compression part of the stroke cycle.

The seals are tested in full scale conditions which circumvents any scaling problems.

The tests are carried out using temperature-controlled pH buffered artificial sea water which is assumed fully aerated.

When upgrading the seal test machine, it would be extremely useful to perform it such that both seal tests and sliding pad tests can be run simultaneously and on the same machine. This will speed up test times and, at the same time, ensure consistent and comparable wear data for all gliding components of the Wavepiston system.

Preliminary identification of needs for upgrading

- To upgrade the test rig to support operational conditions, i.e. mimicking irregular wave motion response as well as the uneven pressure for energizing the seals.
- The test rig needs to be upgraded with a control system as well a data acquisition system which enables continued monitoring of friction and internal pressure.
- As suspended material in the sea water is expected to be very important for the wear of the seal, the test rig should accommodate this feature.

- It would be beneficial if the upgraded test system, after certain test intervals, could interrupt testing and assess seal performance by pressurizing the seals, shut down the high-pressure pump and then measure the gradual decline in pressure.

All in all, it is most likely that a completely new test rig will be constructed within WP5, along the lines of Figure 110.

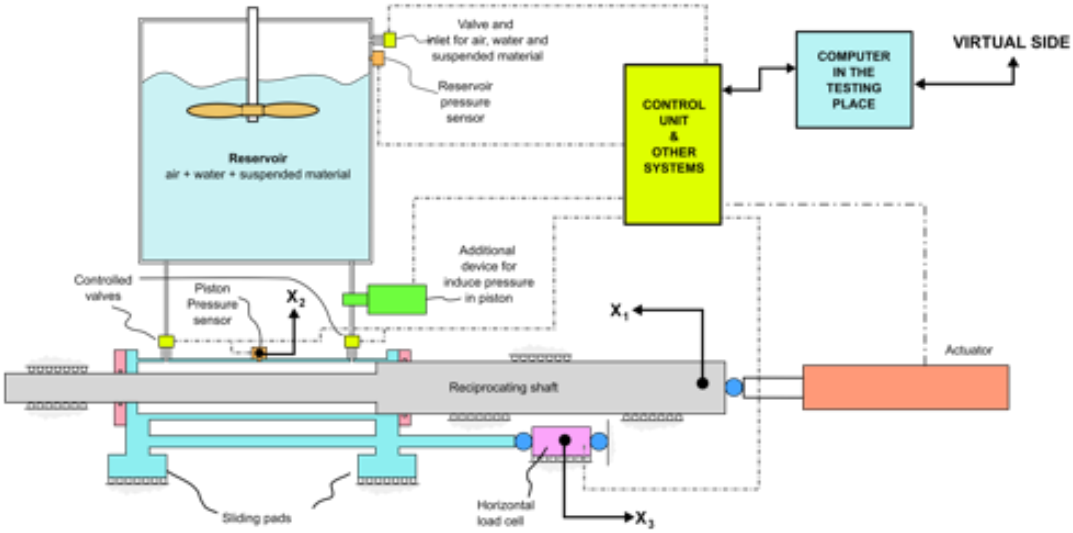

Figure 110: Outline of upgraded seawater hydraulic pump seal test rig.

4.3.3.2 *Gliding Pads Test Rig (Wavepiston)*

Overall description and capabilities

The Wavepiston system is heavily dependent on gliding pads, partly to align the different sections of the hydraulic rams and partly to align the wagon (which drives the hydraulic rams) with the supporting beam. All gliding pads in the Wavepiston system experience movements closely related to the movements of the seals.

The gliding pads test rig is used to assess the wear and fatigue of the gliding pads of the wagon that is part of the primary PTO. It mimics the translation in one degree of freedom motion of the primary PTO, which in turn is caused by the wave motion. Looking at the Wavepiston device the hydro-dynamic sub-system is made up of the energy collectors, i.e. the plate-wagon system. The wagon is attached to the wear bar by several gliding pads (see Figure 111).

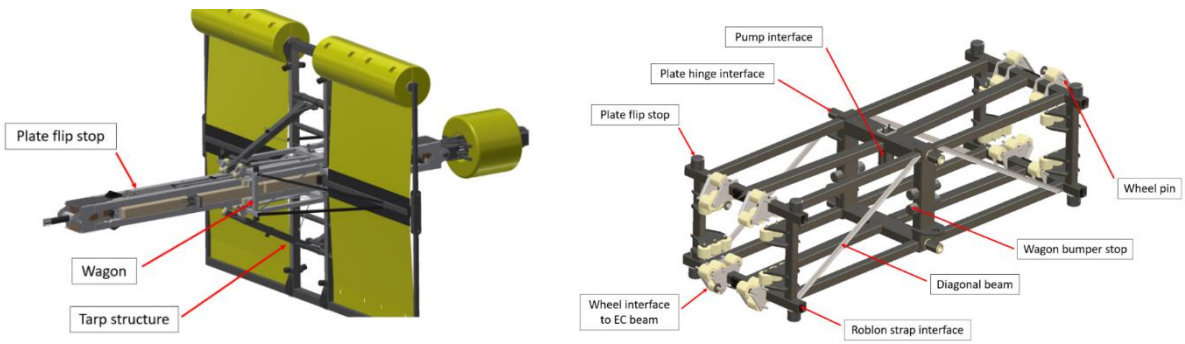

Figure 111: Overview of one Wavepiston energy collector, the wagon and the glider pads/wheels.

The gliding pads test rig set up is similar to the hydraulic seal test rig. It consists of a motor and arm that provided the one degree of motion with a fixed stroke length. The arm is attached to the wear bar. The wear bar moves inside a small basin filled with water. The glider pads are attached to the basin walls (see Figure 112). There are two sets of glider pads in the test rig.

Figure 112: Photos of the glider pads test rig. Left: overview. Right: Glider pads.

Table 25: Glider pads test rig specifications.

	Maximum	Minimum
Motor frequency (rpm)	25	25
Stroke length (m)	1	1
Glider pads diameter (mm)	10	0
Pressure on pads [N]	100	20

The test rig has the following components:

- **Motor:** VEM G43A DM100LC4
- **Data acquisition system:** None, at certain intervals testing is interrupted and wear on pads and polymer liner is estimated using optical inspection and simple analogue measurement methods

Additional communication, software and hardware requirements

As mentioned above, the test rig is not controlled by any software and there is no continuous collection of data.

Initial assessment of applicability to the hybrid testing methodology

As for the hydraulic seal test rig there is presently a shortcoming in only fixed stroke lengths that can be modelled and not responses as for irregular wave cases.

The glider pads are tested in full scale conditions which circumvents any scaling problems.

The tests are carried out using temperature-controlled pH buffered artificial sea water which is assumed fully aerated.

When upgrading the sliding pads test machine, it would be extremely useful to perform the upgrade such that both seal tests and sliding pad tests can be run simultaneously and on the same machine. This would speed up test time and at the same time ensure consistent and comparable wear data for all gliding components of the Wavepiston system.

Preliminary identification of needs for upgrading

- To upgrade the test rig to support operational conditions, i.e. mimicking irregular wave motion response.
- The test rig needs to be upgraded with a control system, an improved actuating system as well a data acquisition system which enables continued monitoring of friction.

This project has received funding from the European Union's Horizon 2020 research and innovation programme under grant agreement No 101006927.

4.4 Virtual testing platform

This section provides a description of the IODP capabilities that AVL provides to the VALID project. Model.CONNECT™ and Testbed.CONNECT™ capabilities.

The mentioned tools can be used to create pure virtual or hybrid prototypes, integrating various models, created in various software tools, with test benches, Figure 113.

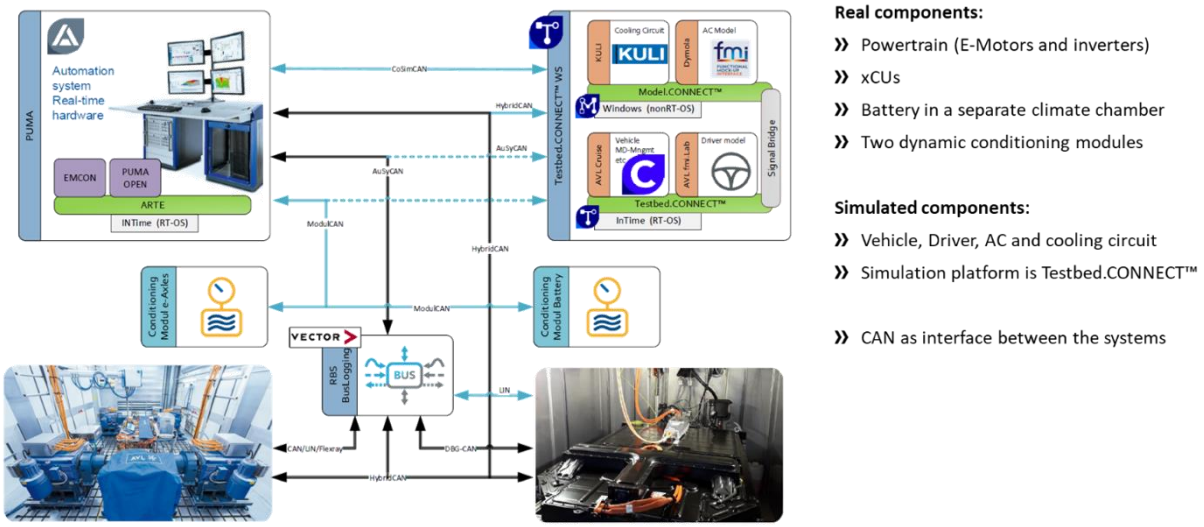

Figure 113: Typical set-up of a hybrid prototype, incorporating multiple simulation models and a test bench

4.4.1 Model.CONNECT™

Model.CONNECT™ is a model integration and co-simulation platform, connecting virtual and real components. Models can be integrated based on standardized interfaces (Functional Mockup Interface, FMI) as well as based on specific interfaces to a wide range of well-known simulation tools.

Model.CONNECT™ supports the user in organizing system model variants. These variants may describe different configurations of the system under investigation as well as different testing scenarios and testing environments.

Through the integration with multiple model execution environments, Model.CONNECT™ supports the continuous functional integration scenarios that form the basis of model-based development processes in particular in the automotive industry.

As a member of the AVL Simulation Desktop, Model.CONNECT™ features powerful model parametrization and batch simulation capabilities, simulation online monitoring, result analysis, and reporting functionalities. Interfaces to various optimization tools enable design studies and optimizations.

The model execution is supported in two flavours which can also be combined:

- Model integration based on models that are provided as executable libraries (FMI for Co-Simulation or Model Exchange). Such model configurations can be executed in one process. Such closely coupled model configurations are prepared for execution on real-time operating systems with later releases of Model.CONNECT™.

- Tool-coupling based on the ICOS technology which is a distributed co-simulation platform with a wide variety of supported simulation tools, industry-leading co-simulation algorithms (e.g. adaptive time step control, NEPCE), and the possibility to connect real-time systems to the co-simulation. The modular architecture provides the possibility for an iterative model developing process. Furthermore, influences of model accuracy, model depth, and nonlinearities on the result can be determined, due to the cross-domain considerations.

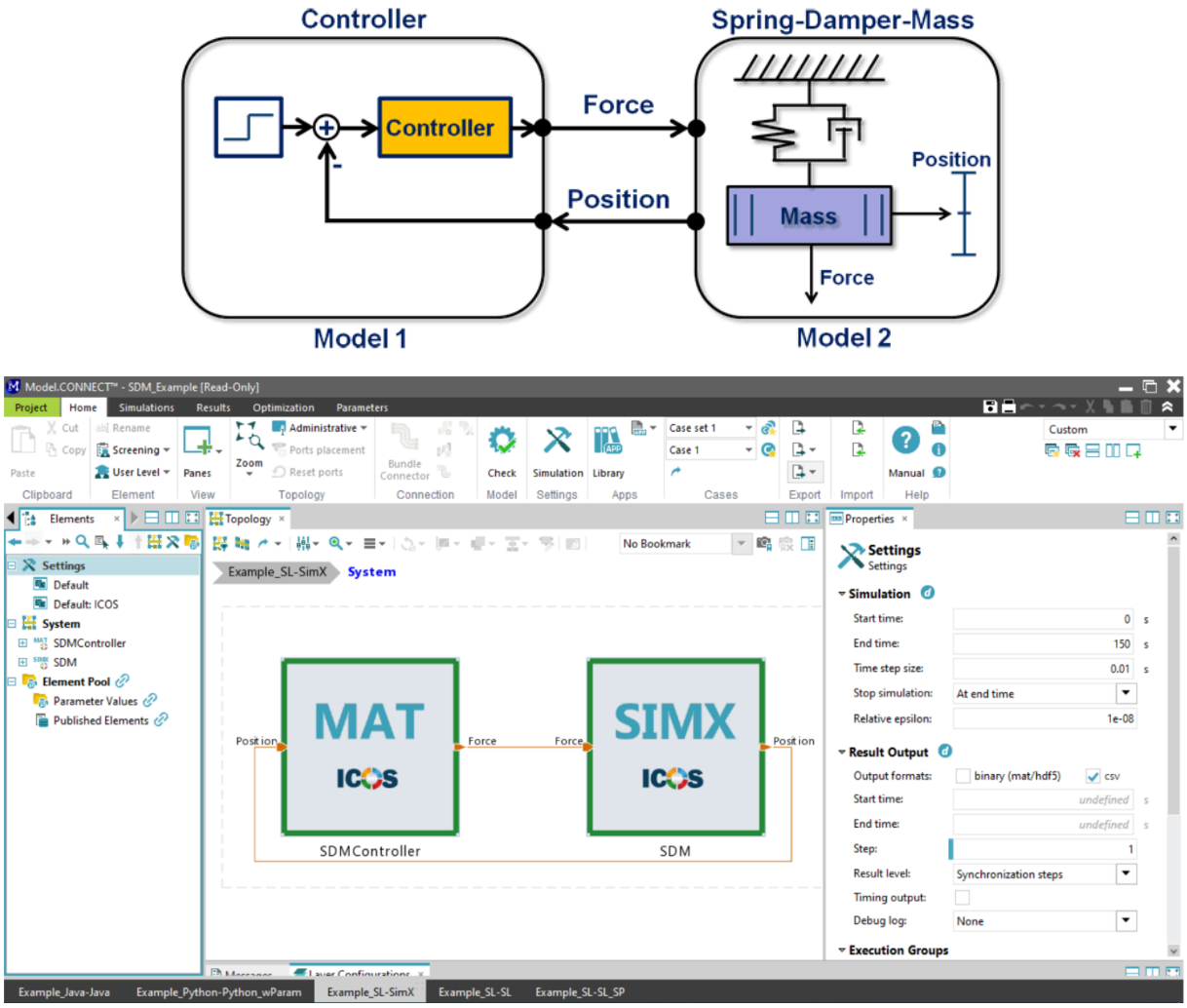

Figure 114: Typical (simple) Co-Simulation problem and setup in Model.CONNECT™

4.4.1.1 *Hardware and software requirements*

The recommended hardware requirements for Linux and Windows are:

- Processor(s) recent x86 or x86_64 processor architecture
- Main Memory >= 8 GB
- Graphic Card hardware OpenGL & Direct-X support / 2 - 4 GB
- Storage >= 256 GB Solid State Drive

Following operating systems are supported:

- Microsoft Windows 10

- Red Hat Enterprise Linux 7 or newer

4.4.1.2 *Supported Tools*

Model.CONNECT™ supports a wide variety of tools with vendor-specific or generic interfaces, see Table 26 and Table 27.

Limited support means, that the interface is no-more maintained or not extensively tested (e.g. due to small demand, or because the interface is new).

The Custom Interface is used for the integration of any simulation tool in Model.CONNECT™. The communication is done via the DllLink.dll and its headers (dllLink.h and dllLinkSpecial.h) which are provided in the installation. Keep in mind that the DllLink.dll is not thread safe. Tested programming languages are python, C, C++, FORTRAN, JAVA. A typical code showing the integration of python-code, is given in section 4.4.1.3. Details are given in the Model.CONNECT™ manual.

Table 26: Supported Software Tools Model.CONNECT 2020R2.

Tool/Interface	Tool vendor	Supported versions
Adams	MSC Software	2015.1, 2016, 2017.2, **2019.2**
AMESim (Simcenter)	Siemens LMS	R13.3-14-14.2-15-15.2-16-17, 2019.1, **2019.2, 2020.1**
AVL BOOST	AVL	2016 – 2020 R1, **2020 R2**
AVL CRUISE	AVL	2011.3 – 2020 R1, **2020 R2**
AVL CRUISE M	AVL	2016 – 2020 R1, **2020 R2**
AVL FIRE	AVL	2014.2, 2017 – 2020 R1, **2020 R2**
AVL Testbed.CONNECT (RT model export)	AVL	1 R2.1, 1 R2.3, 1 R3, 1 R3.1, 1 R4, **1 R5**
AVL Testbed.CONNECT (non-RT model coupling)	AVL	**1 R5**
AVL VSM	AVL	3.13, 4.0, 4.1, 4.2, 4.3, **2020 R1.4**
CAN (RealTime)	n/a	n/a
CarMaker/TruckMaker	IPG Automotive	4.5.4, 5.1.1, 6.0, 7.0, 8.0, **8.1**
CarMaker for Simulink	IPG Automotive	4.5.4, 5.1.1, 6.0, 7.0, 8.0, **8.1**
CarSim Product Family	Mechanical Simulation Corp.	8.2.2, 9.0.3, 2016.2, 2017, 2018, 2018.1, **2019**, **2020.1**
Custom	n/a	n/a
DCP (ACoSar)	n/a	1.0
Dymola	Dassault Systèmes	2015FR01, 2016, 2017, 2018, 2019, 2020
FloMASTER	Mentor	7.9.2, 7.9.4, 7.9.5, **9.x**
FMI	n/a	1.0, 2.0
GT-Suite	Gamma Technologies	7.3, 7.4, 7.5, 2016, 2017, 2018, 2019, 2020

Tool/Interface	Tool vendor	Supported versions
Java	n/a	7, 8, **15**
KULI	MAGNA	9.1, 10, 11, 11.1, 12SR2, 13, 13.1, **13.2**
LabVIEW	NI	2016, 2019
MapleSim	MapleSoft	2018, 2019, **2020**
MATLAB	Mathworks	2012, 2014, 2015b, 2016, 2017, 2018a/b, 2019a/b, 2020a
OpenModelica	Modelica Consortium	1.9.3, 1.9.6, 1.9.7, 1.11(64/32), 1.12(64/32), 1.14
RealTime	n/a	n/a
SaberRD	Synopsys	2018, 2019, **2020**
SIMPACK	Dassault Systèmes	9.4.1, 2017, 2019, 2020
SimulationX	ESI	3.8, 3.9, 4.0, 4.1
VTD	Vires	2.0, 2.1, 2.2, 2019.1, **2020.1**
VI-CarRealTime	VI-grade	**18**

Table 27: Software Tools with limited support.

Tool/Interface	Tool Vendor
Abaqus	Dassault Systèms
Ansys	LMS
CARLA	CARLA
CarMaker 9	IPG Automotive
CFD++	Metacomp
Excel	Microsoft
Generic Wrapper	-
LS-Dyna	LSTC
monoDrive	monoDrive
PreScan	TASS
rFpro	rFpro
SciLab	scilab.org
SUMO	Eclipse Foundation
TAITherm	ThermoAnalytics
VEOS	dSPACE
VISSIM	PTV
WAVE	Ricardo

4.4.1.3 *Code example for Custom wrapper (python 2.7)*

```
from ctypes import *
from time import sleep
import math
from icos import ICOS_Connection
import sys
import os

state_x1 = 0.0
state_x2 = 0.0

def main():

    try:
        # Model.CONNECT UI
        icos = ICOS_Connection(port = 0)
    except Exception as exc:
        print(str(exc))
        sys.exit(-1)

    endTime  = icos.getEndTime()
    dT = 0.01
    num_sim_steps = int(math.ceil(endTime/dT)) # ceil to always end with a
full timestep, even if endtime is not aligned
    couple_stepsize = icos.getModelDefsSpecial()['TimeStep']

    for x in range(num_sim_steps + 1):
        tstep = float(x) *dT
        force  = icos.getScalarInput("Force", tstep)
        position = calcPosition(force, dT)
        icos.postScalarOutput("Position", tstep, position)

def calcPosition(F, dT):
    # dT ... micro time step

    global state_x1 # velocity
    global state_x2 # position
    m = 1.0 # mass
    c = 0.05 # spring coefficient
    d = 0.3 # damper coefficient

    state_x1 += 1/m *(F - d*state_x1 - c*state_x2)*dT
    state_x2 += state_x1*dT

    return state_x2


if __name__ == "__main__":
    main()
```

4.4.2 Testbed.CONNECT™

4.4.2.1 *Overall description and capabilities*

Testbed.CONNECT™ helps harnessing the benefits of model-based testing. As an open platform it facilitates early integration tests by connecting simulation models to the testbed. In alliance with Model.CONNECT™ it opens the testbed to the whole world of office simulation. This prevents long wait times for prototype components and vehicles and allows for quicker and more powerful decision- making throughout the entire development cycle. Testbed.CONNECT™ ensures a seamless connection between advanced office simulation and their utilization in the testfield.

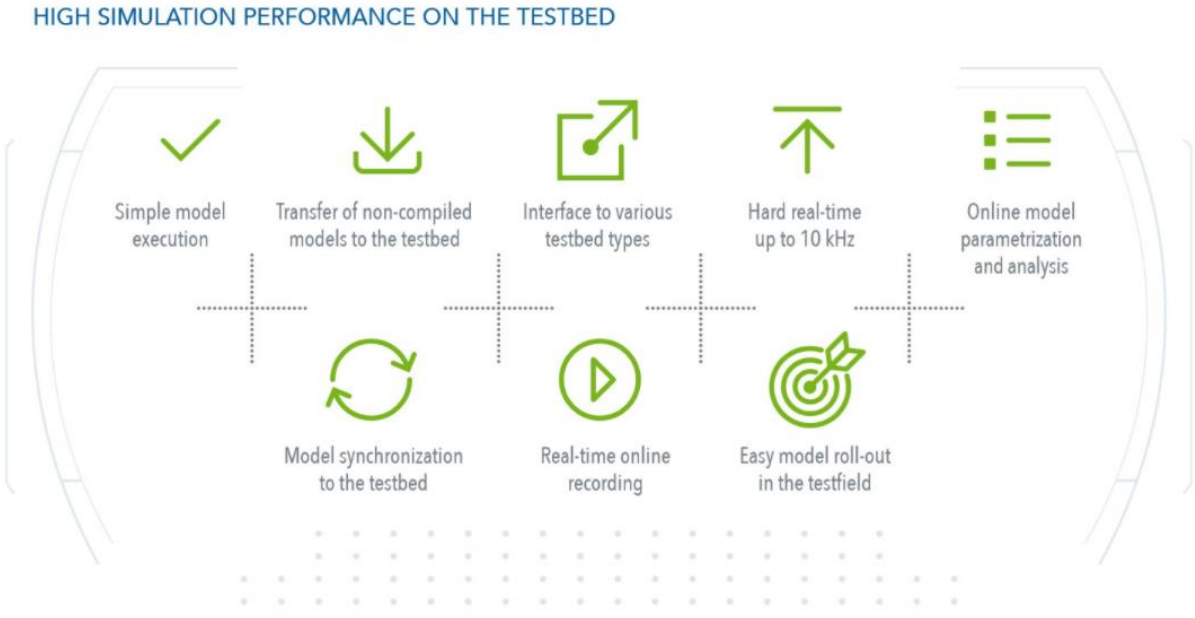

Figure 115: Testbed.CONNECT™ features

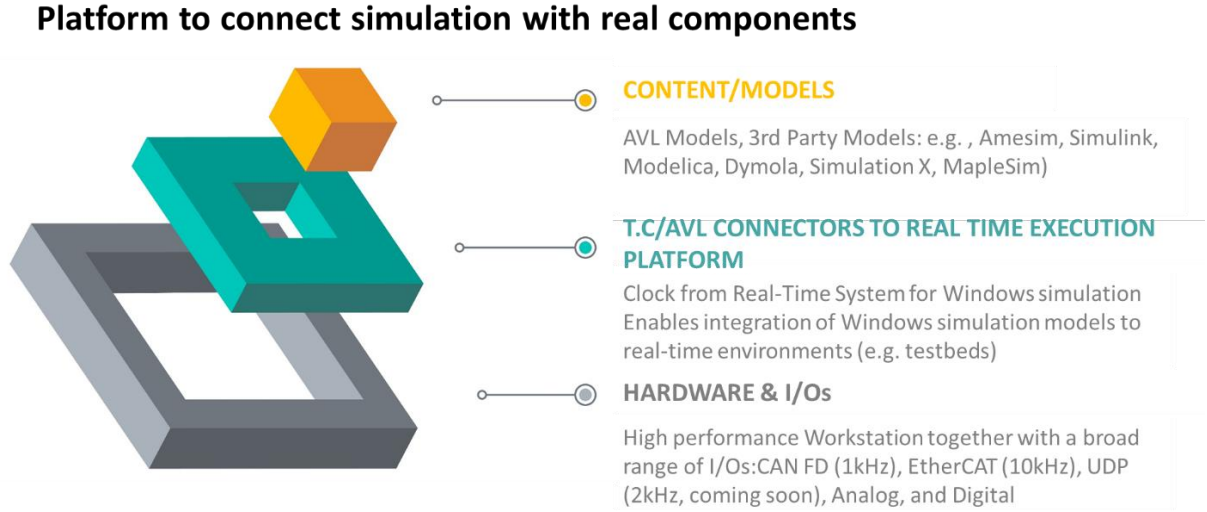

Figure 116: Testbed.CONNECT™ Architecture

4.4.2.2 *Hardware and software requirements*

Testbed.CONNECT™ uses a dedicated high-performance PC (AVL TCW) with pre-installed operating systems (inTime – a real time Windows, and Windows 10), software, and hardware extensions (interface cards) pre-installed.

Workstation

- Dual Operating Systems (Windows & InTime)
- 8 Core Xeon CPU
  - 4 cores for Windows (Model.CONNECT™)
  - 4 cores for InTime (Testbed.CONNECT™)

Connector

- Clock from Real-Time System for Windows simulation
- Patented technology
- Enables integration of *Windows simulation models** to real-time environments (e.g. testbeds)
- *capability to run faster than real-time

TIP (Testbed Integration Package)

- Standard interfaces for Engine Testbed, Powertrain Testbed and Driveline Testbed
- Incl. basic safety features

I/O

- CAN FD (1kHz)
- EtherCAT (10kHz)
- UDP (coming soon)
- Analog, digital and frequency I/Os

Figure 117: Testbed.CONNECT™ Workstation

4.4.2.3 *Preliminary identification of needs for upgrading*

Required implementation of customized interfaces for hardware and software depend on the identification of used software tools and available test bed interfaces. A more detailed analysis of these is planned to be conducted in WP2.

5 Analysis of limitations

5.1 Limitations of modelling approaches

Section 3 of this document presented a review of existing modelling approaches that may be relevant from a WEC's design perspective. These included state-of-the-art theoretical, numerical and experimental / physical models, which were firstly introduced and then extensively discussed. Section 4 reviewed the numerical models, test rigs and platforms currently available for its use in the VALID project.

For the purposes of the VALID project, it is important to critically identify and analyse the limitations of such modelling methods, in preparation of the conceptualisation of a new testing methodology which aspires at embracing both hybrid and accelerated testing principles.

This section aims at identifying and discussing such limitations, focusing on the impact they have on accuracy and computational effort. Furthermore, the practicalities associated with the implementation of such methods in the future VALID testing framework is also considered. For consistency, this sub-section has been structured analogously to Section 3.

5.1.1 Limitations of theoretical models

Theoretical models provide analytical representations of (potentially complex) physical situations, often by e.g. reducing the description of the situation to a simplified set of equations, or by implementing theoretical principles upon which engineering predictions may be derived. This sub-section addresses limitations of theoretical models, categorised in Section 3 as 'Environmental characterisation models', 'Wave-structure interaction models', 'Effects and deterioration models' and 'Reliability and survivability models'. Such analysis is presented in the text below and summarised in Table 28, which provides an overview on possible limitations of theoretical models, both from a general perspective and considering their application within the VALID project.

'*Environmental characterisation models'* typically provide inputs to a WEC's design process. Metocean data acquisition systems have the potential to provide the most accurate description of relevant metocean variables used in these models, via e.g. wave buoys and satellite observations. While providing the greatest fidelity due to their direct presence into the wave regime, in-situ measurements are limited by the fact that can rarely be extended to other geographical locations due to local wave transformation, which might be significant even at a short geographical distance depending on the site characteristics. Furthermore, wave buoys may be limited in their characterisation of extreme events due to station-keeping restrictions associated with standard mooring configurations. Alternatively, satellite observations can provide data related to vast portions of sea, however at the cost of discontinuous data sampling (due to periodical orbits around Earth) and reduced accuracy close to the coastline (distance less than ~20 km). Finally, and importantly in a context of accelerated testing, measurement and observation of ocean waves for offshore structures, due to typical long-term design requirements, would require years to be carried out if initiated at the project start date.

Wave models offer a complementary solution to overcome the limitations of measurement / observations. Although a variety of models is available, they generally all provide accurate results assuming the setup and calibration is appropriate. Within the VALID project, it is envisaged that a hybrid approach, which builds on relatively short observations and the complementary use of wave models ('*measure, correlate, predict'*), may offer a possible way forward.

Estimates of environmental conditions related to long-term return periods play an important role in the design of offshore structures. Extreme value analysis, among other techniques, is an accepted method in the offshore engineering industry that allows the estimation of key metrics. Within its potential limitations, the possibility of producing results with different

probability distributions – and the limited guidance from standards on using these – can represent a significant challenge.

Moving from resource modelling to '*wave-structure interaction'* modelling, multiple theoretical approaches can be considered (see Section 3.1.2). Frequency-domain models are the simplest and the least computationally expensive, finding their major limitation in being unable to model any nonlinear hydrodynamic effect – or other any nonlinear phenomenon related to e.g. mechanically applied forces. Gradually increasing complexity, and thus moving to time-domain formulations and finally to CFD models (RANSE, SPH, …), may in turn lead to an increase in the accuracy of predictions, at the cost of additional computational effort – see Table 28 for details. In the context of VALID, envisaging that hybrid approaches may include Hardware-In-the-Loop (HIL) approaches, wave-structure interaction models shall therefore offer the right (and non-trivial) balance between sufficient accuracy and computational cost.

Theoretical models may also be used to assess critical effects related to specific operational modes. Models categorised under '*effects and deterioration'* include models to quantify corrosion, wear, fatigue or biofouling on a WEC. Fatigue models – namely the Palmgren–Miner linear damage rule and an S-N curve following the Basquin expression– are simple yet representative models which support the estimation of the fatigue life of a structure. Use of such models is limited to elastic, single-type loading where high- and low-cycle fatigue occur in similar fashion. Wear models, which are represented by Archard's model in this context, are based on simplified physical representation of wear (adhesive wear on spherical elements) and is generally valid for the mild-wear region. "Effects and deterioration" models, within VALID, play a significant role as witnessed by the studied user-cases, see e.g. Section 4.2. Accelerated testing for such phenomena would be valuable during a WEC's development, noting that the timescale for these to affect reliability are typically very long. The limitations underlined above shall be properly taken into consideration when framing a hybrid / accelerated testing platform, noting that a combination of phenomena could also be important from a WEC's reliability perspective.

Finally, '*reliability and survivability models*' are conceptualised to estimate the risk of failure (under a range of operational and environmental conditions) of complex systems. From a theoretical perspective, reliability and survivability models span from deterministic to probabilistic models, with an increasing rate of complexity with the benefit of statistically more relevant predictions. Within VALID, and to a wider extent in a future hybrid testing methodology, deterministic models may be used at a pre-processing stage, prior to any test being executed, in an attempt to anticipate – within the models' capabilities – where the main criticalities may lie. The results of deterministic models, together with those of physical testing, could then inform probabilistic models, which could in turn to be used in a post-processing stage to characterise a wide range of conditions and infer key design metrics. Such principles will be explored in Section 6 and in future deliverables within the VALID project.

This project has received funding from the European Union's Horizon 2020 research and innovation programme under grant agreement No 101006927.

Table 28: Limitations of theoretical models

	Model type	General limitations	Specific limitations in the context of VALID
Environmental characterisation	Metocean input data	• In-situ measurements observations are limited only to measurement location. Extreme weather could bias observations due to mooring length / ability to cope with such events. • Satellite observations of significant length require time, they offer discontinuous data sampling and reduced accuracy close to the coastline.	• Observations of significant length require time and hardly cope with the requirements of accelerated testing.
	Wave models	• Require calibration. • Tend to over-estimate wave heights at high frequencies, and under-estimate at low frequencies.	• None
	Extreme value analysis & environmental contours	• Different functions may provide (substantially) different results. • Multi-variate analysis needs standardised variables if PCA is used to reduce the dataset	• Requires long-term data which acquisition hardly copes with accelerated testing, see "In-situ measurements" and "Satellite observations".
	Frequency domain	• Unable to model nonlinear hydrodynamic effects which may be dominating / significantly impacting the system dynamic. • PTO and mooring forces must be linearised.	• Possibly not providing a sufficient level of detail at the development stage at which the VALID framework would be adopted.

This project has received funding from the European Union's Horizon 2020 research and innovation programme under grant agreement No 101006927.

	Model type	General limitations	Specific limitations in the context of VALID
Wave-structure interaction formulations	Linear BEM time-domain	• Unable to model nonlinear hydrodynamic effects which – depending on the WEC type and the wave conditions – may be dominating / significantly impacting the system dynamic.	• In-house codes should first follow steps to ensure they are accurate
	Nonlinear BEM time-domain	• Capability of real-time modelling / simulation is to be investigated.	• Likely unable to cope with real-time testing requirements
	CFD	• Requires significant setup and running time	• Unable to cope with real-time testing requirements.
	Fatigue – Basquin model	• May not be appropriate if different L- (Low) and H- (High) CF (Cycle Fatigue) regimes are present. • Strain range is dominated by elastic rather than plastic strain. • Applies only to one component of loading.	• Unclear if theoretical model works for accelerated testing.
Effects and deterioration	Wear – Archards model	• Valid only in the mild wear region, where the wear rate is constant. • Assumes adhesive wear sliding spherical asperities which deform fully plastically in contact to form a junction.	• Unclear if theoretical model works for accelerated testing.
	Corrosion & biofouling	• Known stress factors but lack of analytical formulation to model degradation	• Environmental effects may be difficult to model and reproduce during lab testing
	Deterministic models	• May oversimplify physics and provide biased reliability information. • Unable to effectively model component damage / degradation / wear which inherently require probabilistic models.	• Likely applicable only at pre-processing stage.

This project has received funding from the European Union's Horizon 2020 research and innovation programme under grant agreement No 101006927.

	Model type	General limitations	Specific limitations in the context of VALID
Reliability and survivability	Probabilistic models	• Require statistical data related to components failure to feed the algorithms. • May require significant setup and computational effort. • Deterministic and pseudo-probabilistic methods are not practical for coupling operating conditions and component damage/degradation/failure • Survivability definitions are not unified	• Likely applicable only at post-processing stage.

5.1.2 Limitations of numerical models

Numerical models are typically based on one, or a combination of more, theoretical model(s). As such, and for relatable topics, when looking at possible limitations of numerical models a strong cross-coupling exist with the previous Section 5.1.1. This sub-section addresses limitations of numerical models, previously framed in Section 3 as '*Environmental characterisation models*', '*Wave-structure interaction models*' and '*Critical sub-system models*'. Such analysis is presented in the text below and summarised in Table 29, where specific limitations which apply for the VALID methodology are highlighted.

To characterise the site's environmental conditions, wave models, as part of '*environmental characterisation models*', inherit the benefits and setbacks of the theoretical models analysed in the previous section. Additionally, considering implementation features, a wide range of solution approaches exist (e.g. deterministic or probabilistic models, based on phase-resolving or phase-averaged approaches) and require careful use, depending on the application requirements. In the context of VALID, wave models may play a role, at pre-processing stage, in compensating time-related limitations of in-situ / satellite observations – see Section 6.

'*Wave-structure interaction models*', building on the theoretical models described in Section 3.1.2, are typically used to characterise the response of the WEC under a range of DLCs. The definition and analysis of a range of significant DLCs represents a foundation in the formulation of a WEC's Design Basis. Wave-structure interaction numerical models represent the main tool to analyse the selected DLCs and set the basis for both concept and detailed design – see Section 3.2.2. Modelling a wide range of design situations, in both normal and extreme environmental conditions, may require the use of multiple numerical models which, depending on the complexity of the situation, may require a significant (overall) computational time. Within VALID, wave-structure interaction models may be used to assess a wide range of DLCs (as a pre-processing step) – which on turn assist in the definition of critical cases that may be investigated in more detail / with more accuracy in a hybrid setup. Additionally, the models may also be used at processing stage, during testing, offering a hybrid solution through the use of e.g. real-time platforms to simulate e.g. wave-structure interaction in conjunction with the use of physical models; however, this may require a significant computational effort which shall match the hardware capabilities.

Finally, numerical models of critical sub-systems may increase the level of detail of a WEC's modelling programme, at the cost of adding complexity and computational time. This applies to complete sub-systems e.g. dynamic mooring models, PTO models and flexible-body models but may also apply to a more detailed component level – thus emphasising a possible hybrid setup, where one component is replaced with a physical equivalent.

This project has received funding from the European Union's Horizon 2020 research and innovation programme under grant agreement No 101006927.

Table 29: Limitations of numerical models

	Model type	General limitations	Specific limitations in the context of VALID
Environmental characterisation models	Wave models	• Different models exist and accuracy / reliability depends on assumptions / application type. • Ability to model non-linear applied forces and constraints • Fully coupled WEC models – rigid & elastic coupling	• In-house codes should first follow steps to ensure they are accurate
Wave-structure interaction models	Selection of design load cases (DLCs)	• Modelling of a wide range of DLCs requires use of multiple types of numerical models to address performance, reliability and survivability	• Unclear if hybrid formulations may be easily conceptualised. • Computationally expensive, if real-time testing is to be conceived.
Critical sub-system models	PTO	• Mostly addresses hydraulic PTOs – to date • Challenging to model PTOs down to component level • Simple mass-spring-damper models are unsuitable for reliability analysis	• Computationally expensive, if real-time testing is to be conceived.
	Mooring	• Lumped-mass formulation.	• Computationally expensive, if real-time testing is to be conceived.
	Hulls	• Peak loads may not be well estimated, depending on the WEC type	• Computationally expensive, if real-time testing is to be conceived.

5.1.3 Limitations of physical models

Physical models represent a widely used engineering mean of investigating the behaviour of a complex system – such as a WEC, or one of its sub-systems / components. In the context of the VALID project, and building on the user cases defined in Section 4, physical models will likely be used to represent (scaled) versions of key sub-systems and, as such, their limitations need to be extensively assessed.

In Table 30, a number of limitations are compiled and categorised – following Section 3.2 – within 'hydrodynamic models', '*energy transformation models*' and '*degradation and failure models*'. Limitations associated with models in each of these categories are discussed sequentially below.

'*Hydrodynamic models*' are typically deployed in size-limited, controlled environments which, by definition, can replicate only selected environmental conditions. Additionally, physical limitations may induce loads which are non-existent in the real world (due to e.g. reflected waves in the flume / tank). Moreover, depending on the scaling approach, specific hydrodynamic forces may not be modelled correctly e.g. if Froude's law is used, viscous forces at model scale may not be representative of those at full-scale. In addition, the typical scale of hydrodynamic models may not allow for a (true) scaled representation of representative sub-systems (e.g. the PTO). For the purposes of VALID, an additional limitation is related to the possibility of performing accelerating testing on hydrodynamic models. Given the limitation of wave tanks / flumes related to e.g. build-up of reflected waves, it is unlikely that a hydrodynamic model can be subject to a test where wave loading is accelerated.

'*Energy transformation models*', if conceived at scale, require careful consideration before being built and tested. Firstly, an adequate scaling factor is required to make sure that all the dominant effects of the energy transformation system are correctly scaled (i.e. the scale should not be too small to alter dominant forces[2]), while matching the requirements to the actuation capabilities (i.e. the scale should not be too big). Secondly, a scaled energy transformation model is unlikely to include the same components to be used at full-scale. This makes it unclear whether failure modes at full-scale can be replicated at scale. Finally, and from a practical perspective, the scale of an energy transformation model may have a lower limit given by the availability of components (bearings, gears, electrical motors / generators, pumps etc.) which form the sub-system under test, and / or the actuation system.

Finally, '*degradation and failure models*', similar to the 'energy transformation models', are likely to play a relevant role in VALID – see e.g. Section 4 of this report, where user cases involve dynamic seals, pump seals and glider pads which are subject to such phenomena. At a high-level, degradation and failure models are widely used in the industry when coming to reliability and survivability testing. However, it is essential, that such models are representative of components that will be used on the field, and that test conditions include all relevant loading sources such that real-world failure modes – such as those possibly arising from e.g. a combination of corrosion, wear and fatigue – are effectively replicated. Within VALID, and related to accelerated testing, it is unclear whether this would trigger the correct failure modes – noting the possible combination of loads that induce a path to failure.

[2] A typical example is related to scaled PTO systems where friction forces may be significantly larger than the corresponding ones at full-scale.

This project has received funding from the European Union's Horizon 2020 research and innovation programme under grant agreement No 101006927.

Table 30: Limitations of physical models

	General limitations	Specific limitations in the context of VALID
Hydrodynamic models	• Controlled wave conditions may differ from real-world environmental conditions. • Possibly suffer from loading conditions which are not present in real-world (e.g. wall reflected waves). • Depending on scaling law, specific hydrodynamic forces may not be correctly scaled. • Scaled representation of representative sub-systems may not be feasible and require simplifications.	• Accelerating the wave-structure interaction loads for a hydrodynamic model in a wave tank may be unfeasible.
Energy transformation models	• Small scales may alter the ratio of dominant forces and require components which are unavailable. • Large scales may violate actuation limits. • Unclear if failure modes at scale are representative of failure modes at full-scale. • The experimental model set-up might limit the failure mechanisms that can be tested at laboratory. • Reproducing WEC accelerations and component set-up (vertical vs horizontal orientation)	• Testing procedures should include the test rig set-up and calibration of the actuators. • Actuator performance and PTO system dynamics should be carefully assessed. Uncertainty ranges should be considered.
Degradation and failure models	• Testing may not be representative of complete real-world conditions, where multiple factors play a role in path to failure.	• Accelerated testing may trigger failure modes which are not representative of real-world applications.

5.2 Limitations of available models, rigs and platforms

In Section 4, the existing numerical models and test rigs of the three user cases were introduced. In addition, the IODP virtual testing platform from AVL (Model.CONNECT™ and Testbed.CONNECT™) was also briefly presented. This section aims at identifying the limitations discussed in Section 5.1 in the context of the available models and test rigs. The section follows the outline of Section 4 and discusses VALID's user cases sequentially.

5.2.1 User Case #1: Dynamic seals

The available models and test rigs for User case #1 are presented in Sections 4.1.2 and 4.1.3, respectively. Focusing here on the Waves2Wire hydrodynamic model, and the seal test rig, we list the limitations in Table 31.

Table 31: Limitations of available models and test rigs for User Case #1

	User Case #1
Limitations numerical models	• The hydrodynamical models are based on the linear BEM time-domain approach. Thus, the models have fundamentally a linear hydrodynamic approach to the highly nonlinear system of a resonant WEC. • BEM time-domain models require calibration of drag coefficients. Drag coefficients obtained from experiments typically lumps all nonlinearities into one which makes scaling difficult. • None of the models addresses biofouling. Biofouling alters over time both the hydrodynamic properties and drag of the WEC and mooring system. • The Waves2Wire model uses simplified mooring block • The Orcaflex model uses a simplified PTO/Controller block • Unlikely that the Wave2Wire model is fast enough for real-time simulations
Limitations physical test rigs	• The test rig uses a harmonic sinusoidal motion. It does not mimic the irregular wave motion response. • Scaling effects for the dynamic seals have to take into account both the diameter and length of the rods. It is possible to test the full-scale diameter, but not the full-scale length. • Scaling of the length in turn influences the speed and accelerations achievable. It is possible to test either the desired speed, or the desired accelerations, but not both at the same time. • Methods to accurately initiate predicted failure modes are lacking. • Corrosion and biofouling effects are missing. • Using quarter-scale diameter rods it is possible to test 4 rods simultaneously, however the actuation is controlled by a single motor, meaning that all rods and seals sets experience the same speeds/accelerations.

5.2.2 User Case #2: Generator failure

The available models and test rigs for User case #2 are presented in Sections 4.2.2 and 4.2.3, respectively. Focusing here on the Marmok hydrodynamic model, and the Tecnalia test rig, we list the limitations in Table 32.

Table 32: Limitations of available models and test rigs for User Case #2

	User Case #2
Limitations numerical models	• The hydrodynamical models are based on the BEM time-domain approach. Thus, the models have fundamentally a linear hydrodynamic approach. • BEM time-domain models require calibration of drag coefficients. Drag coefficients obtained from experiments typically lumps all nonlinearities into one which makes scaling difficult. • The Marmok model only work in heave. • Uniform pressure and flow are assumed in the chamber. • The model does not address biofouling. Biofouling alters over time both the hydrodynamic properties and drag of the WEC and mooring system. • No ageing effect on performance has been accounted for, such as Biofouling; corrosion (structure/turbine blades); generator insulation… • Compressibility model assumes air to be an isentropic gas. • Turbine performance is based on physical testing in laboratory conditions and constant rotational speed. • Generator performance is based on numerical fittings of relevant loss coefficients and assumes stationary working conditions. • Accumulated damage on the generator is independent of the actual state of it.
Limitations physical test rigs	• The converter that controls the motor (Leroy Somer UMV 4301 22T), has output power of 15kW at 400 V and the following limitations for switching frequency of 3kHz : continuous rated current of 34A, Overload current for 60s of 50.6A ,Peak current for 4s of 60A. Regarding overload capacity: 150% of controller rated current for 60s and 175% of controller rated current for 4s • The motor is a Leroy Somer LSMV160LU-T with a P_{nom}=15kW, has a 1460 rpm nominal speed (max speed of 1800rm). Rated torque=97,6Nm, rated current= 27,4A, maximum torque 3 times rated one. Similar and newer motor has the following relation between speed, torque and current. 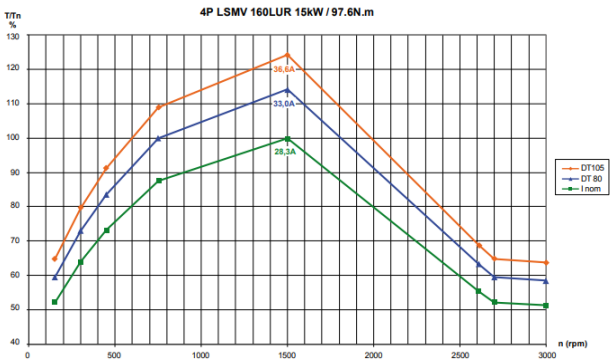

	User Case #2
	• The currently available generator has the same nominal power as the drive motor which limits the capacity of generating overcurrents for accelerating the tests. • The converter ACS800-11-0016-3 has a continuous rated current of 34A, maximum current of 52A, nominal power of 15kW, 32A continuous rms current 10% overload for one minute every 5 min, 50% current overload for one minute every 5 min at heavy-duty use. • Several stress factors that affect the UC failure mode cannot be reproduced in the laboratory environment (i.e. salinity, humidity, etc.).

5.2.3 User Case #3: Seawater hydraulic pump seals and glider pads

The available models and test rigs for User case #3 are presented in Sections 4.3.2 and 4.3.3, respectively. The focus here are on the WEC-SIM and Orcaflex hydrodynamic models, and the seal test rig, we list the limitations in Table 33.

Table 33: Limitations of available models and test rigs for User Case #3

	User Case #3
Limitations numerical models	• The hydrodynamical models are based on the nonlinear BEM time-domain approach. Thus, the models have fundamentally a linear hydrodynamic approach. • BEM time-domain models require calibration of drag coefficients. Drag coefficients obtained from experiments typically lumps all nonlinearities into one which makes scaling difficult. The multi-EC plate design should make this problem even more pronounced for User Case #3. • The BEM model has difficult to provide reliable hydrodynamic coefficients for up to 24 interacting bodies. • None of the models addresses biofouling. Biofouling alters over time both the hydrodynamic properties and drag of the WEC and mooring system. • The WEC-SIM model is limited to surge motion of the ECs only and thus disregards the motion of the macro-structure. • The WEC-SIM model does not include mooring restoring forces. • The WEC-SIM model does not include bending/torsion of the drill pipe. • The Orcaflex model does not consider wave diffraction/radiation. • Neither WEC-SIM model nor Orcaflex is expected to be fast enough for real-time simulations. • The models hydraulic pump and pipe system are treated as quasi-static. • There are no models for predicting the wear of the seal and glider pads. • The models do not include the electrical generator/reverse osmosis system. • The models do not include grid connection.

	User Case #3
Limitations physical test rigs	• The test rig gives harmonic sinusoidal motion. It does not mimic the irregular wave motion response. • The test rig does not support forces caused by end-stops. • The test rig has constant pressure on the seals, which is incompatible with the true time-dependent pressure that energize the seals. • The test rig lacks control system as well data acquisition system to enable continued monitoring of friction and internal pressure. • A way to accelerate initiation of seal failure is missing. • Suspended material in the sea water is expected to be very important for the wear of the seal. The test rig does not accommodate this feature. • Corrosion effects are missing. • Biofouling effects are missing. • Scaling effects for the dynamic seals must consider both the diameter and length of the rods. It is possible to test the full-scale diameter, but not the full-scale length. • Scaling of the length in turn influences the speed and accelerations achievable. It is possible to test either the desired speed, or the desired accelerations, but not both at the same time.

5.2.4 The virtual platform

The IODP model for virtual models (Model.CONNECT) and test rigs (Testbed.CONNECT) are presented in Sections 4.4.1 and 4.4.2 respectively. The identified limitations are listed in Table 34.

Table 34: Limitations of the virtual platform.

	Virtual platform
Limitations of model.CONNECT	• Missing support for industry standard tools in ocean engineering e.g. Orcaflex and DeepC[1]. • Only simulations in the time domain are supported. • Very high number of channels will slow down simulation [2]. • Limited support for field coupling (e.g. CFD or FEA tools). • (Very) long simulation times might lead to memory issues [3].
Limitations of testbed.CONNECT	• All limitations as listed for Model.CONNECT, as well as: • Possibly missing support for hardware (e.g. interface / bus) used by the user cases. • Each individual model has to be real time capable (realistically ~20% faster to account for overhead).

[1] basically, interfaces can be developed, as long as the tool to be integrated offers a proper API (application programmable interface)
[2] basically not too critical for pure office simulation
[3] depending on coupling time step and number of result channels

This project has received funding from the European Union's Horizon 2020 research and innovation programme under grant agreement No 101006927.

6 Moving forward: hybrid testing framework

Following the review of modelling approaches (Section 3), the compilation of the current models, test rigs and testing platforms available in the VALID consortia (Section 4), and the analysis of the associated limitations with both modelling approaches and current capacity within VALID (Section 5), initial considerations related to a new framework for accelerated hybrid testing can be issued. It is expected that such considerations will have a first application in the VALID user cases, assisting in the conceptualisation of a testing methodology that shall be compiled in the final WP1 deliverable (D1.5). The learnings from such initial application will inform the re-contextualisation of a final methodology, promoting wider adoption in the wave energy community.

6.1 Framework for accelerated hybrid testing

At a high-level, a framework for accelerated hybrid testing may encompass three key stages, as illustrated in Figure 118. Such stages – pre-processing, processing and post-processing – form the foundation of a hybrid testing methodology, by housing the key tasks and functions that must be addressed in a successful hybrid testing campaign. Additionally, such stages may benefit from being coupled via an integrated platform – ensuring that core aspects such as the communication between all stages are preserved from inception. It is noted that in the VALID application of such conceptual framework, the integrated testing platform role is performed by AVL's virtual testing platform (see also Section 4.4).

Figure 118 describes some of the aspects associated with each of the proposed key stages. Immediate follow-up questions include which modelling approaches are best suited to each stage, and why are these best suited. Such critical questions are addressed in Section 6.2.

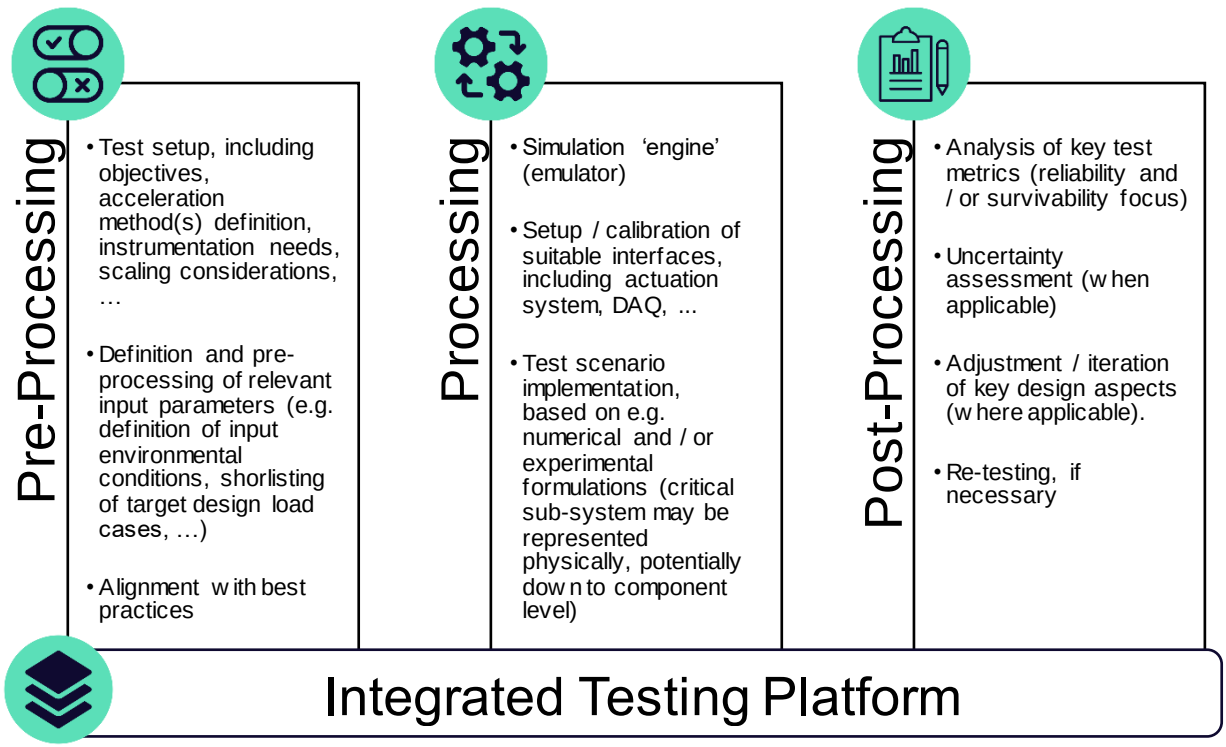

Figure 118: Conceptual framework for accelerated hybrid testing

6.2 Modelling approaches vs. testing stage

Having defined in Section 6.1 the three key stages that form the base of a hybrid testing framework, it is relevant to consider which type(s) of modelling approach – theoretical, numerical and / or experimental – best suit each stage. Such assessment will in turn inform the conceptualisation of a (practical) methodology for hybrid testing, by focusing development efforts at each key stage on the best suited modelling methods.

Following the layout of Section 3, theoretical models may be firstly considered. Owing to their analytical nature, a theoretical model of a complete WEC and / or of a WEC sub-system is likely to feature a number of high-level assumptions and / or simplifications (e.g. consideration of a reduced number of degrees-of-freedom), potentially limiting the applicability of such models in the 'Processing' stage of a hybrid testing framework. The use of a theoretical modelling approach is more pressing at both the 'Pre-Processing' and 'Post-Processing' stages, as a means of preparing for the test by e.g. assist in the assessment of what is critical, and assessing the test result by e.g. quantifying the key metrics emanating from the tests, by applying e.g. key reliability and survivability assessment consideration (as detailed in Section 3.1). Additionally, crucial aspects such as the formulation and type of accelerated test, and the assessment of the uncertainty across the I/O structure of the hybrid testing framework, can be seen as critical areas that theoretical methods can contribute to.

Naturally, baseline theoretical principles are at the core of any numerical models – thus to an extent, numerical models are also limited by the theory over which they are built on. However, the inherent flexibility of numerical models offers them the potential to create a virtual environment where a WEC can be described in a coupled approach, i.e. where the influences of all relevant sub-systems in the WEC response are simultaneously accounted for, in modules of increasing complexity / different formulations, adapting to the needs of a WEC development programme. Overall, the majority of WEC numerical models proposed to date aim to address overall behaviour (forces, displacements, …), and thus models of critical sub-system(s) aim to address the impact of such sub-system(s) on the functional behaviour of a WEC. However, such sub-system models do not typically provide a component-level breakdown, which could in turn influence the detailed design of the sub-system and of the WEC itself. This is particularly clear for the PTO sub-system, where numerical models are often reduced to simple mass-spring-damper representations at early development stages – and thus require additional complexity to fully emulate the characteristic response of a (real) WEC.

Experimental / physical models offer the potential to add additional degree(s) of realism, if required down to component level. However, it is important to note that the inherent limitations of a 'model' still apply even if the model itself is an experimental / physical system – thus unless a full-scale replica is used, modelling uncertainty may still have a significant impact on the test results. Even with such caveat present, the role of experimental / physical models in hybrid testing is likely to be key at the 'Processing' stage – and one that can jointly stimulate:

a) the acceleration of a WEC's technology roadmap, by more readily assessing critical components in a controlled environment.
b) The refinement and validation of (increasingly more) realistic accurate numerical models of both the critical sub-system(s) and of the entire WEC.

While the identification of criticality may include or exclude the use of experimental models (potentially in an isolated, non-hybrid test setup), the use of experimental models may also be constrained depending on which sub-system is judged to be critical. For example, an experimental test in a wave tank will likely limit the scale of the models, which may be more or less relevant depending on the sub-system of interest. To mitigate such limitation, and where feasible, a test scenario using large and / or full-scale versions of critical components may more immediately yield relevant results for the objectives associated with the VALID project, when compared to a scaled model test in a controlled environment. The assessment of such compromise between scale and feasibility of the hybrid test is likely to benefit from the ongoing

work within the VALID project – namely WP3 to WP5 – and later inform the hybrid testing methodology to be proposed in Task 1.5.

Hybrid testing, i.e. the combination of a numerical model of the WEC and an experimental / physical model of the critical sub-system(s) at a suitable scale, may therefore play a key role in increasing the detailed understanding of a critical sub-system and of its overall influence in the design of the WEC. Hybrid testing introduces the possibility of coupled modelling while intrinsically allowing a higher fidelity approach in the development and design of critical sub-systems. Such higher fidelity approach may be introduced numerically, where multiple numerical simulation tools for different sub-systems are coupled in a virtual platform; or experimentally, via e.g. a full-scale PTO coupled to a numerical model of the WEC. While a hybrid approach involving experimental / physical representations of critical sub-systems may be required to more immediately assess features that warrant critical design decisions, a numerical (virtual) environment, especially once validated, is likely to have a key role in ongoing development activities, assisting in the transition from concept to detailed design..

Importantly, hybrid testing can serve multiple test objectives – which should be made clear at the 'Pre-Processing' stage. This may include e.g. Real-Time simulation (leading to system validation, fault identification, …); limit state testing (where post-processed simulated loads are used as the actuation loads); and component characterisation (where e.g. different components of similar specification are compared for final selection in the sub-system). Numerical models are likely to be essential to any of these objectives, although they may have different roles depending on the overall test objective. For example, if component and / or sub-system accelerated tests are to be considered, then using output data from coupled numerical models as actuation loads may be sufficient, noting that the load time-series would require suitable pre-processing. From a computational perspective, the requirements for such setup are likely less demanding, which may be relevant if e.g. a fully coupled hybrid environment proves unfeasible in real-time for certain design situations. Additionally, this approach may be valuable in e.g. the gradual increase in the level of detail of a fully coupled WEC numerical model down to component level, leading to creation of a 'digital-twin' suitable for the detailed design of the WEC.

Table 35 provides a summary of the perceived suitability of each modelling approach to the proposed three stages that form a hybrid testing framework. While the connection between numerical and experimental models is immediately clear in a hybrid testing context (see also Section 3.3), a further connection to theoretical models should not be neglected (see also Section 3.1). Theoretical models are likely essential for pre- and post-processing in hybrid testing, preparing input variables and assessing the outputs, to enable the evaluation of the test objectives. For example, the preparation of input conditions for accelerated testing, including e.g. environmental conditions beyond metocean considerations (e.g. marine growth, salinity, temperature, …) should follow standard practices, from a theoretical basis and / or related industries. Additionally, clear metrics to assess the test objectives should form the core of a post-processing methodology; however, and as alluded to in [198], there is currently a lack of consensus on which post-processing methodologies to implement, which may lead to considerable uncertainty when analysing key test results (see also [175]). Further research into this issue is planned under VALID's Task 1.3.

A clear challenge of the VALID project is therefore to combine best practices from a theoretical, numerical and experimental perspective, under the umbrella of hybrid testing and aligned with specific test objectives. Some guiding principles that may be followed when devising a novel hybrid testing methodology – and applied when drafting testing plans – are documented in Section 6.3.

Table 35: Suitability of modelling approach to key hybrid testing framework stages

	Pre-Processing	Processing	Post-Processing
Theoretical	✓	✗	✓
Numerical	✓	✓	✓
Experimental	✗	✓	✗

6.3 Guiding principles of a novel hybrid testing methodology

When devising a novel hybrid testing methodology for WEC design, alignment with best practices from relevant industries should be sought (where applicable), to ensure that know-how from other industries is incorporated in the novel processes and that compliance with applicable industry standards is met from inception (see also VALID's D1.1 [1] for a review of relevant standards).

In this regard, and at a high-level, two industry processes may prove particularly useful when conceptualising a methodology, and in turn drafting testing plans, suitable for the objectives of the VALID project:

- Technology qualification.
- V-Model.

Technology qualification is defined in [290] as " (…) *the process of providing the evidence that a technology will function within specified operational limits with an acceptable level of confidence*." The overall principles are followed by multiple classification societies and detailed in recommended practices (or similar documents) such e.g. DNV-RP-A203 *Technology Qualification* [290], ABS *Guidance Notes on Review and Approval of Novel Concepts* [291], LR's *Guidance Notes for Technology Qualification* [292], IEC's *Specification for establishing qualification of new technology* [293], etc.. In this section, and for simplicity, the nomenclature and key notes from [290] are followed.

Conceptually, a technology qualification process follows a systematic, risk-based approach. The main guiding principles of the process include:

- Adoption of an iterative qualification strategy, to be clearly defined and documented in a series of key deliverables.
- Definition of a series of activities (related to analysis, testing, documentation of previous experience, etc.) that have the underlying objective of assessing failure modes for the range of relevant design situations.
- Acceptance margins should be defined using recognised methodologies / standards, or in their absence by based on combinations of operational and test data, including all significant sources of uncertainty.
- Validation of model predictions shall be sought (in a quantifiable manner).

The above detailed principles guide the main steps typically involved in a technology qualification process. These are illustrated in Figure 119, where a basic description of the activities associated with each step is also provided. It should be noted that the technology qualification process is iterative – thus prior to achieving a qualified technology, the same steps may need to be followed (potentially) multiple times, to reach agreed qualification states / milestones. Further detail into the definition of each step can be found in [290].

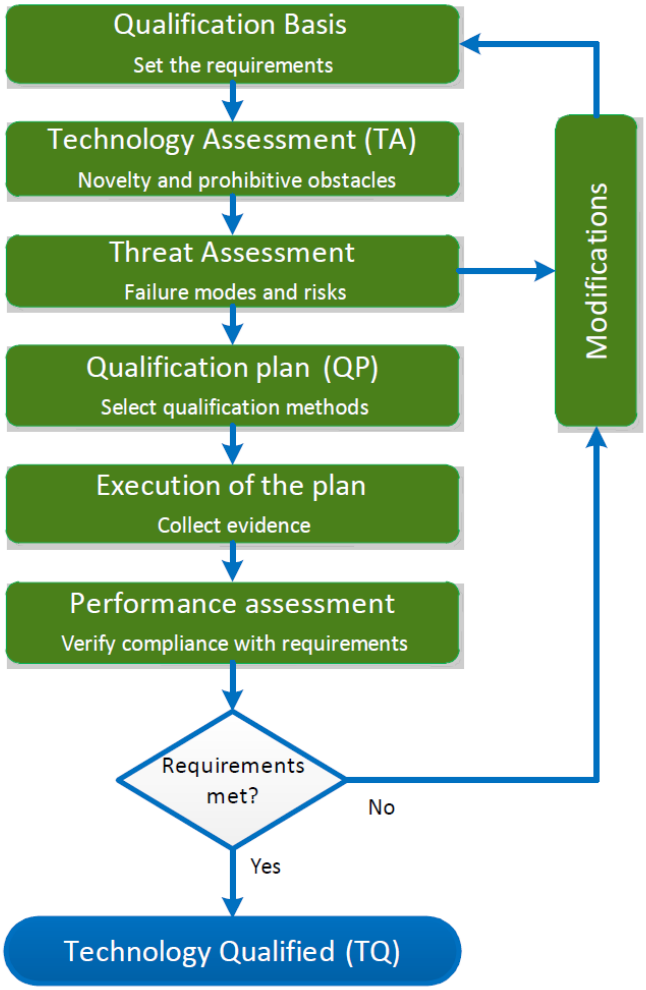

Figure 119: Basic steps of a technology qualification programme [290]

From both a hybrid testing methodology and test plan creation perspective, it is relevant to connect the basic steps illustrated in Figure 119 to the key questions that a hybrid test programme may aim to address. Table 36 summarises a selection of key questions that can associated with a WEC hybrid testing programme, while Figure 120 illustrates the possible connection(s) between the basic steps of a technology qualification programme and such key questions. In the context of the proposed framework for accelerated hybrid testing (see Figure 118), both Table 36 and Figure 120 can be used to develop, in detail, the pre-processing stage of the test programme, while also aligning both the processing and post-processing stages.

It is therefore suggested that such guideline principles are taken into consideration, where applicable, in the initial tasks associated with each VALID user case (namely Tasks 3.1, 4.1 and 5.1).

Table 36: Key questions to be address in a WEC hybrid testing programme

Question	Notes
What is being tested? What are the objectives of the test?	Identify what is to be represented numerically (and how), and what is to be represented physically (to what level) Compile details of tentative approach, e.g. does a metocean design basis exist? Which models are available? Etc. Document approach (preliminary test plan)
What are the key constraints of the test rig and models (e.g. scale, actuation load magnitude, test duration, acceleration method)?	Do these constraints critically affect the test objectives? Is re-iteration needed?
Following the risk / criticality assessment, what design situations are most relevant for the test objectives?	See VALID's D1.1 [1] for guidance on the identification of criticality
How all relevant interfaces between actuation and reaction sides of hybrid platform (per test) should be defined?	Ensure sufficient capacity to actuate each test DLC Align interfaces to allow critical data collection Compile commissioning plan (with customized check list) to mitigate possibility of severe error(s)
How to formalise / document final test plan (from less to most potentially destructive)?	Plan contingency should materials need to be replaced
How to implement test plan, collect and post-process data time-series?	Align with post-processing practices associated with each DLC + test objectives
How to feed qualification process with results?	Assess need to re-design and / or re-test

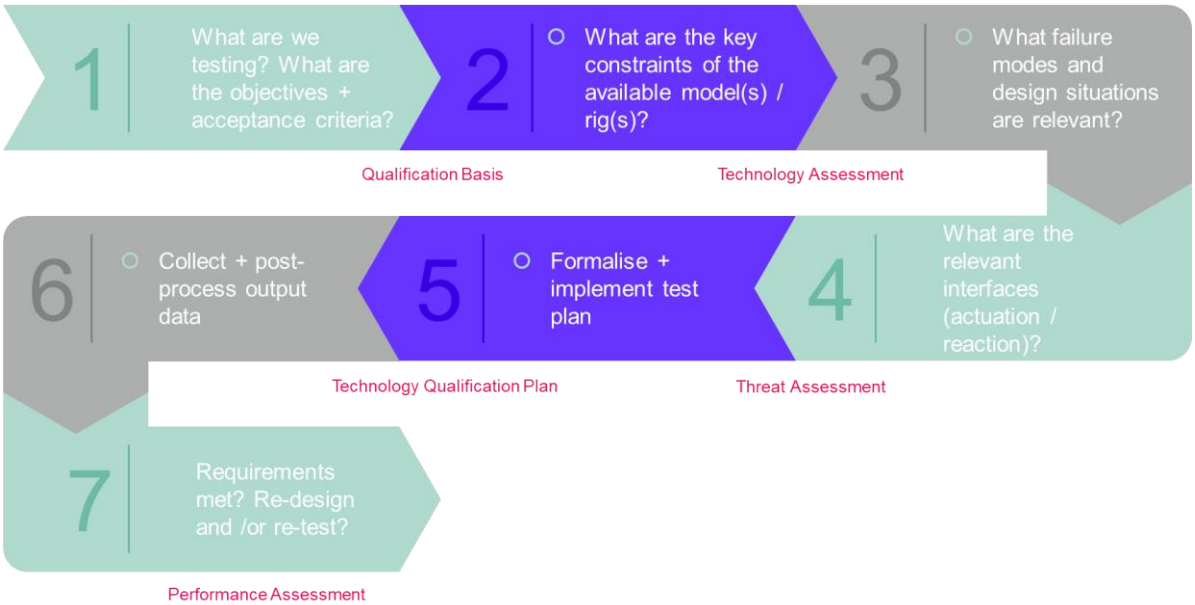

Figure 120: Connection between technology qualification basic steps and key questions associated with a WEC hybrid testing programme

In addition to Technology Qualification, a conceptual model used extensively in the automotive industry – the V-Model or V-Cycle [294], [295] – may also provide guidance when conceptualising a hybrid test programme related to WEC design. The V-Model, originally conceived for software development, aims at guiding the development process of a system by focusing on its multi-level nature, i.e. its capability of being decomposed into building 'elements'. The V-Model plays a significant role in functional safety for automotive applications; for example, it forms the skeleton of ISO 26262 *Road vehicles – Functional safety* [296], which is derived from IEC 61508 *Functional safety of electrical/electronic/programmable electronic safety-related systems* [297].

As illustrated in Figure 121, the V-Model is typically characterised by two phases: a 'Partitioning' phase (left side of the 'V'), and an 'Integration' phase (right side of the 'V').

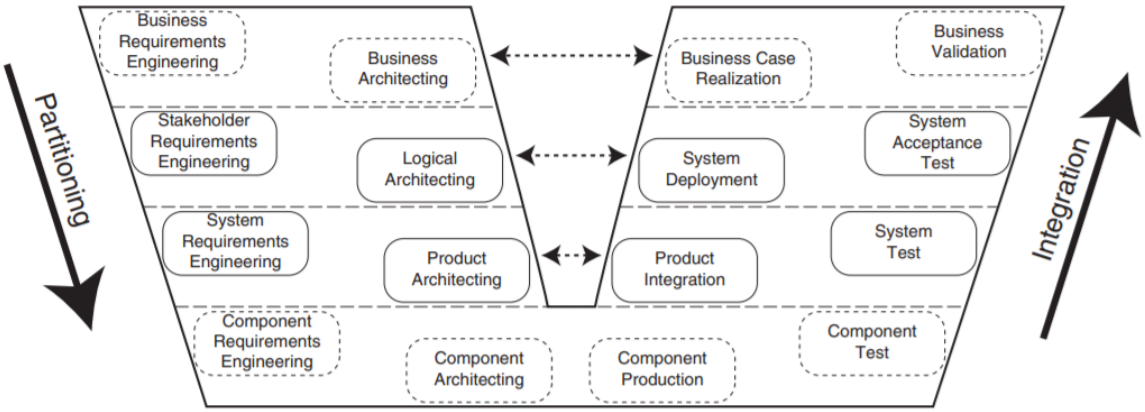

Figure 121: V-Model with exemplary named basic development processes [294]

Starting from the 'Partitioning' phase, and moving from the top to the bottom, the V-Model subsequentially decomposes a system into lower-level building 'elements' – with the lowest 'elements' not requiring any further partitioning (as part of the development process). The 'Partitioning' phase includes, at each level, the dual presence of a 'requirements engineering' and an 'architecting' task: in the V-Model, the precise definition of requirements (which flows down from higher levels), sets the basis for a corresponding architecting activity. As practical as it can be, and focusing the continuous-line blocks of Figure 121 (i.e. neglecting the highest level and the lowest level), a typical 'Partitioning' process for a generic software may include (see also [298] and [299]):

1. Collecting functional requirement(s) ('Stakeholder Requirements Engineering').
2. Transforming the functional requirement into a function, in a model-based environment ('Logical Architecting'), to be verified through Model-In-the-Loop (MIL) tests.
3. Propagating requirements at a lower system level ('System Requirements Engineering') which may include e.g. memory usage, data types, specificities related to the programming language etc.
4. Develop the final product, generating code in the target language ('Product Architecting'), and verifying it through Software-In-the-Loop (SIL) tests which include compiling and running the software on the development laptop / computer.

This last step marks the end of the 'Partitioning' phase and allows the start of the 'Integration' phase. This aims at progressively integrating the product (i.e. the software in this example) into the higher system levels – ultimately, to the highest level (i.e. the vehicle in this example).

Two blocks compose the 'Integration' phase, at each level: 'integration' and 'test'. Building on the example above, the following steps would form part of this phase (see also [298] and [299]):

1. Integrating the product ('Product Integration') with all existing (software) modules required for the specific project, noting that the developed function(s) can have an impact on several software modules.
2. Testing the integrated system ('System test'), to verify the correct interaction between modules and check the impact of functional changes on legacy software. This is typically done through Hardware-In-the-Loop (HIL) tests, where the vehicle is simulated in model-based environment by means of a Real-Time target machine.
3. Deploying the software at the vehicle level ('System deployment'), via a testing laptop connected the target Electronic Control Unit (ECU) located on-board.
4. Finally, testing the software on a pre-defined test scenario ('System acceptance test') to test the limits and capabilities of the developed product under real-world conditions (i.e. through a vehicle test drive).

Significantly, any step during the 'Integration' phase provides feedback (and, possibly, validation) to the corresponding step in the 'Partitioning' phase – this being visualized by the horizontal arrows at the centre of the 'V' in Figure 121.

It is worth highlighting that ISO 26262 *Road vehicles – Functional safety* [296], in its Part 5, suggests the application of the V-Model not only to software but also to hardware development (although for electrical / electronic systems only) – see Figure 122. Notably, this entails two significant steps:

- The evaluation of 'architectural metrics', which shall "*be objectively assessable: metrics are a comprehensible means to differentiate between different architectures*"
- The evaluation of 'safety goal violation due to random hardware failures' i.e. the capability of the hardware to cope with a failure while maintaining appropriate safety levels (as measured against the 'architectural metrics').

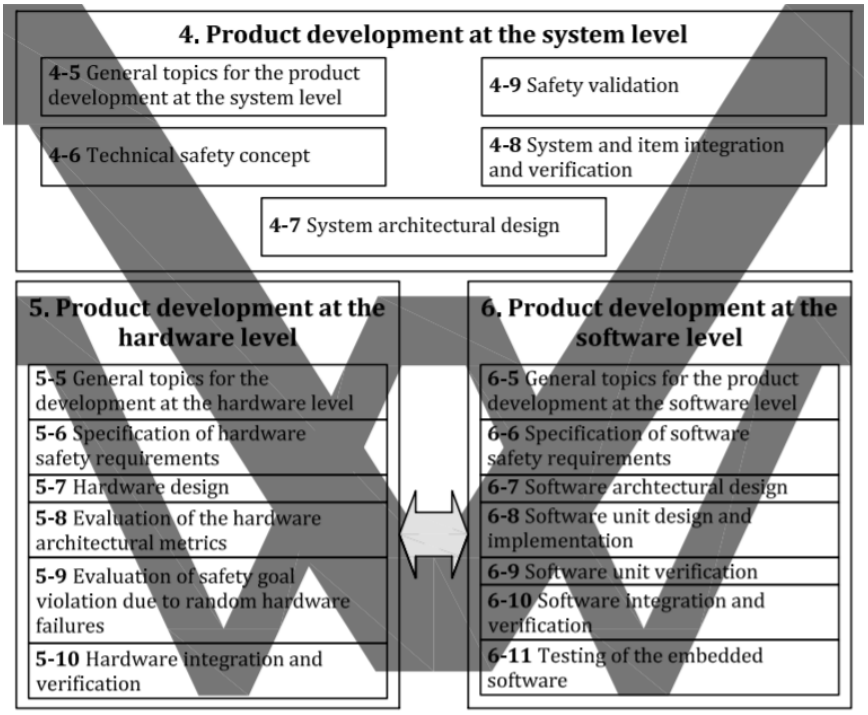

Figure 122: Application of V-Model for product development at system, hardware and software levels [296].

In summary, the V-Model presents features that may match (some of) the requirements of accelerated hybrid testing in the context of VALID, and are aligned with the project objectives (see Section 1.1.3 in the VALID Project Proposal), namely:

- It specifically addresses the topic of functional safety and, thus, directly relates to reliability and survivability as measurable metrics to evaluate whether a (WEC) system is able to work within (predefined) acceptable risk limits.
- It accommodates iteration and incremental development, being characterised by gradual steps accompanied by validation / verification tasks – thus ensuring that design changes can be timely made at an early stage (i.e. low TRL) of the development process.
- It inherently entails a hybrid feature, making use of MIL / SIL / HIL testing throughout the process with an increasing degree of complexity / realism, moving towards the tail-end of the 'Integration' phase.

It should be noted that the V-Model – as originally conceived – may require adaptation for the specific purposes of VALID, and the wider goals of wave energy. Since VALID focuses on critical sub-systems and components of a WEC – as identified in D1.1 – it is envisaged that the V-Model principles may be adapted to the development process of such critical components. Eventual adaptations should also align with additional principles from other processes, such as Technology Qualification, and integrated with the modelling approaches defined in Section 6.2. Additional notes on how next steps in VALID WP1 may address such development and adaptation are provided in Section 7.

7 Concluding remarks

Reliability testing is a recurrent issue in wave energy. At early development stages, there are many uncertainties and design-decisions that need to be explored and consequently this is commonly perceived as a costly investment. However, relegating this activity to later development stages, when a full prototype is manufactured and ready for testing, has also negative implications, namely the design may be too rigid to make significant changes and the associated costs can be prohibitive.

To cope with this challenge, the VALID project aims to develop, implement and enforce a new test procedure based on accelerated hybrid testing techniques. Accelerated hybrid testing allows to integrate the knowledge from real environment (i.e. ocean, uncontrolled testing), the simplified lab environment (i.e. physical test rigs, controlled testing) and a virtually enhanced environment (i.e. numerical models, controlled testing). Once implemented, it will enable the industry to scale-up simulated lab conditions and test a virtual model of the existing structure, and hence reducing current uncertainties, increasing confidence in results, empowering informed decision-making, and thus, largely assisting in the design and development process of WECs, specially at low TRLs.

This report has reviewed and assessed the various modelling theoretical, numerical and experimental approaches that may be relevant in the context of accelerated testing of critical WEC sub-systems / components together with the ones that are available for its use in the VALID project within the partnership. It has also covered the limitations, impact and practicalities associated with the implementation of these modelling approaches in the future VALID testing framework.

Theoretical models provide analytical representations of physical systems by means of a simplified set of equations or by implementing theoretical principles upon which engineering predictions may be derived. Owing to their analytical nature, a theoretical model of WEC sub-systems is likely to feature several assumptions, potentially limiting the applicability of such models in the hybrid testing framework. Additionally, crucial aspects such as the formulation and type of accelerated tests and the assessment of the uncertainty across the I/O structure of the hybrid testing framework can be seen as critical areas that theoretical methods can contribute to.

Numerical models are typically based on one or a combination of more theoretical model(s). In this sense, they are inherently limited by the theory over which they are built on. However, numerical models offer the potential to create a virtual environment where a WEC can be described in a coupled approach. Despite this flexibility, most of numerical models developed to date address the functional behaviour of a WEC and can be suitable for efficiency assessment, but lack the level of detail to represent critical components or sub-systems and to analyse other performance metrics such as reliability.

Finally, experimental/physical models represent a widely used engineering mean of investigating the behaviour of a complex system or one of its sub-systems or components. They add additional degree(s) of realism, but as models they are also limited, unless a full-scale replica is used.

The combination of a numerical model of the WEC and a physical model of the critical sub-system(s) under investigation at a suitable scale, therefore plays a key role in increasing the detailed understanding of the key requirements for the robust design of a WEC at early stages. This hybrid testing offers a coupled modelling while intrinsically allowing a higher fidelity approach in the development and design of critical sub-systems.

The learnings from such initial application of this framework in three user cases will inform the re-contextualisation of a final methodology, promoting wider adoption in the wave energy community.

8 Nomenclature

Abbreviations

ADCP	Acoustic Doppler Current Profiler
AEP	Annual Energy Production
ALARP	As Low As Reasonable Possible
ALWC	Accelerated Low Water Corrosion
AMM	Annual Maxima Method
ANN	Artificial Neural Networks
BAT	Best Available Technology
BEM	Boundary Element Method
BORA	Barrier and Operational Risk Analysis
BTA	Bowtie Analysis
CAPEX	Capital Expenditure
CBM	Condition Based Maintenance
CCA	Cause Consequence Analysis
CEA	Cause-and-Effect Analysis
CFD	Computational Fluid Dynamics
CL	Control Law
CPO	CorPower Ocean
CSN	Climatological Standard Normals
DEG	Dielectric Elastomer Generator
DLC	Design Load Case
EC	European Commission
ECU	Electronic Control Unit
EFTA	Energy Flow/Barrier Analysis
EMG	Electro-Mechanical Generator
ERMO	External Risk Management Options
ESA	Event Sequence Analysis
ETA	Event Tree Analysis
EU	European Union
EVA	Extreme Value Analysis
FEA	Finite Element Analysis
FME(C)A	Failure Modes, Effects (and Criticallity) Analysis
FMI	Functional Mockup Interface
FSI	Fluid Structural Interaction
FTA	Fault tree analysis

FNT	Float-Neck-Tank
GEV	Generalised Extreme Value
GPD	Generalised Pareto Distribution
H2020	Horizon 2020
HAZOP	Hazard and Operability study
HCF	High Cycle Fatigue
HIL	Hardware-In-the-Loop
ICOS	Independent CO-Simulation
IGBT	Insulated Gate Bipolar Transistor
iid	identically independent distributed
LCF	Low Cycle Fatigue
LPA	Layer of protection analysis
MBD	Multi-Body Dynamics
MIC	Microbially Influenced Corrosion
MIL	Model-In-the-Loop
MLER	Most-Likely-Extreme-Response
MLD	Master Logic Diagram
MTBF	Mean Time Between Failures
OEM	Original Equipment Manufacturer
OPEX	Operational Expenditure
OWC	Oscillating Water Column
OWSC	Oscillating Wave Surge Converter
PCA	Principal Component Analysis
PCC	Power Conversion Chain
PCE	Polynomial Chaos Expansion
PDE	Partial Differential Equations
PHA	Preliminary Hazard Analysis
PID	Proportional Integral Derivative
PLC	Programmable Logic Controller
PM	Preventive Maintenance
PMSG	Permanent Magnet Synchronous Generator
POT	Peak-Over-Threshold
PFTE	Polytetrafluoroethylene
PTO	Power Take Off
RAMS	Reliability, Availability, Maintainability and Survivability/Safety
RANSE	Reynolds-Averaged Navier-Stokes Equations
RBD	Reliability Block Diagrams

RBM	Risk-Based Maintenance
RDS	Risk-Directed Survivability
R&S	Reliability and Survivability
SAR	Synthetic Aperture Radar
SCADA	Supervisory Control And Data Acquisition
SCIG	Squirrel Cage Induction Generator
SHM	Structural Health Monitoring
SHP	Smooth Particle Hydrodynamics
SIL	Software-In-the-Loop
SWAN	Simulating WAves Nearshore
SWIFT	Structured What-if technique
TRL	Technology Readiness Level
UV	Uncertainty quantification
VHTP	VALID Hybrid Testing Platform
VMEA	Variation Mode and Effect Analysis
V&V	Verification and Validation
W2W	Wave-to-Wire
WAM	Wave Model
WEC	Wave Energy Converter
WEC^3	Wave Energy Converter Code Comparison
WP	Work Package
WWIII	Wave Watch, 3rd geneartion

9 References

[1] VALID D1.1, 'Accelerated Testing Requirements'.

[2] J. Hodges *et al.*, 'An International Evaluation and Guidance Framework for Ocean Energy Technology', IEA-OES, 2021.

[3] B. Hamedni, C. Mathieu, and C. Bittencourt Ferreira, 'SDWED Deliverable D5.1 Generic WEC System Breakdown', 2014. [Online]. Available: https://www.sdwed.civil.aau.dk/digitalAssets/97/97538_d5.1.pdf

[4] G. Goldschmidt, 'Modeling the Role of Sketching in Design Idea Generation', in *An Anthology of Theories and Models of Design: Philosophy, Approaches and Empirical Explorations*, A. Chakrabarti and L. T. M. Blessing, Eds. London: Springer London, 2014, pp. 433–450. doi: 10.1007/978-1-4471-6338-1_21.

[5] D. Calvo Vélez, 'Modelos teóricos y representación del conocimiento', PhD Thesis, Universidad Complutense de Madrid, Servicio de Publicaciones, Madrid, 2007. [Online]. Available: https://eprints.ucm.es/id/eprint/7367/

[6] R. T. Hudspeth, *Waves and Wave Forces on Coastal and Ocean Structures*, vol. Volume 21. WORLD SCIENTIFIC, 2006. doi: 10.1142/5397.

[7] J. F. Wilson, *Dynamics of offshore structures*. John Wiley & Sons, 2003.

[8] T. Aderinto and H. Li, 'Ocean Wave Energy Converters: Status and Challenges', *Energies*, vol. 11, no. 5, Art. no. 5, May 2018, doi: 10.3390/en11051250.

[9] T. Fazeres-Ferradosa *et al.*, 'Scour Protections for Offshore Foundations of Marine Energy Harvesting Technologies: A Review', *J. Mar. Sci. Eng.*, vol. 9, no. 3, Art. no. 3, Mar. 2021, doi: 10.3390/jmse9030297.

[10] J. D. Zika, N. Skliris, A. T. Blaker, R. Marsh, A. J. G. Nurser, and S. A. Josey, 'Improved estimates of water cycle change from ocean salinity: the key role of ocean warming', *Environ. Res. Lett.*, vol. 13, no. 7, p. 074036, Jul. 2018, doi: 10.1088/1748-9326/aace42.

[11] 'ESA - Mapping salty waters'. https://www.esa.int/Applications/Observing_the_Earth/Space_for_our_climate/Mapping_salty_waters (accessed Oct. 01, 2021).

[12] B. G. Reguero, I. J. Losada, and F. J. Méndez, 'A recent increase in global wave power as a consequence of oceanic warming', *Nat. Commun.*, vol. 10, no. 1, p. 205, Jan. 2019, doi: 10.1038/s41467-018-08066-0.

[13] G. Lavidas and B. Kamranzad, 'Assessment of wave power stability and classification with two global datasets', *Int. J. Sustain. Energy*, vol. 40, no. 6, pp. 514–529, 2020, doi: 10.1080/14786451.2020.1821027.

[14] N. Guillou, G. Lavidas, and G. Chapalain, 'Wave Energy Resource Assessment for Exploitation-A Review', *J. Mar. Sci. Eng.*, vol. 8, no. 9, p. 705, Sep. 2020, doi: 10.3390/jmse8090705.

[15] N. Guillou, 'Estimating wave energy flux from significant wave height and peak period', *Renew. Energy*, vol. 155, pp. 1383–1393, Aug. 2020, doi: 10.1016/j.renene.2020.03.124.

[16] G. Lavidas and H. Polinder, 'North Sea Wave Database (NSWD) and the Need for Reliable Resource Data: A 38 Year Database for Metocean and Wave Energy Assessments', *Atmosphere*, vol. 10, no. 9, 2019, doi: 10.3390/atmos10090551.

[17] M. T. Pontes, M. Bruck, and S. Lehner, 'Assessing the wave energy resource using remote sensed data', Sep. 2009.

[18] S. P. Neill and M. R. Hashemi, 'Fundamentals of Ocean Renewable Energy', in *E-Business Solutions*, S. P. Neill and M. R. B. T.-F. of O. R. E. Hashemi, Eds. Academic Press, 2018. doi: 10.1016/B978-0-12-810448-4.00002-1.

[19] Y. Wan, J. Zhang, and J. Meng, 'A wave energy resource assessment in the China's seas based on multi-satellite merged radar altimeter data', *Acta Oceanol. Sin.*, vol. 34, pp. 115–124, Mar. 2015, doi: 10.1007/s13131-015-0627-6.

[20] J. Vinoth and I. R. Young, 'Global Estimates of Extreme Wind Speed and Wave Height', *J. Clim.*, vol. 24, no. 6, pp. 1647–1665, Mar. 2011, doi: 10.1175/2010JCLI3680.1.

[21] L. Cavaleri, L. Bertotti, and P. Pezzutto, 'Accuracy of altimeter data in inner and coastal seas', *Ocean Sci.*, vol. 15, no. 2, pp. 227–233, Mar. 2019, doi: 10.5194/os-15-227-2019.

[22] D. . Ingram, G. H. Smith, C. . Ferriera, and H. Smith, 'Protocols for the Equitable Assessment of Marine Energy Converters', 2011.

[23] World Meteorological Organization, 'WMO Guidelines on the Calculation of Climate Normals', 2017.

[24] G. Lavidas, V. Venugopal, and D. Friedrich, 'Wave energy extraction in Scotland through an improved nearshore wave atlas', *Int. J. Mar. Energy*, vol. 17, pp. 64–83, 2017, doi: 10.1016/j.ijome.2017.01.008.

[25] G. Lavidas, 'Selection index for Wave Energy Deployments (SIWED): A near-deterministic index for wave energy converters', *Energy*, vol. 196, p. 117131, Apr. 2020, doi: 10.1016/j.energy.2020.117131.

[26] N. Guillou, G. Lavidas, and G. Chapalain, 'Wave Energy Resource Assessment for Exploitation—A Review', *J. Mar. Sci. Eng.*, vol. 8, no. 9, 2020, doi: 10.3390/jmse8090705.

[27] G. Lavidas and H. Polinder, 'North Sea Wave Database (NSWD) and the Need for Reliable Resource Data: A 38 Year Database for Metocean and Wave Energy Assessments', *Atmosphere*, vol. 10, no. 9, 2019, doi: 10.3390/atmos10090551.

[28] IEC TS 62600-101, *IEC TS 62600-101: Marine Energy - Wave, tidal and other water current converters - Part 101: Wave energy resource assessment and characterization*. [Online]. Available: https://webstore.iec.ch/publication/22593

[29] G. Lavidas and V. Venugopal, 'Application of numerical wave models at European coastlines : A review', *Renew. Sustain. Energy Rev.*, vol. 92, no. October 2016, pp. 489–500, 2018, doi: 10.1016/j.rser.2018.04.112.

[30] G. Lavidas, V. Venugopal, and D. Friedrich, 'Sensitivity of a numerical wave model on wind re-analysis datasets', *Dyn. Atmospheres Oceans*, vol. 77, pp. 1–16, 2017, doi: 10.1016/j.dynatmoce.2016.10.007.

[31] J. E. Stopa, 'Wind forcing calibration and wave hindcast comparison using multiple reanalysis and merged satellite wind datasets', *Ocean Model.*, vol. 127, pp. 55–69, Jul. 2018, doi: 10.1016/J.OCEMOD.2018.04.008.

[32] T. Chakraborty and M. Majumder, 'Impact of extreme events on conversion efficiency of wave energy converter', *Energy Sci. Eng.*, vol. 8, no. 10, pp. 3441–3456, 2020, doi: 10.1002/ese3.336.

[33] H. C. M. Smith, D. Haverson, and G. H. Smith, 'A wave energy resource assessment case study: Review, analysis and lessons learnt', *Renew. Energy*, vol. 60, pp. 510–521, 2013, doi: 10.1016/j.renene.2013.05.017.

[34] F. Arena *et al.*, 'Wave climate analysis for the design of wave energy harvesters in the Mediterranean Sea', *Renew. Energy*, vol. 77, pp. 125–141, 2015, doi: 10.1016/j.renene.2014.12.002.

[35] J. Tucker, M, *Waves in Ocean Engineering Measurements, Analysis, Interpretation*. Ellis Horwood Ltd., 1991.

[36] Y. . Goda, *Random seas and desing of maritime structures*, 2nd editio. World Scientific Co.Pte.Ltd., 2000.

[37] M. Mathiesen *et al.*, 'Recommended practice for extreme wave analysis', *J. Hydraul. Res.*, vol. 32, no. 6, pp. 803–814, 1994, doi: 10.1080/00221689409498691.

[38] G. Dodet, X. Bertin, and R. Taborda, 'Wave climate variability in the North-East Atlantic Ocean over the last six decades', *Ocean Model.*, vol. 31, no. 3–4, pp. 120–131, 2010, doi: 10.1016/j.ocemod.2009.10.010.

[39] I. . Young, *Wind Generated Ocean Waves-volume 2*, 1st ed. Elsevier Ocean Engineering Book Series, 1999.

[40] G. P. Harrison and a. R. Wallace, 'Climate sensitivity of marine energy', *Renew. Energy*, vol. 30, no. 12, pp. 1801–1817, Oct. 2005, doi: 10.1016/j.renene.2004.12.006.

[41] I. R. Young, J. Vinoth, S. Zieger, and a. V. Babanin, 'Investigation of trends in extreme value wave height and wind speed', *J. Geophys. Res.*, vol. 117, Mar. 2012, doi: 10.1029/2011JC007753.

[42] L. Bertotti and L. Cavaleri, 'Modelling waves at Orkney coastal locations', *J. Mar. Syst.*, vol. 96–97, pp. 116–121, Aug. 2012, doi: 10.1016/j.jmarsys.2012.02.012.

[43] S. Caires and M. R. a. Van Gent, 'Wave height distribution in constant and finite depths', *Coast. Eng. Proc.*, 2012.

[44] A. Sterl and S. Caires, 'Climatology, variability and extrema of ocean waves: The web-based KNMI/ERA-40 wave atlas', *Int. J. Climatol.*, vol. 25, no. 7, pp. 963–977, 2005, doi: 10.1002/joc.1175.

[45] S. Caires and A. Sterl, 'A new nonparametric method to correct model data: Application to significant wave height from the ERA-40 re-analysis', *J. Atmospheric Ocean. Technol.*, vol. 22, no. 4, pp. 443–459, 2005, doi: 10.1175/JTECH1707.1.

[46] S. Caires and M. R. A. Van Gent, 'Extreme Wave Loads', *Proc. ASME 2008 27th Int. Conf. Ocean. Arct. Eng. OMAE2008*, pp. 1–9, 2008.

[47] S. Coles, *An Introduction to Statistical modelling of extreme values*. Springer Series in Statistics, 2001.

[48] C. Oikonomou, M. Gradowski, C. Kalogeri, and A. J. N. A. Sarmento, 'On defining storm intervals: Extreme wave analysis using extremal index inferencing of the run length parameter', *Ocean Eng.*, vol. 217, pp. 107988–107988, 2020.

[49] C. Michelén Ströfer and R. Coe, *Comparison of methods for estimating short-term extreme response of wave energy converters*. 2015. doi: 10.23919/OCEANS.2015.7401878.

[50] S. Haver, 'Wave climate off northern Norway', *Appl. Ocean Res.*, vol. 7, no. 2, pp. 85–92, Apr. 1985, doi: 10.1016/0141-1187(85)90038-0.

[51] S. Haver, 'On the joint distribution of heights and periods of sea waves', *Ocean Eng.*, vol. 14, no. 5, pp. 359–376, Jan. 1987, doi: 10.1016/0029-8018(87)90050-3.

[52] E. Vanem, 'Environmental contours for describing extreme ocean wave conditions based on combined datasets', *Stoch. Environ. Res. Risk Assess.*, vol. 33, pp. 1–15, Jun. 2019, doi: 10.1007/s00477-019-01670-6.

[53] A. F. Haselsteiner, R. G. Coe, L. Manuel, P. T. T. Nguyen, N. Martin, and A. Eckert-Gallup, 'A Benchmarking Exercise on Estimating Extreme Environmental Conditions: Methodology and Baseline Results', presented at the ASME 2019 38th International Conference on Ocean, Offshore and Arctic Engineering, Jun. 2019. doi: 10.1115/OMAE2019-96523.

[54] H. Hotelling, 'Analysis of a complex of statistical variables into principal components.', *J. Educ. Psychol.*, vol. 24, pp. 498–520, 1933.

[55] I. T. Jolliffe and J. Cadima, 'Principal component analysis: a review and recent developments', *Philos. Trans. R. Soc. Math. Phys. Eng. Sci.*, vol. 374, no. 2065, p. 20150202, Apr. 2016, doi: 10.1098/rsta.2015.0202.

[56] G. J. Komen, S. Hasselmann, and K. Hasselmann, 'On the Existence of a Fully Developed Wind-Sea Spectrum', *J. Phys. Oceanogr.*, vol. 14, no. 8, pp. 1271–1285, Aug. 1984, doi: 10.1175/1520-0485(1984)014<1271:OTEOAF>2.0.CO;2.

[57] E. B. L. Mackay, A. S. Bahaj, and P. G. Challenor, 'Uncertainty in wave energy resource assessment. Part 1: Historic data', *Renew. Energy*, vol. 35, no. 8, pp. 1792–1808, Aug. 2010, doi: 10.1016/j.renene.2009.10.026.

[58] H. L. Tolman, 'A Generalized Multiple Discrete Interaction Approximation for resonant four-wave interactions in wind wave models', *Ocean Surf. Waves*, vol. 70, pp. 11–24, Oct. 2013, doi: 10.1016/j.ocemod.2013.02.005.

[59] 'Equitable Testing and Evaluation of Marine Energy Extraction Devices in terms of Performance, Cost and Environmental Impact 2.4', p. 47.

[60] G. Besio, L. Mentaschi, and A. Mazzino, 'Wave energy resource assessment in the Mediterranean Sea on the basis of a 35-year hindcast', *Energy*, vol. 94, pp. 50–63, Jan. 2016, doi: 10.1016/j.energy.2015.10.044.

[61] L. Cavaleri and L. Bertotti, 'The improvement of modelled wind and wave fields with increasing resolution', *Ocean Eng.*, vol. 33, no. 5, pp. 553–565, Apr. 2006, doi: 10.1016/j.oceaneng.2005.07.004.

[62] G. Lavidas and V. Venugopal, *Influence of Computational Domain Size on Wave Energy Assessments in Energetic Waters*. 2015.

[63] L. Cavaleri, 'Wave Modeling—Missing the Peaks', *J. Phys. Oceanogr.*, vol. 39, no. 11, pp. 2757–2778, Nov. 2009, doi: 10.1175/2009JPO4067.1.

[64] L. Cavaleri, F. Barbariol, and A. Benetazzo, 'Wind–Wave Modeling: Where We Are, Where to Go', *J. Mar. Sci. Eng.*, vol. 8, no. 4, 2020, doi: 10.3390/jmse8040260.

[65] G. Vledder, T. Herbers, R. Jensen, D. Resio, and B. Tracy, *Modelling of Non-Linear Quadruplet Wave-Wave Interactions in Operational Wave Models*, vol. 276. 2000, p. 811. doi: 10.1061/40549(276)62.

[66] M. Zijlema, G. P. van Vledder, and L. H. Holthuijsen, 'Bottom friction and wind drag for wave models', *Coast. Eng.*, vol. 65, pp. 19–26, Jul. 2012, doi: 10.1016/j.coastaleng.2012.03.002.

[67] R. C. Ris, L. H. Holthuijsen, and N. Booij, 'A third-generation wave model for coastal regions: 2. Verification', *J. Geophys. Res. Oceans*, vol. 104, no. C4, pp. 7667–7681, Apr. 1999, doi: 10.1029/1998JC900123.

[68] J. Cruz, *Ocean Wave Energy*, 1st ed. Berlin Heidelberg: Springer-Verlag, 2008.

[69] M. Folley, 'Chapter 1 - Introduction', in *Numerical Modelling of Wave Energy Converters*, M. Folley, Ed. Academic Press, 2016, pp. 1–7. doi: 10.1016/B978-0-12-803210-7.00001-3.

[70] D. V. Evans, 'A theory for wave-power absorption by oscillating bodies', *J. Fluid Mech.*, vol. 77, no. 1, pp. 1–25, 1976, doi: 10.1017/S0022112076001109.

[71] C. C. Mei, 'Power extracted from water waves', *J. Ship Res.*, vol. 20, pp. 63–66, 1976.

[72] K. Budal, 'Theory for Absorption of Wave Power by a System of Interacting Bodies', *J. Ship Res.*, vol. 21, no. 04, pp. 248–254, Dec. 1977, doi: 10.5957/jsr.1977.21.4.248.

[73] J. Newman, 'Panel Methods in Marine Hydrodynamics', in *11th Australasian Fluid Mechanics Conference*, Hobart, Australia, 1992, p. Keynote Paper K-2.

[74] C. Fitzgerald, 'PerAWaT - Report on Comparisons of Nonlinear Models with Experimental Data for both Single Devices and Arrays of Devices (WG1 WP1 D1)', ETI, 2013. doi: 10.5286/UKERC.EDC.000402.

[75] Aalborg University, 'D2.1: Assessment of capabilities of available tools'. DTOcean Project, 2014. Accessed: Mar. 02, 2021. [Online]. Available: https://www.dtoceanplus.eu/content/download/2518/file/DTO_WP2_AAU_D2.1.pdf

[76] C. Mingham, L. Qian, and D. Causon, 'Chapter 6 - Computational Fluid Dynamics (CFD) Models', in *Numerical Modelling of Wave Energy Converters*, M. Folley, Ed. Academic Press, 2016, pp. 105–122. doi: 10.1016/B978-0-12-803210-7.00006-2.

[77] P. Haselbach, A. Natarajan, R. G. Jiwinangun, and K. Branner, 'Comparison of Coupled and Uncoupled Load Simulations on a Jacket Support Structure', *Deep. – Sel. Pap. 10th Deep Sea Offshore Wind RD Conf. Trondheim Nor. 24 – 25 January 2013*, vol. 35, pp. 244–252, Jan. 2013, doi: 10.1016/j.egypro.2013.07.177.

[78] N. Nakata *et al.*, *Hybrid Simulation Primer and Dictionary*. 2014. [Online]. Available: https://datacenterhub.org/resources/8102

[79] N. Nakata *et al.*, 'Hybrid Simulation: A Discussion of Current Assessment Measures', Aug. 2014.

[80] P. Paris and F. Erdogan, 'A Critical Analysis of Crack Propagation Laws', *J. Basic Eng.*, vol. 85, no. 4, pp. 528–533, Dec. 1963, doi: 10.1115/1.3656900.

[81] A. Palmgren, 'Die Lebensdauer von Kugellagern (Life Length of Roller Bearings or Durability of Ball Bearings)', *Z. Vereines Dtsch. Ingenieure*, no. 14, pp. 339–341, 1924.

[82] P. Marcus, *Corrosion Mechanisms in Theory and Practice, Third Edition*. Taylor & Francis, 2011. [Online]. Available: https://books.google.dk/books?id=8Kq7xVUpYuUC

[83] R. P. Gangloff, 'Corrosion fatigue crack propagation in metals', presented at the International Conference on Environment Induced Cracking of Metals, Jun. 1990. Accessed: Apr. 05, 2021. [Online]. Available: https://ntrs.nasa.gov/citations/19900015089

[84] I. Hutchings and P. Shipway, *Tribology: Friction and Wear of Engineering Materials*. Elsevier Science, 2017. [Online]. Available: https://books.google.dk/books?id=yRR2DQAAQBAJ

[85] O. Ditlevsen, *Structural Reliability Methods*. Technical University of Denmark, 2007.

[86] M. H. Faber, *Statistics and Probability Theory: In Pursuit of Engineering Decision Support*. Springer Netherlands, 2012. [Online]. Available: https://books.google.dk/books?id=n0qAFuZU82kC

[87] H. O. Madsen, S. Krenk, and N. C. Lind, *Methods of Structural Safety*. Dover Publications, 2006. [Online]. Available: https://books.google.dk/books?id=e8sZjD7so-AC

[88] J. Kofoed *et al.*, 'State of the Art Descriptions and Tasks for Structural Design of Wave Energy Devices', Aalborg Universitet, Aalborg, Denmark, 1, 2010. [Online]. Available: www.sdwed.civil.aau.dk

[89] N. E. Dowling, *Mechanical Behavior of Materials*, 4th edition. Boston: Pearson, 2012.

[90] P. R. Thies, L. Johanning, and T. Gordelier, 'Component reliability testing for wave energy converters: Rationale and implementation', 2013. [Online]. Available: https://ore.exeter.ac.uk/repository/bitstream/handle/10871/15923/Thies--Component_Reliability_Testing_for_Wave_Energy_Converters-Rationale_and_Implementation--EWTEC2013.pdf?sequence=4&isAllowed=y

[91] T. Svensson and J. Sandström, 'Load/Strength analysis of wave energy components', Borås, SP Rapport 2014:80, 2014.

[92] I. Hutchings and P. Shipway, *Tribology: Friction and Wear of Engineering Materials*. Elsevier Science, 2017. [Online]. Available: https://books.google.dk/books?id=yRR2DQAAQBAJ

[93] S. C. Lim, 'Recent developments in wear-mechanism maps', *Tribol. Int.*, vol. 31, no. 1, pp. 87–97, Jan. 1998, doi: 10.1016/S0301-679X(98)00011-5.

[94] H. Unal, U. Sen, and A. Mimaroglu, 'Study of Abrasive Wear Volume Map for PTFE and PTFE Composites', *Appl. Compos. Mater.*, vol. 14, no. 5, pp. 287–306, Nov. 2007, doi: 10.1007/s10443-007-9047-x.

[95] R. W. Revie and H. H. Uhlig, 'Corrosion and Corrosion Control : An Introduction to Corrosion Science and Engineering', p. 513.

[96] P. Refait, A.-M. Grolleau, M. Jeannin, C. Rémazeilles, and R. Sabot, 'Corrosion of Carbon Steel in Marine Environments: Role of the Corrosion Product Layer', p. 21, 2020.
[97] J. Zuquan, Z. Xia, Z. Tiejun, and L. Jianqing, 'Chloride ions transportation behavior and binding capacity of concrete exposed to different marine corrosion zones', *Constr. Build. Mater.*, vol. 177, pp. 170–183, Jul. 2018, doi: 10.1016/j.conbuildmat.2018.05.120.
[98] R. E. Melchers and R. Jeffrey, 'Corrosion of long vertical steel strips in the marine tidal zone and implications for ALWC', *Corros. Sci.*, vol. 65, pp. 26–36, Dec. 2012, doi: 10.1016/j.corsci.2012.07.025.
[99] B. J. Little *et al.*, 'Microbially influenced corrosion—Any progress?', *Corros. Sci.*, vol. 170, p. 108641, Jul. 2020, doi: 10.1016/j.corsci.2020.108641.
[100] Y. Ma, Y. Zhang, R. Zhang, F. Guan, B. Hou, and J. Duan, 'Microbiologically influenced corrosion of marine steels within the interaction between steel and biofilms: a brief view', *Appl. Microbiol. Biotechnol.*, vol. 104, no. 2, pp. 515–525, Jan. 2020, doi: 10.1007/s00253-019-10184-8.
[101] I. Lazakis, O. Turan, and S. Aksu, 'Increasing ship operational reliability through the implementation of a holistic maintenance management strategy', *Ships Offshore Struct.*, vol. 5, no. 4, pp. 337–357, Oct. 2010, doi: 10.1080/17445302.2010.480899.
[102] M. Abbas and M. Shafiee, 'An overview of maintenance management strategies for corroded steel structures in extreme marine environments', *Mar. Struct.*, vol. 71, p. 102718, May 2020, doi: 10.1016/j.marstruc.2020.102718.
[103] P. A. Vinagre, T. Simas, E. Cruz, E. Pinori, and J. Svenson, 'Marine Biofouling: A European Database for the Marine Renewable Energy Sector', *J. Mar. Sci. Eng.*, vol. 8, no. 7, p. 495, Jul. 2020, doi: 10.3390/jmse8070495.
[104] I. Elishakoff, *Probabilistic Theory of Structures*. Dover Publications, 1999. [Online]. Available: https://books.google.dk/books?id=8ohKdUv6wNwC
[105] ISO/IEC 9126-4, *Software engineering - Product quality - Part 4: Quality in use metrics*. 2004.
[106] D. Warburton, J. E. Strutt, and K. Allsopp, 'Reliability prediction procedures for mechanical components at the design stage', *Proc. Inst. Mech. Eng. Part E J. Process Mech. Eng.*, vol. 212, no. 4, pp. 213–224, Nov. 1998, doi: 10.1243/0954408981529420.
[107] Rausand, Marvin, *Risk Assessment: Theory, Methods and Applications*, First Edition. Wiley & Sons, Inc., 2011. [Online]. Available: https://onlinelibrary.wiley.com/doi/book/10.1002/9781118281116
[108] Yoe, Charles, *Principles of Risk Analysis: Decision Making Under Uncertainty*, 1st edition. 2012. [Online]. Available: https://doi.org/10.1201/b11256
[109] S. Ambühl, M. M. Kramer, and J. D. Sørensen, 'Different reliability assessment approaches for wave energy converters', in *European Wave and Tidal Energy Conference*, 2015, pp. 7D1–4. [Online]. Available: https://energiforskning.dk/sites/energiforskning.dk/files/slutrapporter/appendix_v_ewtec2015_different_reliability_assessment_approaches.pdf
[110] D. Kececioglu, 'Reliability analysis of mechanical components and systems', *Nucl. Eng. Des.*, vol. 19, no. 2, pp. 259–290, May 1972, doi: 10.1016/0029-5493(72)90133-1.
[111] P. R. Thies, L. Johanning, and T. Gordelier, 'Component reliability testing for wave energy converters: Rationale and implementation', 2013. [Online]. Available: https://ore.exeter.ac.uk/repository/bitstream/handle/10871/15923/Thies--Component_Reliability_Testing_for_Wave_Energy_Converters-Rationale_and_Implementation--EWTEC2013.pdf?sequence=4&isAllowed=y
[112] H. Tanizaki, *Computational Methods in Statistics and Econometrics*. Taylor & Francis, 2004. [Online]. Available: https://books.google.dk/books?id=pOGAUcn13fMC

[113] S. K. Au and Y. Wang, *Engineering Risk Assessment with Subset Simulation*. Wiley, 2014. [Online]. Available: https://books.google.dk/books?id=7UhZAwAAQBAJ
[114] C. Bucher, *Computational Analysis of Randomness in Structural Mechanics: Structures and Infrastructures Book Series, Vol. 3*. CRC Press, 2009. [Online]. Available: https://books.google.dk/books?id=nZkt02wl6egC
[115] S. K. Choi, R. Grandhi, and R. A. Canfield, *Reliability-based Structural Design*. Springer London, 2006. [Online]. Available: https://books.google.dk/books?id=BZ1AAAAAQBAJ
[116] S. Ambühl, M. Kramer, and J. D. Sørensen, 'Structural Reliability of Plain Bearings for Wave Energy Converter Applications', *Energies*, vol. 9, no. 2, 2016, doi: 10.3390/en9020118.
[117] S. Ambühl, M. Kramer, and J. D. Sørensen, 'Reliability-Based Structural Optimization of Wave Energy Converters', *Energies*, vol. 7, no. 12, 2014, doi: 10.3390/en7128178.
[118] M. Mueller, R. Lopez, A. McDonald, and G. Jimmy, 'Reliability analysis of wave energy converters', in *2016 IEEE International Conference on Renewable Energy Research and Applications (ICRERA)*, Nov. 2016, pp. 667–672. doi: 10.1109/ICRERA.2016.7884418.
[119] S. Ambühl, 'Reliability of Wave Energy Converters: revised version', 2015.
[120] Y. Yang, 'Reliability, Availability, Maintainability and Survivability Assessment Tool – Alpha version', Apr. 2020.
[121] R. Coe and Y. Yu, 'WDRT : A toolbox for design-response analysis of wave energy converters', 2016.
[122] J. Canning, P. Nguyen, L. Manuel, and R. G. Coe, *On the Long-term reliability analysis of a point absorber wave energy converter*. New York: Amer Soc Mechanical Engineers, 2017, p. UNSP V010T09A024.
[123] R. Coe, Y. Yu, and J. V. Rij, 'A Survey of WEC Reliability, Survival and Design Practices', *Energies*, vol. 11, p. 4, 2017.
[124] A. C. Eckert-Gallup, C. J. Sallaberry, A. R. Dallman, and V. S. Neary, 'Application of principal component analysis (PCA) and improved joint probability distributions to the inverse first-order reliability method (I-FORM) for predicting extreme sea states', *Ocean Eng.*, vol. 112, pp. 307–319, Jan. 2016, doi: 10.1016/j.oceaneng.2015.12.018.
[125] J. Dawson, S. Din, M. Mytton, N. Shore, and H. Stansfield, 'System-reliability studies for wave-energy generation', *Iee Proc.--Sci. Meas. Technol.*, vol. 127, no. 5, pp. 296–300, 1980, doi: 10.1049/ip-a-1.1980.0047.
[126] J. D. Sørensen, J. P. Kofoed, and C. B. Ferreira, *Probabilistic design of wave energy devices*. Boca Raton: Crc Press-Taylor & Francis Group, 2011, pp. 1839–1845.
[127] J. Flinn and C. B. Ferreira, *Uncertain and unavoidable-reliability estimation in wave and tidal energy systems*. Boca Raton: Crc Press-Taylor & Francis Group, 2011, pp. 1799–1804.
[128] S. Ambühl, F. Ferri, J. P. Kofoed, and J. D. Sorensen, 'Fatigue reliability and calibration of fatigue design factors of wave energy converters', *Int. J. Mar. Energy*, vol. 10, pp. 17–38, Jun. 2015, doi: 10.1016/j.ijome.2015.01.004.
[129] A. Kolios, L. F. Di Maio, L. Wang, L. Cui, and Q. Sheng, 'Reliability assessment of point-absorber wave energy converters', *Ocean Eng.*, vol. 163, pp. 40–50, Sep. 2018, doi: 10.1016/j.oceaneng.2018.05.048.
[130] H. Liu *et al.*, 'Reliability Assessment of Water Hydraulic-Drive Wave-Energy Converters', *Energies*, vol. 12, no. 21, p. 4189, Nov. 2019, doi: 10.3390/en12214189.
[131] A. Cretu, R. jr Munteanu, D. Iudean, V. Vladareanu, and P. Karaisas, 'Reliability Assessment of Linear Generator Type Wave Energy Converters', in *2016 International Conference on Applied and Theoretical Electricity (icate)*, New York: Ieee, 2016.

[132] P. R. Thies, J. Flinn, and G. H. Smith, 'Reliability assessment and criticality analysis for Wave Energy Converters', 2009.
[133] H. C. Pedersen, R. H. Hansen, A. H. Hansen, T. O. Andersen, and M. M. Bech, 'Design of full scale wave simulator for testing Power Take Off systems for wave energy converters', *Int. J. Mar. Energy*, vol. 13, pp. 130–156, Apr. 2016, doi: 10.1016/j.ijome.2016.01.005.
[134] S. Chandrasekaran and Harender, 'Failure mode and effects analysis of mechanical wave energy converters', *Int. J. Intell. Eng. Inform.*, vol. 3, no. 1, pp. 57–65, 2015, doi: 10.1504/IJIEI.2015.069089.
[135] M. Mueller, R. Lopez, A. McDonald, and G. Jimmy, 'Reliability Analysis of Wave Energy Converters', in *2016 Ieee International Conference on Renewable Energy Research and Applications (icrera)*, New York: Ieee, 2016, pp. 667–672.
[136] M. Trapanese, V. Boscaino, G. Cipriani, D. Curto, V. Di Dio, and V. Franzitta, 'A Permanent Magnet Linear Generator for the Enhancement of the Reliability of a Wave Energy Conversion System', *Ieee Trans. Ind. Electron.*, vol. 66, no. 6, pp. 4934–4944, Jun. 2019, doi: 10.1109/TIE.2018.2838076.
[137] F. Madhi and R. W. Yeung, 'On survivability of asymmetric wave-energy converters in extreme waves', *Renew. Energy*, vol. 119, pp. 891–909, Apr. 2018, doi: 10.1016/j.renene.2017.07.123.
[138] A. Ben Yaghlane and M. N. Azaiez, 'Systems under attack-survivability rather than reliability: Concept, results, and applications', *Eur. J. Oper. Res.*, vol. 258, no. 3, pp. 1156–1164, May 2017, doi: 10.1016/j.ejor.2016.09.041.
[139] The European Marine Energy Center Ltd, 'Guidelines for Reliability, Maintainability and Survivability of Marine Energy Conversion Systems', 2009.
[140] S. Dharmaraja, R. Vinayak, and K. S. Trivedi, 'Reliability and survivability of vehicular ad hoc networks: An analytical approach', *Reliab. Eng. Syst. Saf.*, vol. 153, pp. 28–38, Sep. 2016, doi: 10.1016/j.ress.2016.04.004.
[141] S. Parmeggiani, J. Kofoed, and E. Friis-Madsen, 'Extreme Loads on the Mooring Lines and Survivability Mode for the Wave Dragon Wave Energy Converter', in *World Renewable Energy Congress-Sweden; 8-13 May; 2011; Linköping; Sweden*, 2011, no. 057, pp. 2159–2166.
[142] J. Hodges *et al.*, 'An International Evaluation and Guidance Framework for Ocean Energy Technology', IEA-OES, 2021.
[143] H. Narasimhan and M. H. Faber, 'Risk Assessment in Engineering: Principles, System Representation and Risk Criteria. Annex - Examples - Assessment of Structural Robustness'. JCSS - Joint Committee on Structural Safety, Jun. 26, 2009. [Online]. Available: https://www.jcss-lc.org/publications/raie/robustness-example_jcss-document.pdf
[144] ISO 31000, 'Risk Management - Guidelines'. 2018.
[145] EN 1991-1-7, 'Eurocode 1 - Actions on structures - Part 1-7: General actions - Accidental actions', Jul. 2006.
[146] A. Brown *et al.*, *Towards a Definition and Metric for the Survivability of Ocean Wave Energy Converters*. New York: Amer Soc Mechanical Engineers, 2010, pp. 917–927.
[147] G. Dodet *et al.*, 'The Sea State CCI dataset v1: towards a sea state climate data record based on satellite observations', *Earth Syst Sci Data*, vol. 12, no. 3, pp. 1929–1951, Sep. 2020, doi: 10.5194/essd-12-1929-2020.
[148] Ove Arup & Partners Ltd and Cruz Atcheson Consulting Engineers, Lda., 'Structural Forces and Stresses for Wave Energy Devices', ARP LS2, Jun. 2016.
[149] A. McCabe, 'An Appraisal of a Range of Fluid Modelling Software', Department of Energy, Lancaster University, SuperGen Marine Report T2.3.4, 2004. Accessed: Jan. 02,

2021. [Online]. Available: https://www.supergen-marine.org.uk/sites/supergen-marine.org.uk/files/publications/McCabe2004.pdf
[150] A. Combourieu *et al.*, 'WEC3: Wave Energy Converter Code Comparison Project', Nantes, France, 2015.
[151] F. Wendt *et al.*, 'Ocean Energy Systems Wave Energy Modelling Task: Modelling, Verification and Validation of Wave Energy Converters', *J. Mar. Sci. Eng.*, vol. 7, no. 11, 2019, doi: 10.3390/jmse7110379.
[152] P. J. Roache, *Verification and Validation in Computational Science and Engineering*. Hermosa Publishers, 1998.
[153] R. Rawlinson-Smith *et al.*, 'The PerAWaT project: Performance Assessment of Wave and Tidal Array Systems', Bilbao, Spain, 2010.
[154] J. Cruz, M. Livingstone, and K. Rhinefrank, 'Validation of a New Wave Energy Converter (WEC) Modelling Tool: Application to the Columbia Power WEC', in *OMAE2011*, Volume 5: Ocean Space Utilization; Ocean Renewable Energy, Jun. 2011, pp. 679–699. doi: 10.1115/OMAE2011-49845.
[155] E. Mackay, J. Cruz, C. Retzler, P. Arnold, E. Bannon, and R. Pascal, 'Validation of a New Wave Energy Converter Design Tool with Large Scale Single Machine Experiments', Jeju, South Korea, 2012.
[156] R. Henderson, 'Case Study: Pelamis', in *Ocean Wave Energy - Current Status and Future Prespectives*, J. Cruz, Ed. Berlin Heidelberg: Springer-Verlag, 2008.
[157] A. Henry, P. Schmitt, T. Whittaker, A. Rafiee, and F. Dias, 'The Characteristics of Wave Impacts on an Oscillating Wave Surge Converter', Jun. 2013.
[158] P. Schmitt and B. Elsaesser, 'On the use of OpenFOAM to model Oscillating wave surge converters', *Ocean Eng.*, vol. 108, pp. 98–104, 2015.
[159] A. Sarmento and G. Thomas, 'Guidelines for Laboratory Testing of WECs', in *Ocean Wave Energy - Current Status and Future Prespectives*, J. Cruz, Ed. Berlin Heidelberg: Springer-Verlag, 2008.
[160] P. Schmitt, H. Asmuth, and B. Elsäßer, 'Optimising power take-off of an oscillating wave surge converter using high fidelity numerical simulations', *Int. J. Mar. Energy*, vol. 16, pp. 196–208, Dec. 2016, doi: 10.1016/j.ijome.2016.07.006.
[161] J. M. Westphalen *et al.*, 'Investigation of Wave-Structure Interaction Using State of the Art CFD Techniques', *Open J. Fluid Dyn.*, vol. 4, pp. 18–43, 2014, doi: 10.4236/ojfd.2014.41003.
[162] P. S. Tromans, A. R. Anaturk, and P. Hagemeijer, 'A New Model For The Kinematics Of Large Ocean Waves-Application As a Design Wave', Aug. 1991.
[163] A. Rafiee and J. Fievez, 'Numerical Prediction of Extreme Loads on the CETO Wave Energy Converter', Nantes, France, 2015.
[164] J. V. Rij and Y. Yu, 'Design Load Analysis for Wave Energy Converters: Preprint', 2017.
[165] P.-H. Musiedlak, E. J. Ransley, M. Hann, B. Child, and D. M. Greaves, 'Time-Splitting Coupling of WaveDyn with OpenFOAM by Fidelity Limit Identified from a WEC in Extreme Waves', *Energies*, vol. 13, no. 13, 2020, doi: 10.3390/en13133431.
[166] J. Davidson and R. Costello, 'Efficient Nonlinear Hydrodynamic Models for Wave Energy Converter Design—A Scoping Study', *J. Mar. Sci. Eng.*, vol. 8, no. 1, 2020, doi: 10.3390/jmse8010035.
[167] P. T. T. Nguyen, L. Manuel, and R. G. Coe, 'On the Development of an Efficient Surrogate Model for Predicting Long-Term Extreme Loads on a Wave Energy Converter', *J. Offshore Mech. Arct. Eng.*, vol. 141, no. 061103, Mar. 2019, doi: 10.1115/1.4042944.

[168] R. So, S. Casey, S. Kanner, A. Simmons, and T. K. A. Brekken, 'PTO-Sim: Development of a Power Take Off Modeling Tool for Ocean Wave Energy Conversion', Denver, CO, USA, 2015.
[169] I. Penesis *et al.*, 'Final report and recommendations of the Specialist Committee on Hydrodynamics Modelling of Marine Renewable Energy Devices', in *28th International Towing Tank Conference (ITTC)*, Wuxi, China, 2017, pp. 579–638.
[170] Y.-H. Yu, K. Ruehl, N. Tom, and J. van Rij, 'Review of WEC-Sim Development and Applications', presented at the PAMEC 2020, San Jose, Costa Rica, 2020.
[171] S. Sirnivas, Y.-H. Yu, M. Hall, and B. Bosma, 'Coupled Mooring Analyses for the WEC-Sim Wave Energy Converter Design Tool', 2016.
[172] J. Scriven and J. Cruz, 'Introducing non-rigid body structural dynamics to WEC-Sim', *Int. Mar. Energy J.*, vol. 3, no. 2, Sep. 2020, doi: 10.36688/imej.3.55-63.
[173] J. Cruz, M. Atcheson, T. Martins, L. Castellini, and M. Martini, 'Preliminary Load Assessment: UMBRA's 250kW EMG Power Take-Off', Napoli, Italy, 2019.
[174] J. van Rij, Y.-H. Yu, Y. Guo, and R. G. Coe, 'A Wave Energy Converter Design Load Case Study', *J. Mar. Sci. Eng.*, vol. 7, no. 8, 2019, doi: 10.3390/jmse7080250.
[175] M. Atcheson, J. Cruz, and T. Martins, 'Quantification of load uncertainties in the design process of a WEC', Napoli, Italy, 2019.
[176] Y. Zhao and S. Dong, 'Probabilistic fatigue surrogate model of bimodal tension process for a semi-submersible platform', *Ocean Eng.*, vol. 220, p. 108501, Jan. 2021, doi: 10.1016/j.oceaneng.2020.108501.
[177] C. B. Li, J. Choung, and M.-H. Noh, 'Wide-banded fatigue damage evaluation of Catenary mooring lines using various Artificial Neural Networks models', *Mar. Struct.*, vol. 60, pp. 186–200, Jul. 2018, doi: 10.1016/j.marstruc.2018.03.013.
[178] D. Xiu and G. E. Karniadakis, 'The Wiener--Askey Polynomial Chaos for Stochastic Differential Equations', *SIAM J. Sci. Comput.*, Jul. 2006, doi: 10.1137/S1064827501387826.
[179] D. Xiu, *Numerical Methods for Stochastic Computations: A Spectral Method Approach*. Princeton University Pres, 2010. doi: 10.2307/j.ctv7h0skv.
[180] A. Chakhunashvili, P. M. Johansson, and B. L. S. Bergman, 'Variation mode and effect analysis', in *Annual Symposium Reliability and Maintainability, 2004 - RAMS*, Jan. 2004, pp. 364–369. doi: 10.1109/RAMS.2004.1285476.
[181] P. Johannesson, T. Svensson, L. Samuelsson, B. Bergman, and J. de Maré, 'Variation mode and effect analysis: an application to fatigue life prediction', *Qual. Reliab. Eng. Int.*, vol. 25, no. 2, pp. 167–179, 2009, doi: 10.1002/qre.960.
[182] P. Johannesson *et al.*, 'A Robustness Approach to Reliability', *Qual. Reliab. Eng. Int.*, vol. 29, no. 1, pp. 17–32, 2013, doi: 10.1002/qre.1294.
[183] P. Johannesson, 'Reliability Guidance for Marine Energy Converters.', 2016. [Online]. Available: http://riasor.com/wp-content/uploads/2016/12/ReliabilityGuidanceMECs_v1.0_20161216.pdf
[184] P. Johannesson, T. Svensson, and H. Gaviglio, 'Reliability Evaluation using Variation Mode and Effect Analysis: Application to CorPower's mooring pre-tension cylinder', presented at the EWTEC 2019 - 13th European Wave and Tidal Energy Conference, Naples, Italy, Sep. 2019.
[185] S. W. G. NAFEMS, 'NAFEMS - What is Uncertainty Quantification (UQ)?', 2018. https://www.nafems.org/publications/resource_center/wt08/ (accessed Nov. 03, 2021).
[186] R. Ghanem, D. Higdon, and H. Owhadi, *Handbook of Uncertainty Quantification*. Cham: Springer International Publishing, 2017. doi: 10.1007/978-3-319-12385-1_1.

[187] C. J. Freitas, 'Standards and Methods for Verification, Validation, and Uncertainty Assessments in Modeling and Simulation', *J. Verification Valid. Uncertain. Quantif.*, vol. 5, no. 2, Jun. 2020, doi: 10.1115/1.4047274.
[188] W. L. Oberkampf and C. J. Roy, *Verification and validation in scientific computing*. New York: Cambridge University Press, 2010.
[189] A. Sarmento and G. Thomas, 'Laboratory Testing of Wave Energy Devices. Wave Energy Converters Generic Technical Evaluation Summary', CEC, Brussels, Annex Report B1, Device Fundamentals / Hydrodynamics, 1993.
[190] (HMRC) Hydraulic & Marine Research Centre, 'Ocean Energy: Development and Evaluation Protocol, Part 1: Wave Power', University College Cork, Ireland, 2003.
[191] Supergen Marine, 'Guidance for the experimental tank testing of wave energy converters', University of Edinburgh, 2008.
[192] (EMEC) European Marine Energy Centre, 'Tank Testing of Wave Energy Conversion Systems. EMEC Marine Renewable Energy Guides.', Orkney, Scotland, 2009.
[193] EquiMar, 'Deliverable 3.3 - Assessment of Current Practices for Tank Testing of Small Marine Energy Devices', University of Strathclyde, University College Cork, University of Southampton, DNV, European Commission FP7 Project, GA number: 213380, 2010.
[194] EquiMar, 'Deliverable 3.4 – Best Practice Testing of Small Marine Energy Devices', University of Strathclyde, University College Cork, University of Southampton, DNV, European Commission FP7 Project, GA number: 213380, 2010.
[195] I. E. A. (IEA) O. E. S. (OES) IEA-OES, 'Development of Recommended Practices for Testing Ocean Energy Systems - Annex II Report', 2010.
[196] I. T. T. C. ITTC, 'Recommended Guidelines. Wave Energy Converter Model Test Experiments. Procedure 7.5-02-07-03.7.', 2017.
[197] I. E. C. IEC TS 62600-103, 'Marine Energy – Wave, Tidal, and Other Water Current Converters – Part 103: Guidelines for the Early Stage Development of Wave Energy Converters – Best Practices and Recommended Procedures for the Testing of Pre-Prototype Devices', Geneva, Switzerland, 2018.
[198] R. Coe, G. Bacelli, S. Spencer, and H. Cho, *Initial results from wave tank test of closed-loop WEC control*. 2018.
[199] E. Angelelli, B. Zanuttigh, J. P. Kofoed, and K. Glejbøl, 'Experiments on the WavePiston, Wave Energy Converter', presented at the 9th European Wave and Tidal Conference, 2011.
[200] A. Pecher, J. P. Kofoed, and E. Angelelli, 'Experimental Study on the WavePiston Wave Energy Converter', Aalborg University, DCE Contract Report No. 73, 2010.
[201] O. Choupin, M. Henriksen, A. Etemad-Shahidi, and R. Tomlinson, 'Breaking-Down and Parameterising Wave Energy Converter Costs Using the CapEx and Similitude Methods', *Energies*, vol. 14, no. 4, 2021, doi: 10.3390/en14040902.
[202] CorPower Ocean, 'User-Project: HiWave Tank testing of high-efficiency phase-controlled Wave Energy Converter', Infrastructure Access Report: HiWave MARINET-TA1-HiWave, 2015.
[203] R. Yemm, 'Pelamis WEC – Full-Scale Joint System Test', DTI Report V/06/00191/00/00/REP (DTI URN 03/1435), 2003.
[204] Rico Hjerm Hansen, 'Design and Control of the PowerTake-Off System for a Wave Energy Converter with Multiple Absorbers', Department of Energy Technology, Aalborg University, 2013.
[205] F. . C. da F. L.M.C. Gato;, A.A.D. Carrelhas;, and J.C.C.Henriques, 'H2020 OPERA-D3.2 Turbine-generator set laboratory tests in variable unidirectional flow', 2017.
[206] 'MaRINET2 Offshore Renewable Energy Testing | MaRINET Infrastructures Network', *MaRINET2*. http://www.marinet2.eu/ (accessed Mar. 22, 2021).

[207] G. Bracco, E. Giorcelli, G. Mattiazzo, V. Orlando, and M. Raffero, 'Hardware-In-the-Loop test rig for the ISWEC wave energy system', *Mechatronics*, vol. 25, pp. 11–17, Feb. 2015, doi: 10.1016/j.mechatronics.2014.10.007.
[208] S. Robertson, D. Noble, H. Jeffrey, L. Castellini, M. Martini, and N. van Velzen, 'Progress update on the development and testing of an advanced power take-off for marine energy applications', p. 18.
[209] UmbraGroup spa, 'EMERGE- WES PTO Stage 3', Public Report, Nov. 2019.
[210] Lafoz, Marcos and Nájera, Jorge, 'SeaTitan- Deliverable D5.2. Description of the PTO testing laboratory facility provided to carry out the tests', 2020.
[211] N. Delmonte *et al.*, 'An Iterative Refining Approach to Design the Control of Wave Energy Converters with Numerical Modeling and Scaled HIL Testing', *Energies*, vol. 13, no. 10, p. 2508, May 2020, doi: 10.3390/en13102508.
[212] FP7 Marinet, 'D4.02. Report on dynamic test procedures'. T4.4 Commission deliverable, 2014.
[213] J. C. N. Cavagnaro Robert J., François-Xavier Faÿ, and Joseba Lopez Mendia, 'Evaluation of Electromechanical Systems Dynamically Emulating a Candidate Hydrokinetic Turbine'. https://ieeexplore.ieee.org/document/7321812/ (accessed Apr. 23, 2021).
[214] 'Marinet Project website'. http://www.fp7-marinet.eu/
[215] G. Moretti *et al.*, 'Hardware-in-the-loop simulation of wave energy converters based on dielectric elastomer generators', *Meccanica*, vol. 56, no. 5, pp. 1223–1237, May 2021, doi: 10.1007/s11012-021-01320-8.
[216] Sandia National Labotarories, 'SWEPT Lab Factsheet'. Nov. 2021. [Online]. Available: https://energy.sandia.gov/download/43985/
[217] 'Integrated Modular Plant and Containerised Tools for Selective, Low-impact Mining of Small High-grade Deposits', *H2020-IMPaCT*. http://www.impactmine.eu/ (accessed Apr. 23, 2021).
[218] CEN-CENELEC, 'Methodology, procedures and equipment required for the laboratory testing of a modular and crosscutting Power Take-Off for wave energy converters', 2021.
[219] G. Bacelli, S. J. Spencer, R. G. Coe, A. Mazumdar, D. Patterson, and K. Dullea, 'Design and Bench Testing of a Model-Scale WEC for Advanced PTO Control Research', p. 8.
[220] J. Todalshaug *et al.*, 'Tank testing of an inherently phase-controlled Wave Energy Converter', *Int. J. Mar. Energy*, vol. 15, May 2016, doi: 10.1016/j.ijome.2016.04.007.
[221] P. Johannesson, 'Advanced PTO for enhanced reliability and performance of Wave Energy Converters', D3.6, Oct. 2019. [Online]. Available: https://ec.europa.eu/research/participants/documents/downloadPublic?documentIds=080166e5c8e7279f&appId=PPGMS
[222] 'R&D of dynamic low voltage cables between the buoy and floating hub in a marine energy system', RISE Research Institutes of Sweden, Borås, Projekt nr 41240-1, 2018. [Online]. Available: http://www.energimyndigheten.se/forskning-och-innovation/projektdatabas/sokresultat/GetDocument/?id=84a98f98-1062-40ba-b849-a0721176b8ed&documentName=SLUTRAPPORT%20Energimyndigheten%20final%202.docx.pdf
[223] T. L. Anderson, *Fracture Mechanics: Fundamentals and Applications, Fourth Edition*, 4th edition. Boca Raton: CRC Press, 2017.
[224] S. Ambühl, F. Ferri, J. P. Kofoed, and J. D. Sorensen, 'Fatigue reliability and calibration of fatigue design factors of wave energy converters', *Int. J. Mar. Energy*, vol. 10, pp. 17–38, Jun. 2015, doi: 10.1016/j.ijome.2015.01.004.
[225] *Guide to Load Analysis for Durability in Vehicle Engineering av P Johannesson, M Speckert (Bok)*, 1st ed. John Wiley & Sons Inc, 2013.

[226] G. W. Stachowiak, A. W. Batchelor, and G. B. Stachowiak, '4 - Measurement of Friction and Wear', in *Tribology Series*, vol. 44, G. W. Stachowiak, A. W. Batchelor, and G. B. Stachowiak, Eds. Elsevier, 2004, pp. 79–102. doi: 10.1016/S0167-8922(04)80020-8.
[227] 'ASTM G44-21 Standard Practice for Exposure of Metals and Alloys by Alternate Immersion in Neutral 3.5 % Sodium Chloride Solution', ASTM International, Jun. 2021. doi: 10.1520/G0044-21.
[228] 'ASTM B117-18 Standard Practice for Operating Salt Spray (Fog) Apparatus', ASTM International, Oct. 2018. doi: 10.1520/B0117-18.
[229] 'ISO 9227:2017 Corrosion tests in artificial atmospheres - Salt spray tests', Apr. 2017.
[230] 'ISO 10289 Methods for corrosion testing of metallic and other inorganic coatings on metallics substrates - Rating of test specimens and manufactured articles subjected to corrosion tests', Apr. 2001.
[231] 'ISO 11997-1:2018 Paints and varnishes - Determination of resistance to cyclic corrosion conditions - Part 1: Wet (salt fog)/dry/humid', Jan. 2018.
[232] 'ISO 12944-6:2018 Paints and varnishes - Corrosion protection of steel structures by protective paint systems - Part 6: Laboratory performance test methods', Mar. 2018.
[233] 'ASTM G5-14 (Reapproved 2021) Reference Test Method for Making Potentiodynamic Anodic Polarization Measurements', ASTM International, Aug. 2021. doi: 10.1520/G0005-14R21.
[234] 'ASTM G59-97 (Reapproved 2020) Test Method for Conducting Potentiodynamic Polarization Resistance Measurements', ASTM International, Nov. 2020. doi: 10.1520/G0059-97R20.
[235] 'ASTM G61-86 (Reapproved 2009) Test Method for Conducting Cyclic Potentiodynamic Polarization Measurements for Localized Corrosion Susceptibility of Iron-, Nickel-, or Cobalt-Based Alloys', ASTM International, May 2009. doi: 10.1520/G0061-86R09.
[236] 'ASTM G100-89 (Reapproved 2021) Test Method for Conducting Cyclic Galvanostaircase Polarization', ASTM International, Aug. 2021. doi: 10.1520/G0100-89R21.
[237] 'ASTM G150-18 Test Method for Electrochemical Critical Pitting Temperature Testing of Stainless Steels and Related Alloys', ASTM International. doi: 10.1520/G0150-18.
[238] L. Lichtenstein, 'Corrosion protection design according to DNV GL standards and recommended practices - possibilities and boundaries', p. 9.
[239] 'ISO 12944-9:2018 Paint and varnishes - Corrosion protection of steel structures by protective paint systems - Part 9: Protective paint systems and laboratory performance test methods for offshore and related structures', Feb. 2018.
[240] 'IEC 60068-2-11:2021 Environmental testing - Part 2-11: Tests - Test Ka: Salt mist', Mar. 2021.
[241] 'IEC 60068-2-52 Environmental testing - Part 2-52: Tests - Test Kb: Salt mist, cyclic (sodium chloride solution)', Nov. 2017.
[242] 2012 CEPE, *Efficacy evaluation of antifouling products Conduct and reporting of static raft tests for antifouling efficacy*. brussels: CEPE - The European Council of producers and importers of paints, printing inks and artists' colours - CEPE Guidance developed by the CEPE Antifouling Working Group, 2012. [Online]. Available: http://cepe-myeteam.eudata.be/EPUB//easnet.dll/GetDoc?APPL=1&DAT_IM=107E41&DWNLD=2012%20CEPE%20Efficacy%20Methodology%20-%2019%20June%202012.pdf
[243] *ASTM D5618-20: Standard Test Method for Measurement of Barnacle Adhesion Strength in Shear*. West Conshohocken, PA: ASTM International, 2020. [Online]. Available: http://www.astm.org/cgi-bin/resolver.cgi?D5618

[244] 'Evaluation of measurement data — Guide to the expression of uncertainty in measurement'. BIPM, Sep. 2008. Accessed: Jun. 24, 2021. [Online]. Available: https://www.bipm.org/documents/20126/2071204/JCGM_100_2008_E.pdf/cb0ef43f-baa5-11cf-3f85-4dcd86f77bd6
[245] G. S. Ásgeirsson *et al.*, 'Loads summary based on tank tests, Orcaflex simulations and wave-2-wire model output', NR15002, 2015.
[246] H. Gaviglio, J. Todalshaug, and P. Lourdais, 'C3 Dry and Ocean performance tests analysis, metrics and improved loss mapping', CorPower Ocean, NR17005, 2018.
[247] Orcina Ltd, *OrcaFlex*. [Online]. Available: https://www.orcina.com/orcaflex/
[248] M. Swenson, 'Submodeling: Simple Solutions for Large-Scale Problems', Nov. 23, 2016. https://www.ansys.com/blog/submodeling-made-easy (accessed Aug. 20, 2012).
[249] 'IDOM | CONSULTORÍA, INGENIERÍA, ARQUITECTURA'. https://www.idom.com/es/ (accessed Mar. 22, 2021).
[250] 'BiMEP – Biscay Marine Energy Platform'. https://www.bimep.com/en/ (accessed Mar. 22, 2021).
[251] 'Home - OPERA H2020'. http://opera-h2020.eu/ (accessed Mar. 22, 2021).
[252] 'Report on Numerical Methods for PTO Systems'.
[253] A. Pecher and J. P. Kofoed, *Handbook of Ocean Wave Energy*. Springer Verlag, 2017.
[254] Delmonte Nicola, 'Multi-chamber oscillating water column device for harvesting Ocean Renewable Energy'. Mar. 21, 2014.
[255] P. Ricci, 'Modelling, optimization and control of wav energy conveerters'.
[256] Wamit Inc., *WAMIT v7.1 User manual*. Chestnut, Massachusetts, USA: Wamit Inc., 2015. Accessed: May 04, 2016. [Online]. Available: http://www.wamit.com/manualupdate/v71_manual.pdf
[257] 'Ansys | Engineering Simulation Software'. https://www.ansys.com/ (accessed Mar. 22, 2021).
[258] P. Ricci *et al.*, 'Control strategies for a wave energy converter connected to a hydraulic power take-off', *Iet Renew. Power Gener.*, vol. 5, no. 3, pp. 234–244, 2011, doi: 10.1049/iet-rpg.2009.0197.
[259] W. E. . Cummins, 'The Impulse Response Function and Ship Motions', pp. 101–109, 1962.
[260] 'OE Buoy', *OceanEnergy*. https://oceanenergy.ie/oe-buoy/ (accessed Mar. 22, 2021).
[261] 'Hydraulics & Maritime Research Centre', *University College Cork*. https://www.ucc.ie/en/civileng/civil-engineering-facilities/hydraulicsandmaritime/ (accessed Mar. 22, 2021).
[262] R. Alcorn, A. Blavette, M. Healy, and A. Lewis, 'FP7 EU funded CORES wave energy project: a coordinators' perspective on the Galway Bay sea trials', *Underw. Technol. Int. J. Soc. Underw.*, vol. 32, no. 1, pp. 51–59, Mar. 2014, doi: 10.3723/ut.32.051.
[263] 'Marine Renewables Infrastructure Network for Emerging Energy Technologies | MARINET Project | FP7 | CORDIS | European Commission'. https://cordis.europa.eu/project/id/262552/es (accessed Mar. 22, 2021).
[264] 'Simulink - Simulación y diseño basado en modelos'. https://es.mathworks.com/products/simulink.html (accessed Mar. 22, 2021).
[265] 'Real-Time Interface - dSPACE'. https://www.dspace.com/en/inc/home/products/sw/impsw/real-time-interface.cfm#175_25029 (accessed Mar. 22, 2021).
[266] 'TwinCAT | Automation software | Beckhoff USA'. https://www.beckhoff.com/en-us/products/automation/twincat/ (accessed Mar. 22, 2021).
[267] F.-X. Faÿ, 'Modelling and Control for the Oscillating Water Column in Wave Energy Conversion'.

[268] 'PCI-6221'. https://www.ni.com/es-es/support/model.pci-6221.html (accessed Mar. 22, 2021).
[269] B. A. G. & C. K. Germany Hülshorstweg 20, 33415 Verl, 'CX1020 | Basic CPU module', *Beckhoff Automation*. https://www.beckhoff.com/es-es/products/ipc/embedded-pcs/cx1020-intel-celeron-m/cx1020.html (accessed Mar. 22, 2021).
[270] 'DTOceanPlus - Design tools for ocean energy systems', *DTOceanPlus - Design tools for ocean energy systems*. https://www.dtoceanplus.eu/ (accessed Mar. 23, 2021).
[271] J. Pyrhonen, T. Jokinen, and V. Hrabovcová, *Design of rotating electrical machines*. Chichester, West Sussex, United Kingdom ; Hoboken, NJ: Wiley, 2008.
[272] G. C. Stone, Ed., *Electrical insulation for rotating machines: design, evaluation, aging, testing, and repair*. Piscataway, NJ : Hoboken, NJ: IEEE ; Wiley-Interscience, 2004.
[273] D. Roberts and University of Liverpool, 'The application of an induction motor thermal model to motor protection and other functions', 1986.
[274] 'Electrical insulation. Thermal evaluation and designation':, BSI British Standards. doi: 10.3403/30146695.
[275] S. Ceballos, J. Rea, I. Lopez, J. Pou, E. Robles, and D. L. O'Sullivan, 'Efficiency Optimization in Low Inertia Wells Turbine-Oscillating Water Column Devices', *Ieee Trans. Energy Convers.*, vol. 28, no. 3, pp. 553–564, 2013, doi: 10.1109/TEC.2013.2265172.
[276] S. Ceballos, J. Rea, E. Robles, I. Lopez, J. Pou, and D. O' Sullivan, 'Control Strategies for Combining Local Energy Storage with Wells Turbine Oscillating Water Column Devices', *Elsevier Renew. Energy*, vol. 83, pp. 1097–1109, Nov. 2015.
[277] R. . Read and H. . Bingham, 'Wavepiston Report 1: Frequency-Domain Analysis of Plate Loads in Regular Waves', Technical University of Denmark, 2018.
[278] R. . Read and H. . Bingham, 'Wavepiston Report 2: Frequency-Domain Analysis of Energy Absorption in Regular Waves', Technical University of Denmark, 2018.
[279] H. . Bingham, *DTU Motion Simulator*. [Online]. Available: https://gitlab.gbar.dtu.dk/oceanwave3d/DTUMotionSimulator
[280] NREL and Sandia, *WEC-Sim*. [Online]. Available: https://wec-sim.github.io/WEC-Sim/
[281] Y.-H. Yu, M. Lawson, K. Ruehl, and C. Michelen, 'Development and demonstration of the WEC-Sim wave energy converter simulation tool', 2014.
[282] Simcenter, *Star-CCM+*. [Online]. Available: https://www.plm.automation.siemens.com/global/en/products/simcenter/STAR-CCM.html
[283] MSC Software, *Nastran*. [Online]. Available: https://www.mscsoftware.com/product/msc-nastran
[284] SCANSCOT, *Abaqus*. [Online]. Available: https://scanscot.com/products/simulia/abaqus
[285] M. Lawson, Y.-H. Yu, A. Nelessen, K. Ruehl, and C. Michelen, 'Implementing Nonlinear Buoyancy and Excitation Forces in the WEC-Sim Wave Energy Converter Modeling Tool', 2014.
[286] G. M. Paredes, C. Eskilsson, J. Palm, J. P. Kofoed, and L. Bergdahl, 'Coupled BEM/hp-FEM Modelling of Moored Floaters', in *Vietnam Symposium on Advances in Offshore Engineering*, 2018, pp. 504–510.
[287] Global Maritime, 'Wavepiston Design: Mooring and Flexible Export Pipe Design', 2020.
[288] T. T. Christensen, 'CFD simulations on an oscillating flat plate in water, at the surface and deep below', Technical University of Denmark, 2017.
[289] Sigma Energy & Marine, 'FE analysis of tarp and wagon structure', 2020.
[290] *DNV-RP-A203: Technology Qualification*. 2013.

[291] ABS, *Guidance Notes on Review and Approval of Novel Concepts*. American Bureau of Shipping, 2017.
[292] Lloyd's Register, *Guidance Notes for Technology Qualification*. Lloyd's Register, 2017.
[293] IEC TS 62600-4, *Marine energy - Wave, tidal and other water current converters. Part 4: Specification for establishing qualification of new technology*. International Electrotechnical Commission (IEC), 2020.
[294] T. Weilkiens, J. G. Lamm, S. Roth, and M. Walker, *Model-Based System Architecture*. Wiley & Sons, Inc., 2015.
[295] O. Knaus and J. C. Wurzenberger, 'System Simulation in Automotive Industry', in *Systems Engineering for Automotive Powertrain Development*, H. Hick, K. Küpper, and H. Sorger, Eds. Cham: Springer International Publishing, 2020, pp. 1–34. doi: 10.1007/978-3-319-68847-3_34-1.
[296] *ISO 26262:2018 Road vehicles - Functional safetly*. International Organization for Standardization, 2018.
[297] *IEC 61508 Functional safety of electrical/electronic/programmable electronic safety-related systems*. International Electrotechnical Commission (IEC), 2010.
[298] National Instruments, 'Accelerating the Product Development Lifecycle with Faster Test: Navigating the V Diagram', 2020. Accessed: Feb. 11, 2021. [Online]. Available: https://www.ni.com/pt-pt/innovations/white-papers/18/accelerating-the-product-development-lifecycle-with-faster-test-.html
[299] MathWorks, 'Validation and Verification for System Development'. [Online]. Available: https://www.mathworks.com/help/ecoder/gs/v-model-for-system-development.html